The role of low oxygen microenvironments in microbial polyhydroxyalkanoate production using *Pseudomonas putida* and application to bioreactor operations for improved productivity

By

Warren Blunt

A Thesis Submitted to the Faculty of Graduate Studies of

The University of Manitoba

In partial fulfillment of the requirements for the degree of

DOCTOR OF PHILOSOPHY

Department of Biosystems Engineering

University of Manitoba

Winnipeg

Copyright © 2019 by Warren Blunt

Thesis Abstract

Synthesis of medium chain-length polyhydroxyalkanoates (mcl-PHAs) is an oxygen-requiring process. Maintaining an adequate supply of dissolved oxygen (DO) is a significant engineering challenge, and can be costly in large-scale bioreactors. The objective of this work was to understand the effect(s) that low-DO environments have on mcl-PHA synthesis in *Pseudomonas putida* LS46. This work focuses on two main aspects: 1) investigating fundamental physiology in microaerophilic environments; and 2) understanding how the findings could be applied to process design for bioreactor operations. In the first aspect, low-DO environments were studied in lab-scale bioreactors, mimicking conditions that might be encountered in large-scale vessels. At low DO, carbon flux to mcl-PHA exhibited considerable dependence on the carbon substrate and hence the biochemical pathway used for mcl-PHA biosynthesis. It was found that significant mcl-PHA was synthesized from β-oxidation intermediates (an oxidative process), but not when precursor monomers were obtained via a *de novo* fatty acid biosynthetic pathway (a reductive process). In the latter case, most of the carbon was respired as CO_2. For substrates that use both pathways to some degree, low DO increased the content of monomers incorporated from β-oxidation intermediates. In the second aspect of this work, an O_2-limited high-cell density fed-batch strategy was developed and implemented for improved productivity, and the effects of culture rheology on process performance were assessed. Finally, a lab-scale semi-continuous sequencing-batch system was pursued to investigate long-term performance in a non-sterile environment. It was found that fatty acid carbon substrates were highly selective for mcl-PHA producing organisms, such that the productivity of this system was comparable to a similar process in a sterile environment.

Collectively, this work represents the most comprehensive study available on the effects of O_2-limitation in mcl-PHA synthesis. The findings improve fundamental understanding of how *P. putida* LS46 metabolism responds to its environment and also have implications for process design, including: 1) under what conditions low-DO environments can benefit mcl-PHA synthesis; 2) possibilities for co-feeding substrates to improve residual growth or PHA yield; 3) how DO might alter monomer compositions; and 4) process configurations that can improve productivity under microaerophilic conditions.

Acknowledgements

I think its safe to say that five years ago I hadn't the slightest idea what I was signing up for. It's been quite a ride, to say the least. It has been a fun and challenging experience, and has certainly helped to mold me into a different (hopefully improved) version of myself. A version that is definitely more humble, and yet somehow more confident (in how much I don't know, I suppose) at the same time. Research certainly has its ups and downs; the euphoric moments of discovery and innovation are interspersed by seasons of stress, anxiety, disappointment, and frustration. This section is for those moments (which are not at all represented in the subsequent chapters) and those that helped me through them.

Firstly I must acknowledge my family in this sense: my parents, Bryan and Edna, and siblings Matthew and Marney. Thanks for being supportive of what I've been trying to achieve, lending an ear during the tough times, providing solid comic relief, and all the while politely pretending that whatever I was working on was actually interesting. Marns – thanks for playing me up to be much smarter than I actually am at every opportunity. Little do they know…

To my fellow graduate students and teammates in the Levin, Cicek, and Sparling labs (and at Scion), you're as important of a support group as any. The complete list has grown too extensive to include everyone (owing to the fact I've been around too long) since those early days of learning the ropes in a new environment with Valery Agbor, but you all know who you are. During those early days I met some of my best friends, who were amazing to hang out with whether talking shop over coffee, working ridiculous hours for the sake of furthering science, or perhaps even more ridiculous hours kept on the odd road trip. Scott Wushke, Marcel Taillefer, and Tom Rydzak, it sure was fun, and I learned a lot from you, but I don't think I could have survived as a full-time member of the Microbiology Department. Back in the Biosystems

Department, I've got to thank the PHA team (Dr. Parveen Sharma and Jilagamazhi Fu) for being patient and teaching me how be a microbiologist and molecular biologist, or at least fake it as best I could. I hope there was at least a bit of payback there. Riffat Munir, I'm not sure where to put you in all this since we've worked together in just about every context over the years. But thanks for being a great colleague, mentor, friend, and life coach. Ditto Joe Ackerman from the Cicek lab, only I wish we could have worked on more of the same projects over the years. I guess until that day comes, we'll just stick to solving all the world's problems over a cup of coffee. Ryan Sestric, I couldn't imagine life in the Levin lab without you, man. Thanks for teaching me that it's ok to have emotions, its not ok to be a robot (try as I may), what an IPA is, as well as some of the finer technical points of the game of dodgeball. Chris Dartiailh - thanks for being a good brainstorming buddy, gym buddy, and travel companion on trips to New Zealand and Australia. Come to think of it, after sharing office/lab space for most of the past 9 years, it actually amazes me that we're still friends. Joking aside, I thought we worked pretty well together and I'm proud of the publications we've got to show for it. I remain convinced that squash will supplant golf as the game over which business is conducted. Keep your racket handy.

Thanks to my committee for having enough confidence in my abilities to give me this opportunity and making room for me in your labs. You all provided unique and invaluable perspectives that have helped me navigate through the past five years. Dr. Sparling - thanks for making me a member of your lab, for being a tough reviewer, and for helping me to articulate how an engineer working at the interface with microbiology is a unique and valuable skillset. Dr. Gapes - I can't quite put my finger on the mixture of chemistry and engineering perspective that you brought - so needless to say it often challenged me big-time and I'm thankful for that. Thanks also for bringing enthusiasm and seeing reason to get excited over my work, and for

helping to bring me over to Scion for a stint. That experience was brought up in every job interview. Also worth noting is that you were also the only member of my committee crazy enough to accompany me running in the rain and muck, trail running in 30 °C heat, and mountain biking in November (and not in New Zealand). Someday, I hope to keep up. Dr. Levin - thanks for looking out for everyone, creating opportunities for us, for teaching me patience, perseverance, balance, and all the tips on pruning and gardening. Thanks also for emphasizing the individual relationships within a team. I'm betting your summertime BBQs are the envy of the entire department. Dr. Cicek - thanks for being willing to supervise me all these years and for keeping the big-picture perspective always present. I wish I could articulate my own thoughts and ideas half as well as you. Thanks also for showing me just how much work my tennis game needs. Maybe with all time that I'm sure will free up after I defend this thesis…

Ariadne Amorim, thank you for being a part of this journey and helping to get me here. The proofreading, support, encouragement, patience, as well as all of the travels and adventures along the way, were all invaluable. I wish you could help to co-author the chapters yet to be written. I'll sign off with one of my favorite Keane lyrics: "*Its not for me to try and steer your ways, I wish you well in all you do*."

Finally, and most importantly, thanks to my saviour, sustainer, and lighthouse, Jesus Christ. Thanks for the blessings of life and all its learning opportunities, as well as the patience and humility to persevere through. All glory to God!

Pride only breeds quarrels, but wisdom is found in those who take advice

Proverbs 13:10

Table of Contents

Thesis Abstract ..... **ii**

Acknowledgements ..... **iv**

List of Tables ..... **xii**

List of Figures ..... **xiv**

Abbreviations ..... **xvi**

List of Copyrighted Material with Permission ..... **xx**

Chapter 1: Overview of the thesis **1**

1.1. Research objectives 1

1.2. Motivation and background for this research 1

1.3. Structure of thesis 4

Chapter 2: Literature Review **5**

2.1. Preface 5

2.2. Introduction: the plastic age 5

2.3. PHA structure and nomenclature 8

2.4. PHAs: a promising alternative? 11

2.5. Synthesis of short chain length (scl-) and medium chain length (mcl-) PHAs 12

2.5.1. Short chain length (scl-) PHAs 12

2.5.2. Medium chain length (mcl-) PHAs 16

2.6. Fundamental bottlenecks for industrial PHA production 20

2.7. Fed batch processes for improved PHA productivity 23

2.7.1. Control of fed-batch cultivations 31

2.7.2. Scale-up of fed-batch PHA production processes 35

2.8. Oxygen transfer limitations in aerobic bioprocesses 42

2.8.1. Mass transfer theory 42

2.8.2. Gas-to-liquid oxygen mass transfer in submerged biological systems 44

2.8.3. Strategies for overcoming oxygen transfer limitations in PHA production 49

2.9. The role of oxygen-limited environments in PHA production 51

2.9.1. Synthesis of scl-PHA under O_2-limtation 53

2.9.2. Effect of OTR on scl-PHA polymer properties 62

2.9.3. Synthesis of mcl-PHA under O_2-limtation 66

2.9.4. General discussion on DO as a modulator of microbial PHA synthesis 68

2.10. Continuous and semi-continuous strategies 70

2.10.1. Continuous culture in PHA production 72

2.10.2. Cyclic/repeated (semi-continuous) processes in PHA production 77

2.10.3. Sterility challenges 81

2.11. Conclusions and outlook 82

Chapter 3: Materials and Methods 85
3.1. Preface 85
3.2. Microorganism and medium 85
3.3. Sample treatment 86
3.4. Sample preparation for analysis by GC 86
3.4.1. Alkylation of PHAs to 3-hydroxyacid methyl esters (3-HAME) 86
3.4.2. Esterification of fatty acids to fatty acid methyl esters (FAMEs) 87
3.5. Quantification of methyl esters by GC-FID 88
3.5.1. GC setup and operating method 88
3.5.2. Determination of RFs and PHA content, composition of sample biomass 88
3.6. PHA titer, non-PHA residual biomass, and specific growth rates 90
3.7. Productivity calculations 90
3.8. Yield calculations 91
3.9. Estimation of residual free ammonium 92
3.10. Reactor setup 92
3.10.1. Calibration of pH and DO electrodes 93
3.10.2. Reactor preparation and sterilization 94
3.11. Detection and quantification of CO_2 94
3.12. Carbon balancing 97
3.13. Determination of volumetric oxygen transfer coefficient (k_La) 97

Chapter 4: Microaerophilic environments improve the productivity of medium chain-length polyhydroxyalkanoate biosynthesis from fatty acids in *Pseudomonas putida* LS46 100
4.1. Preface 100
4.2. Abstract 100
4.3. Introduction 101
4.4. Materials and Methods 103
4.4.1. Micro-organism, medium, and substrates 103
4.4.2. Bioreactor setup and preparation 103
4.4.3. Oxygen transfer conditions 104
4.4.4. Reactor Monitoring 104
4.4.5. Measurement techniques 105
4.5. Results and Discussion 106
4.5.1. Growth rate 106
4.5.2. PHA synthesis characteristics 108
4.5.3. Monomer composition of the polymer 111
4.5.4 PHA productivity and yield 112
4.5.5. Carbon dioxide and carbon balance 116
4.5.6. Engineering applications 117
4.6. Conclusions 117
4.7. Acknowledgements 118

Chapter 5: Carbon flux to growth or polyhydroxyalkanoate synthesis under microaerophilic conditions is affected by fatty acid chain-length in *Pseudomonas putida* LS46 119
5.1. Preface 119
5.2. Abstract 120
5.3. Introduction 121
5.4. Materials and Methods 123
5.4.1. Microorganism, medium, and substrates 123
5.4.2. Reactor setup and preparation 123
5.4.3. Feeding rates 124
5.4.4. Co-feeding and prolonged LCFA cultivation experiments 125
5.4.5. Sample treatment and analyses 126
5.4.6. Carbon balance and yield analysis 127
5.5. Results 127
5.5.1. Dissolved oxygen 130
5.5.2. Total biomass and PHA accumulation in single substrate comparison 130
5.5.3. Analysis of X_r and residual concentrations of carbon and NH_4 131
5.5.4. Co-feeding and prolonged LCFA cultivation experiments 133
5.5.5. Volumetric productivity 138
5.5.6. Carbon balancing and yield analysis 138
5.5.7. Monomer composition of the polymer 140
5.6. Discussion 141
5.7. Conclusions 144
5.8. Acknowledgements 145

Chapter 6: *De novo* fatty acid biosynthesis is not an effective route to medium chain-length polyhydroxyalkanoates 146
6.1. Preface 146
6.2. Abstract 147
6.3. Introduction 148
6.4. Materials and Methods 151
6.4.1. Microorganism and medium 151
6.4.2. Bioreactor setup and experimental conditions 151
6.4.3. Sample treatment and analyses 153
6.4.4. CO_2 measurement, carbon balancing, and yield analysis 153
6.5. Results 154
6.5.1. Growth and PHA synthesis 154
6.5.2. Monomer composition 163
6.5.4. Yield analysis 167
6.6. Discussion 169
6.7. Conclusions 177

6.8. Acknowledgements 177

Chapter 7: Development of an oxygen-limited fed-batch process for improved polyhydroxyalkanoate productivity using *Pseudomonas putida* LS46 179

7.1. Preface 179
7.2. Abstract 179
7.3. Introduction 180
7.4. Materials and Methods 182
7.4.1. Microorganism, medium, substrates 182
7.4.2. Reactor setup and operation 182
7.4.3. Yield coefficients 183
7.4.4. Measurement of residual carbon, NH_4-N, PO_4-P and trace medium components. 184
7.5. Results 184
7.5.1. Pulse feed strategy 184
7.5.2. Residual concentrations of octanoic acid, NH_4-N and PO_4-P 185
7.5.3. Carbon flux and yield analysis 186
7.5.4. Residual trace elements 188
7.5.5. Modeling of feeding rates – continuous drip feed strategy 190
7.6. Discussion 194
7.7. Conclusions 197
7.8. Acknowledgements 197

Chapter 8: Rheological characterization of high-cell density cultures of *Pseudomonas putida* LS46 199

8.1. Preface 199
8.2. Abstract 199
8.3. Introduction 200
8.4. Materials and Methods 202
8.4.1. Micro-organism, medium and substrates 202
8.4.2. Reactor setup and operation 202
8.4.3. Sample treatment and analyses 204
8.4.4. Viscosity measurements 204
8.4.5. Off-line k_La determination 205
8.4.6. Analysis of organic products in the supernatant 206
8.5. Results and Discussion 208
8.5.1. Rheological characterization of the cultivation medium 208
8.5.2. Quantifying extracellular components in the supernatant matrix 213
8.5.3. Effects on k_La 216
8.6. Conclusions 218
8.7. Acknowledgements 219

Chapter 9: Towards continuous cultivation: tailoring selective conditions for mcl-PHA production in a non-sterile environment 220
9.1. Preface 220
9.2. Abstract 220
9.3. Introduction 221
9.4. Materials and Methods 224
9.4.1. Microorganism, medium, and substrates 224
9.4.2. Cultivation techniques/platforms 224
9.4.3. Contamination assessment 227
9.4.4. Analytical methods 227
9.4.5. Statistical analyses 227
9.5. Results 228
9.5.1. Micro-plate tests 228
9.5.2. Mcl-PHA production in non-sterile flask cultures 232
9.5.3. Prolonged mcl-PHA production in non-sterile (semi-continuous) SBR 236
9.6. Discussion and engineering significance 241
9.7. Conclusions 244
9.8. Acknowledgements 245

Chapter 10: Discussion, engineering significance, and future work 246
10.1 Overview and discussion of findings 246
10.1.1. Microaerophilic mcl-PHA synthesis in P. putida LS46 (Chapters 4-6) 247
10.1.2. Process optimization under oxygen-limited conditions (Chapters 7-9) 251
10.2 Engineering Significance 254

References 258

Appendix A: Scaling up production of mcl-PHA to pilot-scale bioreactors **290**

Appendix B: Zoomed-in profile of DO and off-gas CO_2 signals for control of pulse-feed experiments (Chapter 7) **300**

Appendix C: Effects of culture rheology on downstream processing operations **301**

Appendix D: Application of a high cell-density fed batch process for non-sterile mcl-PHA production **304**

Appendix E: The potential of non-sterile mcl-PHA production from biodiesel waste free fatty acids and mixed culture mcl-PHA production **307**

List of Tables

Table 2.1. Nomenclature system for PHAs based on structure. 10
Table 2.2. Current commercial-scale PHA production operations. 21
Table 2.3. High-productivity fed-batch cultivation processes in mcl-PHA research. 26
Table 2.4. High-productivity fed-batch cultivations processes in scl-PHA research. 28
Table 2.5. Exponential fed-batch strategies applied in mcl-PHA research. 34
Table 2.6. Operating costs for mixing and aeration in 30 to 19000 L bioreactors. 37
Table 2.7. Research on scale-up to at least a 100 L for various PHA production processes. 39
Table 2.8. Diffusion of an oxygen molecule from the gas bubble to the site of the biological reaction. 46
Table 2.9. The impact of oxygen limitation when producing scl-PHA from carbohydrate-based carbon substrates using pure cultures. 55
Table 2.10. The impact of oxygen limitation when producing scl-PHA from VFAs or LCFAs using pure cultures. 58
Table 2.11. Summary of studies that investigated the impact of oxygen limitation on PHA production using MMCs. 60
Table 2.12. Summary of polymer properties (molecular mass, thermal, and mechanical) for various scl- and mcl-PHAs. 63
Table 2.13. Research on continuous cultivation in PHA production. 74
Table 2.14. Semi-continuous (cyclic) batch, fed-batch, and cell recycle processes applied in PHA production. 79

Table 3.1. Molecular masses of 3-hydroxyacid monomers detected in mcl-PHA analysis by GC. 90

Table 4.1. Summary of the tested bioreactor OTRs and DO concentrations. 105
Table 4.2. Observed monomer compositions produced from octanoic acid at different OTRs. 112
Table 4.3. Literature values for mcl-PHA yield from mcl-fatty acids using *P. putida* grown and various cultivation strategies. 116

Table 5.1. Determination of appropriate specific growth rate for exponential feeding of octanoic acid to *P. putida* LS46. 129
Table 5.2. Comparison of key process performance indicators during mcl-PHA production by *P. putida* LS46 from LCFAs or octanoic acid as the sole carbon source, or when co-fed in C-mol equivalent proportions. 137
Table 5.3. Final monomer compositions of mcl-PHA polymers synthesized from LCFAs and octanoic acid by *P. putida* LS46. 141

Table 6.1. Summary of experimental conditions used in the bioreactors. 152

Table 6.2. Specific growth rate, carbon uptake rate, and oxygen uptake rate observed during the growth phase, and under limiting (N or O_2) conditions. 160
Table 6.3. Biomass titer and PHA synthesis characteristics from 320 C-mmol L^{-1} of the indicated carbon substrates that utilize the *de novo* pathway to varying degrees, under conditions of strict NH_4-limitation or O_2-limitation. 161
Table 6.4. Monomer composition of PHA obtained from carbon substrates that utilize the *de novo* pathway to varying degrees, under conditions of strict NH_4 limitation or O_2-limitation. . 166
Table 6.5. Yield analysis for unrestricted growth conditions and growth-limited (NH_4 and O_2) conditions for each substrate. 168
Table 6.6. Possible enzymes responsible for reactions that reduce $NADP^+$ in *P. putida* LS46. 171

Table 7.1. Yield coefficients for C, N, P, and certain (detectable) trace elements. 188
Table 7.2. Comparing process performance of previous batch cultivations with the described fed batch processes 193

Table 8.1. Model parameters for fitting the rheological data with the Power Law. 212
Table 8.2. Summary of average viscosity at a shearing rate of 10 rad s^{-1} and onset of shear thickening. 212

Table 9.1. Statistical analysis of $\%_{PHA}$ and Q_v using a two-tailed comparison of means ($\alpha = 0.05$) between sterile and non-sterile flasks cultures of *P. putida* LS46 using different concentrations of octanoic acid.. 234
Table 9.2. Monomer composition of mcl-PHA obtained for sterile and non-sterile flask cultures. 234
Table 9.3. Summary of mcl-PHA production in a non-sterile environment during a 28-day SBR cultivation.. 239

List of Figures

Figure 2.1. Occurrence of intracellular PHA granules with generic chemical structure. 10
Figure 2.2. Pathway for synthesis of scl-PHA from glucose, VFAs, and LCFAs. 15
Figure 2.3. Pathways for synthesis of mcl-PHA from *de novo* synthesis and fatty acid β-oxidation. 18
Figure 2.4. Two-dimensional graphical representation of two-film theory. 43
Figure 2.5. Mass transport of oxygen from a gas bubble to the cell. 45
Figure 2.6. Summary schematic for development of subsequent chapters in this thesis. 84

Figure 3.1. Typical DO profile during N_2-sparging and aeration phases for k_La determination via the dynamic method. 98

Figure 4.1. Representative growth and mcl-PHA synthesis curves from octanoic acid at high and low DO conditions. 107
Figure 4.2. Specific growth rates and maximum $\%_{PHA}$ from octanoic acid at different OTRs. 109
Figure 4.3. Maximum Q_s and Q_v of mcl-PHA synthesized from octanoic acid at indicated OTR. 114
Figure 4.4. Distribution of carbon flux from octanoic acid at tested OTRs. 115

Figure 5. 1. Results from *P. putida* LS46 growth on either octanoic acid or LCFAs when grown in fed-batch at $\mu = 0.25\ h^{-1}$. 132
Figure 5.2. Results from cultivation of *P. putida* LS46 in prolonged LCFA and co-feed fed batch cultivations at 0.25μ. 135
Figure 5.3. Uptake of each carbon source during the co-feed experiments. 136

Figure 6.1. Growth and PHA synthesis from glucose using *P. putida* LS46 on under a) O_2-limited or b) NH_4-limited conditions. 155
Figure 6.2. Growth and PHA synthesis from acetate using *P. putida* LS46 on under a) O_2-limited or b) NH_4-limited conditions. 156
Figure 6.3. Growth and PHA synthesis from valerate using *P. putida* LS46 on under a) O_2-limited or b) NH_4-limited conditions. 157
Figure 6.4. Growth and PHA synthesis from hexanoate using *P. putida* LS46 on under a) O_2-limited or b) NH_4-limited conditions. 158
Figure 6.5. Mcl-PHA synthesis characteristics from a spectrum of substrates in low DO environments. 176

Figure 7.1. Supporting data obtained over the course of the pulse-feed experiments. 187
Figure 7.2. Uptake of trace metals in fed-batch culture of *P. putida* LS46. 189

Figure 7.3. Modeled cumulative uptake of carbon and ammonium over the time course of the pulse-feed experiments. 191
Figure 7.4. Results for the continuous, drip-feed fed-batch cultivation. 192

Figure 8.1. Plexi-glass reactor constructed for off-line determinations of k_La using a minimal amount of sample. 206
Figure 8.2. a) Growth and PHA synthesis curves and b) appearance of culture after centrifugation for fed-batch experiments at the cultivation time indicated. 209
Figure 8.3. Flow sweep curves for growth medium from fed-batch cultures. a) *P. putida* LS46 cultures and b) supernatants from *P. putida* LS46 cultures. 210
Figure 8.4. Changes in power-law constants describing culture rheology as a function of the total biomass in the fed batch cultivation at varying points over time 213
Figure 8.5. Carbonaceous products detected in the supernatant over time 214
Figure 8.6. Relationship between select components of the VS with the observed viscosity ... 215

Figure 9.1. Effect of different initial concentrations of octanoic acid in medium at pH 7.0. 230
Figure 9.2. Effect of medium pH at 20 mM initial concentration of octanoic acid.. 232
Figure 9.3. Final $\%_{PHA}$ and Q_v observed at 24 h when *P. putida* LS46 was grown in flasks under sterile and non-sterile conditions. 233
Figure 9.4. Growth of non-sterile control cultures (no inoculum) at different initial concentrations of octanoic acid. 236
Figure 9.5. Long term performance of $[X_t]$ and $\%_{PHA}$ during the 28-day non-sterile SBR cultivation. 238
Figure 9.6. Long-term performance of Q_v and $Y_{PHA/S}$ during the 28-day non-sterile SBR cultivation.. 240

Abbreviations

a	gas-liquid interfacial area
ATP	adenosine triphosphate
CDM	cell dry mass (g L^{-1})
C_i	the ith component (*C*) in a mathematical series
C_L	liquid phase concentration (of O_2)
C_L^*	equilibrium liquid phase concentration (of O_2)
CoA	coenzyme A
C/N	carbon-to-nitrogen ratio
C/P	carbon-to-phosphate ratio
C_T	total dissolved carbonate species
C(t)	time-dependent amount of carbon fed to a bioreactor (grams)
D	dilution rate (h^{-1})
Df	diffusivity (m^2 s^{-1})
DO(C)	dissolved oxygen (content) (% of relative saturation with atmospheric air at 30 °C, unless otherwise specified)
EPS	extracellular polymeric substance
f	molar fraction
FAD/$FADH_2$	oxidized/reduced flavin adenine dinucleotide
FadG	3-ketoacyl-CoA reductase
FFA	free fatty acid
FAME	fatty acid methyl ester
G_{CO2}	molar flow rate of CO_2 (mol min^{-1})
GC-FID	gas chromatograph with a flame ionization detector
HAME	3-hydroxyacid methyl ester
HCD	high-cell density
HPLC	high performance liquid chromatography

HRT	hydraulic retention time
IS	internal standard
K_0, K_1, K_2	equilibrium constant of the dissolved carbonate buffer system
k_H	Henry's law coefficient
k_L	liquid film coefficient *(distance time^{-1})*
k_La	volumetric oxygen mass transfer coefficient (h^{-1} or s^{-1})
$K_{s,\ O2}$	oxygen half saturation constant
LB	Luria-bertrani broth
LCA	life cycle analysis
LCFA	long chain fatty acid
LPM	liters per minute
mcl-	medium chain-length
MIMS	membrane-inlet mass spectrometer
MMC	mixed microbial culture
M (M_v, M_w, M_n, M_r)	molecular mass, (viscosity average, weight average, number average, relative)
m/z	mass-to-charge ratio
n	power law rate index (dimensionless)
N_a	rate of bioreactor agitation or orbital shaking rate (rpm)
NAD(P)/NAD(P)H	oxidized/reduced nicotinamide adenine dinucleotide (phosphate)
$N(t)$	time-dependent amount of NH_4 fed to a bioreactor (grams)
OD_{600}	optical density at 600 nm wavelength
OTR	oxygen transfer rate
OUR	oxygen uptake rate
P	pressure
$P_{CO2,\ O2}$	partial pressure of a gas phase (CO_2, O_2) above a liquid
PBS	phosphate-buffered saline
PHA	polyhydroxyalkanoate

PhaC	PHA synthase enzyme
PhaJ	R-specific enoyl-CoA hydratase enzyme
PHB	poly(3-hydroxybutyrate)
PHBV	poly(3-hydrxybutyrate-co-3-hydroxyvalerate)
PHO	poly(3-hydroxyoctanoate)
Q_s	specific productivity (g PHA g X_r^{-1} h^{-1})
Q_v	volumetric productivity (g PHA L^{-1} h^{-1})
R	ideal gas constant
Re	Reynold's number
RF	response factor
SBR	sequencing batch reactor
scl-	short chain-length
SRT	solids retention time
TCA	tricarboxylic acid cycle or citric acid cycle
t	time in hours (h), minutes (min) or seconds (s)
T	temperature
T_g	glass transition temperature
T_m	melt temperature
TV	total volume
$\dot{V}_a$	volumetric airflow rate (VVM or LPM)
VFA	volatile fatty acid
V_g, V_L	volume occupied by gas phase and liquid phase, respectively
VS	volatile solids
VVM	volumes air per liquid volume per minute
WV	working volume
X_{PHA}	PHA biomass
X_r	non-PHA residual biomass

X_t	total biomass
$Y_{PHA/S}$	yield of PHA from carbon substrate (on a mole or gram basis)
$Y_{Xr/C}$, $Y_{Xr/N}$	yield coefficients of X_r from carbon and ammonium, respectively
η	apparent viscosity (Pa.s or mPa.s)
μ, μ_{max}	specific growth rate, maximum specific growth rate (h^{-1})
τ	shear stress (mPa)
φ	power law viscosity constant
ω	shear rate (s^{-1})
[ ]	concentration braces
$\%_{PHA}$	intracellular PHA content (% g g^{-1})

List of Copyrighted Material with Permission

Permission was obtained from either Springer-Nature or Elsevier through the RightsLink® service available online from the Copyright Clearance Center for use of the following material for parts of this thesis:

1. Blunt W, Dartiailh C, Sparling R, Gapes DJ, Levin DB, Cicek N. (2018). Carbon flux to growth or polyhydroxyalkanoate synthesis under microaerophilic conditions is affected by fatty acid chain-length in *Pseudomonas putida* LS46. *Appl Micrbiol Biotechnol*, 1-13.
2. Blunt W, Sparling R, Gapes DJ, Levin DB, Cicek N. (2018). The role of dissolved oxygen content as a modulator of microbial polyhydroxyalkanoate synthesis. *World J Microbiol Biotechnol* 34(8): 106.
3. Figure 2.5 in this thesis is a modified version of Figure 10.8 (p. 397) in the text *Bioprocess Engineering Principles* (2nd Edition, Doran 2013).
4. Table 2.6 in this thesis is a modified version of of Table 1 in the journal article *Scale-up methodologies for Escherichia coli and yeast fermentation processes* (Junker 2004).

Sections of Chapter 2 (2.2, 2.7, 2.8.3, and 2.10) were published as an invited review article entitled *Bioreactor operating strategies for improved polyhydroxyalkanoate productivity* in the MDPI journal *Polymers* 10(11): 1197. This is an open access journal, and as such the work has been licensed for unlimited redistribution and re-use in accordance with the Creative Commons Attribution license. Chapters 4 and 6 were published in the Elsevier journal *Process Biochemistry*. In those cases, the author (myself) retained the right to include it as part of a thesis or dissertation provided it is not published commercially, and permission was not required.

Chapter 1: Overview of the thesis

1.1. Research objectives

The overall objective of this research was to extend medium chain length polyhydroxyalkanoate (mcl-PHA) production using *Pseudomonas putida* LS46 to the bioreactor scale and seek understanding of how these environments affect microbial metabolism, mcl-PHA synthesis characteristics, and process design. More specifically, this work examines how carbon flux, mcl-PHA synthesis rates, yields, and productivities were affected by aspects of: 1) the chemical environment, including the dissolved oxygen (DO) concentration and choice of carbon substrate; 2) the physical environment, including the effect(s) of shearing on culture rheology and oxygen transfer; and 3) the biological environment, including the presence of contaminating organisms in non-axenic cultures.

1.2. Motivation and background for this research

The motivation of this work was to improve mcl-PHA productivity in a cost-effective manner. Prior to this work being undertaken, multiple studies had been done at the flask scale, but little work was done at the bioreactor scale. The latter was not only a requisite for further study and characterization of the PHA polymers produced (not directly part of this research), but also crucial to understand and anticipate scale-up challenges. This scale-up was a necessary milestone for the project entitled *Fibre Composite and Biomatrix Genomics* (FiCoGEN), a Genome-Prairie-funded project supporting our lab. The objective of this project was to produce a biodegradable bio-composite material (of flax fibers embedded in a PHA matrix) for the manufacture of a prototype interior panel for a small vehicle (also not directly part of this research).

1.3. Thesis hypotheses

Preliminary bioreactor experiments using octanoic acid as the carbon substrate were designed to simply mimic previously obtained results in flask studies. The bioreactor studies showed that growth and mcl-PHA production from octanoic acid is characterized by very high oxygen demand. Furthermore, a stark disagreement in mcl-PHA titer was consistently observed between previous flask studies and bioreactors run under what we (at the time) thought were similar conditions. These observations, to a large extent, determined the map for this research (this is outlined in Figure 2.6). Assessment of the literature (Chapter 2) showed there was a fundamental lack of understanding of how low-DO environments affect mcl-PHA synthesis, product characteristics, and carbon flux in mcl-PHA-producing organisms in general. This led to the first major hypothesis of this work, which was that low-DO environments induce synthesis of mcl-PHA from fatty acids in *P. putida*, and this was addressed in Chapter 4. This work led to additional hypotheses that carbon flux under oxygen-limited conditions depends on the substrate being metabolized, and hence the biochemical pathway used to obtain monomers for synthesis of PHA (i.e. *de novo* fatty acid biosynthesis or β-oxidation). These investigations were reported in Chapter 5 (for long-chain fatty acids, LCFAs) and Chapter 6 (glucose or short-chain volatile fatty acids, VFAs).

Equipped with a fundamental understanding of carbon flux and mcl-PHA synthesis characteristics in low DO environments, the next task focused on applying these findings to bioreactor operations for improved productivity. Since fatty acids were efficiently incorporated to mcl-PHA under microaerophilic conditions, it was hypothesized that O_2-limitation could be used to drive mcl-PHA synthesis in a high-cell density (HCD) fed batch process without the need to restrict or manage the supply of another nutrient (many of which are conserably more difficult

to measure and control in real time). This may also result in reduced aeration requirement during the polymer storage phase. This hypothesis was developed and tested in Chapter 7, and scaled up to 150 L to demonstrate robustness of this process. The latter part of this work is described in Appendix A, and was done in the Biotransformation Lab at Scion, a Crown Research Institute in Rotorua, New Zealand.

These HCD cultures (and their supernatants) showed significantly different rheological behavior compared to batch or simple fed-batch cultivations described in Chapters 4-6. While working in the Biotransformation lab at Scion, the opportunity came about to investigate and quantify this behavior. In keeping with the overall research objective of this thesis, it was hypothesized that the observed viscosity effect had a significant detrimental impact on the oxygen mass transfer coefficient in HCD processes (Chapter 8).

The final research work of this thesis (Chapter 9) aimed to evaluate the efficacy of mcl-PHA production in non-sterile environments. This was done with the motivation of mitigating sterility concerns as a constraint for development and application of semi-continuous or fully continuous bioreactor systems for mcl-PHA production. The central hypothesis of this work was that maintaining a sufficient concentration of fatty acids in the medium applies a selective pressure for *P. putida* (or other mcl-PHA producing organisms) such that non-sterile operation could be achieved without significant detriment to the overall productivity. Although non-sterile operation may not be realistic, this work demonstrates the resilience of mcl-PHA production from fatty acids to process upsets by contamination, which allows considerable flexibility in process design or application of continuous bioreactor systems.

1.3. Structure of thesis

This is a sandwich-format thesis, in which each chapter is a stand-alone manuscript. Certain chapters (or sections of chapters) have been published in internationally recognized, peer-reviewed journals. When this is the case, it will be described in the preamble section at the forefront of individual chapters. Following the literature review (Chapter 2), the methods that are common to several subsequent experimental chapters (Chapters 4 through 9) are described in Chapter 3 to avoid redundancy throughout the chapters. Chapter 10 closes out the body of this thesis. This section summarizes the findings and draws some brief conclusions from this work with particular emphasis on the engineering significance of the work, as well as pointing toward some of the future challenges and research directions.

Chapter 2: Literature Review

2.1. Preface

This chapter serves as an introduction and review of all background information pertinent to this work. Sections 2.4 and 2.9 were combined and published as an invited review article entitled *The role of dissolved oxygen as a modulator of microbial polyhydroxyalkanoate synthesis* for a special issue on "Manipulation of the oxygen transfer rate to optimize microbial product formation" in *World Journal of Microbiology and Biotechnology* (2018) 34:106. Sections 2.2, 2.7, 2.8.3, and 2.10 were combined and published as an invited review article entitled *Bioreactor operating strategies for improved polyhydroxyalkanoate productivity* in a special issue on "Recent advances in bioplastics" in the journal *Polymers* (2018) 10(11): 1197.

2.2. Introduction: the plastic age

The term 'plastic' refers to a diverse group of materials that are synthesized from polymerization of petroleum-derived monomer building blocks, including methanol, ethylene, propylene, butadiene, benzene, toluene, and xylene (Thompson et al. 2009b). The plastics industry has a relatively brief history that only dates back to the Second World War, when metallic materials like steel, aluminum, and copper were diverted for military requirements. This created a need for alternative materials to produce domestic goods, a niche that was filled by petroleum-derived plastics (Hammer et al. 2012). Applications for plastics have become so widespread since that the past 70 years have been described as "The Plastic Age" (Thompson et al. 2009b). In 1950, global plastic production was approximately 0.5 million tonnes per annum (Thompson et al. 2009a). By 2015, global production reached 322 million tonnes (Worm et al. 2017), and if current consumption rates continue, the total production is projected to reach 33

billion tonnes by 2050 (Rochman et al. 2013). Plastic polymers are extremely durable, versatile, and can be produced from a relatively inexpensive and seemingly abundant supply of oil. These attributes have made plastics into an industry that generates revenues of $600 billion annually (Gourmelon 2015) and represents a great success story for materials science in the 20th century.

However, for all the past commercial success, we are becoming aware of the hazards associated with the production, use, and disposal of plastics. According to Rochman et al. (2013), of the total plastic produced less than half is recycled or landfilled. Of the remainder, an overwhelming portion ends up unaccounted for in terrestrial, marine, and freshwater ecosystems (Koller and Braunegg 2018). It is estimated that 10 to 20 million tonnes of plastic accumulate in the oceans alone each year (Bergmann et al. 2015) and significant quantities of plastic have been detected along some of the most remote coastlines in the world (Lavers and Bond 2017) Thus, the materials that were supposed to make for "a brighter and cleaner world" (Yarsley and Couzens 1945) have, somewhat ironically, ended up having the opposite effect.

Although the high degree of polymerization and complex molecular structure of plastic polymers gives these materials very high molecular mass (M) and excellent durability, it also makes them highly recalcitrant to bio-degradation in the natural environment, causing deleterious environmental effects (Teuten et al. 2009; Hammer et al. 2012; Philp et al. 2013). Plastics can contain a number of harmful toxins in the form of additives, including plasticizers, stabilizers, flame-retardants, fillers, biocides, and pigments (Lithner et al. 2011). Research has shown that these additives may not be chemically bound in the polymer and are able to migrate to the surface and leach into the surrounding environment (Bejgarn et al. 2015). Plastics have also been shown to absorb, concentrate, and transport persistent organic pollutants (Mato et al. 2001), which can be consumed by native fauna and bio-accumulate in the food web of an ecosystem

(Besseling et al. 2013). This effect is particularly problematic as the size of the plastic fragments is reduced to micro- to nano-sized particles, which are typically less than five mm in size (Germanov et al. 2018). Much of the plastic material accumulating in oceans is in the form of micro-sized particles that bio-accumulate in filter-feeding animals, posing a significant threat to marine ecosystems (Bergmann et al. 2015). Recent evidence also suggests that particles less than ten μm may pose significant risks to human health through inhalation and penetration of pulmonary surfaces (Gasperi et al. 2018; Hale 2018).

Current disposal methods for plastics include landfills, incineration, and recycling. Each of these methods has problems associated with it. The bulky nature of plastics is putting pressure on increasingly finite landfill space (Philp et al. 2013), causing some to regard this disposal method as little more than "storing a problem for the future" (Barnes et al. 2009). Incineration can also release toxins, such as hydrogen chloride and hydrogen cyanide, which are harmful to both the environment and human health (Reddy et al. 2003; Keshavarz and Roy 2010). Although recycling may be promising, recycling rates are relatively low due to cost, sorting challenges, and limited application for post-recycled materials (Barnes et al. 2009; Hammer et al. 2012; Carey 2017). Given that many plastic products are used once and discarded, an appropriate solution could be a biodegradable alternative that is completely broken down to biomass, water, and CO_2 through enzymatic activity of microorganisms (Braunegg et al. 1998). Although some plastics have biodegradable components added to them (starch or photo-biodegradable pigments for example), these components degrade and leave smaller fragments of plastic to persist, which as already discussed, may be even more problematic.

Production of completely biodegradable materials from renewable resources is therefore an urgent challenge for mitigating the environmental impact of petroleum-based plastics.

Microbial polyhydroxyalkanoates (PHAs) are a class of bio-based and biodegradable polyesters that have a broad range of characteristics and may help displace traditional plastic materials, at least for certain applications (Madison and Huisman 1999; Zheng et al. 2005; Iwata 2015). Because of the wide range of properties, they have perhaps greater upside than other known bio-polymers (polylactic acid, for example) and have attracted significant interest since the oil embargo of the 1970s (Akiyama et al. 2003).

2.3. PHA structure and nomenclature

PHAs are hydroxyalkanoic acids synthesized as intracellular inclusion bodies as a carbon and energy storage mechanism during sub-optimal growth conditions. Dutch-born microbiologist Martinus Beijerinck originally observed these structures as early as 1888, although the chemical structure and function was not identified until 1926 by French researcher Maurice Lemoigne during his work with *Bacillus megaterium* (Możejko-Ciesielska and Kiewisz 2016). Since then, PHA synthesis has been reported in more than 90 genera of archaea and bacteria (Zinn et al. 2001). PHA synthesis has been observed in more than 300 species of bacteria, both gram positive and gram-negative (Madison and Huisman 1999; Braunegg et al. 2004; Keshavarz and Roy 2010). Some of the more common PHA-synthesizing bacterial species include *Cupriavidus necator* (formerly *Alcaligenes eutrophus*, *Hydrogenomonas eutrophus*, *Wausteria eutropha*, *Ralstonia eutropha)*, *Azotobacter vinelandii*, *Pseudomonas putida*, *Azohydromonas lata* (formerly *Alcaligenes latus*), *Bacillus megaterium*, and recombinant strains of *Escherichia coli*, amongst others (Khanna and Srivastava 2005a; Keshavarz and Roy 2010). Production of PHA has been identified in several species of archaea, including *Haloferax*, *Haloarcula*, *Halobacterium*, and *Halococcus* amongst others (Poli et al. 2011).

Selection criteria for PHA production strains include the ability to achieve a high maximum specific growth rate (μ_{max}) on inexpensive and available carbon sources, ability to grow at relatively high temperatures, lack of sensitivity to precursors used for copolymer production, ability to produce a polymer with *M* of at least 500 kDa, genetically stable over long periods, and be capable of polymer accumulation during growth phase (Braunegg et al. 1995). While the ability to accumulate PHAs during active growth is desirable, most strains require nutrient limitation (N, P, C[1], or O_2) to induce optimal polymer synthesis. Some exceptions include *A. lata, A. vinelandii,* and recombinant strains of *E. coli*, which are known to synthesize PHAs concurrently to growth (Braunegg et al. 2004; Singhaboot and Kaewkannetra 2015). Although poly(3-hydroxybutyrate) (PHB) biosynthetic capability has been reported in native species of *E. coli* (Reusch et al. 1986), the majority of studies examining PHB synthesis in *E. coli* utilize recombinant strains (discussed later in this literature review). Therefore, use of the term *E. coli* implies a recombinant strain for the remainder of this thesis, unless otherwise stated.

A schematic of the basic chemical structure of a PHA molecule is shown in Figure 2.1. The carboxyl group of one monomer subunits forms an ester bond with the hydroxyl group of the adjacent monomer to create a polymer (Madison and Huisman 1999; Zinn et al. 2001). The degree of polymerization can range between 100 and 30,000, and thus *M* can range from 50 to 1000 kDa or higher (Zinn et al. 2001; Keshavarz and Roy 2010; Raza et al. 2018). As shown in Table 2.1, different side-chain radical groups give rise to different 3-hydroxy polyesters with a

[1] Although C-excess conditions are a requisite for PHA synthesis, multiple fed-batch studies (Sun et al. 2007a, 2009a; Maclean et al. 2008) have shown that if the growth rate is restricted by the feeding rate, a continual state of "carbon limitation" is created and this causes accumulation of mcl-PHAs concurrently to growth. These studies are summarized in Table 2.3, and further details are available in Section 2.7 of this literature review.

three-carbon backbone (n = 1). When the number of methyl groups in the carbon backbone is increased to two (n = 2) this gives rise to 4-hydroxy monomers. For the remainder of this thesis, abbreviations such as PHB, PHV, PHO, etc. (defined in Table 2.1) will refer to 3-hydroxy monomers, whereas 4-hydroxy monomers will be specifically referred to as P(4-HB), P(4-HV), and so on.

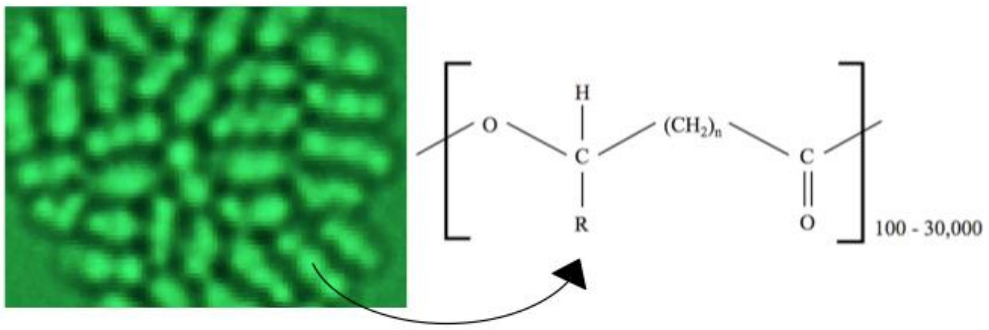

Figure 2.1. Occurrence of intracellular PHA granules with generic chemical structure.

Table 2.1. Nomenclature system for PHAs based on structure.

Carbon Backbone (n)	Side Chain Radical (R)	Name of PHA monomer	Abbreviation
n=1	hydrogen	poly(3-hydroxypropionate)	P(3-HP) or PHP
	methyl	poly(3-hydroxybutyrate)	P(3-HB) or PHB
	ethyl	poly(3-hydroxyvalerate)	P(3-HV) or PHV
	propyl	poly(3-hydroxyhexanoate)	P(3-HHx) or PHHx
	pentyl	poly(3-hydroxyoctanoate)	P(3-HO) or PHO
	hexyl	poly(3-hydroxynonanoate)	P(3-HN) or PHN
	heptyl	poly(3-hydroxydecanoate)	P(3-HD) or PHD
	nonyl	poly(3-hydroxydodecanoate)	P(3-HDD) or PHDD
	octyl	poly(3-hydroxytetradecanoate)	P(3-HTD) or PHTD
n=2	methyl	poly(4-hydroxybutyrate)	P(4-HB)
	propyl	poly(4-hydroxyvalerate)	P(4-HV)

2.4. PHAs: a promising alternative?

The advantages of using PHAs for biodegradable biopolymer applications may be several-fold. They have a unique attribute over other biodegradable polymers in that they are synthesized directly by bacteria, whereas many other bio-based polymers are synthesized chemically from biologically derived precursor molecules (de Jong et al. 2012). More than 150 blends of monomer subunits have been described giving different PHA polymers an extensive range of properties (Chen 2009; Akaraonye et al. 2010). These bio-polyesters have been shown to possess properties that are comparable with some conventional plastics (mostly polyethylene and polypropylene), and can thus be molded, extruded, spun into fibers and made into films (Khanna and Srivastava 2005a; Noda et al. 2010; Chanprateep 2010; Li et al. 2018). PHAs can be produced from a variety of (waste) renewable carbon sources, which create disposal challenges of their own due to high biochemical oxygen demand (Du et al. 2012; Nikodinovic-Runic et al. 2013; Cruz et al. 2016; Ravindran and Jaiswal 2016). As already mentioned, PHAs are completely biodegradable, and could reduce recalcitrant plastic waste in terrestrial, marine, and aquatic environments (Madison and Huisman 1999; Zheng et al. 2005; Iwata 2015).

Perhaps most importantly, life cycle analysis (LCA) studies have shown that PHAs can out-perform polyethylene, polypropylene and polystyrene in several major impact categories including CO_2 production, ecological footprint, and environmental toxicity (Harding et al. 2007; Shahzad et al. 2013; Dietrich et al. 2017). Harding et al. (2007) have shown that PHA out-performed polypropylene across ten major impact categories, and outperformed polyethylene in eight of these ten categories. Studies have reported that PHAs can reduce global warming potential and non-renewable energy consumption compared to petrochemical plastics (Akiyama et al. 2003; Gurieff and Lant 2007; Kendall 2012). However, multiple reports have indicated the

production of PHA required more fossil fuels than petrochemical plastics (Lynd and Wang 2003; Khoo and Tan 2010). The impact appears to be largely dependent on production context, and specifically the available carbon feedstock as well as the nature of the electricity source used during the production processes. Furthermore, the disposal method for biodegrdable packaging plays a significant role and must be considered (Dilkes-Hoffman et al. 2018). Despite mixed reports on LCA of PHAs, it is anticipated that as production technology evolves, life cycle analyses will increasingly favor PHAs (Koller et al. 2013; Yates and Barlow 2013).

2.5. Synthesis of short chain length (scl-) and medium chain length (mcl-) PHAs

Based on the length of the carbon chains of the monomer unit, two major groups of PHA have been established, and are hence identified as either short chain-length (scl-) or mcl-PHAs (already defined). Longer chain monomers have also been reported (Zinn et al. 2001), although little information is currently available. While most bacterial species synthesize either scl- or mcl-PHAs, some are capable of synthesizing co-polymers of both (Chen et al. 2001; Woo et al. 2012; Kourmentza et al. 2017; Lee et al. 2018). This section discusses the nature of both scl- and mcl-PHAs, and a brief overview of their general properties.

2.5.1. Short chain length (scl-) PHAs

The scl-PHAs have monomer subunits with chain lengths of 3-5 carbon atoms (C3-C5). When PHA was first identified by Lemoigne in 1926, it was as granules of PHB accumulated in *B. megaterium*. To date, PHB and copolymers of PHB with PHV (P(HB-co-HV) or PHBV) are the most commonly studied and best-characterized scl-PHAs (Khanna and Srivastava 2005a; Laycock et al. 2013). The scl-PHAs are synthesized by a wide variety of organisms, some of which reportedly accumulate up to 90% of their cell dry mass (CDM) as PHB (Janes et al. 1990;

Quillaguamán et al. 2008). PHB tends to be brittle, highly crystalline, and has a high melt point close to the thermal decomposition temperature, which limits its ability to be processed (Lee, 1996; Madison and Huisman, 1999). Copolymers of P(HB-co-HV) were first discovered from activated sludge samples from a treatment facility for grain-processing wastewater in Peoria, IL (Wallen and Rohwedder 1974). The addition of relatively small quantities of C5 monomers can have a significant impact on the thermal and mechanical properties of the polymer and increase its ability to be processed (Zinn et al. 2003; Salehizadeh and Van Loosdrecht 2004; Modi et al. 2011).

Synthesis of PHB occurs via a three-enzyme pathway in which acetyl-CoA is the precursor (Figure 2.2). Briefly, acetyl-CoA molecules (produced from the Entner-Doudoroff pathway, β-oxidation cycle, pentose phosphate pathway, or Embden-Meyerhof-Parnas pathway) are condensed into acetoacetyl-CoA via the enzyme β-ketothiolase. Acetoacetyl-CoA is then reduced to 3-hydroxybutyrl-CoA via acetoacetyl-CoA reductase and is subsequently polymerized into PHB via a PHA synthase (PhaC) enzyme (Sudesh et al. 2000). In this step, NADPH is used as the electron donor in most species, including *C. necator*, although an NADH-dependent acetoacetyl-CoA reductase has been observed but apparently does not play a role in PHB synthesis (Haywood et al. 1988; Shi et al. 1997; Budde et al. 2010). The only known NADH-dependent acetoacetyl-CoA reductase that is functional in PHB synthesis has been reported in *Allochromatium vinosum* (Liebergesell and Steinbüchel 1992; de las Heras et al. 2016). In *C. necator*, the NADPH consumed in the reduction of acetoacetyl-CoA to (R)-3-hydroxybutyryl-CoA may be regenerated to $NADP^+$ by: 1) the Entner-Doudoroff pathway via the enzyme glucose-6-phosphate dehydrogenase; 2) the TCA cycle via the enzyme iso-citrate dehydrogenase; 3) the malic enzyme; or 4) transhydrogenases, which catalyze inter-conversion

of NADPH to NADH, and allow NADH to be oxidized via electron transport (Grousseau et al. 2013). However, in *C. necator*, transhydrogenase activity is reportedly low although regions of the genome and subunits of the proteome been identified as putative transhydrogenase enzymes (Grousseau et al. 2013).

Incorporation of PHV subunits into the polymer relies on condensation of propionyl-CoA with acetyl-CoA. Propionyl-CoA may be produced from succinyl-CoA in the methylmalonyl-CoA pathway, activation of propionate with propionyl-CoA synthetase, or β-oxidation of odd-chain length fatty acids (Madison and Huisman 1999).

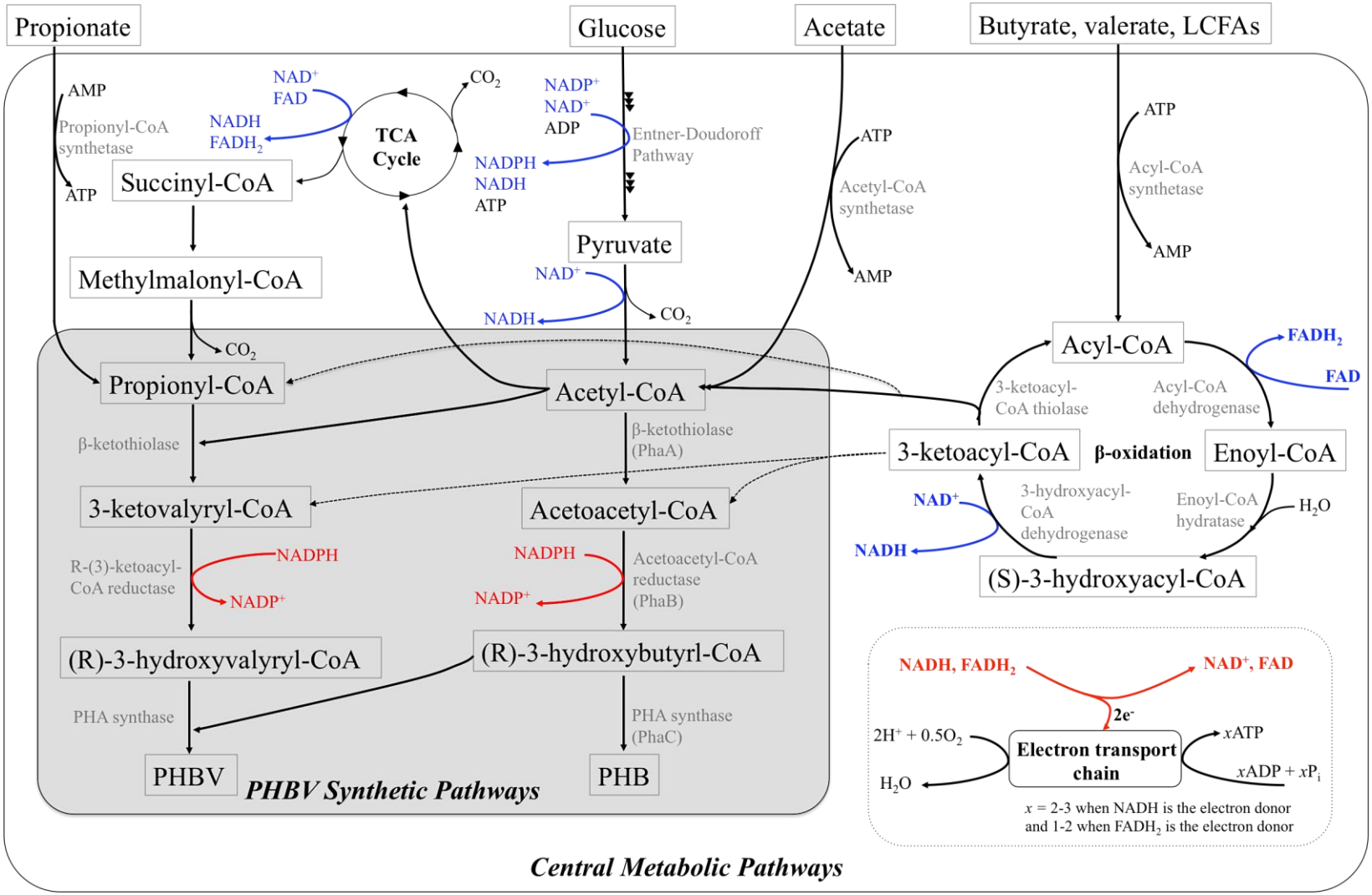

Figure 2.2. Pathway for synthesis of scl-PHA from glucose, VFAs, and LCFAs.

2.5.2. Medium chain length (mcl-) PHAs

The mcl-PHAs have monomer subunits ranging from 6-14 carbon atoms (C6-C14) (Huijberts et al. 1992). The mcl-PHAs tend to be elastomeric, with low crystallinity, low melting points, low tensile strength, and high elongation to break ratio (Akaraonye et al. 2010). Mcl-PHAs account for 95% of the more than 150 identified monomers (Chen 2009) and can contain double and triple bonds in the side chains, which are reactive and can be used to incorporate various chemical moieties to tailor the polymer to many potential applications (Kellerhals et al. 2000; Braunegg et al. 2004; Hartmann et al. 2006; Tortajada et al. 2013).

Mcl-PHAs are synthesized primarily by *Pseudomonas* sp. (Huisman et al. 1989; Prieto et al. 2016). The first observation of mcl-PHA was in *P. putida* GPo1, (formerly *P. oleovorans*) (de Smet et al. 1983). Other common mcl-PHA production strains include *P. putida* KT2440 and its rifampicin-resistant mutant *P. putida* KT2442, which have been well characterized and used in a diversity of applications, including bioremediation, desulfurization of petroleum feedstocks, and recombinant protein production (Prieto et al. 2016). *P. putida* KT2440 is a derivative of *P. putida* mt-2 (formerly *P. arvilla*) which was isolated from enriched soil samples in Osaka, Japan for its ability to degrade meta-toluates (Nakazawa 2002). *P. putida* KT2440 lacks the TOL plasmid encoding for a specific pathway for degradation of benzoates and toluates (Regenhardt et al. 2002). *Pseudomonas* sp. are promising biocatalysts for PHA production because of their metabolic versatility, rapid growth rates, high tolerance to extreme conditions, and natural PHA biosynthetic capability (Poblete-Castro et al. 2012a; Prieto et al. 2016).

Mcl-PHA is synthesized using two central metabolic pathways (Figure 2.3): 1) *de novo* fatty acid biosynthesis (also a reductive process that uses NADPH as the electron donor) from structurally-unrelated carbon substrates (glucose, glycerol, acetate); and 2) fatty acid β-oxidation

(an oxidative process that uses NAD^+ and FAD as the electron acceptors) for fatty acids and alkanes (Madison and Huisman 1999; Prieto et al. 2016). Although one pathway or the other is primarily used to synthesize mcl-PHA from a given substrate, studies have shown that both pathways can function simultaneously (Huijberts et al. 1994). It has been shown that mcl-PHA synthesis is regulated by ratios of both acetyl-CoA/CoA and $NADH/NAD^+$ (Bae and Rittmann 1996; Ren et al. 2009).

2.5.2.1. Production of mcl-PHAs by de novo synthesis (reductive synthesis)

Production of mcl-PHA from structurally unrelated carbon substrates (i.e. glucose, glycerol, acetate) relies on successive condensation of acetyl-CoA precursors into 3-hydroxyacyl-ACP monomers. Like the PHB biosynthetic pathway, the *de novo* pathway is a reductive process and consists of two reactions that use NADPH as the electron donor (Figure 2.3). The composition of mcl-PHA synthesized by the *de novo* pathway is not particularly dependent on the substrate (Eggink et al. 1992; Madison and Huisman 1999), and usually has monomer composition of primarily C10 followed by C8, and traces of C6, C12, C14, C12:1 and C14:1 have been reported (Huijberts et al. 1992; Eggink et al. 1992; de Waard et al. 1993).

Although glycerol and carbohydrate-based substrates are not generally associated with high intracellular PHA content *($\%_{PHA}$)* in native species (Lageveen et al. 1988; Haywood et al. 1990; Huijberts et al. 1992; Sharma et al. 2012; Fu et al. 2014), a few studies have obtained $\%_{PHA}$ as high as 67% CDM from glucose and 47% CDM from glycerol (Poblete-Castro et al. 2014b; Poblete-Castro et al. 2014a) using recombinant strains of *P. putida* KT2440. Another study obtained 63% CDM as mcl-PHA from glucose/fructose using *P. putida* IPT046 (Diniz et al. 2004).

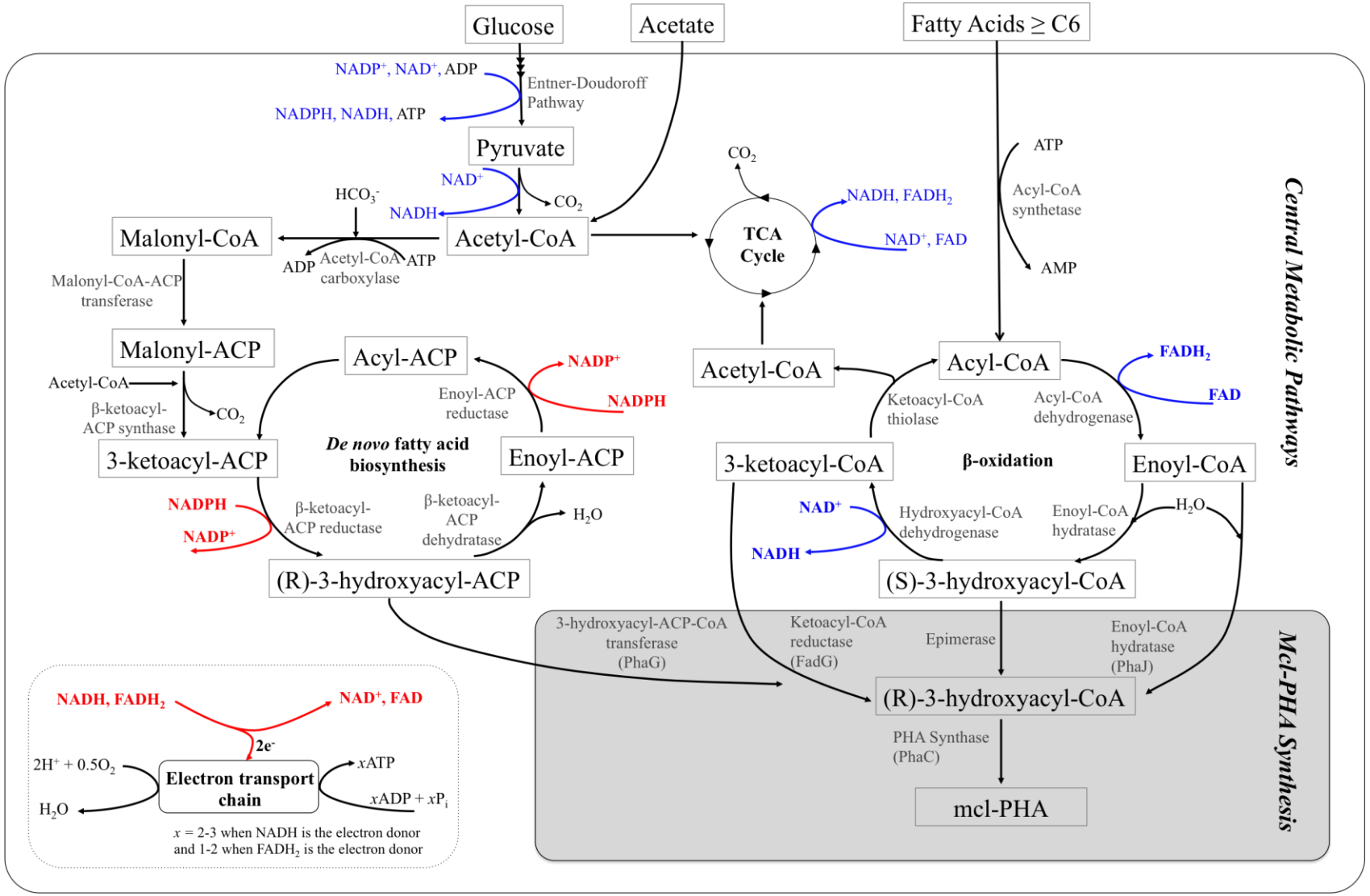

Figure 2.3. Pathways for synthesis of mcl-PHA from *de novo* synthesis and fatty acid β-oxidation.

2.5.2.2. Production of mcl-PHAs by β-oxidation (oxidative synthesis)

Synthesis of PHA from fatty acid β-oxidation (Figure 2.3) is a catabolic process in which intermediates of the cycle are incorporated into PHA. This was originally hypothesized by Lageveen et al. (1988) and subsequently confirmed in several NMR-based studies (Eggink et al. 1992; de Waard et al. 1993; Huijberts et al. 1994). It is widely accepted that enoyl-CoA, hydroxyacyl-CoA and 3-ketoacyl-CoA can all be converted to (R)-3-hydroxyacyl-CoA via the enzymes 1) trans-enoyl-CoA hydratase (PhaJ); 2) epimerase; and 3) R-specific ketoacyl-CoA reductase (FadG), respectively (Magdouli et al. 2015; Prieto et al. 2016). In contrast to synthesis of PHB or mcl-PHA by the *de novo* pathway, production of PHA from related substrates is an oxidative process, producing one $FADH_2$ from oxidation of acyl-CoA to enoyl-CoA. Depending which intermediate is incorporated by PhaC, NADH may also be produced from oxidation of (S)-3-hydroxyacyl-CoA to 3-ketoacyl-CoA. The polymer produced from β-oxidation intermediates is somewhat dependent on the chemical structure of the substrate, and thus different feeding strategies can be used to some extent to tailor the monomer composition of the polymer (Kellerhals et al. 2000; Hartmann et al. 2006; Sun et al. 2009a; Tripathi et al. 2013). However, for most fatty acids or alkanes (containing even-numbered carbon chain lengths) the dominant monomer subunits produced are C8 closely followed by C10 (Lageveen et al. 1988; Huisman et al. 1989; Eggink et al. 1992).

Fatty acids and alkanes are good substrates for mcl-PHA synthesis due to their high yield ($Y_{PHA/S}$), defined as PHA produced per substrate utilized on a mole or gram basis) (Weusthuis et al. 1997). Studies have obtained very high $Y_{PHA/S}$ of 0.86 g PHA g decanoic $acid^{-1}$ (Gao et al. 2016). Furthermore, storage capacity in native species appears to be quite high for such

structurally related carbon substrates, with $\%_{PHA}$ as high as 75% CDM (Jiang et al. 2013; Gao et al. 2016).

2.6. Fundamental bottlenecks for industrial PHA production

PHAs have been produced commercially since the 1980s and several companies continue to produce PHAs on scales approaching 50,000 tonnes per annum today, as shown in Table 2.2 (Dietrich et al. 2017; Kourmentza et al. 2017). As of 2013, global bio-based polymer production was only 5.1 million tonnes (Aeschelmann and Carus 2015) and represented at most 5% of the current global plastic market (Shahzad et al. 2013). While this number (of which PHAs represent an even smaller fraction) is a very small percentage of global plastic production, the global PHA market has shown rapid growth in recent years and is expected become a $100 million industry within the next three years (Dietrich et al. 2017; Kourmentza et al. 2017). However, expansion of the PHA industry to these levels (and beyond) requires significant process development inputs (Kaur and Roy 2015). The high production cost of PHAs has limited their application mostly to niche markets and significant cost reduction is needed to allow more broad application of PHAs (Możejko-Ciesielska and Kiewisz 2016). There are a number of factors that contribute to the cost of PHAs, for which estimates range from three to fifteen-fold higher than polyethylene or polypropylene (Możejko-Ciesielska and Kiewisz 2016; Kourmentza et al. 2017). The carbon source accounts for a large portion (most estimates are 40-50%) of PHA production costs (Salehizadeh and Van Loosdrecht 2004; Koller et al. 2017; Rodriguez-Perez et al. 2018). This is exacerbated by low yields, titers, and productivities (Kaur and Roy 2015). Increasing oil prices could reduce this gap, but the recent resurgence in oil production from exploitation of shale oil reserves means this is not a likely outcome in the near future (Chen 2012).

Table 2.2. Current commercial-scale PHA production operations.

Company (Country)	Trade Name	Product	Substrate	Strain	Capacity (tonnes/year)
Biomer (Germany)	Biomer™	PHB pellets	Sucrose	*A. lata*	1,000
Bio-On Srl. (Italy)	Minerv®	PHB and PHBV spheres	Sugar beet sucrose	*C. necator*	10,000
Danimer Scientific (USA)	Seluma™	PHB-co-PHHx	Canola oil	Soil bacteria	15,000
ETH (Switzerland)	?	Mcl-PHA	Fatty acids	*P. putida*	?
Metabolix (USA)	BioPol	P(3-HB-co-4-HB)	Glucose	*C. necator*	50,000
PHB Industrial S.A. (Brazil)	Biocycle®	PHB, PHBV	Sucrose	*Bacillus* sp.,	3,000
Polyferm (Canada)	VersaMer™	mcl-PHA	Sugars, fatty acids	*P. putida*	?
P&G (USA)/ Jiangmen Biotech (China)	Nodax®	PHB-co-PHHx	Glucose/lauric acid	*Aeromonas hydrophila*	?
P&G (USA)/ Kaneka Corporation (Japan)	Nodax®	PHB-co-PHHx	Fatty acids	*C. necator*	3,500
Shenzen Ecomann Biotech Co. Ltd. (China)	AmBio®	PHA pellets, resins, microbeads	Corn starch	?	5,000
TianAn Biologic Materials Co. Ltd. (China)	Enmat™	PHB and PHBV	Glucose and propionate	*C. necator*	10,000
TianJin Green Biomaterials Co. (China)	Sogreen®	P(3-HB-co-4-HB) films, pellets, foams	Glucose and 1,4-butanediol	Recombinant *E. coli*	10,000

Sources: Dietrich et al. (2017), Kourmentza et al. (2017), Mozejko-Ciecielska and Kiewicz (2016), Levett et al. (2016).

Since carbon and energy must be channeled to biosynthetic production of non-PHA residual biomass (X_r, consisting of proteins, membranes, nucleic acids), maintenance of viable cells, and respiration, the yield of PHA from the carbon susbtrate ($Y_{PHA/S}$) is always less than the theoretical maximum (i.e. that which could be achieved assuming the growth, maintenance, and respiration requirements were nil). A common goal of fed batch studies (discussed below) is to use inexpensive substrates (i.e. biodiesel waste glycerol) for growth while supplying higher quality substrates (usually mcl-fatty acids, which are generally high-yielding) only for PHA synthesis (Kim et al. 1997; Sun et al. 2009a; Jiang et al. 2013; Cerrone et al. 2014b; Davis et al. 2015). Experimental $Y_{PHA/S}$ of mcl-PHA from fatty acids have been reported as high as 0.6-0.9 g g^{-1} (Cerrone et al. 2014b; Gao et al. 2016)[2]. By comparison, the $Y_{PHA/S}$ of PHB from a variety of carbohydrate-based substrates, short-chain alcohols, VFAs can be 0.2-0.5 g g^{-1} (Ackermann and Babel 1998; Salehizadeh and Van Loosdrecht 2004). Wang et al. (2014) report that in general, experimental $Y_{PHA/S}$ values of about 0.33 g g^{-1} are typical, which is roughly one third of what is obtained in the chemical industry. Because of the inefficiency of carbon conversion, much recent focus has been given to identifying inexpensive and readily available carbon substrates for PHA synthesis (Du et al. 2012; Nikodinovic-Runic et al. 2013; Fu et al. 2014; Jiang et al. 2016; Koller et al. 2017; Gillis et al. 2017; Rodriguez-Perez et al. 2018). As pointed out by Wang et al. (2014) other bottlenecks that limit commercial production of PHAs include variation in properties of the product, difficulty in processing, as well as a lack of demonstrated high-value applications.

[2] With regard to reported $Y_{PHA/S}$ values, it is important to distinguish if the value considers carbon required for growth or just the mcl-PHA synthesis phase. As important indicated in the footnotes at the bottom of Tables 2.3 and 2.4, this distinction isn't always made clear. In many cases, the language and terminology used around this difference can be subject to interpretation by the reader, and often needs to be more explicitly stated.

2.7. Fed batch processes for improved PHA productivity

In addition to using low-cost carbon feedstock, efficient cultivation techniques aimed at obtaining high rates, yields, and product titers are crucial factors for commercial viability of PHAs (Kaur and Roy 2015; Koller et al. 2017). The objective of this section of the literature review is to summarize previous research on novel bioreactor configurations for improving PHA productivity. These include fed-batch, cyclic or repeated processes (i.e. semi-continuous), and fully continuous bioreactor systems. In addition, where possible, we also examine the degree to which these technologies have been scaled up to pilot or industrial levels. Although the primary focus of this section is given to mcl-PHAs, the literature on scl-PHAs is often referred to as a useful point of reference. In addition to the terms X_r, $\%_{PHA}$, and $Y_{PHA/S}$, which have already been defined, additional terms used throughout this section are defined here, including: total biomass concentration, [X_t] (g L^{-1}); PHA biomass concentration, [X_{PHA}] (g L^{-1}); and volumetric productivity, Q_v (g L^{-1} h^{-1}).

The objective of applying fed-batch cultivation to PHA production is to combine HCD cultures with high $\%_{PHA}$ of the biomass to maximize overall Q_v. Fed-batch cultures are usually started in batch mode, and the culture is fed with growth nutrients (carbon, ammonium, etc.) to prolong exponential-phase growth at a high rate and maximize cell density as quickly as possible (Ienczak et al. 2013). To date, HCD fed-batch cultures have demonstrated the highest Q_v in both scl- and mcl-PHA production (Wang and Lee 1997b; Maclean et al. 2008) and are also used in most industrial production settings (Koller and Muhr 2014).

Obtaining high $\%_{PHA}$ is also an important factor for high Q_v, and improving ease of downstream processing (Choi and Lee 1999). For most production strains in which PHA synthesis is not growth-associated, the growth phase is followed by continued carbon feeding in

the absence of another nutrient, often NH_4^+ or PO_4^{3-}, to promote high $\%_{PHA}$ at the time of harvest. The cultivation process is usually divided into a growth phase and a PHA storage phase. These are separated temporally but occur in the same vessel, although this is not always the case. Previous studies have shown that mcl-PHA can be produced from nonanoic acid concurrently to growth when the carbon uptake rate is limited by the feeding rate (Sun et al. 2007a; Sun et al. 2009a). Other studies have employed organisms that are known to accumulate PHA simultaneous to growth, like *A. lata* or recombinant strains of *E. coli*, and do not require nutrient limitation (Yamane et al. 1996; Wang and Lee 1997a; Wang and Lee 1997b). However, for the general case where growth and PHA synthesis occur in separate phases, fed-batch cultivations can also be used to improve the $Y_{PHA/S}$ for a given substrate. This is usually done by supplying a lower-cost carbon source (often glucose) for cell production during the growth phase, with subsequent feeding using substrates that allow higher $Y_{PHA/S}$, but may be more expensive (Kim et al. 1997; Sun et al. 2009a; Cerrone et al. 2014b; Davis et al. 2015; Gao et al. 2016). However, as noted in footnote 2 (see bottom of p. 22) as well as footnotes for Tables 2.3 and 2.4, this can lead to confusion over interpretation of reported $Y_{PHA/S}$ values, and should thus be used cautiously.

Several high-productivity fed batch cultivations are shown in Table 2.3 for mcl-PHA and Table 2.4 for scl-PHA studies using pure cultures. Most of the mcl-PHA studies have used relatively expensive medium chain length fatty acids to obtain $\%_{PHA}$ as high as 76% CDM (Jiang et al. 2013), Q_v as high as 2.13 g L^{-1} h^{-1} (Maclean et al. 2008), and $Y_{PHA/S}$ as high as 0.86-0.93 g g^{-1} (Gao et al. 2016). In the latter study, the reported yield refers only to mcl-PHA accumulated from decanoic acid (although it is not clear if this includes the growth phase as well). In that case, decanoic acid was co-fed with glucose and acetic acid (mass ratio of 5:1:4) and presumably acetic acid and glucose satisfied a large portion of the growth and maintenance requirements.

Despite some promising results shown in Table 2.3 for fed-batch mcl-PHA cultivations, comparison with Table 2.4 shows that, in general, the Q_v of mcl-PHA cultivations is low in comparison to scl-PHA production processes. Ryu et al. (1997) report achieving [X_t] of more than 280 g L^{-1} CDM with [X_{PHA}] of more than 230 g L^{-1} ($\%_{PHA}$ = 83% CDM) using *C. necator* grown on glucose. While these are the highest known experimental values for X_t and X_{PHA}, Wang and Lee (1997b) report the highest Q_v (5.13 g L^{-1} h^{-1}) using *A. lata* cultured on sucrose. By comparison, Maclean et al. (2008) have reported the highest mcl-PHA Q_v from inoculation to harvest at 2.13 g L^{-1} h^{-1}. As shown in Table 2.3, the [X_t] seldom exceeds 100 g L^{-1} in mcl-PHA cultivations, and only one study has reported [X_{PHA}] of more than 70 g L^{-1} (Lee et al. 2000b)

Table 2.3. High-productivity fed-batch cultivation processes in mcl-PHA research.

Ref	Organism	Substrate; limitation	$[X_t]$ (g L^{-1})	$\%_{PHA}$ (% CDM)	$Y_{PHA/S}$ (g g^{-1})	Q_v (g L^{-1} h^{-1})	C_L*	Contribution
(Preusting et al. 1993b)	*P. putida* GPo1	Octane; N-limited	37.1	33	-	0.25	Air	First HCD process in two-liquid phase media
(Hazenberg and Witholt 1997)	*P. putida* GPo1	Octane; N-limited	40	26	-	0.34	?	Economic evaluation of mcl-PHA production systems
(Kim et al. 1997)	*P. putida* BM01	OA + glc; N, O_2-limited	35.9	65.6	0.4	0.92	Air	Enhanced $Y_{PHA/OA}$ by co-feeding glucose
(Dufresne and Samain 1998)	*P. putida* GPo1	OA	47	55	0.31	0.54	Air	Studied granule morphology *in vivo* during fed-batch cultivation
(Kellerhals et al. 1999b)	*P. putida* KT2442	OA; N-limited	51.5	17.4	-	0.41[a]	$+O_2$	Closed-loop fed-batch control strategies based on online GC-measurements
(Kellerhals et al. 1999a)	*P. oleovorans*	Octane; O_2-limited	112	5	-	0.09	$+O_2$	Highest $[X_t]$ from octane, but found to be inversely proportional to $\%_{PHA}$
(Lee et al. 2000b)	*P. putida* KT2442	Oleic acid; P-limited	141	51.4	-	1.91	$+O_2$	Highest known $[X_t]$ and highest Q_v from oleic acid
(Kim 2002)	*P. putida* GPo1	OA; N-limited	63	62	-	1	Air	Highest $\%_{PHA}$ (75% CDM) did not correspond to max. Q_v
(Diniz et al. 2004)	*P. putida* IPT046	Glc + fructose; P-limited	50	63	0.19[b]	0.8	Air	Highest Q_v, $\%_{PHA}$ from glucose in a native strain
(Sun et al. 2007a)	*P. putida* KT2440	NA; C-limited	56	67	0.6[b]	1.44	$+O_2$	Mcl-PHA accumulation under C-limitation
(Maclean et al. 2008)	*P. putida* KT2440	NA; C-limited	109	63	-	2.13	$+O_2$	Highest Q_v yet reported for mcl-PHAs
(Shang et al. 2008)	*P. putida* KT2440	Corn oil LCFAs, P-limited	103	28.5	-	0.61	$+O_2$	High Q_v from mixed LCFA substrate
(Sun et al. 2009b)	*P. putida* KT2440	NA + UDA; C-limited	48.1	55.8	0.5[c]	1.09	$+O_2$	Control of PHA monomers through feeding

Table 2.3. *(con't)*

(Sun et al. 2009a)	*P. putida* KT2440	Glc + NA; C-limited	71	56	0.66[b]	1.44	$+O_2$	Improved $Y_{PHA/NA}$ by co-feeding glucose
(Jiang et al. 2013)	*P. putida* KT2440	Glc + NA; C-limited	71.4	75.5	0.78[c]	1.8	$+O_2$	Used acrylic acid as a β-oxidation inhibitor to obtain elevated C9 content
(Cerrone et al. 2014b)	*P. putida* CA-3	Butyric acid + DA; P-limited	90	65	0.61[b]	1.63	Air	First use of VFA feedstock, highest Q_v without the use of enriched air
(Davis et al. 2015)	*P. putida* KT2440	Glc + NA; no limitation	102	32	0.56[b]	0.95[d]	Air	Highest $[X_t]$ without enriched air
(Poblete-Castro et al. 2014b)	Recombinant *P. putida* Δgcd	Glc; C-limited	61.8	67	-	0.83	$+O_2$	Highest $\%_{PHA}$, Q_v from glucose
(Gao et al. 2016)	*P. putida* KT2440	DA, acetic acid, glc (5:1:4); C-limited	75	74	0.86[c]	1.16	$+O_2$	Highest $Y_{PHA/S}$ in mcl-PHA production
(Andin et al. 2017)	*P. putida* KT2440	Oleic acid (80%); N-limited	125.6	54.4	0.7[e]	1.01	0.3 bar	Improved $Y_{PHA/S}$ coupled to anabolism

[a]final Q_v reported at 42.75 h, whereas maximum Q_v reported as 1.18 g L^{-1} h^{-1} at 23 h; [b]$Y_{PHA/S}$ accounts for polymer storage phase only; [c]unclear if $Y_{PHA/S}$ considers total cultivation or storage phase only; [d]Q_v of 2.85 g L^{-1} h^{-1} reported only during 11 h PHA accumulation phase when supplied with nonanoic acid. Factoring in the 21 h growth phase results in a Q_v of 0.95 g L^{-1} h^{-1}; [e]$Y_{PHA/S}$ reported yield on a C-mol C-mol^{-1} basis. Abbreviations: C_L^* - equilibrium oxygen concentration, which may be enhanced using O_2-enriched air ($+O_2$) or elevated pressure (specified in bar or mbar); OA – octanoic acid; glc – glucose; NA – nonanoic acid; DA – decanoic acid; UDA – undecenoic acid; LCFAs – long chain fatty acids. The question mark indicates where it was not explicitly stated if aeration was done with atmospheric air or purified O_2. The dash in the $Y_{PHA/S}$ column indicates where values were not reported. Note: *P. putida* GPo1 formerly known as *P. oleovorans* (strain ATCC 29347).

Table 2.4. High-productivity fed-batch cultivations processes in scl-PHA research.

Ref	Organism; (product[a])	Substrate; conditions	$[X_t]$ (g L^{-1} CDM)	$\%_{PHA}$ (% CDM)	$Y_{PHA/S}$ (g g^{-1})	Q_v (g L^{-1} h^{-1})	C_L^*	*Contribution*
(Suzuki et al. 1986)	*Methylobacterium extorquens*	MeOH; N-limited	233	64	0.2	0.88	$+O_2$	Highest $\%_{PHA}$ obtained using a methylotroph
(Kim et al. 1992)	*E. coli* XL1-Blue	Glc; O_2-limited	116.6	76	-	2.11	$+O_2$	First HCD fed batch using recombinant *E. coli* for PHB production
(Kim et al. 1994)	*C. necator* NCIMB 11599	Glc; N-limited	164	76	0.3	2.42	Air	Timing of N-limitation and maintaining a residual [glc] of 10-20 g L^{-1} important
(Kim et al. 1996)	*Methylobacterium organophilum*	MeOH; K-limited	250	52	0.19	1.86	$+O_2$	Highest $[X_t]$ obtained using a methylotroph
(Bourque et al. 1995)	*M. extorquens* ATCC 55366	MeOH; N-limited	114	46	0.22[b]	0.56	Air	Highest $[X_t]$, Q_v from a methylotroph without using purified O_2
(Yamane et al. 1996)	*A. lata* DSM 1123	Sucrose; none	142	50	-	3.97	$+O_2$	First HCD process using *A. lata*; Highest Q_v without nutrient limitation
(Ryu et al. 1997)	*C. necator* NCIMB 11599	Glc; P-limited	281	83	0.38	3.14	?	Highest $[X_t]$ obtained in a fed-batch system for PHA production
(Wang and Lee 1997b)	*A. lata* DSM 1123	Sucrose; N-limited	111.7	88	0.42	4.94[c]	$+O_2$	Highest Q_v reported in PHA production
(Wang and Lee 1997a)	*E. coli* XL1-Blue	Glc; O_2-limited	204.3	77	0.28	3.2	$+O_2$	Highest $[X_t]$ obtained using *E. coli*
(Choi et al. 1998)	*E. coli* XL1-Blue	Glc; not stated	194.1	73	-	4.63	?	Highest Q_v reported using *E. coli*
(Wang and Lee 1998)	*E. coli* XL1-Blue	Glc; not stated	149	70	-	2.4	$+O_2$	
(Wong and Lee 1998)	*E. coli* CGSC 6576	Whey; not stated	87	80	0.33	1.4	$+O_2$	First use of a waste industrial substrate for PHB production using *E. coli*.

Table 2.4. *(con't)*

(Lee et al. 2000a)	*A. hydrophila;* PHB-co-PHHx	Oleic acid; P-limited	95.7	45	0.51[d]	1.01	$+O_2$	First HCD process for PHB-co-PHHx production
(Shang et al. 2003a)	*C. necator* NCIMB 11599	Glc; P-limited	208	67	-	3.1	$+O_2$	Maintaining residual glc at 9 g L^{-1} gave highest $Q_{v,\,PHB}$
(Quillaguamán et al. 2008)	*Halomonas boliviensis* LC1	MSG; N-limited	23	90	-	1.15	Air	Demonstrated *H. boliviensis* viable for HCD production of PHB
(Cavalheiro et al. 2009)	*C. necator* DSM 529	Crude glycerol, N-limited	76	50	0.34	1.1	$+O_2$	Demonstrated high $Q_{v,\,PHB}$ obtained using crude glycerol
(Ibrahim and Steinbüchel 2009)	*Zorbellella denitrificans* MW1	Glycerol; 20 g L^{-1} NaCl	81.2	67	0.25	1.09	Air	Highest known $Y_{PHB/S}$ using crude glycerol as the sole carbon source
(Chanprateep et al. 2010)	*C. necator A-04*; P(3-HB-co-4-HB)	Fructose + BDO; C/N ratio of 4 then 200	112	64	-	0.76	Air	Highest obtained [X_t] in P(3-HB-co-4-HB) production
(Pradella et al. 2010)	*Burkholderia sacchari* IPT 189	Sucrose; N, O_2 limited	150	42	0.22	1.7	?	Utilized an airlift bioreactor (instead of STR) for HCD production of PHB
(Pradella et al. 2012)	*C. necator* DSM 545	Soybean oil; N, P, metals limiting	83	80	0.85	2.5	?	Highest Q_v obtained from edible oils as the sole carbon source.
(Riedel et al. 2012)	Recombinant *C. necator*; PHB-co-PHHx	Palm oil; N-limited	139	74	0.78[b]	1.07	$+O_2$	Amongst the highest [X_t] and Q_v for production of PHB-co-PHHx using recombinant *C. necator*
(Grousseau et al. 2013)	*C. necator* DSM 545	Butyric acid; P-limited	46.7	82	0.62[e]	0.57	75 mbar	Highest [X_t], $\%_{PHA}$, and Qv for *C. necator* grown on butyric acid and favorable impact of coupling residual growth and PHB synthesis on Q_v

Table 2.4. *(con't)*

(Kanjanachumpol et al. 2013)	*B. megaterium* BA-019	Sugarcane molasses; C/N = 10	73	43	-	1.73	Air	Highest obtained Q_v for PHB production using *B. megaterium*
(Cesário et al. 2014)	*B. sacchari* DSM 17165	WSH; P-limited	146	72	0.22	1.6	Air	Highest Q_v from a waste agricultural residue
(Kachrimanidou et al. 2014)	*C. necator* DSM 7237; PHBV	Crude glycerol and SMH; C/N = 17.05	27.9	74.5	0.34	0.27	Air	Among the highest $\%_{PHBV}$ and $[X_{PHBV}]$ produced using levulinic acid as the precursor
(Mozumder et al. 2014)	*C. necator* DSM 545	Glc; N-limited	128	76	0.24	2.03	$+O_2$	Developed fed-batch control strategy independent of the carbon source
(Huschner et al. 2015)	*C. necator* H16; PHBV	Mixed VFAs; N-limited	112.4	83	-	2.13	$+O_2$	Highest $[X_t]$, Q_v in production of PHBV
(Thinagaran and Sudesh 2017)	*C. necator* Re2058/pCB113; PHB-co-PHHx	SPO; N-limited	88.3	57	0.5	1.1	Air	Demonstrated efficacy of SPO as a substrate for high-Qv production of PHB-co-PHHx
(Miranda De Sousa Dias et al. 2017)	*B. sacchari* DSM 17165; P(3-HB-co-4-HB)	Saccharose + GBL; N-limited	74.6	72	0.08	1.87	Air	Highest known Q_v for the product P(3-HB-co-4HB)

[a]Product is PHB unless otherwise specified; [b]$Y_{PHA/S}$ values reported only for polymer synthesis phase. All other values reported appear to be total yields obtained over the entire duration of the fermentation, although this is rarely made explicit and subject to interpretation. [c]Q_v values reported at time of harvest (20 h), highest Q_v of 5.13 g L^{-1} h^{-1} observed at 16 h; [d] $Y_{PHA/S}$ corrected to exclude residual oleic acid adhering to internal surfaces of bioreactor (0.26 g g^{-1} obtained without correction; [e]$Y_{PHA/S}$ reported as C-mol C-mol^{-1}. Abbreviations: GBL - γ-butyrolactone, BDO – 1,4 butanediol; MeOH – methanol; WSH – wheat straw hydrolysate; SMH – sunflower meal hydrolysate; SPO – sludge palm oil; C/N – carbon-to-nitrogen ratio.

Interestingly, the number of studies targeting cultivation strategies for achieving the highest possible Q_v appeared to peak in the mid-1990s for scl-PHAs, and perhaps 10-15 years later for mcl-PHAs. While these studies are valuable tools for understanding process engineering design and limitations, they are hindered by a few key impracticalities. These include use of high-purity carbon substrates, O_2-enriched air for aeration, are generally limited to lab-scale bioreactors. More recently, there appears to have been somewhat of a shift toward PHA production from waste substrates like crude glycerol (Cavalheiro et al. 2009; Kachrimanidou et al. 2014), plant-based oils (Shang et al. 2008; Riedel et al. 2012; Pradella et al. 2012; Andin et al. 2017; Thinagaran and Sudesh 2017), and lignocellulose-based hydrolysates (Cesário et al. 2014), and strategies to achieve HCD cultures without use of purified O_2 streams (Cerrone et al. 2014b; Davis et al. 2015; Miranda De Sousa Dias et al. 2017).

2.7.1. Control of fed-batch cultivations

A significant challenge in fed-batch cultivation is predicting the nutritional requirements of the culture in real-time so that an appropriate feeding strategy can be implemented. Direct and rapid measurement of the parameters of interest (i.e. $[X_t]$, $\%_{PHA}$, residual concentrations of carbon, NH_4, PO_4^{3-}, Mg^{2+}, etc.) is often not possible, or the existing methods require expensive analytical equipment with a considerable time delay (Lee et al. 1999; Riesenberg and Guthke 1999; Harms et al. 2002). Nonetheless, some studies have used online or rapid offline measurements of residual carbon levels using analytical techniques such as gas chromatography (GC) (Kim et al. 1996; Kellerhals et al. 1999b), high-performance liquid chromatography (HPLC) (Quillaguamán et al. 2008; Ibrahim and Steinbüchel 2009), and mass spectrometry (MS) (Kim et al. 1992). Others have made use of online glucose analyzers (Kim et al. 1994; Kim et al. 1997; Ryu et al. 1997; Shang et al. 2003a; Sun et al. 2006).

Most often, feeding rates are predicted indirectly using other parameters that can be rapidly and reliably measured using standard bioreactor equipment. Some of the more popular methods involve off-gas CO_2 measurements (Suzuki et al. 1986; Sun et al. 2006; Follonier et al. 2015; Andin et al. 2017), DO measurements (Wang and Lee 1997b; Kellerhals et al. 2000; Shang et al. 2008; Poblete-Castro et al. 2014b), pH measurements, (Yamane et al. 1996; Wang and Lee 1997a), optical density (Lee et al. 2000a; Lee et al. 2000b), and combinations thereof (Lee et al. 2000a; Lee et al. 2000b; Huschner et al. 2015). In general with these approaches, carbon-limitation results in reduced oxygen demand, which manifests itself as a large drop in CO_2 production, reduced agitation rates, and a rise in the DO signal. A rise in pH may also be detected with exhaustion of the carbon source, assuming a negligible impact on pH from production of acetate, amino acids, and the nitrogen source (Kim 2002). With these methods, the carbon source is often fed pulse-wise upon detection of a limitation in order to bring the concentration back up to the desired level (Wang and Lee 1997a; Wang and Lee 1997b; Wang and Lee 1998; Lee et al. 2000a; Riedel et al. 2012; Pradella et al. 2012; Cesário et al. 2014; Możejko and Ciesielski 2014; Thinagaran and Sudesh 2017). There is evidence to suggest the method of carbon addition can influence PHA synthesis. One study showed a significant increase in $\%_{PHA}$ (from a maximum of 25% CDM to 44% CDM) in *Pseudomonas* sp. G101 when the carbon source (waste canola oil) was fed to the bioreactor by a pulse-feed strategy in comparison to a continuous drip-feed addition of an equivalent aliquot of waste canola oil (Możejko and Ciesielski 2014). These results may suggest that short feast-famine cycling favors mcl-PHA storage in cultures of *Pseudomonas* sp.

Alternatively, a more proactive strategy may be applied in which the culture is fed to maintain a predetermined (typically exponential) growth rate (μ). This method has been quite

successful in several studies, achieving [X_t] nearing 100 g L^{-1} CDM for growth of *Pseudomonas* sp. on both fatty acid and carbohydrate-based carbon sources (Maclean et al. 2008; Cerrone et al. 2014b; Davis et al. 2015). Typically, these models require the initial [X_t], the change in μ over time, as well as establishing constant (Jiang et al. 2013), linear (Davis et al. 2015; Gao et al. 2016), or decaying (Dufresne and Samain 1998; Maclean et al. 2008) feeding rates during the PHA accumulation phase. According to Maclean et al. (2008), sudden decreases in feeding rates result in cell lysis and foaming, so it is important to make the transition between different stages of feeding smoothly. Several feeding strategies have been investigated and are shown in Table 2.5.

Significant efforts have gone into developing various models that allow the culture to grow as quickly as possible at the start of the process, before curbing the feeding rate to match the transient carbon uptake rate as the culture transitions to PHA storage. Sun et al. (2007a) have shown that controlling μ via the rate of carbon addition allows higher [X_t] to be obtained before the process is terminated due to inadequate oxygen mass transfer. Lower μ brings a trade-off in biomass productivity, but some studies have suggested carbon-limitation causes PHA accumulation concurrently to growth without the need to limit another nutrient (Sun et al. 2007a; Maclean et al. 2008; Sun et al. 2009a). The onset of oxygen limitation inevitably limits Q_v in HCD cultivations for PHA production and causes uncontrollable foaming and accumulation of the carbon source to potentially toxic levels (depending on the feeding strategy) (Lee 1996; Lee et al. 2000b; Kellerhals et al. 2000; Sun et al. 2007a; Sun et al. 2009a; Cerrone et al. 2014b).

Table 2.5. Exponential fed-batch strategies applied in mcl-PHA research.

Study	Feeding Strategy	Results
(Maclean et al. 2008)	Exponential feeding of NA: 1) From 0-9 h starting at μ=0.25 h^{-1} followed by linearly-decaying feeding rate over the next 21 h 2) Quadratic decay in feeding rate (5-15 h) with initial μ=0.45 h^{-1} followed by a constant feed rate (8.75 g NA $L^{-1}h^{-1}$)	1) [X_t] = 90 g L^{-1} CDM with 65% PHA 30 h, Q_v = 1.9 g L^{-1} h^{-1} in 30 h. 2) [X_t] = 109 g L^{-1} CDM with 63% PHA in 30 h, Q_v = 2.13 g L^{-1} h^{-1}
(Gao et al. 2016)	Exponential feeding (mixture of DA and acetic acid) at μ=0.15 h^{-1} for 23 h followed by constant feeding rate of 5 g substrate L^{-1} h^{-1} until 40 h	[X_t] = 75 g L^{-1} CDM containing 74% PHA in 40 h, Q_v = 1.16 g L^{-1} h^{-1}
(Davis et al. 2015)	Exponential feeding of glc: 1) At constant μ of 0.25 h^{-1} until DO limitation 2) At μ_{max} (0.67 h^{-1}) for 0-9 h followed by constant feeding when DO became limiting 3) At μ_{max} (0.67 h^{-1}) for 0-9 h followed by a linearly increasing feed rate when DO became limiting	1) [X_t] = 53 g L^{-1} CDM in 22 h. Ended by DO limitation causing glucose accumulation 2) [X_t] = 43 g L^{-1} CDM in 18 h. No DO limitation but C limitation slowed growth 3. 102 g L^{-1} CDM in 33 h, limited by DO
(Elbahloul and Steinbüchel 2009)	1) Cells allowed to grow for 4-5 h, pH adjusted with NH_4OH 2) At 6-7 h, 0.5 mM Amm-OA and 0.05 mM $MgSO_4$ were fed per hour for 5 successive hours then feeding exponentially increased to 5 mM Amm-OA and 0.5 mM $MgSO_4$ per hour for 5 h, 3) 1.8 mM Amm-OA and 0.27 mM $MgSO_4$ were added per hour	[X_t] = 53 g L^{-1} CDM containing 50% PHA obtained in 48 h, Q_v = 0.76 g $L^{-1}h^{-1}$
(Poblete-Castro et al. 2014b)	Phase 1: batch operation until 12 h when 20 g L^{-1} glc initially consumed Phase 2: exponential feeding with μ=0.2 h^{-1} until 21 h (50 g L^{-1} CDM), DO limitation causes glc accumulation Phase 3: glc fed in response to DO rise above set point to maintain a residual concentration of 30-35 g L^{-1}	[X_t] = 61.8 g L^{-1} CDM containing 67% PHA in 50 h for a Q_v of 0.83 g L^{-1} h^{-1}

Abbreviations: Amm-OA – ammonium octanoate.

2.7.2. Scale-up of fed-batch PHA production processes

According to Choi and Lee (1999), increasing scale can significantly decrease costs (both operating and capital costs) for production capacities up to 15,000 tonnes PHA per annum. Scale-up presents many challenges, which can be biological, chemical, or physical in nature, and some of these are discussed below. As already discussed for lab scale fed-batch operations in PHA production, O_2 mass transfer limitations are problematic. In conventional bioreactor design, these occur in the vertical direction since feeding is done from the top and aeration from the bottom (Bylund et al. 1998; Enfors et al. 2001; Lara et al. 2006a). Significant hydrostatic pressure can also influence solubility near the bottom of large reactors (Schmidt 2005), and these factors also complicate measurement of important process variables because the measurement can be highly dependent on the location of the probes (Byrom 1992). Such gradients in the physical and chemical environment are the primary reason large-scale bioreactors often do not behave the same as bench-scale, and in the case of O_2-limitation, usually results in rearrangement of flux through central carbon metabolism (Zimmermann et al. 2006). This is more thoroughly discussed in Section 2.8.

There are many criteria that can be used to scale-up an aerobic bioprocess, including similar geometry, constant impeller tip speed, constant Reynolds number, constant k_La, circulation time, or constant power input (either gassed or un-gassed) per unit reactor volume (Junker 2004). Ultimately, these criteria are simply different ways of measuring energy requirement, which almost inevitably ends up being the limiting factor in scale-up. According to Lara et al. (2006a), circulation time-based scale-up from 80 L to 1000 L would result in a 25-fold increase in power dissipation per unit volume. This is further demonstrated in Table 2.6, which shows mixing power costs for a variety of bioreactor volumes. This data was obtained from a

survey (of actual bioreactors setups operating at maximum oxygen transfer capacity) conducted by Junker (2004). The additional calculations assume that 40% of the electrical energy is lost in the lipseals, bearings, and motor of the stirrer (Asciano et al. 2004), and current Manitoba Hydro electricity rates[3]. As shown, the mixing cost at the 30 L scale is about four times that of the 1000 L scale, and more than ten times that of the 1000 L scale. With respect to large-scale bioreactors, maintaining the same degree of energy dissipation as the smaller bioreactors (throughout the entire liquid phase) for a well-mixed, homogeneous environment becomes cost prohibitive and impractical (Oldshue 1997). Whereas well-mixed lab scale bioreactors dissipate 10-20 kW m^{-3}, large-scale bioreactors dissipate only 0.5 to 5 kW m^{-3} (Doran 2013), and generally have reduced overall mass transfer capability (Byrom 1992; Lara et al. 2006a; Garcia-Ochoa et al. 2010).

The combined effects of friction from vigorous mixing and generation of metabolic heat can also require significant cooling capcity, particularly in HCD cultures. A relatively recent study showed that for a facility producing 100,000 tonnes/year PHB using mesophilic cultures, cooling costs could be as much as 28% of the total operating costs (Levett et al. 2016). This assumed that a refrigerant would be required to prevent the need to extensive and intricate heat exchange surfaces required if water were used as the coolant. The study also assumed use of airlift bioreactors, which generally have lower shear forces, and may generate less heat than a mechanically agitated bioreactor.

[3] Electricity rates obtained as \$0.0672 kW-h^{-1} for small general service up to 11,000 kW-h, obtained May 19, 2018 from https://www.hydro.mb.ca/accounts_and_services/rates/commercial_rates/#e-sgs

Table 2.6. Operating costs for mixing and aeration in 30 to 19000 L bioreactors.

Total Volume (TV)	**Working Volume (WV)**	**Max. Agitation, N_a**	**Max. Airflow rate, $\dot{V}_a$**	**Installed power**	**Gassed power at $N_{a,\,max}$**	**Cost per 24 h operation**
L	L	rpm	LPM	kW	kW/1000 L	$ CDN/1000L
30	20	875	30	1.34	56.86	152.80
100	75	400	120	4.02	34.87	93.70
280	180	460	300	10.06	25.21	67.75
800	600	330	600	10.06	16.09	43.25
1000	750	300	1200	13.41	14.89	40.00
1200	900	282	1200	20.12	13.95	37.48
1900	1500	230	1500	20.12	11.53	30.99
19000	15000	155	15000	80.46	4.96	13.33

Adapted from Junker (2004) with permission**.** Abbreviations: rpm – revolutions per minute; LPM – liters per minute

In the literature reviewed so far, the majority of the focus in PHA research has been on strategies to improve productivity in lab-scale bioreactors, typically with working volumes of 5 L or less. Studies that have investigated some aspect of scale-up comparatively few, but are shown in Table 2.7. This thesis considers 'scale-up' as volumes of at least 100 L, but if the bioreactor size is set a lower limit to 30-50 L, Table 2.7 would include a number of additional studies (Wang and Lee 1997a; Ryu et al. 1997; Kellerhals et al. 2000; Nath et al. 2008; Shang et al. 2008; Ibrahim and Steinbüchel 2009).

As indicated in Table 2.7, a few studies have achieved scl-PHA productivities of 1 g L^{-1} h^{-1} or higher at scales of up to 300 L (with a 100-150 L working volume) (Park et al. 2002; Choi

et al. 2002), whereas up to 0.75 g L^{-1} h^{-1} has been demonstrated for mcl-PHA production at a similar scale (Elbahloul and Steinbüchel 2009). These productivities are less than half many of the reported Q_v values summarized in Tables 2.3 and 2.4 for mcl- and scl-PHA research, respectively. A large part of this discrepancy may be due to use of purified O_2 as the aeration medium in the bench-scale studies, which can increase the driving force for oxygen transfer nearly five-fold (Doran 2013). However, this can be a challenge to implement, and can also add significant fixed and operating costs to PHA production (Choi and Lee 1999; Lopes et al. 2014).

A recent study performed a k_La-based scale up and obtained a Q_v of 1.66 g L^{-1} h^{-1} (of the product P(3-HB-co-4-HB) in a 5,000 L bioreactor, which is perhaps the most promising pilot-scale result in PHA production to date (Ye et al. 2018). Interestingly, in that same study the Q_v obtained at 5,000 L was slightly higher than that achieved at the 1,000 L scale and significantly better than the result achieved at lab-scale (7.5 L, see Table 2.4). However, in this study the estimated k_La in both the 1,000 L and 5,000 L bioreactors was similar, and surprisingly, significantly better than the 7.5 L bioreactor.

Table 2.7. Research on scale-up to at least a 100 L for various PHA production processes.

Ref	Organism, Product	Conditions	WV (TV)	$[X_t]$	$\%_{PHA}$	$Y_{PHA/S}$	Q_v	C_L^*
			(L)	(g L^{-1})	(% CDM)	(g g^{-1})	(g L^{-1} h^{-1})	
(Chen et al. 2001)	*A. hydrophila* 4AK4, PHB-co-HHx	Glc during growth and lauric acid during P-limited accumulation phase.	10,000 (20,000)	50	50	-	0.54	Air
(Gorenflo et al. 2001)	*P. putida* GPp104, P(3-HB-co-3-HV-co-4-HV)	DO-stat feeding of gluconic acid during growth, with levulinic acid during N-limited accumulation phase	500 (650)	19.7	50	-	-	Air
			25[a]	25	50	-	-	Air
(Choi et al. 2002)	Recombinant *E. coli*, PHBV	pH-stat feeding of glc + oleic acid + propionic acid. k_La = 108 h^{-1} in 300 L bioreactor and k_La = 396 h^{-1} in 30 L bioreactor.	100 (300)	29.6	69	-	1.06	Air
			10 (30)	42.2	70.1	-	1.37	Air
(Park et al. 2002)	Recombinant *E. coli* CGSC 4401, PHB	Whey solution containing 200 g L^{-1} lactose fed via pH-stat method	150 (300)	30	67	-	1.01	Air
			10 (30)	51	70	-	1.35	Air
(Shang et al. 2003b)	*C. necator* NCIMB 11599, PHB	Glc controlled at 9 g L^{-1} with online glc analyzer	300[a]	23.4	36	-	0.18	Air
			30[a]	49.2	45	-	1.09	Air
			5[a]	96.4	58	-	1.03	Air
(Elbahloul and Steinbüchel 2009)	*P. putida* GPo1 mcl-PHA	Exponential followed by constant feeding of OA with N-limited conditions	350-400 (650)	53	50	0.41	0.76	Air
(Zhu et al. 2009)	*Burkholderia cepacia* ATCC 17759, PHB	Biodiesel waste glycerol concentration maintained at 10-40 g L^{-1} with N-limitation	200 (400)	23.6	31	-	0.06	Air

Table 2.7 *(con't)*

(Heinrich et al. 2012)	*C. necator* H16, PHB	Gluconate with N limitation	400 (650)	24.2	65.2	-	0.23	Air
(Kshirsagar et al. 2012)	*Halomonas campisalis* MCMB-1027, PHB	Batch cultivations using maltose with O_2 limitation after 12 h (1-5%). Scale up based on constant k_La of 14.2-18.4 h^{-1}	85 (120)	1.3	49.2	0.06	0.03	0.5 bar
			8 (14)	1.7	56.2	0.09	0.04	0.5 bar
(Follonier et al. 2015)	*P. putida* KT2440, mcl-PHA	Batch growth on grape pomace with subsequent N-limited polymer accumulation on OA and UDA	100 (300)	14.2	41.1	0.79[b]	0.1	Air
(Ye et al. 2018)	*Halomonas bluephagenesis* TD40, P(3-HB-co-4-HB)	Glucose, GBL, waste CSL fed with PHA synthesis triggered by N limitation. Scale up based on similar reactor geometry and k_La	3,500 (5,000)	99.6	60	-	1.66	Air
			700 (1,000)	89.5	64	-	1.58	Air
			4 (7.5)	81.4	74	-	1.25	Air

[a]not indicated if volume referred to WV or TV; [b]$Y_{PHA/S}$ values include only fatty acids (OA, UDA) fed during the polymers storage phase. Abbreviations not already defined: CSL - corn steep liquor.

A study from 2003 evaluated growth and PHB synthesis from *C. necator* using air compared to purified O_2 as the aeration medium in 5 L and 30 L bioreactors, as well as a 300 L bioreactor where air was the sole aeration medium (Shang et al. 2003b) Although the focus of that study was the effects of CO_2 inhibition arising from poor liquid-to-gas mass transfer at lower gas flow rates (used to minimize use of purified O_2), the study presents a useful comparison to help de-convolute the effects of increasing the driving force for oxygen transfer by gassing the reactor with pure O_2. The use of pure O_2 instead of atmospheric air caused [X_t] to more than double (from 96 to 208 g L^{-1}) in the 5 L bioreactor, and more than triple (from 49 to 186 g L^{-1}) in the 30 L bioreactor. Furthermore Q_v displayed a two-fold increase from approximately 1 to 3 g L^{-1} h^{-1} in both the 5 L and 30 L bioreactors. Interestingly, the PHB content was elevated when pure O_2 was used at both the 5 L and 30 L scale. This is somewhat unexpected since PHB is known to be synthesized from glucose in low-DO environments (Senior et al. 1972; Du et al. 2000; Berezina 2013). Oxygen limitation became very prevalent at the 300 L scale, which achieved two-fold less biomass than the 30 L, and four-fold less than the 5 L when air was used as the sole aeration medium.

It is worthwhile mentioning that Shang et al. (2003b) concluded that there was a significant effect of CO_2-inhibition on both growth and PHA synthesis in *C. necator*. Another study evaluated the effect of elevated CO_2 concentrations in a pressurized bioreactor system, and concluded that dissolved CO_2 concentrations of up to 540 mg L^{-1} did not negatively affect mcl-PHA synthesis, but did result in a decreased μ in cultures of *P. putida* KT2440 (Follonier et al. 2012). Both of these studies suggest that buildup of CO_2 from liquid-to-gas mass transfer limitations also merit consideration during process scale-up since they have been shown to negatively impact both growth and PHA synthesis.

2.8. Oxygen transfer limitations in aerobic bioprocesses

Gas-to-liquid mass transfer limitations are frequently encountered in aerobic bioprocesses primarily because of the solubility of oxygen in aqueous medium and poor gas-to-liquid transfer efficiency. Since oxygen mass transfer limitations inevitably affect Q_v in high-cell density fed batch operations in PHA production, this section is devoted to a brief review of mass transfer theory, as well as application to scale-up of PHA production processes.

2.8.1. Mass transfer theory

Due to its simplicity and visual representation, a popular model for gas to liquid mass transfer is (stagnant) film theory (Whitman 1962). The concept of two-film theory (applied in the context of diffusion of O_2 from a gas bubble into an aqueous medium) is shown in Figure 2.4, in which C_L^* is the equilibrium O_2 concentration, $C_{L,interface}$ is the O_2 concentration at the gas-liquid interface, C_L is the DO concentration in the bulk liquid phase, and δ_g and δ_l are the thickness of the gas and liquid film layers, respectively. This model requires several key assumptions that limit its applicability. These include: 1) steady state conditions (i.e. no reaction so the flux across the gas-phase film is equal to the flux across the liquid-phase film); 2) zero velocity and linear concentration profiles throughout the stagnant film; 3) equilibrium is achieved instantaneously and therefore resistance to mass transfer at the gas-liquid interface is negligible; 4) transport by bulk diffusion is not rate limiting; and 5) the solution is dilute, and therefore Henry's law may be applied; 6) the gas-liquid interface is a sharp boundary.

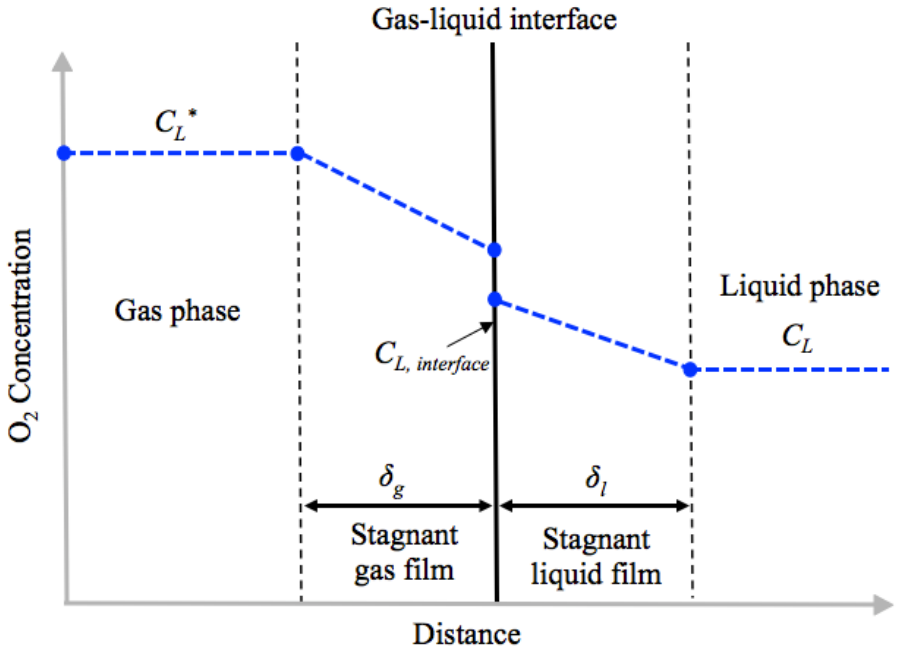

Figure 2.4. Two-dimensional graphical representation of two-film theory.

Fick's first law describes an analytical representation of mass transport between two arbitrary points (1 and 2) along in the x-direction. This relates flux of a component to the concentration gradient as shown in Equation 2.1. It should be noted that this is for the case of a linear concentration gradient in the stagnant film.

$$J_{i,x} = -\mathcal{D}\frac{dC_i}{dx} = -\mathcal{D}\frac{C_{i,2}-C_{i,1}}{x_2-x_1} = -\frac{\mathcal{D}_{i,x}}{\delta_s}\left(C_{i,2}-C_{i,1}\right) = k_{L,i}\left(C_{i,2}-C_{i,1}\right) \qquad \text{Equation 2.1}$$

where $J_{i,x}$ is the mass (or molar) flux of a component i along a particular plane (g m^{-2} s^{-1} or mol m^{-2} s^{-1}), $\mathcal{D}$ is the diffusivity of i in the medium (m^2 s^{-1}), C_i is the concentration of component i, δ_s is the film thickness of the stagnant layer (m), and $k_{L,i}$ is the liquid film mass transfer coefficient. The negative sign is a convention implying that the net flux of i is down the concentration gradient.

As previously mentioned, this model has some inherent limitations. Most notably, the film is in fact not stagnant, and the velocity profile only reaches zero immediately adjacent to the

interface. Therefore, the concentration profile is not linear (Gapes 2002). Other theories have been proposed to address these limitations by using more realistic models of the hydrodynamic conditions encountered at the interface. The most common models include penetration theory (Higbie 1935) and surface renewal theory (Danckwertz 1951), amongst others. Further details are available elsewhere (Gapes 2002; Garcia-Ochoa and Gomez 2009). Extension of these theorems to real biological systems is often not possible due to complicated geometries of gas bubbles and liquid-solid interfaces, as well as the onset of turbulent hydrodynamic conditions at the interfaces. A number of empirical correlations have been proposed that allow description of mass transfer under turbulent fluid flows using the dimensionless parameters like the Reynolds or Sherwood numbers (Garcia-Ochoa and Gomez 2009).

2.8.2. Gas-to-liquid oxygen mass transfer in submerged biological systems

In a three-phase system containing gas bubbles, an aqueous medium, and a solid (biomass) phase, the mass transfer process is more complex than depicted in Figure 2.4. For aerobic bioprocesses, O_2 must be transported from the gas bubble to the reaction site (oxidative phosphorylation) within a cell. This consists of several individual mass transfer processes, which are shown in Figure 2.5. Each mass transfer process has its own transfer resistance (Table 2.8), but generally it is thought that the main resistance (i.e. the rate determining step) for the case of dispersed cells in a well-mixed bioreactor is diffusion through the relatively stagnant gas-liquid boundary layer. As described in Table 2.8, other mass transfer processes can also contribute significant resistance depending on the conditions.

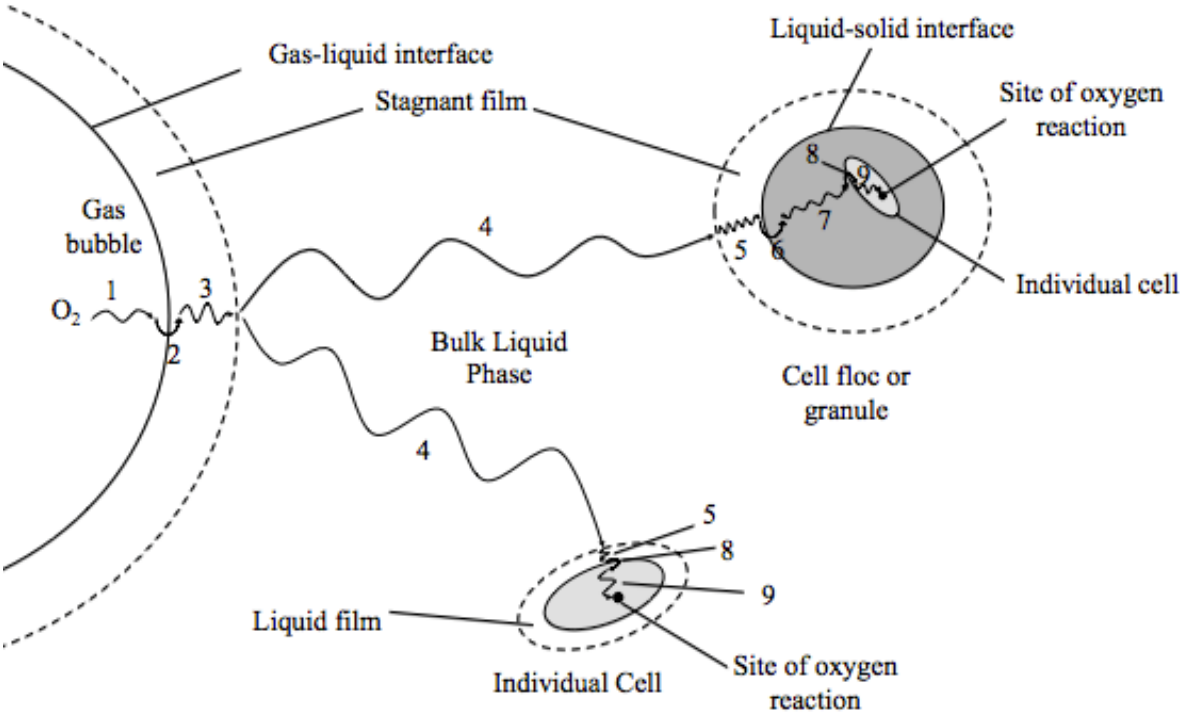

Figure 2.5. Mass transport of oxygen from a gas bubble to the cell. Refer to Table 2.8 for description of the individual (numbered) transport steps. Adapted from Doran (2013) with permission.

Table 2.8. Diffusion of an oxygen molecule from the gas bubble to the site of the biological reaction.

Transport Step (Figure 2.5)	Description	Assumptions/conditions
1	Transport through the bulk gas to the gas-liquid interface.	This step occurs relatively rapidly.
2	Transport across the gas-liquid interface	Resistance at the gas-liquid interface is negligible.
3	Transport through the relatively stagnant boundary layer surrounding the gas bubble	This step is, generally, the major resistance to oxygen transfer.
4	Transport through the bulk liquid	In a well-mixed bioreactor the concentration is assumed to be homogenous. However, in large-scale bioreactors or viscous medium, concentration gradients may develop.
5	Transport through the relatively stagnant boundary layer surrounding the biomass (cell or floc)	Stagnant film surrounding cells much thinner than that surrounding gas bubbles. However, for large flocs, the contribution to resistance may be significant.
6	Transport through the liquid-biomass interface (in the case of a floc)	Resistance at the liquid-cell interface is considered negligible.
7	Transport through the floc to the surface of the cell	Resistance to diffusion of oxygen through a solid medium (cell floc) likely significant.
8	Transport across the cell membrane or wall	Resistance at the liquid-cell interface is considered negligible.
9	Transport through the cytoplasm to the reaction site.	Intracellular resistance is negligible due to the small distance.

Sources: Garcia-Ochoa and Gomez (2010) and Doran (2013).

Multiplying Equation 2.1 by the interfacial liquid-gas area per unit volume, *a*, (i.e. assuming the main resistance to mass transfer is the gas-liquid boundary layer surrounding the gas bubbles), gives the volumetric mass transfer rate of O_2 to the liquid phase (N_{O2}, in units of mol s^{-1} or g s^{-1}).

$$J_{i,x}\, a = N_{O2} = k_L a(C_L^* - C_L) \qquad \text{Equation 2.2}$$

In Equation 2.2, the term (C_L^* - C_L) is the DO concentration gradient between two points, which is the potential or driving force for mass transfer. This is the difference between the O_2 partial pressure in the gas bubble and the average concentration in the bulk liquid phase. The primary reason that O_2 mass transfer is a bottleneck is aerobic bioprocesses is the low solubility of O_2 in aqueous medium, which is related to C_L*. At equilibrium with atmospheric conditions and 25 °C (O_2 partial pressure = 0.2095 atm), the solubility of O_2 in pure water is about 8 mg L^{-1} (Sander 1999). Gas solubility in aqueous solutions decreases with the presence of electrolytes in what has been termed a "salting-out" effect (Schumpe 1993). The change in solubility of an electrolyte solution (i.e. microbial culture medium) can be approximated using empirical constants that are specific to the gas and the individual ions in solution using the Sechenov relation (Schumpe et al. 1982; Schumpe 1993; Weisenberger and Schumpe 1996). The presence of organic molecules also generally decrease the solubility of gases in liquid culture medium, with the exception of a few short chain alcohols (Rischbieter et al. 1996). Vendruscolo et al. (2012) investigated changes to O_2 solubility over the time course of *Monascus ruber* cultivation in a mineral-salts medium with glucose and glycine as the carbon source. In that study, the O_2 solubility of the medium itself was determined to be 6.77 mg L^{-1}. Within the first 24 h of cultivation, the O_2 solubility decreased to 6.39 mg L^{-1}, but then by 72 h it had increased to 7.74 mg L^{-1}. Surprisingly, this value was close to that measured in distilled water (7.67 mg L^{-1}).

The O_2 mass transfer rate is also proportional to the liquid film mass transfer coefficient (k_L, i.e. distance time^{-1}), and the interfacial area between the gas and the liquid (a). Predicting experimental values for either k_L or a is difficult. Such predictions are impacted by medium composition, rheological properties, bioreactor design, and hydrodynamic conditions (Garcia-Ochoa and Gomez 2009). Analytical determination of k_L is often not possible under realistic conditions encountered in a biological system, so these terms are usually lumped together and determined experimentally as the volumetric oxygen mass transfer coefficient k_La. A number of studies have proposed dimensionless empirical correlations for k_La under specific conditions that take into account the type of bioreactor, operating regime, and rheological properties of the fluid. Garcia-Ochoa and Gomez (2009) have reviewed these correlations and further details can be found there. Most often, k_La is determined experimentally using several methods, with the dynamic out-gassing method being the most common. Further details on methods for k_La determination are available elsewhere (Garcia-Ochoa and Gomez 2009; Garcia-Ochoa et al. 2010; Doran 2013), and the approach followed in this work is described in Chapter 3.

If k_La is known, the oxygen uptake rate (OUR) of the culture can be estimated from the rate of change of DO with respect to time.

$$\frac{dC_{O_2}}{dt} = OTR - OUR = k_La(C_L^* - C_L) - OUR \qquad \text{Equation 2.3}$$

Assuming no buildup of oxygen in the liquid phase (i.e. steady state conditions) the OUR can be assumed to be equal to the OTR, which can be written as shown in Equation 2.4 (Pratt et al. 2003).

$$OUR \approx OTR = k_La(C_L^* - C_L) \qquad \text{Equation 2.4}$$

2.8.3. Strategies for overcoming oxygen transfer limitations in PHA production

With the onset of oxygen limitation being problematic in strictly aerobic bioprocesses, many studies have focused on enhancing the OTR to achieve faster growth rates, higher cell densities, and ultimately higher productivity. Implicit from Equation 2.4 is that several approaches may be taken to do this, including manipulation of C_L^*, a, or k_L.

In PHA production, all fed-batch studies use very high stirring rates to enhance the oxygen transfer rate by increasing both the tortuosity of the path taken by the bubble and the residence time of the bubble in the liquid phase (gas hold up, which can be measured as the total liquid volume that is occupied by gas). While this increases k_L, stirring also helps to break up larger bubbles into smaller bubbles to increase a. This requires a significant input of mechanical energy to the bioreactor, and is frequently used in conjunction with other techniques. Many studies also increase the driving force for oxygen transfer by increasing C_L^*. This has included use of an aeration medium with enriched O_2 content (see Tables 2.3, 2.4, and 2.7) as well as pressurization of the bioreactor headspace (Follonier et al. 2012). Interestingly, while pressurization does increase C_L^*, it has also been shown to have a detrimental impact on k_La (Lopes et al. 2013). Other approaches involve increasing the interfacial area for mass transfer using micro-bubbler devices (Inan et al. 2016). Although not used in a PHA production context, another study applied a microfluidic device to generate bubbles with an average diameter of around 110 μm, and obtained nearly ideal mass transfer (i.e. 90% of the oxygen in the gas phase was delivered to the liquid phase), which is a promising development for industrial (aerobic) biotechnology in general (Baker et al. 2016).

Other approaches have focused on modifying the medium through the addition of a second phase (liquid or solid) that effectively increases the solubility of oxygen in the medium.

Magnetic functionalized nanoparticles have been used to increase the oxygen transfer coefficient (both k_L and a) in bioreactors (Olle et al. 2006). However, no reports could be found on use of functionalized nanoparticles being applied to improve PHA productivities. Two-liquid phase systems (in which small quantities of certain immiscible liquids are dispersed into the aqueous medium) reportedly can significantly improve OTR (Dumont and Delmas 2003; Dumont et al. 2006; Gomes et al. 2007; Kundu et al. 2008). A few studies have investigated two-liquid phase bioreactor systems in PHA production (Preusting et al. 1993b; Kellerhals et al. 1999a) but in those cases *n*-octane served as the carbon source, and its effect on OTR was not reported. Interestingly, soybean oil (which along with other plant-based oils are high-yielding PHA substrates) has been found to significantly improve k_La when dispersed in aqueous medium (Rols and Goma 1991; Jia et al. 1999).

In summary, maintaining adequate DO in HCD cultures is a significant challenge for commercial-scale PHA production. As discussed in this section, this is due to a combination of the low solubility of O_2 in aqueous medium and poor gas-to-liquid mass transfer of O_2. Although a number of techniques, some of which appear quite promising, may be applied to delay the onset of O_2-limited conditions and achieve higher cell densities and increased productivities, there are drawbacks to many of these techniques. In addition to cost, a drawback of purified O_2 is it can undergo partial reduction to create toxic reactive oxygen species (Lopes et al. 2014). Bioreactor pressurization may be a more attractive alternative, but requires specialized equipment and also makes feeding less straightforward due to the need for bioreactor addition ports and fittings that are compatible with pressure. Use of microbubble devices can significantly improve gas-to-liquid mass transfer but can also require high-energy input (Li et al. 2016) and be prone to fouling (Liu et al. 2012). Even the high mechanical energy required for vigorous

agitation and aeration accounts for a large portion of the environmental impact, and cost, of PHA production (Akiyama et al. 2003; Koller et al. 2013). Because of these challenges, the ability to synthesize PHAs in low-DO environments is desirable and important to consider when screening and/or genetically engineering potential PHA-producing strains (Chen 2009; Wang et al. 2014). The following sections examine the available literature for the effect(s) of O_2-limited PHA synthesis.

2.9. The role of oxygen-limited environments in PHA production

As stated earlier, synthesis of PHAs (which can be an oxidative or reductive process) is relatively expensive for their putative uses as biodegradable replacements for polyethylene or polypropylene. Cost reduction can be achieved (partially) by increasing the productivity at the bioreactor level on a large scale (Dietrich et al. 2017). It is widely accepted that the best way to do this is through fed-batch cultivations, in which cultures are rapidly grown to HCDs (Ienczak et al. 2013). These cultures have very high oxygen demand, and therefore the DO is an important factor for maximizing Q_v. In many cases, insufficient OTR has limited high productivity PHA processes (Lee et al. 2000b; Maclean et al. 2008; Cerrone et al. 2014b; Gao et al. 2016). These studies have increased the OTR by improving k_La through high-intensity mixing and aeration. Others have also increased the driving force (C_L^*-C_L) by increasing C_L^* through use of purified O_2 (Lee et al. 2000b; Maclean et al. 2008; Gao et al. 2016) or reactor pressurization (Follonier et al. 2012). While such techniques have certainly improved PHA productivities in bench-scale systems, they are often impractical to scale up to improve the inherently poor mass transfer characteristics of large-scale bioreactors (Byrom 1992). The overall energy requirement for aeration and high-intensity mixing in PHA production contributes significantly to its high cost and environmental impact (Koller et al. 2013). It is therefore important to understand how low

OTR and DO impact PHA production, since these conditions are likely to be encountered during scale up of aerobic bioprocesses (Lara et al. 2006a; Garcia-Ochoa et al. 2010). Since nutritional imbalance is generally needed to promote PHA synthesis, limiting O_2 rather than N, P, or another nutrient, would be expected not only to promote PHA synthesis but also reduce power input to the bioreactor. Given that low DO environments are likely to persist in large-scale bioreactors, anticipating these effects could be a valuable point of reference for trouble-shooting process scale-up. This can be done through study of physiology under fluctuating conditions simulated in scaled-down systems (Junker 2004; Lara et al. 2006a).

The role of O_2 limitation in scl-PHA production using pure cultures has been relatively well studied, and has also attracted recent attention using mixed microbial cultures (MMCs), as will be discussed in the following sections. However, very little information is available on how synthesis of mcl-PHA is affected by low DO environments. This section summarizes past research regarding the effect of low DO environments on PHA synthesis characteristics from carbohydrates, VFAs, and long-chain fatty acids (LCFAs) in both pure cultures and MMCs. The objectives of this review are to understand the mechanisms for PHA synthesis in low DO environments and identify gaps in the literature, particularly for mcl-PHAs, in order to facilitate efficient management of OTR during process scale-up. Specific focus is given to key performance metrics including $\%_{PHA}$, $Y_{PHA/S}$, and the specific productivity, Qs (g PHA g Xr^{-1} h^{-1}). Although perhaps not as important in this context, other metrics that are often referred to are [X_{PHA}] and Q_v. Polymer characteristics discussions focus on monomer composition, M, melting temperature (T_m), glass transition temperature (T_g), and tensile properties, where information is available.

2.9.1. Synthesis of scl-PHA under O_2-limtation

2.9.1.1. scl-PHA synthesis from carbohydrates

Several studies throughout the 1970s extensively examined PHB synthesis from glucose at low DOC using *Azotobacter beijerinckii*. While little PHB was accumulated in N- or C-limited chemostat cultures, significantly improved PHB synthesis (up to 50% of CDM) under O_2-limited conditions was observed with DO below detectable limits (Senior et al. 1972). It was proposed that the reductive step of PHB synthesis (Figure 2.2) is a sink for electrons, allowing ATP synthesis via substrate-level phosphorylation to proceed during O_2 limitation (Senior and Dawes 1971; Senior et al. 1972). In addition, intracellular levels of NADH, NADPH, and ATP were linked to repression of enzymes of the Entner-Doudoroff pathway (glucose 6-phosphate dehydrogenase), TCA cycle (citrate synthase, iso-citrate dehydrogenase), and PHB degradation (β-3-hydroxybutyrate dehydrogenase), while the intracellular concentration of PHB biosynthetic enzymes (β-ketothiolase and acetoacetyl-CoA reductase) decreased upon relaxation of O_2 limitation (Senior and Dawes 1971; Senior and Dawes 1973; Jackson and Dawes 1976). Much of the early work in this area was completed using *Azotobacter* sp., in which PHB synthesis is complicated by the demand for reducing power for N_2-fixation (particularly at low DO) and can cause lower PHA contents in an N-limited medium (Ward et al. 1977; Pozo et al. 2002).

In other species (*C. necator*, *Pseudomonas* sp., recombinant *E. coli*), subsequent studies have confirmed the role of NADH/NAD^+, NADPH/$NADP^+$, and acetyl-CoA/CoA ratios in promoting PHA synthesis (Lee et al. 1995; Bae and Rittmann 1996; van Wegen et al. 2001; Ren et al. 2009), as well as their effect on enzymes associated with glucose metabolism and the TCA cycle (Mitchell and Dawes 1982). A summary of other works that have examined PHB synthesis from carbohydrate-based substrates at low DO is shown in Table 2.9. While mixed results have

been reported, these studies generally indicate that PHB synthesis can be initiated by limiting DO to 5% or less (expressed as a percent of saturation with atmospheric air at 30 °C throughout this review, unless stated otherwise)[4], and support that PHB synthesis is a sink for electrons at low DO.

[4] Most studies choose to express DO concentration as a percent of saturation, as stated. However, depending on the composition of the medium, presence of carbon substrates, biological macromolecules, anti-foam agents, temperature, pressure, etc., the actual concentration (expressed in mg L^{-1} or mmol L^{-1}) can vary. Vendruscolo et al. (2012) determined the solubility of O_2 in pure water (at 30 °C and with O_2 partial pressure of 0.20946 atm) to be 7.68 mg L^{-1}. In a mineral-salts medium, the O_2 soubility was determined to be 6.77 mg L^{-1}. Since most PHA-based studies perform a DO calibration in a saturated bioreactor (at 30 °C) prior to inoculuation, we assume that 5% of air saturation would be a DO concentration of approximately 0.34 mg L^{-1}.

Table 2.9. The impact of oxygen limitation when producing scl-PHA from carbohydrate-based carbon substrates using pure cultures.

Study	Organism, substrate	Conditions	Key Results
(Ahn et al. 2000)	Recombinant *E. coli*, lactose	6.6 L pH-stat fed batch BR with 1.3 L initial WV, $N_a \leq 1000$	Step-wise decrease from 40 to 15% DO during accumulation phase resulted in highest $\%_{PHA}$ (81% CDM), [X_{PHA}] (96.2 g L^{-1}) and Q_v (2.6 g L^{-1} h^{-1})
(de Almeida et al. 2010)	Recombinant *E. coli*, glc or glycerol	5.6 L BR with 3 L WV, N_a = 125 or 500, $\dot{V}_a$ = 3 LPM	At the lower OTR, $\%_{PHA}$ from glycerol-grown cultures increased from 16.9 to 30.1% CDM but decreased from 37.2 to 20.4 % CDM in glc grown cultures at lower OTR
(Berezina 2013)	*C. necator*, glc/ glutamate	Flasks with either 200 mL or 300 mL headspace volumes	Increased $\%_{PHA}$ increased (~50% to 70% CDM) as the headspace volume was reduced from 300 mL to 200 mL
(Castillo et al. 2013)	*A. vinelandii*, glc	500 mL flasks without baffles (100 mL WV) and with baffles (50 mL WV), N_a = 200, DO measured with optical sensors	DO reached nearly zero values in both conditions, but only for a brief period at the higher OTR, $Y_{PHA/S}$ increased from 0 to 0.21 C-mol C-mol^{-1} at lower OTR
(Díaz-Barrera et al. 2016)	*A. vinelandii*, sucrose	3 L batch BR with 2 L WV, N_a = 300-600, $\dot{V}_a$ = 2 LPM, DO below detectable limits	In wild type *A. vinelandii*, highest $\%_{PHA}$ (84% CDM) achieved at N_a = 300, OTR = 6-16 mmol O_2 L^{-1} h^{-1}
(Du et al. 2000)	*C. necator*, glc	Fed batch BR with 0-5% DO (12-40 h), N_a = 600, $\dot{V}_a$ = 1.2 VVM	0-5% DO increased $\%_{PHA}$ to 45.3% CDM and doubled Q_s compared to non-limiting conditions, but less effective than N limitation
(Faccin et al. 2013)	*B. megaterium*, sucrose	5 L batch BR with 4 L WV, N_a = 100-600, $\dot{V}_a$ = 4 LPM (k_La = 7-133 h^{-1}), DO dropped to 0% in all conditions	Highest $\%_{PHA}$ (62% CDM) and $Y_{PHA/S}$ (0.21 g g^{-1}) at second-to-lowest OTR tested ($k_La \leq 22$ h^{-1}) which compared well to flask results. Highest Q_v (0.017 g L^{-1} h^{-1}) at moderate OTRs
(García-Torreiro et al. 2016)	*H. boliviensis*, glc/MSG	2 L fed batch BR with1 L WV, N_a = 400-650, $\dot{V}_a$ = 1-5 LPM (max. k_La of 168 h^{-1})	Obtained 37% and 45% PHB using O_2 and N limitation, respectively. N limitation at low OTR gave 73% PHB with highest $Y_{PHA/S}$ (0.37 mol%) and Q_v (1.32 g L^{-1} h^{-1})
(Kshirsagar et al. 2012)	*H. campisalis*, maltose	14 L batch BR, N = 100-200, $\dot{V}_a$ = 0.5-1.5 LPM, 0.5 bar pressure, k_La =18.4 h^{-1}	1-5% DO during accumulation phase gave highest $\%_{PHA}$ (56%), [X_{PHA}] (1.7 g L^{-1}), and Q_v (0.04 g L^{-1})

Table 2.9. *(con't)*

(Millán et al. 2016)	*A. vinelandii*, sucrose	Batch BR with 2 L WV, 1% or 15% DO (0.0021 and 0.0137 mmol O_2 L^{-1}, respectively) controlled via N_2 and O_2 flow rates, N_a = 500	At lower DO, $\%_{PHA}$, [X_{PHA}], and $Y_{PHA/S}$ increased from 45 to 80% CDM, 1.7 to 3 g L^{-1}, and 0.04 to 0.32 g g^{-1}, respectively.
(Lillo and Rodriguez-Valera 1990)	*Haloferax mediterranei*, glc	Continuous BR 1.5 L WV, dilution rate = 0.1 h^{-1}; OTRs of 0.02, 0.07, and 0.4 mmol O_2 L^{-1} h^{-1}	PHB protein^{-1} ratio and $Y_{PHA/S}$ (5.13 and 0.21 g g^{-1}, respectively) highest at 0.4 mmol O_2 L^{-1} h^{-1}, and decreased to 0.83 and 0.048 g g^{-1} at 0.02 mmol O_2 L^{-1} h^{-1}
(Pozo et al. 2002)	*Azotobacter chroococcum*, olive mill WW[g]	250 mL flasks with 50 mL WV, N_a varied 50-300	In medium without NH_4, higher $\%_{PHA}$ (51%) and [X_{PHA}] (3 g L^{-1}) obtained at lower *N*, but little difference in medium with NH_4
(Quillaguamán et al. 2005)	*H. boliviensis*, maltose	2 L batch BR with varied N_a (≤ 800) and $\dot{V}_a$ (≤1.7 LPM) to meet cell demand	0% DO caused $\%_{PHA}$ to increase from 21 to 41%, which matched results obtained in flasks
(van Wegen et al. 2001)	*E. coli*, glc	5 L BR with 2.5 L WV, N_a = 700, $\dot{V}_a$ = 4 LPM (k_La = 66 h^{-1})	DO fell to 0-5% causing increased Q_s but also significant synthesis of formic, pyruvic, acetic, lactic, and succinic acids
(Vollbrecht et al. 1979)	*C. necator*, gluconate	4 L BR with N_a = 630, $\dot{V}_a$ = 5-140 mL min^{-1}, k_La = 6-140 h^{-1}	Maximum $\%_{PHA}$ obtained when respiration rate restricted to 40-50% of that observed at the end of exponential growth

Abbreviations not already defined: BR – bioreactor; VVM– volumes of air per liquid volume per minute; WW – wastewater.

2.9.1.2. scl-PHA synthesis from VFAs and LCFAs

Fatty acids are a common substrate for scl-PHA synthesis, which may be activated directly (acetate, propionate) or utilized via β-oxidation (butyrate, valerate, LCFAs) (Figure 2.2). In either case, the $NADP^+$ produced from PHB synthesis may be regenerated by glucose-6-phosphate dehydrogenase, iso-citrate dehydrogenase, the malic enzyme, or transhydrogenase activity (Grousseau et al. 2013). At least one of these reactions allows synthesis of PHB or PHBV from VFAs to proceed at low DO; several studies in Table 2.10 have found improved $\%_{PHA}$ or $Y_{PHA/S}$ using VFA mixtures or medium supplemented with VFAs. However, in many cases this was accomplished using simultaneous N-limitation. Several MMC studies, which are discussed below, have reported similar results. Butyrate and valerate can be partially oxidized via the β-oxidation cycle to 3-ketoacyl-CoA intermediates for PHBV synthesis (Shi et al. 1997; Serafim et al. 2008). In low DO environments, direct incorporation of butyrate or valerate to PHA could allow some ATP conservation via oxidative phosphorylation while reducing minimal O_2 via electron transport. This may help explain why lower specific uptake rates of propionate and acetate (compared to butyrate and valerate) at low DO were observed using MMCs (Wang et al. 2017). Few studies (shown at the bottom of Table 2.10) have examined PHB synthesis from highly reduced LCFAs in low DO environments, but these have also reported that lower OTRs resulted in improved $\%_{PHA}$.

Table 2.10. The impact of oxygen limitation when producing scl-PHA from VFAs or LCFAs using pure cultures.

Study	Organism, substrate	Conditions	Key Results
(Cavalheiro et al. 2012)	*C. necator*, glycerol + γ-butyrolactone with propionate	2 L fed batch BR with 2% and 20% DO during N-limited accumulation phase, $N_a \leq 1500$, $\dot{V}_a$ = 3.6 LPM	Improved maximum Q_v (0.15-0.35 g L^{-1} h^{-1}) $\%_{PHA}$ (15-25% CDM) and [X_{PHA}] (4-11 g L^{-1}) at 2% DO compared to results without propionate, in which case 20% DO was more favorable for PHB synthesis
(Ganzeveld et al. 1999)	*C. necator*, mixed VFAs (acetic to hexanoic)	1 L BR with 750 mL WV, 30% DO >0.1 % DOC during O_2-limited phase with N_a = 400, $\dot{V}_a$ = 2.8-16.4 mL min^{-1}	0.1% DO initiated synthesis of PHBV, optimum [X_{PHA}] (1.1 g L^{-1}) and $\%_{PHA}$ (40% CDM), and Q_s (15 mg g^{-1} h^{-1}) was observed with $\dot{V}_a$ = 5.5-6.4 mL min^{-1} (0.24 mol O_2 kg biomass^{-1} h^{-1})
(Kourmentza et al. 2015)	*Pseudomonas* isolates, acetate, propionate, butyrate	Batch experiments with DO > 2 mg L^{-1} or DO < 2 mg L^{-1} with simultaneous N limitation, N_a = 250	Lower Q_v with DO < 2 mg L^{-1} in most isolates, but one isolate showed improved $\%_{PHA}$ (24-51% CDM) at lower DO
(Lefebvre et al. 1997)	*C. necator*, glc with propionate	1.7 L fed batch BR with 1-4% DO or 50-70% DO during N-limited accumulation phase	Lower Q_v, but 2-3 times higher yield of PHV from propionate at 1-4% DO (0.48 -0.73 mol mol^{-1}), compared control with 50-70% DO (0.25 mol mol^{-1}). Yield of PHB from glc unaffected
(Mumtaz et al. 2009)	*Comomonas* sp. EB172, acetate, propionate, butyrate	2 L pH-stat fed batch BR, $N_a \leq 1200$, $\dot{V}_a$ = 1-8 VVM, DO dropped to 0% within 20 h with gradual depletion of NH_4	O_2-limitation caused $\%_{PHA}$ to increase (5%-73% CDM), which was higher than 30% DO during the accumulation phase (42% CDM). Higher $Y_{PHA/S}$ under O_2-limited conditions
(Mumtaz et al. 2016)	*Comomonas* sp. EB172, acetate, propionate, butyrate	150 L pH-stat fed batch BR (50 L WV) with $N_a \leq 258$ rpm	DO dropped to 10% after 38 h with simultaneous NH_4 limitation, causing $\%_{PHA}$ to increase to 73% by 47 h
(Kek et al. 2008)	*C. necator*, acidified palm kernel oil	Reduced OTR by increasing culture volume 25-200 mL in 250 mL flasks, N_a = 200	$\%_{PHA}$ improved 60-77% CDM as the WV increased 50-100 mL and reached 79% at 200 mL WV, maximum [X_{PHA}] at 100 mL WV
(Shantini et al. 2015)	*Cupriavidus* sp. USMAA2, oleic acid and pentanol	DO-stat fed batch BR at high OTR (k_La = 45 h^{-1}) and low OTR (k_La = 11 h^{-1}), NH_4 excess	DO fell to 0% in all cases, but lower OTR during storage phase improved $\%_{PHA}$ (52-66% CDM) and Q_v (0.38-0.48 g L^{-1} h^{-1})

2.9.1.3. scl-PHA synthesis from mixed cultures

PHA metabolism is known to play a vital metabolic role as both an electron donor and energy source under transient conditions encountered in in wastewater treatment processes (Third et al. 2003; Salehizadeh and Van Loosdrecht 2004). The synthesis and metabolic role of PHAs in MMCs are thought to behave similarly to pure cultures (Serafim et al. 2008). The potential of activated sludge for PHA production was recognized in 1997 (Van Loosdrecht et al. 1997), but only 20-30% PHA was typically achieved under anaerobic-aerobic conditions (Dias et al. 2006). Using a microaerophilic-aerobic process, $\%_{PHA}$ was improved to 62% CDM, but this was not stable over prolonged operation (Satoh et al. 1998; Takabatake et al. 2000). Significant PHA storage capacity in MMCs was also observed under fully aerobic conditions cycling between the presence (feast) and absence (famine) of exogenous substrate, which has given rise to the feast-famine process or aerobic dynamic feeding (ADF) (Majone et al. 1996; Van Loosdrecht et al. 1997). ADF has become a popular strategy for operation of sequencing batch reactors (SBRs) for selection of MMCs enriched for PHA production, with subsequent PHA production done in batch or fed-batch reactors (Johnson et al. 2009). Despite the process being entirely aerobic, management of OTR or DO to mitigate operating costs during the culture selection or PHA production steps remain significant optimization challenges that have attracted attention recently. Table 2.11 shows several studies that have investigated the effect of OTR on PHA production with MMCs primarily from VFAs, but also from glucose and glycerol. Mixed results have been reported, with only some studies reporting improved $\%_{PHA}$ at lower OTRs. However, improved yield of PHA from both carbon and reducing equivalents, and higher C5 content appears to be a common occurrence.

Table 2.11. Summary of studies that investigated the impact of oxygen limitation on PHA production using MMCs.

Study	Substrate	Conditions	Key Results
(Amulya et al. 2016)	Glucose	250 mL batch BRs (110 mL WV) with aerobic (3.1 mg L^{-1} DO) and microaerophilic (0.6 mg L^{-1}) conditions and limiting amounts of P and N	Higher $\%_{PHA}$ (56% CDM) and C5 proportion (21%) obtained in microaerophilic environment corroborated with higher reduction potential (-0.74 μA) and dehydrogenase activity
(Coats et al. 2016)	Fermented dairy manure	1.2 L enrichment SBRs with k_La varied 4-20 h^{-1} ($\dot{V}_a$ = 15-600 mL min^{-1}), PHA production in pulse-fed 300 mL reactors with DO >1 mg L^{-1}	No statistical difference of OTR on Q_s, Q_v, $\%_{PHA}$, X_{PHA} or $Y_{PHA/S}$ during the feast phase in enrichment reactors. Little impact of enrichment reactor OTR on production reactors
(Gobi and Vadivelu 2015)	Palm mill oil effluent (VFA)	2 L SBRs (1 L WV) operated at $\dot{V}_a$ = 1, 2, 3, and 4 LPM (k_La = 6-330 h^{-1})	Maximum $\%_{PHA}$ (75% CDM) unaffected, but Q_s doubled at 3-4 LPM. C5 content increased (11-31%) as $\dot{V}_a$ was reduced from 4 LPM to 1 LPM
(Moralejo-Gárate et al. 2013)	Glycerol	2 L enrichment SBR operated in ADF regime, k_La = 45.6 h^{-1} (air diffuser) or k_La = 9.5 h^{-1} (surface aeration) with subsequent batch PHA production at k_La 7.4–15.6 h^{-1} (DO = 0.3-3.8 mg L^{-1})	Improved $Y_{PHA/S}$, Q_s in high DO enrichment, low DO favored formation of polyglucose over PHB. In batch PHA production the high DO enrichment achieved faster conversion rates and higher $\%_{PHA}$ at higher OTR
(Pratt et al. 2012)	Acetate and propionate (70:30)	0.6 L WV batch BR with DO controlled at 0.2 mg L^{-1} and 5.5 mg L^{-1} with intermittent aeration	$\%_{PHA}$ (35% TSS[a]) unaffected by DO and $Y_{PHA/S}$ improved at low DO, but Q_s was significantly (3 times) slower at low DO
(Reddy and Mohan 2012)	Unfermented and fermented food wastes	250 mL SBRs with 110 mL WV and N_a = 100, operated under aerobic (unsealed) and anoxic (sealed with intermittent aeration) conditions	Slightly higher $\%_{PHA}$ (36-40%) and C5 content (32-36%) under anoxic conditions compared to aerobic (32-35% PHA, 6-35% C5)
(Third et al. 2003)	Acetate	2 L SBR with ADF at high (DO > 0.9 mg L^{-1}, k_La = 30-51 h^{-1}) and low (0 mg L^{-1}, k_La = 6-16 h^{-1}) OTRs	Yield of PHB from both carbon and reducing equivalents increased (0.48-0.68 C mol C-mol^{-1} and 0.54-0.77, respectively) at low DO
(Vjayan and Vadivelu 2017)	Palm mill oil effluent (VFA)	2 L SBR operated at $\dot{V}_a$ = 2 LPM for 2 h (feast phase) then reduced to 0, 0.5, 1, or 2 LPM from 2-8 h (famine phase)	Decreased $\dot{V}_a$ during famine phase increased C5 content (21% at 2 LPM up to 35% at 0 LPM), and reduced the time until maximum $\%_{PHA}$ (65% CDM) in the feast phase

Table 2.11. *(con't)*

(Wang et al. 2017)	Mixed VFAs (acetate to valerate)	2 L SBR with at high (3.5 mg L^{-1}) and low (0.9 mg L^{-1}) DO during culture enrichment and subsequent PHA production steps	$\%_{PHA}$ (>60%), $Y_{PHA/S}$ (>0.9 C-mol C-mol^{-1}), and rate of butyrate and valerate uptake of culture selected at low DO less affected by low DO during PHA production step

2.9.2. Effect of OTR on scl-PHA polymer properties

The properties of the polymer can have significant impact on the final application. It is therefore important to understand how cultivation parameters impact polymer properties. For reference, Table 2.12 shows generic literature values obtained for various PHA polymers in comparison to petrochemical plastic materials (shown at the bottom of the table). Although a few values are shown for *M* to give context, these should be intpreted with caution as various studies report values that may be different due to the carbon substrate, the production strain, and the cultivation conditions. The remainder of this section discusses the available literature on how the DO and/or OTR maintained during the cultivation process might impact the polymer composition and polymer properties. Or perhaps more specifically, how OTR affects parameters such as the molecular mass distribution, which might in turn affect polymer properties.

Table 2.12. Summary of polymer properties (molecular mass, thermal, and mechanical) for various scl- and mcl-PHAs.

Polymer	Composition	Molecular mass (kDa)		Young's Modulus	Tensile Strength	Elongation at break	T_m	T_g
		M_w	M_n	(GPa)	(MPa)	(%)	(°C)	(°C)
PHB		300	254	3.5-4.0	40	3-8	173-180	5-9
P(4-HB)				149	104	1000	53	-50
PHBV	3% HV			2.9	38	-	170	-
	20% HV	948.2	319	1.2	32	-	145	-1
P(3HB-*co*-4HB)	3% 4-HB			-	28	45	166	-
	90% 4-HB			100	65	1080	50	-42
P(HB-*co*-HHx)	10% HHx			135	20	400	127	-1
P(HB-*co*-HO)	30% HO			189	11	9.6	169	-
P(HB-*co*-HD)	6% HD			-	17	680	130	-8
P(HHx-*co*-HO)	11% HHx			8	10	300	61	-36
PHO	C8 (C6)	187-230	78-98	9.8-11.0	6-10	300-450	56-58	-40
PHA, oleic	C8, C10, (C12, C14, C12:1, C14:1)	125-135	46-49	0.8-0.85	-	-	-	-43.5 to -45
PP				1.0-1.7	29.3-38.6	500-900	170-176	-10
HDPE				0.4-1.0	17.9-33.1	12-700	112-132	-80
LDPE				0.05-0.1	15.2-78.6	150-600	88-130	-36
PS				3.0-3.1	50	3-4	80-110	21
PET				2.2	56	7300	262	3400

Note: PHA polymers are the 3-hydroxy form unless otherwise specified. Abbreviations: PP – polypropylene; HDPE – high-density polyethylene; LDPE – low-density polyethylene; PS – polystyrene; PET – polyethylene terephthalate. The dash line indicates where values not reported in the literature found, most likely beucase the test parameter was not a suitable measure for type of PHA. Adapted from multiple sources (Madison and Huisman 1999; Kellerhals et al. 2000; Zinn et al. 2003; Khanna and Srivastava 2005a; Hartmann et al. 2006; Liu and Chen 2007; Akaraonye et al. 2010; Nerkar et al. 2014; Anjum et al. 2016; Możejko-Ciesielska and Kiewisz 2016)

2.9.2.1. Monomer composition

The OTR has also been reported to cause shifts in the PHA monomer composition. Increased incorporation of P(4-HB) monomers was reported at lower OTRs using *C. necator* cultured on glycerol supplemented with γ-butyrolactone (Cavalheiro et al. 2012) and *Comomonas acidovorans* grown on glucose supplemented with 1,4-butanediol (Lee et al. 2004). PHBVs produced from VFA mixtures have shown increased C5 content at lower OTR in both pure cultures (Mumtaz et al. 2009; Zafar et al. 2012) as well as in several mixed culture studies (Amulya et al. 2016; Vjayan and Vadivelu 2017). Several isolates of *Pseudomonas* sp. showed lower C5 and increased C6 content with DO < 2 mg L^{-1} when grown on VFA mixtures (Kourmentza et al. 2015).

2.8.2.2. Molecular mass and thermal characteristics

Although the monomer composition can provide some interesting insights into metabolism, the effect of culture conditions on final properties of the polymer are pertinent considerations that may not be reflected by the monomer composition. In several examples in the literature, the OTR has impacted polymer properties in PHB homopolymers. Peña et al. (2014) evaluated *M* of PHB synthesized from sucrose in *A. vinelandii* OP (and a mutant strain OPN) at different OTRs. These were achieved by increasing the working volume from 100 to 200 mL in a 500 mL flask with orbital shaking at 200 rpm, and unfortunately neither DO nor k_La was reported. Remarkably, the viscosity-average molecular mass (M_v) tripled in the wild type and doubled in the mutant strain as the working volume was increased to 200 mL. The weight-average molecular masses (M_w), were also measured and found to be significantly higher than M_v, although the overall trends were similar regardless of the method (Peña et al. 2014). Myshkina et al. (2008) reported similar results for PHB synthesized by *A. chroococcum* grown in

flasks under various conditions from aerobic (with shaking) to microaerophilic (no shaking) to anaerobic (N_2-atmosphere). In that study, the M_v increased from 1480 kDa at maximum aeration to 2215 kDa under anaerobic conditions (Myshkina et al. 2008).

Bioreactor studies in which DO or OTR can be measured and controlled have reported mixed results on polymer properties. One study explored bioreactor agitation rates on properties of PHB synthesized from either glucose or glycerol using recombinant *E. coli* (de Almeida et al. 2010). When the substrate was glycerol (in which each mole of carbon is more reduced than in glucose) the M_r, T_m, T_g, and crystallinity were reduced at 500 rpm compared to the corresponding observations at 125 rpm or 1000 rpm. When the substrate was glucose, a slight increase in T_g was observed at 500 rpm compared to 125 rpm, while other properties showed little change. Higher agitation rates (1000 rpm) were not tested with glucose. Shantini et al. (2015) studied properties of PHBV synthesized by *C. necator* from oleic acid and pentanol at high OTR (k_La = 45 h^{-1}) and low OTR (k_La = 11 h^{-1}). Although the low-OTR polymer had slightly higher C5 content, (i.e. 24% compared to 23% at high OTR), the number-average molecular mass (M_n) and M_w both increased significantly (from 23 to 51 kDa and 233 to 313 kDa, respectively). Minor increases in T_m and T_g were demonstrated in the high-OTR polymer. In addition, polydispersity increased from 6.1 to 7.8 at low OTR (Shantini et al. 2015).

In a separate study, the M_n of PHB synthesized by *A. vinelandii* was measured in cultures grown on sucrose and yeast extract and controlled at 1% and 15% DO (Millán et al. 2016). In that work, there was little difference in M_n of the PHB produced at either oxygen condition, but changes in the M_n distribution (and hence mean molecular mass) were observed depending on whether the PHA was obtained from exponential-phase cultures or stationary-phase cultures. In an earlier bioreactor study, in which PHB synthesized from beet molasses at various DO contents

(5%, 10%, and 20%) using *A. vinelandii*, little change was observed in M_n, M_w, or polydispersity (Chen and Page 1994).

2.9.2.3. Tensile properties

Peña et al. (2014) also evaluated the tensile properties of PHB produced under the aeration conditions described above. The films were cast in chloroform, dried overnight, and then further dried under vacuum at 90 °C for 4 h. Interestingly, the Young's modulus of the PHB film synthesized at the lower aeration condition increased 25-fold (12 to 320 MPa) in strain *A. vinelandii* OP and more than two-fold (180 to 560 MPa) in strain mutant OPN (Peña et al. 2014). Shantini et al. (2015) examined tensile properties of PHBV films synthesized at k_La values described above. A significant increase in tensile strength (14.1 to 19.1 MPa), Young's modulus (107 to 187 MPa) and elongation at break (113 to 193%) were observed for the film made at higher OTR. Unfortunately, specific details of the preparation methods for these films were not given. Although these two studies give merit to consideration of DO and/or OTR effects on mechanical properties, little research is available on this matter and further investigation may be worthwhile. Again, the need to distinguish if changing polymer properties was a direct effect of a cultivation parameter such as aeration, or a consequence of changes in molecular mass distribution, for example, is important.

2.9.3. Synthesis of mcl-PHA under O_2-limtation

2.9.3.1. Mcl-PHA synthesis from carbohydrate substrates

Carbohydrates, short-chain VFAs, and glycerol are converted to mcl-PHA via fatty acid *de novo* biosynthesis (Figure 2.3). Like the PHB biosynthetic pathway, the *de novo* pathway is a reduction, requiring NADPH as the electron donor (Figure 2.3). Mitchell and Dawes (1982)

found that enzymes of glucose metabolism and the TCA cycle in *P. aeruginosa* responded to changes in DO similarly to N_2-fixing *Azotobacter* sp. (Mitchell and Dawes 1982). Therefore it might be hypothesized that mcl-PHA synthesis, at least from glucose, would behave similarly to PHB synthesis from glucose under O_2-limiting conditions. Few studies have looked at the effect of OTR on *de novo* mcl-PHA synthesis. In glucose-grown chemostat cultures using a *Pseudomonas* sp., the $\%_{PHA}$ increased slightly (from 4.4% to 7% CDM) when the DO was reduced from 70% to 1% in NH_4-limited medium with a dilution rate (D) of 0.1 h^{-1} (Haywood et al. 1990). In that study, no PHA was synthesized using O_2 as the sole limiting nutrient (DO below detectable limits). Similarly, Diniz et al. (2004) found that *P. putida* did not synthesize PHA from a equimolar mixture of glucose and fructose with DO as low as 1%, and concluded that DO should be maintained at 15% or higher (Diniz et al. 2004). Silva et al. (2014) reported that O_2-limited conditions were encountered below 13% DO, and obtained 6.5% CDM as mcl-PHA when *P. oleovorans* was grown on sugary cassava waste under O_2 limited conditions with excess NH_4 (Silva et al. 2014).

2.9.3.2. Mcl-PHA synthesis from fatty acids

In contrast to synthesis of PHB from glucose or mcl-PHA by *de novo* synthesis, production of mcl-PHA from β-oxidation intermediates is an oxidative process. Only a few studies have investigated the impact of DO on mcl-PHA synthesis from fatty acids. Two studies have suggested that addition of fatty acids to glucose-grown cultures improved mcl-PHA content at low DOC using *P. putida* with simultaneous N-limitation (Kim et al. 1997), and *P. oleovorans* in the presence of excess NH_4 (Silva et al. 2014). Huijberts and Eggink (1996) operated a high cell density chemostat under DO limitation (15%) and achieved 23% CDM as mcl-PHA from oleic acid at D = 0.1 h^{-1} and a C/N ratio of 20 (mol mol^{-1}). Unfortunately in that work, details on

how the DO was optimized were not given, and comparisons of monomer composition and polymer characteristics were only done on the basis of dilution rate, and not variable DO (Huijberts and Eggink 1996).

Fernández et al. (2005) reported that PHA content and [X_{PHA}] in flasks were not significantly affected by cultivation at two OTRs (k_La of 216 h^{-1} or 360 h^{-1}), but it should be pointed out that the OTRs used in that study are relatively high compared to other studies. In that study, it was also reported that the lower OTR produced a polymer containing a lower proportion of C8, C10, C12, and C14:1 monomers, but also a significant (20%) increase in C12:1 content as well as appearance of C14:2 that accounted for 13.2% of the polymer. This is the only known study that reported a difference in mcl-PHA monomer composition in response to OTR.

2.9.4. General discussion on DO as a modulator of microbial PHA synthesis

Multiple studies have shown that O_2-limtiation can be an appropriate stressor for synthesis of significant amounts of PHB from sugars or glycerol. These collectively support the reduction of acetoacetyl-CoA to (R)-3-hydroxybutryl-CoA acting as an electron sink, and allowing ATP production to proceed via substrate-level phosphorylation in low DO environments. In contrast, synthesis of mcl-PHA from sugars via *de novo* biosynthesis (also a reductive process using NADPH as the electron donor) has not yet been shown to occur to any significant extent under O_2 limitation. Thus, this process does not appear to act as a 'sink' for electrons in low DO environments in the same way that PHB synthesis does. However, when mcl-PHA is synthesized from intermediates of the β-oxidation cycle (an oxidative process), a few studies have shown significant capacity for storage of fatty acids as mcl-PHA under O_2-limited conditions. According to Vollbrecht et al. (1979), sufficient ATP is needed to drive the synthesis of PHB and maintenance requirement of the cells, and several studies have reported

that the most efficient utilization of carbon or reducing equivalents for PHB or mcl-PHA synthesis occurs when DO is below detectable limits in the bulk liquid using standard polarographic DO probes (Third et al. 2003; Faccin et al. 2013). This makes flask studies in which DO is often not measured or controlled problematic because in many cases only two aeration conditions (typically defined by filling volume or orbital shaking rates) are used, and both observations could lie on one side of the optimum. Furthermore, since k_La or OTR are seldom reported in flask cultures, the results are difficult to interpret and should be used cautiously. Fortunately, optical DO sensors have made it possible to monitor DO in flask cultures (Castillo et al. 2013), which could significantly expedite process development in this area. Several bioreactor studies have shown flask cultures (even at relatively low working volumes) behave as if they are O_2-limited (Quillaguamán et al. 2005; Faccin et al. 2013), which could disguise the true effect of other parameters often examined in flasks, such as C/N or carbon-to-phosphorus (C/P) ratios.

Due to the challenges described above in measuring DO, it would be ideal if k_La values were consistently reported. This is not always done, and many studies have described aeration conditions using aeration rates, agitation rates, and DO as a percent of saturation. While this may be appropriate for bench-scale studies in which the OTR (mixing and aeration rates) are simply maximized, a more rigorous understanding of the impact of lower OTRs can save costs as the process is scaled up (Coats et al. 2016). From this review, storage of carbon as PHA is generally favored when DO is reduced below 5-10%, but a robust definition for O_2-limitation appears to be lacking. This is supported by the variety in methodologies and reporting criteria described in this review, and is a long-standing problem that was outlined more than 40 years ago (Ward et al. 1977). Regardless, there is room for considerable study and optimization efforts for carbon flux

to PHA at low OTRs, particularly for the field of mcl-PHA production in which only a few reports have examined some aspect of this in any amount of detail. Further studies might include measurements of the O_2 half saturation constants, specific O_2 uptake rates, carbon and redox balances, measurement of oxidation-reduction potentials, and/or yield analysis to understand how a particular organism might redirect carbon flux from growth to PHA synthesis under a spectrum of precisely controlled OTR conditions – ideally described using k_La at below detectable DO contents.

The monomer composition of the polymer (even if it does not change in response to OTR), as well as physical and thermal characteristics should also be reported. The monomer composition can affect the physical and thermal properties of the final polymer (Salehizadeh and Van Loosdrecht 2004) and has been impacted by OTR in several scl-PHA studies, and in one instance of mcl-PHA from oleic acid using *P. aeruginosa* (Fernández et al. 2005). Even synthesis of PHB homopolymers at different OTRs had an effect on polymer properties including M, T_m, T_g, and crystallinity (de Almeida et al. 2010; Peña et al. 2014). Little information is available regarding the effect of OTR on scl-PHA properties, and no studies were found that describe changes in physical or thermal characteristics of mcl-PHA polymers synthesized at different OTRs. The work that has been done in this area with scl-PHA suggests an opportunity to tune polymer properties by manipulating the bioreactor OTR. Furthermore, considerations regarding the desired final polymer application could play a highly pertinent role in management of bioreactor OTR.

2.10. Continuous and semi-continuous strategies

In continuous culture, fresh medium is constantly supplied to the bioreactor, and a portion of the culture is removed at the same rate - the dilution rate (D). Using this method, the

conditions inside the reactor (substrate, cell, and product concentrations) remain at steady state. Because of this, continuous cultures are often referred to as chemostats, which is short for "chemical environment is static" (Koller and Braunegg 2015). Steady state operation has a number of advantages. It is an attractive platform to study bioprocess physiology and implement control strategies due to the constant growth rate, and is less laborious to operate and maintain once steady state operation is reached (Braunegg et al. 2004; Sun et al. 2007b; Koller and Braunegg 2015). Steady state operation also circumvents the major challenge of optimal control of fed-batch strategies, which is predicting μ over time and under highly dynamic conditions (Koller and Muhr 2014).

However, the main reason continuous bioreactor configurations may be of interest is that they can theoretically achieve higher *average* productivity (over time) in comparison to discontinuous processes (Braunegg et al. 1995). This is done by maintaining the culture at a moderate but constant growth rate for prolonged periods and avoiding non-productive downtime required for harvest, cleaning, preparation of new medium, sterilization, cooling, and culture lag in a discontinuous process (Braunegg et al. 2004; Koller and Braunegg 2015). Ultimately, higher productivities could result in a smaller reactor volume requirement, less capital investment (for both the production and downstream processing requirements), lower operating costs, and would avoid some of the typical mass transfer issues associated with scale up of discontinuous processes, which have already been discussed (Braunegg et al. 1995; Huijberts and Eggink 1996; Hartmann et al. 2010; Koller and Braunegg 2015). Furthermore, manipulation of chemostat cultures has also been shown to reproducibly tailor monomer composition (Hartmann et al. 2006; Hartmann et al. 2010; Zinn et al. 2011) and M_w (Koyama and Doi 1995), giving the process considerable flexibility.

Despite significant upside, there are a number of challenges with continuous culturing that have perhaps limited its industrial application. These include: 1) higher risk of infection due to a large number of fittings and pumping operations; 2) risk of back-growth into the feed medium reservoir; 3) the production strain must be genetically stable over many generations; 4) cell wash out as the *D* approaches μ_{max} (Ramsay et al. 1991; Preusting et al. 1993a; Koller and Muhr 2014); and 5) to date, experimental values for fed-batch processes are reported to have higher productivity (Hartmann et al. 2010).

2.10.1. Continuous culture in PHA production

The *D* is an important parameter in continuous systems, and is defined as the quotient of the bioreactor working volume to the incoming flow rate (h^{-1}). This can have a significant impact on the growth rate, PHA content of the cells, and hence the productivity. Unless cell retention techniques are employed, the *D* is equal to the reciprocal of both the hydraulic retention time (HRT) and solids retention time (SRT). Manipulation of *D* can change both the growth rate of the cells, cellular PHA content, and ultimately the productivity (Heijnen et al. 1992; Zinn et al. 2001). The *D* must be lower than μ_{max} to prevent cell washout or wasting the carbon source (which unless recycled must be subject to post-treatment to remove biochemical oxygen demand of the waste effluent), but high enough to allow productive growth, keep toxic substrates dilute, and remove any accumulation of toxic end products.

It must be acknowledged that application of continuous culture for PHA production is a significant challenge. In general, PHA synthesis is not growth-associated and cannot therefore be simultaneously optimized in a reactor operating at steady state (Koller and Braunegg 2015) (Koller and Muhr 2014). This may be the reason that continuous cultures are often applied as a tool to study physiology rather than a bioreactor configuration to improve PHA productivity.

One solution has been to implement a two-stage process in which the two phases (growth and PHA synthesis) are separated spatially by adding a second reactor in-series, where conditions favorable to PHA accumulation can be implemented. Typically the second reactor is operated at a lower dilution rate and may also have higher C/N or C/P ratios. This has been done in multiple instances with promising results (Jung et al. 2001; Du et al. 2001; Hartmann et al. 2010). One study producing PHB from glucose using *C. necator* has used a cascade of five bioreactors in series (i.e. to simulate plug flow) in order to optimize PHA content of the biomass (Atlić et al. 2011).

These, and other past studies of PHA production in continuous cultures are summarized in Table 2.13, along with the novel contributions of each study showing the development of continuous processes over time. It is worth noting that Ramsay et al. (1991) carried out the original study of mcl-PHA production in continuous culture as a way to circumvent the toxicity effect of related substrates using *P. putida* GPo1 grown on octanoate (Ramsay et al. 1991). While this study showed a relationship of decreased PHA content with increased *D*, the $\%_{PHA}$ was low and ultimately it was concluded that a fed-batch strategy should be pursued. This group of researchers subsequently channeled their efforts into development of high-productivity fed batch strategies (Table 2.3). Comparison back to Table 2.3 and 2.4 will quickly reveal that Q_v (for both mcl- and scl-PHA) is significantly lower in continuous processes (to date) than in fed-batch processes. However, it is important to note that fed batch productivities are always reported on a timescale from inoculation to harvest. To be able to compare these values with those in Table 2.13, productivity should be reported on a timescale from one harvest to the next – factoring in the downtime for cleaning, preparation, sterilization, and cooling, of the subsequent cultivation.

Table 2.13. Research on continuous cultivation in PHA production.

Ref	Organism, substrate (polymer)	Conditions	X_t (g L^{-1})	$\%_{PHA}$ (% CDM)	$Y_{PHA/S}$ (g g^{-1})	Q_v (g L^{-1} h^{-1})	Contribution
(Senior et al. 1972)	*A. beijerinckii*, glc (PHB)	Single stage, O_2-limited with D = 0.05 h^{-1}.	-	45	0.13	-	First application of PHA production in a chemostat
(Ramsay et al. 1990)	*C. necator* DSM 545, glc + propionate, (PHBV)	Single stage with N-limited conditions D = 0.15 h^{-1}	-	33	-	-	Demonstrated co-polymer production dependent on ratio of feed components, also first implementation of a two-stage cont. system for improved $\%_{PHA}$
(Ramsay et al. 1990)	*A. lata* ATCC 29714, sucrose, propionate (PHBV)	Two-stage with N-limitation, D = 0.15 h^{-1}	-	58	-	-	(see above)
(Lillo and Rodriguez-Valera 1990)	*Hfx. mediterranei* DSM 1411, glc (PHB)	Single-stage with D = 0.02 h^{-1}, OTR = 0.4 mmol O_2 L^{-1} h^{-1}	3.1	48		0.03[a]	First cont. PHA production with using archaea – and first under non-sterile conditions.
(Ramsay et al. 1991)	*P. oleovorans* ATCC 29347, OA (mcl-PHA)	Single stage, various D and C/N ratios tested (D = 0.24 h^{-1} shown)	4.2	13	0.09	0.14[a]	First mcl-PHA production in cont. culture. Demonstrated little effect of feed C/N ratio on $\%_{PHA}$ at D = 0.24 h^{-1} and showed some dependence of monomer composition on D.
(Preusting et al. 1993a)	*P. putida* GPo1, n-octane (mcl-PHA)	Single stage, D = 0.2 h^{-1} NH_4 limiting	11.6	23	-	0.58	First cont. study with two-liquid phase medium and first to use a cont. platform for enhanced Q_v. Demonstrated effect of D on $\%_{PHA}$

Table 2.13 *(con't)*

(Koyama and Doi 1995)	*C. necator*, fructose + pentanoic acid (PHBV)	Single-stage, D= 0.17 h^{-1}, NH_4-limiting	-	-	-	0.31	First study to use continuous scl-PHA production as a platform for improved Q_v. Showed effect of D on HV content.
(Huijberts and Eggink 1996)	*P. putida* KT2440, oleic acid (mcl-PHA)	Single stage, O_2 limited (DO <15% AS) with D = 0.1 h^{-1}	30	23	-	0.69	Highest steady state X_t reported for a cont. system in mcl-PHA production
(Hazenberg and Witholt 1997)	*P. putida* GPo1, octane (mcl-PHA)	Single stage, N limited with D = 0.2 h^{-1}	12.4	30	0.63	0.74	Highest Q_v for a single-stage cont. PHA production system
(Durner et al. 2000)	*P. putida* GPo1, OA (mcl-PHA)	Single stage, D = 0.05 – 0.4 h^{-1}, C/N ratio = 5-25 (mol mol^{-1})	-	56.1	0.25	-	First study exploring dual nutrient limited growth. Results reported at D = 0.1 h^{-1}
(Du et al. 2001)	*C. necator*, glc (PHB)	Two-stage, D =0.075 h^{-1} and with N-limiting conditions in second stage	42	72.1	0.36	1.23	Highest [X_t] and Q_v in cont. culture for PHA production. Max. $\%_{PHA}$ and $Y_{PHA/S}$ with D = 0.075 h^{-1} in S2
(Jung et al. 2001)	*P. oleovorans* ATCC 29347, octane (mcl-PHA)	2 stage (S1: D = 0.21 h^{-1} and S2: D = 0.16 h^{-1})	71.4	63	-	1.06	Highest mcl-PHA Q_v to date in a cont. bioreactor system.
(Hartmann et al. 2006)	*P. putida* GPo1, OA, UDA (mcl-PHA)	Single stage, D = 0.1-0.4 h^{-1}, dual C- and N-limitation	1.75	23	-	0.08	Monomer composition shown to be a function of D and not C/N ratio. Preference for incorporation of aliphatic monomers at lower D. Results reported for C/N = 23 and D = 0.1 h^{-1}.

Table 2.13. *(con't)*

(Hartmann et al. 2010)	*P. putida* GPo1, fatty acids, (mcl-PHA)	2 stage (S1- OA S2 – UDA, D = 0.1 h^{-1} for both dual C and N limitation	1.53 (S2)	52.4 (S2)	-	0.08[a]	Synthesis of two mcl-PHA co-polymers when fed different fatty acids in S1 (OA) and S2 (UDA). Results shown for D = 0.1 h^{-1} and C/N = 19.1
(Atlić et al. 2011)	*C. necator* DSM 545, glc (PHB)	5 CSTRs with D = 0.13-0.17 h^{-1}; S1 7.5 L growth reactor (DO = 40%) and S2-S5 - 3.6 L accumulation reactors (DO = 20%)	81 (S5)	77 (S5)	0.29	1.85	First time more than two in-series CSTRs used for PHA production. Highest reported Q_v for any cont. PHA production system.
(Follonier et al. 2012)	*P. putida* KT2440, OA + UDA	High pressure (7 bar) chemostat with DO = 235%, D = 0.15 h^{-1} and C/N = 12.5 g g^{-1}	13.8	45.1		0.9	First application of a pressurized chemostat for improved OTR and overall Q_v.

[a]Q_v calculated on the basis of [X_t] and $\%_{PHA}$, or [X_{PHA}], and D. Abbreviations: CSTR – continuous stirred tank reactor. Note: *P. putida* GPo1 formerly *P. oleovorans* (strain ATCC 29347)

2.10.2. Cyclic/repeated (semi-continuous) processes in PHA production

A repeated batch, fed-batch or sequencing batch reactor (SBR) process could also be adopted as a method to increase PHA productivity by decreasing non-productive downtime between batches. Although still a discontinuous process, the growth and PHA production phases can be accomplished in a single bioreactor operated under transient conditions. During SBR operation, a portion of the reactor is decanted, refilled with fresh medium to re-start the process immediately after the end of the last cycle (Ienczak et al. 2013). This principle is similar to sequential batch reactors (SBRs), which have become a popular culture selection tool with subsequent scl-PHA production using mixed microbial cultures, allowing for quick and easy manipulation of process conditions to favor PHA production (Salehizadeh and Van Loosdrecht 2004). Although developed primarily as a selection tool for robust PHB-producing populations from mixed cultures, they may also be a reliable method for producing mcl-PHA effectively using pure cultures. Although harvest is done at intervals (i.e. discontinuously) there is still a considerable time savings advantage by using the remaining broth as a seed for the subsequent reactor, eliminating time required to clean, sterilize, and prepare new inoculum (Singhaboot and Kaewkannetra 2015). Several instances of this type of process are shown in Table 2.14, and some have reported highly competitive productivities. However, in multiple cases shown in Table 2.14, only a few cycles were done (Khanna and Srivastava 2005b; Ibrahim and Steinbüchel 2010) and the cultures did not even appear to achieve a steady state. Ideally, more prolonged operation would be required to take advantage of the time saved by using a cyclic approach.

Because waste carbon sources are usually dilute (lactose in whey solution, for example) often these cyclic processes are employed in conjunction with a cell retention technique

(typically an external membrane module) to overcome the volumetric limitation imposed by feeding a dilute carbon source (Ahn et al. 2001; Schmidt et al. 2016; Haas et al. 2017). This is generally not the case with studies reported in Tables 2.3 and 2.4. Cell techniques allow decoupling of the SRT from the HRT, meaning a group of cells can be exposed to more carbon and thus accumulate high $\%_{PHA}$, and also prevent washout of cells with the effluent. As shown, some of these studies have reported cell densities approaching 150-200 g L^{-1}, with $\%_{PHB}$ of up to 87% CDM.

Table 2.14. Semi-continuous (cyclic) batch, fed-batch, and cell recycle processes applied in PHA production.

Ref	Organism	Substrate (polymer)	Conditions	$[X_t]$ (g L^{-1})	$\%_{PHA}$ (% CDM)	$Y_{PHA/S}$ (g g^{-1})	Q_v (g L^{-1} h^{-1})	C_L^*
(Ahn et al. 2001)	Recombinant *E. coli* CGCS 4401	Whey (PHB)	2.3 L pH-stat fed batch with constant volume and cell recycle via external membrane module (36.5 h total cultivation time)	194	87	-	4.6	O_2
(Khanna and Srivastava 2005b)	*C. necator* NRRL B14690	Fructose (PHB)	Fed batch with 20% volume removal at 27 and 41 h (2 cycles, 68 h total cultivation time)	49	51	0.31	0.42	?
(Huang et al. 2006)	*Hfx. mediterranei* ATCC 33500	ERB and ECS (1:8) + YE (PHB)	5 L pH-stat repeated fed batch with 90% withdrawal at end of cycle (3 cycles – 118 h total cultivation time)	140	55.6	-	3.2	?
(Ibrahim and Steinbüchel 2010)	*Chelatococcus* sp. MW10	Glc (PHB)	Fed batch with 20 - 40% volume removal (2 cycles, 265 h total cultivation time)	115	11.8	0.11[a]	-	Air
(Yue et al. 2014)	Recombinant *Halomonas campaniensis* LS21	Mixed (proteins, fats, cellulose) (PHB)	Fed batch with 40 mL of culture removed every 12 h and addition of 2 L substrate (day 25 and 49) and 0.5 L seawater on day 7 and 34 (65 d total cultivation time)	69[b]	70	-	-	?
(Singhaboot and Kaewkannetra 2015)	*A. lata* TISTR 1403	Sugar cane juice (PHB)	2 L repeated batch with 90% withdrawal at the end of each cycle (4 cycles – 84 h total cultivation time)	4.5	69	0.38[c]	0.21	?
(Ienczak et al. 2016)	*C. necator* DSM 545	Glc, fructose (PHB)	5 L repeated fed batch with periodic 25% withdrawal and complete cell recycle via external membrane (8 cycles, 42 h total)	61.6	69	-	1.0	Air

Table 2.14. *(con't)*

(Schmidt et al. 2016)	*C. necator* DSM 545	Glc + propionic acid (PHBV)	Fed batch with cell recycle via an external membrane, 1 L periodically withdrawn and replaced with fresh medium (52 h total cultivation time)	80	73	-	1.24	Air
(Haas et al. 2017)	*C. necator* DSM 545	Dilute glc (PHB)	3 L fed batch, continuously added and removed through external membrane after 18 h batch operation (36 h total cultivation time)	148	76	0.33	3.1	Air
(Gahlawat 2018)	*Azohydromonas australica* DSM 1124	Sucrose (PHB)	20% volume removed when sucrose concentration reached 8 g L^{-1}, and replenished with fresh medium. Three cycles completed (69 h total cultivation time)	27.9	74	0.59[d]	0.29	Air

[a] maximum $Y_{PHA/S}$ reported at end of second cyclic fed batch cycle; [b]maximum $[X_t]$ reported at day 12; [c]maximum $Y_{PHA/S}$ reported at 18 h; [d]maximum $Y_{PHA/S}$ reported at 48 h; the dashed line indicated $Y_{PHA/S}$ values not reported. Abbreviations: ECS – extruded cornstarch; ERB – extruded rice bran; YE – yeast extract

2.10.3. Sterility challenges

One of the challenges of semi-continuous or continuous operation is increasing risk of contamination (Li et al. 2014). Although pure cultures are generally preferred in PHA production because of reproducibility, the cost of sterilization processes is one of the main disadvantages compared with mixed culture PHA production (Wang et al. 2014). If, however, an environment can be established that precludes or minimizes growth of competitors, then the lack of need for sterilization could be a cost saving measure for pure culture production as well. Such techniques are used in PHA production with MMCs, in which feast-and-famine cycles (aerobic dynamic feeding) are used to select for PHA-producing bacterial populations, because the ability to store carbon gives them a competitive advantage under starvation conditions (Van Loosdrecht et al. 1997). Tan et al. (2011) isolated the halophilic bacterium *Halomonas bluephagenesis* TD01 from a salt lake in China (Tan et al. 2011). This organism was cultured under non-sterile conditions (37 °C, pH 9.0), and produced 80 g L^{-1} CDM containing 80% CDM as PHB in 56 h using a fed-batch method. In a two-stage continuous bioreactor, the steady state concentration of biomass in the first reactor was 40 g L^{-1} with 60% PHB content, and the $\%_{PHB}$ rose to 70% CDM after being transferred to the second stage with N-limiting conditions. In an un-inoculated blank study, 3.5 g L^{-1} of cellular contaminants was observed after 48 h, but no contaminants could be detected in the presence of *H. bluephagenesis* TD01. In a similar study, Yue et al. (2014) were able to maintain relatively steady biomass and PHB levels, with no evident contamination using wild type and recombinant *H. campaniensis* LS21 in a 65-day open process that was periodically fed (Yue et al. 2014). Lillo and Rodriguez (1990) made use of the salt-tolerant properties of the haloarcula *Hfx. mediterranei* ATCC 33500 to maintain a continuous culture for three months under non-sterile conditions with stable PHB production. Other studies have employed

methanotrophs (Wendlandt et al. 2001) as well as thermophilic strains (Ibrahim and Steinbüchel 2010) for production of PHA under non-sterile conditions.

2.11. Conclusions and outlook

With recalcitrant plastic waste accumulating in natural ecosystems, production of a renewable and biodegradable alternative for single-use applications is an urgent challenge. Microbial PHAs are a promising candidate to serve in some of these applications, and particularly mcl-PHAs because of their extensive and diverse range of properties, and ability to be functionalized. In order to reduce production costs and make PHAs more commercially attractive, scaling up production processes is necessary. However, scaling up of this technology is significantly lagging behind efforts occurring at the bench scale. Currently, the main limiting factor in HCD cultivations and large-scale bioreactors is DO, and its role in microbial PHA synthesis and physical or thermal properties is poorly understood, particularly for mcl-PHAs. A better understanding of how the organism responds to O_2 mass transfer limitations can be simulated in the lab scale and would help to anticipate challenges encountered in large-scale bioreactors.

Time is a significant factor in advancing PHA productivities. While the preferred mode of operation in PHA production certainly appears to be fed batch, continuous processes may have higher average productivity over prolonged operation due to lack of downtime between batches. Continuous cultures of both scl- and mcl-PHA have given productivities in excess of 1 g L^{-1} h^{-1}, but little research has been published within the past eight years to drive this technology forward. Cyclic processes have recently shown great promise (particularly when cell retention is used), but generally these were not operated long enough to take advantage of time saved from minimal downtime in a cyclic process.

In light of these current gaps in the literature, the following chapters of this thesis examine some of these limitations with the overall motivation of improving mcl-PHA productivity and addressing potential scale-up challenges with *Pseudomonas putida* LS46 (as a representative of most mcl-PHA producers). These challenges include:

1) Understanding how *P. putida* LS46 metabolism responds to varying degrees of oxygen availability in its environment. Specifically, how mcl-PHA synthesis characteristics were impacted by oxygen limited conditions (which was found to be a default condition even in low cell density flask cultures), as well as the substrate choice and biochemical pathway used to obtain monomers for mcl-PHA synthesis. These investigations of fundamental physiology are described in Chapters 4-6.
2) Evaluation of strategies for improved bioreactor productivity through the development of oxygen-limited HCD fed batch processes, and exploration of the oxygen-transfer challenges associated with the rheological properties of HCD mcl-PHA cultivation medium. This is explored in Chapters 7-8, as well as Appendix A.
3) Evaluating the efficacy of growth and mcl-PHA synthesis in non-sterile environments to open up new opportunities for fully continuous or semi-continuous process configurations. This is described in Chapter 9, with some supplemental information available in Appendix D and Appendix E.

A schematic of how the chapters were developed and fit together is shown in Figure 2.6, along with a brief outline of the approach applied in each. Further details of the methods applied are available in Chapter 3, or in the methods section of each subsequent chapter.

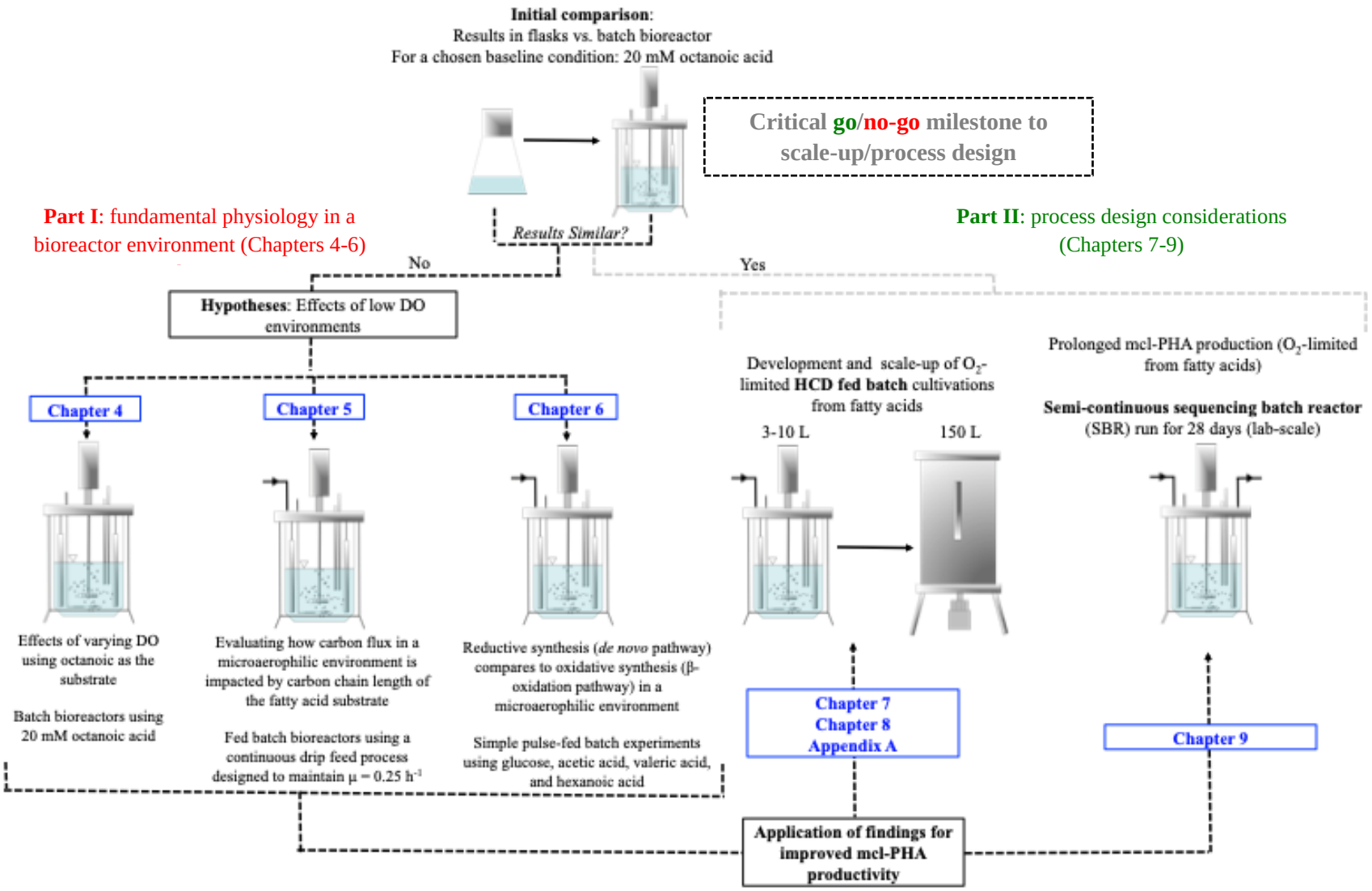

Figure 2.6. Summary schematic for development of subsequent chapters in this thesis.

Chapter 3: Materials and Methods

3.1. Preface

To avoid redundancy throughout this document, this section describes methods that are common to more than one subsequent chapter. Methods that are specific to a particular chapter will be described in that chapter.

3.2. Microorganism and medium

The strain used in this thesis research was *Pseudomonas putida* LS46 (International Depository Authority of Canada Accession Number 181110-03). This strain was isolated from enriched hog barn wash and showed promise as a biocatalyst for mcl-PHA production (Sharma et al. 2012). The strain was preserved in 60% glycerol and stored at -80 °C. Glycerol stock cultures were periodically revived and maintained on agar plates stored at 4 °C. Experimental inoculums were prepared using single colonies from these plates. Single colonies were revived in Luria-Bertani broth (LB) before being sub-cultured at least once using the same growth medium and substrate as was to be used in the subsequent experiment. The experimental inoculums were prepared in 1000 mL, 500 mL, or 250 mL baffled shaker flasks with working-volumes of 250 mL, 100 mL, and 50 mL, respectively.

The medium used in all studies was a mineral salts medium described previously (Ramsay et al. 1990). Briefly, this medium contains (per L distilled water): 6.7 g Na_2HPO_4, 1.5 g KH_2PO_4, 1 g $(NH_4)_2SO_4$, 0.2 g $MgSO_4.7H_2O$ (or 0.1 g anhydrous $MgSO_4$), 60 mg ferric ammonium citrate, 10 mg $CaCl_2.2H_2O$, and 1 mL trace element solution. The composition of the trace element solution (per L distilled water) was: 0.3 g H_3BO_3, 0.2 g $CoCl_2.6H_2O$, 0.1 g $ZnSO_4.7H_2O$, 30 mg $MnCl_2.4H_2O$, 30 mg $NaMoO_4.2H_2O$, 20 mg $NiCl_2.6H_2O$, and 10 mg

$CuSO_4.5H_2O$. The medium used was as described for most studies, although concentrations of $(NH_4)_2SO_4$, $MgSO_4$, $CaCl_2$, and trace element solution were altered as described in subsequent chapters.

3.3. Sample treatment

Culture samples of 40 mL were taken in 50 mL conical tubes and centrifuged at $4500 \times g$ for 20 minutes (min) using a ThermoFisher Sorvall RC-6 centrifuge with an SH-3000 swinging-bucket rotor. The supernatant was decanted and stored at -20 °C until further analysis could be performed. The pellet was suspended in phosphate-buffered saline (PBS), and centrifuged again at the same conditions described above. The PBS was then decanted, and the pellet was re-suspended in distilled water and transferred to pre-weighed 20 mL aluminum trays. These were then put in an oven at 60 °C until no further loss in mass was detected, generally 24 hours (h). The total biomass (X_t) was determined gravimetrically on a cell dry mass (CDM) basis as shown in Equation 3.1.The terms m_f and m_i represent the final and initial masses of the aluminum trays, respectively. Square braces indicate concentration.

$$[X_t] = \frac{[m_{f,tray} - m_{i,tray}\,(g)] \times 1000}{sample\ volume\ (mL)}\ (g\ L^{-1}\ CDM) \qquad \text{Equation 3.1}$$

3.4. Sample preparation for analysis by GC

3.4.1. Alkylation of PHAs to 3-hydroxyacid methyl esters (3-HAME)

Sample preparation for determination of the PHA content of the dried bacterial biomass and monomer composition of the PHA followed the acid-catalyzed methanolysis procedure described previously (Brandl et al. 1988). In this process, 5-to10 mg (exact mass was noted) of dried biomass was weighed and placed into a 10 mL reaction vial. Following this, 1 mL of 15% H_2SO_4 in methanol and 1 mL of chloroform with a 1 mg mL^{-1} benzoic acid internal standard (IS)

were added to the reaction vial. These were then sealed tightly with a screw-cap lid and placed in a boiling water bath for 5 h. After removal from the water bath and cooling to room temperature, 1 mL of distilled H_2O was added to the reaction vial. The vial was the capped, vortexed, and left undisturbed overnight to allow phase separation. The chloroform layer was then extracted (taking care not to extract any of the upper aqueous layer) using a needle with a 1 mL syringe and transferred to 2 mL vials to be analyzed by GC with a flame ionization detector (GC-FID).

3.4.2. Esterification of fatty acids to fatty acid methyl esters (FAMEs)

Fatty acids were converted to fatty acid methyl esters (FAMEs) using the same methanolysis procedure described in Section 3.4.1. For estimation of residual free fatty acids (FFAs) in the culture medium, 1 mL of culture supernatant (allowed to come to room temp and vortexed vigorously) was added to the reaction vial. This vial was then placed in a 60 °C oven overnight (no more than 16 h) to remove approximately 75% of the water in the sample. The latter step was found to improve reliability of the results compared to direct methanolysis of 1 mL of the culture supernatant, probably due improved reaction efficiency because of: 1) lack of dilution of the H_2SO_4 catalyst and methanol alkylation agent; and 2) lack of phase separation when mixing aqueous culture medium with chloroform.

Although a commercial fatty acid standard (described in Section 3.5) was used to obtain the GC response factors (RFs) for FAME components, separate fatty acids standards were prepared each time this analysis was done to confirm the RFs and account for any volatilization during the oven-drying process. These were prepared by adding known masses of the appropriate fatty acids to the reaction vial, suspending them in Ramsay medium, and putting them in the 60 °C oven simultaneously with the samples, and then methanolysed and analyzed with the sample set.

3.5. Quantification of methyl esters by GC-FID

3.5.1. GC setup and operating method

The methyl esters were quantified using an Agilent 7890 GC equipped with a split-splitless inlet, an Agilent DB-23 capillary column (30 m × 250 μm × 0.25 μm) and flame ionization detector (Aglient Technologies, Santa Clara, CA). Helium (He) was used as the carrier gas in constant flow mode at a flow rate of 1.78 mL min^{-1}. The inlet was operated in split mode (split ratio 10:1) and maintained at 260 °C. A sample volume of 1 uL was injected using a CombiPAL automated injector (CTC Analytics AG, Zwingen, Switzerland). Following injection, the oven and column were maintained at 60 °C for 2 min and then the temperature was subsequently ramped at 15 °C min^{-1} to 250 °C and held at 250 °C for 5 min. The detector was maintained at 275 °C and used compressed air and H_2 at flow rates of 400 and 35 mL min^{-1}, respectively, with a makeup flow rate (He) of 25 mL min^{-1}. All gases were ultra-high purity (5.0) and were purchased from Welders Supply (Winnipeg MB).

3.5.2. Determination of RFs and PHA content, composition of sample biomass

The RFs for mcl-PHA monomers were quantified using C_6, C_8, C_{10}, C_{12}, and C_{14} 3-hydroxyacid analytical standards (Sigma-Aldrich, St. Louis MO). Since standards with unsaturation ($C_{12:1}$, $C_{14:1}$)were not available commercially, the RFs for these compounds were assumed to be the same as C_{12} and C_{14} respectively. The standards were methanolysed as described above using a 1 mg mL^{-1} benzoic acid IS. The RFs for individual fatty acids were obtained a Supelco 37-FAME standard (Sigma-Aldrich St. Louis MO). The samples were then analyzed using the GC-FID method described and RFs for a given i^{th} component (C_i) were determined as shown in Equation 3.2.

$$RF_i = \frac{Response\ ratio}{Amount\ ratio} = \frac{\frac{C_i\ peak\ area}{IS\ peak\ area}}{\frac{mass\ C_i}{mass\ IS}} \qquad \text{Equation 3.2}$$

The mass of each C_i in the sample biomass was determined from the chromatogram peak areas as shown in Equation 3.3.

$$Mass\ C_i = \frac{C_i\ peak\ area \times IS\ mass}{IS\ peak\ area} \times RF_i \qquad \text{Equation 3.3}$$

The $\%_{PHA}$ was determined on a mass basis as summation of the masses of individual detected mcl-PHA monomer components (C_i) divided by the total sample mass as shown in Equation 3.4. For study of mcl-PHA, i = 6, 7, 8, 9, 10, 12, 14, and can even include mono- and poly-unsaturated monomers of C_{12} ($C_{12:1}$, $C_{12:2}$) and C_{14} ($C_{14:1}$, $C_{14:2}$) depending on the growth substrate. However, in this work, the most relevant monomers for much were even-chain lengths.

$$\%_{PHA} = \frac{100 \times \sum_{i=6}^{n} Mass\ C_i}{total\ sample\ mass\ added\ to\ reaction\ vial}\ (\%\ g\ g^{-1}) \qquad \text{Equation 3.4}$$

The mole fraction (f) of a given PHA monomer component, C_i, was determined as shown in Equation 3.5. As previously defined, M is used to denote molar mass and M_{Ci} represents the molecular mass of the ith 3-hydroxyacid monomer component C.

$$f_{C_i} = \frac{\frac{Mass\ Ci}{M_{C_i}}}{\sum_{i=6}^{n} \frac{Mass\ C_i}{M_{C_i}}}\ (mol\ mol^{-1}) \qquad \text{Equation 3.5}$$

The monomer composition of the polymer was determined on a mole basis using the values for M shown in Table 3.1.

Table 3.1. Molecular masses of 3-hydroxyacid monomers detected in mcl-PHA analysis by GC.

Saturated mcl-PHA monomers	*M* (g mol^{-1})	Unsaturated mcl-PHA monomers	*M* (g mol^{-1})
C6	132	C12:1	214
C8	160	C14:1	242
C10	188		
C12	216		
C14	244		

3.6. PHA titer, non-PHA residual biomass, and specific growth rates

The PHA concentration or titer, [X_{PHA}], was determined as the concentration of PHA per liter of aqueous medium as follows:

$$[X_{PHA}] = [X_t] \times \%_{PHA} \ (g\ L^{-1}) \qquad \text{Equation 3.6}$$

The concentration of non-PHA residual biomass, [X_r], is an important indicator of cell growth. This was determined as the difference between [X_t] and [X_{PHA}].

$$[X_r] = [X_t] - [X_{PHA}] \ (g\ L^{-1}) \qquad \text{Equation 3.7}$$

Since the accumulation of PHAs causes neither OD_{600} nor total biomass to be reflective of cell growth the specific growth rates (μ) were quantified using X_r as follows, where t_2 and t_1 represent two time points (h) and square braces indicate concentration. The μ_{max} for a given set of conditions was estimated as the maximum value for μ between any two consecutive time points, t_2 and t_1.

$$\mu = \frac{\ln(X_r|_{t_2}) - \ln(X_r|_{t_1})}{t_2 - t_1} \ (h^{-1}) \qquad \text{Equation 3.8}$$

3.7. Productivity calculations

Two indications of productivity were used in this work. The Q_v (volumetric productivity) is regarded as the most fundamental indicator of overall process rates or performance. As

indicated in Equation 3.9, Q_v for a process is highly dependent on [X_t], $\%_{PHA}$, as well reaction rates, as indicated by cultivation time (h).

$$Q_V = \frac{[X_{PHA}]}{Cultivation\ time} \quad (g\ L^{-1}h^{-1}) \qquad \text{Equation 3.9}$$

The Q_s (specific productivity) is an indicator of the PHA synthesis rate (per gram X_r) and is not dependent on [X_t]. As indicated in the denominator in Equation 3.10, the X_r is assumed to be the mean value of the measured X_r at the start of the interval (t_1) at the end of the interval (t_2).

$$Q_s = \frac{X_{PHA}|_{t_2} - X_{PHA}|_{t_1}}{\left(\frac{X_r|_{t_2} + X_r|_{t_1}}{2}\right)(t_2 - t_1)} \qquad \text{Equation 3.10}$$

3.8. Yield calculations

The $Y_{PHA/S}$ was calculated as the slope of a plot between substrate uptake on the x-axis and PHA titer on the y-axis, and in this work is expressed on either a mass or C-mol basis. The maximum theoretical yield of mcl-PHA from a fatty acid substrate was calculated using a modified version of a previous approach (Weusthuis et al. 1997). While that work had assumed that palmitic acid was converted solely to 3-hydroxydecanoic acid (four β-oxidation cycles), in this approach we have corrected the analysis to account for the relatively amorphous composition of mcl-PHAs produced from most fatty acid substrates other than octanoic acid. However, for the sake of consistency, this approach was followed with octanoic acid. It was assumed that the molar composition of mcl-PHA was the weighted average of the content of the GC-detectable monomers. The molar composition of substrates with mixed composition, such as LCFAs derived from canola oil, was determined in the same way. The maximum theoretical (chemical) yield was then determined as the ratio of molar masses for an average PHA monomer to that of an average substrate molecule. Following this analysis, it was determined that each mole of polymer derived from octanoic acid contained on average 7.9 moles of carbon and had

an average molecular mass of 159.4 g mol^{-1}. Likewise, it was calculated that each mole of LCFA PHA monomers contained 10.3 moles of carbon had an average molecular mass of 194.7 g mol^{-1}. This resulted in maximum theoretical yields for octanoic acid, oleic, and canola-derived LCFA of 0.98 g g^{-1}, 0.69 g g^{-1}, and 0.71 g g^{-1}, respectively. As described in Chapter 2, this analysis assumes that the maintenance requirement and/or anabolic demand during PHA-producing conditions are negligible.

3.9. Estimation of residual free ammonium

Residual ammonium in the culture medium was determined via the Lachat QuikChem® Method 10-107-06-1-J. Briefly, this method uses a spectrophotometer coupled to a flow injection system (Lachat Instruments, CO) that measures the blue color change resulting from the reaction of alkaline phenol and sodium hypochlorite with ammonia to form indophenol blue, which is measured at 630 nm. The samples were filtered through a 0.45 μm filter and diluted in distilled water (minimum 3 mL total volume) such that the total concentration of free NH_4 did not exceed 25 mg L^{-1}. This resulted in approximately a 10-fold dilution for every 1 g L^{-1} of $(NH_4)_2SO_4$.

3.10. Reactor setup

All reactor experiments were conducted in a 7 L glass, round-bottom reactor (total aspect ratio: 2.3). The reactor was equipped with a lip-sealed direct drive stirring motor, external heating jacket, automated peristaltic pumps for pH control, 12 mm x 325 mm Applisens® electrochemical DO probe (unless otherwise specified) and gel-type pH electrode. The inside of the reactor was consisted of a single Rushton impeller (60 mm OD), three baffles, an adjustable liquid sampling pipe (4 mm ID), and a heat exchanger that formed a loop just below the impeller. Tap water was circulated through this heat exchanger for cooling when necessary. Heating was

accomplished via an 80W external jacket that received feedback from a Pt-100 temperature probe. Aeration was accomplished with an L-type sparging tube with small holes in the bottom of the tube located beneath the impeller, although this setup could be modified as described in subsequent chapters. The reactor top plate was equipped with a water-cooled condenser, gas-sampling port, a triple inlet port for pH control or addition of other reagents, a sleeve for the temperature sensor, and a vacuum bottle for liquid sampling. All reactor equipment was purchased from Applikon Biotechnology (Foster City, CA).

3.10.1. Calibration of pH and DO electrodes

The pH electrode was calibrated using standards of pH 4.0 and 7.0 (Fisher Scientific, Toronto, ON) prior to autoclaving. Good calibrations were assumed to have a slope of approximately 1 and an offset less than ± 0.5. If either the slope or offset was outside this range, the calibration was repeated. The DO electrolyte solution (Applikon Biotechnology, Foster City, CA) was discarded prior to each run and the membrane was rinsed with distilled water, and then rinsed again with electrolyte solution, before 1 mL of new electrolyte solution was added.

Calibration of the DO electrode was performed just prior to the experiment at the same temperature (30 °C) and aeration rate as was to be maintained during the experiment. Air was used as the aeration medium in all studies unless otherwise indicated. A two-point calibration was carried out by gassing the reactor with N_2 at 500 mL min^{-1} until the electrode current was stable at 0 mA, then aeration was turned on at 6 LPM. After the electrode current had stabilized, this was assigned a value of 100% of air saturation at 30 °C, which will be referred to simply as a percentage hereafter. It was assumed that the solubility of O_2 in the medium at 30 °C was 6.77 mg L^{-1} (Vendruscolo et al. 2012). Since the slope of a one-point calibration was found to be in

good agreement with the described two-point calibration, one-point calibrations (at operating conditions) were subsequently performed.

3.10.2. Reactor preparation and sterilization

The medium was prepared and added to the reactor to an initial working volume of 3 L. Either a silicone-based anti-foaming agent obtained from Husky Energy (Minnedosa, MB) or Antifoam 204, an organic mixture of polyether dispersions (Sigma-Aldrich Antifoam 204, St. Louis, MO) was added. The silicone-based antifoam was added at a concentration of 200 uL per 3 L, whereas the polyether-based solution was added 50 uL per 3 L. The reactor was then autoclaved at 121 °C for 40 min, and the tubing on the top of the condenser was left un-clamped to relieve pressure. Following sterilization, the reactor was set up and allowed to cool to 30 °C. During this time, mixing was left on at 250-350 rpm and aeration was left on at a low flow rate to achieve slight positive pressure. To avoid evaporation losses due to aeration through the medium at elevated temperatures, cold water was circulated from an insulated ice bath to the condenser with a peristaltic pump.

Once the temperature reached 30 °C, the carbon source was added aseptically (either sterilized separately and added with a needle and syringe or filter-sterilized directly into the reactor, depending on the nature of the substrate). The acid and base lines were then primed and connected to the reactor and the pH was adjusted to the set point. The pH dosing monitors were then reset, and this setup was left overnight and ready for inoculation the next morning.

3.11. Detection and quantification of CO_2

Water vapour was removed from the reactor off-gas using the factory condenser mounted on the bioreactor top-plate. The condenser was chilled using water from an ice bath that was

circulated with a peristaltic pump. CO_2 in the condensed reactor off-gas stream was measured with a Hiden HPR-40 dissolved species membrane inlet mass spectrometer (MIMS, Hiden Analytical, Warrington, UK) or a Blue-in-One Cell infrared CO_2/O_2 sensor (Bluesens Gas Sensor, GmbH, Germany). The MIMS was equipped with a HAL 201 RC quadrupole mass analyzer (70 eV electron impact ionization energy), Faraday Cup detector, and MasSoft 7 software. CO_2 was measured at a mass-to-charge ratio (*m/z*) of 44. Calibration of the MIMS for CO_2 was done using a four-point background subtracted calibration curve. Known concentrations of CO_2 (in the range 0-5 mol%) were diluted from purchased gas mixtures of known concentration (Welder's Supply, Winnipeg, MB). The dilutions were performed in N_2 gas using thermal mass flow controllers (EL-Flow, Bronkhorst Hi-Tech, Ruurlo, The Netherlands). These gases were bubbled through the reactor (under operating conditions but without cells) and passed through the ice-bath cooled condenser mounted to the reactor top plate to mimic experimental conditions. The reactor was sparged with N_2 until the *m/z* 28 spectrum was stable, and then each step increase in concentration was given two hours to ensure stable signals. The standard factory calibrations of 0-25 mol% CO_2 and 0-50 mol% O_2 were used for the Blue-in-One sensor, although periodic recalibrations were done using by purging room air through it with an aquarium pump.

The measured CO_2 in the reactor off-gas was related to the concentration of dissolved CO_2 concentration through Henry's Law, as shown in Equation 3.11. Use of this equation assumes that the gas phase is at a state of thermodynamic equilibrium with the liquid phase.

$$[CO_2]_{(aq)} = k_H \times P_{CO_2} \qquad \text{Equation 3.11}$$

where, $[CO_2]_{(aq)}$ is the concentration of dissolved CO_2 in the medium, k_H is the Henry's Law coefficient for CO_2 (0.0352 mol L^{-1} atm^{-1}) and was obtained as the temperature-corrected value

(Sander 1999) and P_{CO2} is the partial pressure of $CO_{2(g)}$ in the reactor headspace. The total dissolved carbonate species were determined following a previous approach (Blunt 2013), which is summarized in Equation 3.12-3.16:

$$CO_{2(aq)} + H_2O \overset{K_0}{\leftrightarrow} H_2CO_3 \overset{K_1}{\leftrightarrow} HCO_3^- + H^+ \overset{K_2}{\leftrightarrow} CO_3^- + 2H^+ \quad \text{Equation 3.12}$$

$$[H_2CO_3] = \frac{[CO_2]_{(aq)}}{K_0} \quad \text{Equation 3.13}$$

$$[HCO_3^-] = \frac{K_1[H_2CO_3^*]}{10^{-pH}} \quad \text{Equation 3.14}$$

$$[CO_3^{2-}] = \frac{K_1K_2[H_2CO_3^*]}{10^{-2pH}} \quad \text{Equation 3.15}$$

In the above equations, K_0 (350-990), K_1 (4.46×10^{-7}), and K_2 (4.69×10^{-11}) are equilibrium constants (Goldberg et al. 2002). The equilibrium for the reaction involving K_0 lies far to the left (at room temperature and irrespective of pH) such that $[CO_2]_{(aq)} >> [H_2CO_3]$ (Pratt et al. 2003; Yang et al. 2003). Therefore Since H_2CO_3 is difficult to measure, it is typically lumped together with $[CO_2]_{(aq)}$ in the term $[H_2CO_3^*]$, which is known as the total analytical concentration of dissolved CO_2 (Stumm and Morgan 1995). The $[H_2CO_3]$ accounts for only 0.2% of $[H_2CO_3^*]$ (Yang et al. 2003). The total concentration of dissolved carbonate species (C_T) was then determined as shown in Equation 3.16.

$$[C_T] = [H_2CO_3^*] + [HCO_3^-] + [CO_3^{2-}] \quad \text{Equation 3.16}$$

The total CO_2 production in moles at any time ($G_{CO2}(t)$) was estimated as the summation of dissolved carbonate species in the liquid, the CO_2 in the reactor headspace, and the sum of CO_2 that had been purged through the reactor (i.e. the measured concentration integrated over the gas flow rate to the reactor) as shown in Equation 3.17. It was assumed that the reactor headspace was completely mixed and biological CO_2 production rate was negligible in comparison to the gas flow rate to the reactor.

$$G_{CO_2}(t) = \left([C_T]V_L + [CO_2]_{(g)}V_g\right)|_t + \frac{P\dot{V}_a}{RT}\int_{t=0}^{t-1}[CO_2]_{(g)}\,dt \qquad \text{Equation 3.17}$$

where V_L and V_g are the liquid and headspace volumes in the bioreactor, respectively. P is the pressure in the reactor headspace (open to the atmosphere and assumed to be 1 atm), $\dot{V}_a$ was defined previously as the volumetric air flow rate to the reactor (LPM), R is the ideal gas constant (0.0821 L mol^{-1} K^{-1}), and T is the reaction temperature (303.15 K).

3.12. Carbon balancing

Carbon recovery (C-mol C-mol^{-1}) was determined at any point in time during the cultivation with knowledge of CO_2 production (Equation 3.16) X_r, X_{PHA}, monomer composition of the PHA, and substrate consumption as shown in Equation 3.18.

$$Carbon\ recovery\ = \frac{\sum_{i=6}^{n} iX_{PHA}f_{C_i} + 4\times\frac{X_r V_L}{101} + G_{CO_2}}{C\text{-}mol\ susbtrate\ consumed} \qquad \text{Equation 3.18}$$

where i represents the number of C-moles per mole of PHA monomer component C_i. f_{Ci} represents the molar fraction of component C_i in the polymer (Equation 3.5). For most analyses performed in this work i = 6, 8, 10, 12, and 14. It was assumed that the non-PHA bacterial biomass (X_r) had the elemental composition $C_4H_7O_2N$ and had a molecular mass of 101 g mol^{-1} (Guedon et al. 1999).

3.13. Determination of volumetric oxygen transfer coefficient (k_La)

The k_La was determined in medium without cells but otherwise under operating aeration rate and temperature using the dynamic out-gassing (Garcia-Ochoa et al. 2010). Briefly, the reactor was gassed with N_2 at 500 mL min^{-1} until the DO signal was stable. Subsequently, aeration was turned on at the experimental flow rate (generally 3-6 LPM) and the DO response was measured and recorded in LabBoss software in 10 second (s) intervals. This generated a DO profile as is exemplified in Figure 3.1 using distilled water.

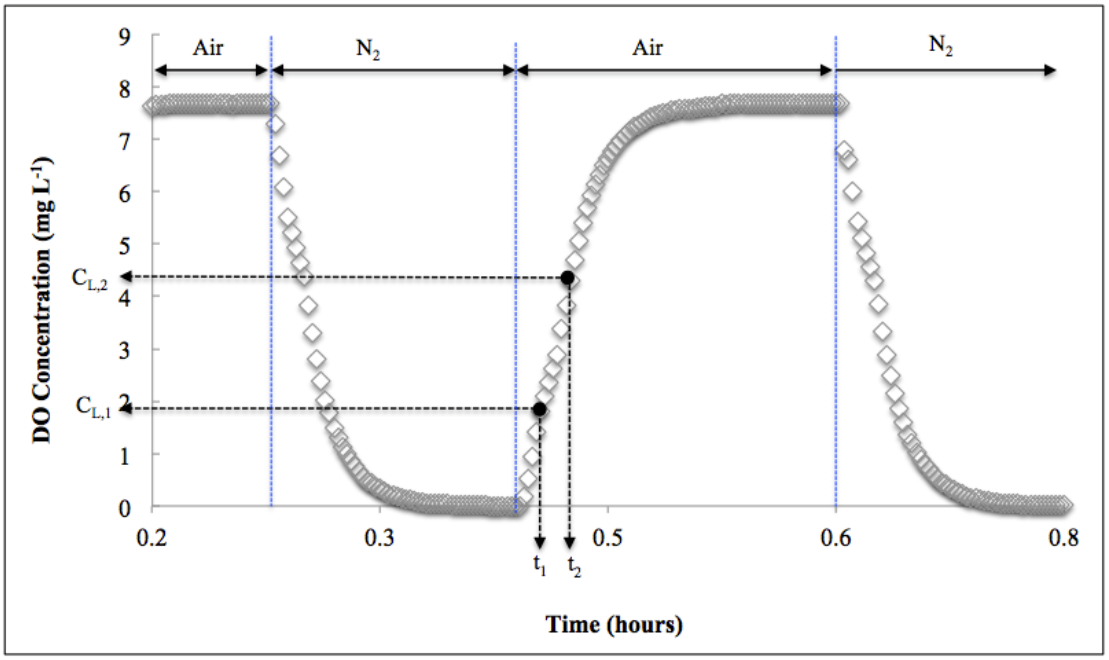

Figure 3.1. Typical DO profile during N_2-sparging and aeration phases for k_La determination via the dynamic method.

As shown in Figure 3.1 two points were selected at time t_1 and t_2 during the aeration phase corresponding to DO concentrations $C_{L,1}$ and $C_{L,2}$ respectively. The k_La was then determined as the slope of a plot between the natural logarithm of the difference between the equilibrium DO concentration and $C_{L,1}$ and $C_{L,2}$ and time. This is shown in Equation 3.19. In practice, this was done for many points for $C_{L,1}$ and $C_{L,2}$ along the aeration curve, although a better fit was obtained using a curve where the extreme values were omitted (Merchuk et al. 1990).

$$k_L a = \frac{ln\left(\frac{C^* - C_{L,2}}{C^* - C_{L,1}}\right)}{t_2 - t_1} \qquad \text{Equation 3.19}$$

It was assumed that the probe response could be modeled as first order, and this was accounted for following a previous approach (Merchuk et al. 1990). The response time was determined to

be 24 s, which was measured as the time to reach 63.2% of the final DO value when subject to a step change in DO concentration (Doran 2013).

Chapter 4: Microaerophilic environments improve the productivity of medium chain-length polyhydroxyalkanoate biosynthesis from fatty acids in *Pseudomonas putida* LS46

4.1. Preface

This chapter represents the earliest research that was done with the objective of investigating why shake flask cultures of *P. putida* LS46 behaved so differently from initial bioreactor cultures using octanoic acid as the carbon source under supposedly similar conditions. It was suspected that oxygen limitation was responsible for driving mcl-PHA accumulation in flask cultures. This work aimed to show how growth and mcl-PHA synthesis characteristics (from octanoic acid) were affected by varying degrees of oxygen limitation in simple low-cell density batch experiments. The work described in this chapter is original research that was published in a "*Polymer/Fibre*" special issue of *Process Biochemistry* 59: 18-25. I alone was responsible for the experimental design, performing of experiments, analyzing and interpreting the data, and preparation of the manuscript. Christopher Dartiailh contributed with thoughtful and challenging discussions on the results and, along with the other co-authors, reviewed the manuscript prior to publication.

4.2. Abstract

Synthesis of medium chain length polyhydroxyalkanoates (mcl-PHA) from fatty acids is an oxidative process. Growth and mcl-PHA synthesis were studied in *Pseudomonas putida* LS46 when subjected to a spectrum of oxygen transfer rates, which were intended to simulate DO gradients likely to be encountered during process scale-up. It was found that maintaining DO at 1–5% (of air saturation at 30 °C) initiated significant mcl-PHA synthesis and concurrent growth at < 0.5 μ_{max} was also observed. Further reductions in DO resulted in nearly negligible growth,

but improved biopolymer synthesis. When k_La was reduced to 38 h^{-1}, DO was below detectable limits and both the PHA content (57.3 ± 3.8% CDM) and yield (0.62 ± 0.06 g mcl-PHA g octanoic $acid^{-1}$) reached the maximum observed values. Under these conditions, the maximum rate of polymer synthesis was also observed (227.9 ± 9.8 mg PHA g X_r^{-1} h^{-1}), and this value was higher than that which could be achieved using NH_4 limitation. Further reductions in oxygen transfer rate did not improve productivity, and PHA synthesis completely ceased when aeration was replaced with N_2 gassing. These results suggest that manipulation of the bioreactor oxygen transfer rate during the PHA accumulation phase could be a strategy used to improve overall productivity during a fed batch or continuous feed process.

4.3. Introduction

Medium chain length polyhydroxyalkanoates are C_6-C_{14} polyesters synthesized by bacteria and have potential value for diverse set of applications (Madison and Huisman 1999; Masood et al. 2015). Currently production costs are too high for economically viable, commercial scale mcl-PHA production (Fu et al. 2014). Development and subsequent scale up of production strategies targeting high overall productivity (a function of reaction rates, yield, and product titer) can help reduce costs and secure the future of mcl-PHA as a commercially valuable biopolymer (Hazenberg and Witholt 1997; Kaur and Roy 2015).

To synthesize a significant amount of mcl-PHA, most bacteria require nutrient imbalance and to achieve this, medium components like carbon, ammonium, or phosphate are added in growth-limiting quantities (Braunegg et al. 2004). During mcl-PHA production and many strictly aerobic bioprocesses, gas-to-liquid mass transfer of O_2 is often rate limiting and has a significant impact on the overall productivity (Lara et al. 2006b; Maclean et al. 2008; Garcia-Ochoa and Gomez 2009). Several studies have supplemented aeration of the medium with pure O_2 to

increase the driving force for mass transfer (Lee et al. 2000b; Maclean et al. 2008; Sun et al. 2009a; Gao et al. 2016). Operating bioreactors at elevated pressure has also been used to increase the driving force, although increased pressure has also been shown to have a negative impact on k_La (Follonier et al. 2012; Lopes et al. 2013). Both strategies aim to prolong the growth phase before oxygen mass transfer becomes rate limiting to achieve higher cell densities and increased Q_v. However, the effect that low DO environments, likely to be encountered in larger-scale and high cell density cultivations, have on mcl-PHA synthesis has not been considered in detail. Low DO has been reported to increase the $\%_{PHA}$ in several microorganisms that produce PHB from a variety of substrates (Senior et al. 1972; Kshirsagar et al. 2012; Faccin et al. 2013). Using mixed microbial cultures, Pratt et al. (2012) observed increased yield during the early stages of growth in low DO environments, but the rate of accumulation was lower than in high DO environments (Pratt et al. 2012). Some studies have also reported changes in the monomeric composition of both scl-and mcl-PHA when the culture was subject to low DO environments (Lefebvre et al. 1997; Fernández et al. 2005).

Given that cellular redox state has been linked to mcl-PHA synthesis (Ren et al. 2009), availability of O_2, the redox state of the substrate could play a role in mcl-PHA synthesis. Structurally related substrates (alkanes, alkanoic acids) are highly reduced and are preferred for mcl-PHA synthesis due to the high yield (Maclean et al. 2008; Sun et al. 2009a; Gao et al. 2016). Production of mcl-PHA from such substrates requires intermediates of the β-oxidation cycle (Huijberts and Eggink 1996). This is an oxidative process (in contrast to synthesis of PHB from glucose) in which FAD and/or NAD^+ are used as electron acceptors, and these must be regenerated by electron transport to O_2. Therefore, mcl-PHA synthesis from highly reduced substrates (i.e. longer-chain fatty acids compared to glucose) under oxygen-limited conditions

would be a phenomenon of interest. Little information is available regarding how mcl-PHA production (from fatty acids or other substrates) responds to low DO environments, particularly compared to short chain length (scl-) PHA production. Several studies have reported improved scl-PHA polymer production from carbohydrate substrates in low DO environments (Senior et al. 1972; Kshirsagar et al. 2012; Faccin et al. 2013).

In this work, we have used a scaled-down approach to assess mcl-PHA production rates in low DO environments using *Pseudomonas putida* LS46 grown on octanoic acid in bench scale bioreactors operated in batch mode. The objective of this study was to understand how O_2 mass transfer limitations affect growth and mcl-PHA biosynthesis from fatty acids.

4.4. Materials and Methods

4.4.1. Micro-organism, medium, and substrates

The microorganism, strain maintenance practices, and medium were all as described in Sections 3.2. However, the medium for bioreactor experiments was slightly modified by increasing the concentration of $(NH_4)_2SO_4$ to 11.35 mM (1.5 g L^{-1}) to ensure excess ammonium throughout each trial. The substrate for all studies was octanoic acid, added to an initial concentration of 20 mM (2.88 g L^{-1}).

4.4.2. Bioreactor setup and preparation

The bioreactor setup, sterilization and calibration procedures were the same as that described in Section 3.10. The transfer capability of the reactor was improved through the addition of two Pyrex microbubblers, which were connected to the existing sparging tube with Masterflex LS25 tubing (4.8 mm inner diameter), and located underneath the impeller. In all experiments, the pH was controlled at 6.5 through the addition of 1 M NaOH or 1 M HCl by

automated peristaltic pumps.

4.4.3. Oxygen transfer conditions

Atmospheric air was used for sparging the culture in all studies. The volumetric flow airflow rate was held constant in all experiments at either three or six LPM, equal to one or two VVM, respectively. A mixing cascade (250–900 rpm) was used to maintain DO at levels above detectable limits (non-zero readings with the DO electrode). Since some of the conditions tested were below the threshold of detection of the DO electrode, these were characterized by k_La, which was measured via the dynamic out-gassing method (see Section 3.12). It was assumed that the probe response could be modeled as first order (Merchuk et al. 1990). Due to insufficient response time of the DO electrode, k_La could not be reliably measured for $k_La > 310$ h^{-1}, which corresponded to mixing rates of approximately 600 rpm. An HPR-40 dissolved species MIMS equipped with a HAL 201 RC quadrupole mass analyzer and Faraday Cup detector (Hiden Analytical, Warrington, United Kingdom) was also used to estimate DO concentrations for conditions below the detection threshold of the DO electrode. A summary of the oxygen transfer conditions tested is presented in Table 4.1, and a minimum of two biological replicates was performed for each condition. It was assumed that the oxygen solubility in the culture medium at 30 °C and under atmospheric conditions was 6.77 mg L^{-1}, which was measured previously in a minimal medium (Vendruscolo et al. 2012). When DO is expressed as a percentage, it refers to these conditions.

4.4.4. Reactor Monitoring

Experiments were initiated with the addition of 1% (vol vol^{-1}) inoculum. At this time, the medium at 30 °C was saturated with air, (DO = 100%) and the DO was allowed to fall until the

indicated set point was reached. A 40 mL sample of culture was taken in one to two hour intervals from the reactor for analyses.

Table 4.1. Summary of the tested bioreactor OTRs and DO concentrations.

DOC			k_La	$\dot{V}_a$	N_a
%	mg L^{-1} O_2	μM O_2	h^{-1}	LPM	rpm
0	0.02[a]	0.53	38	3	250
0	0.04[a]	1.28	78	6	250
1	0.07[b]	2.12	$78 < k_La < 145$	6	250-410
5	0.34[b]	10.58	$78 < k_La < 310$	6	250-620
10	0.68[b]	21.16	$78 < k_La < 540$[c]	6	250-740
40	2.71[b]	84.65	$78 < k_La < 1016$[c]	6	250-900

[a]reported results were measured with a MIMS; [b]results measured with electrochemical DO probe; [c]k_La values > 310 $hour^{-1}$ could not be reliably measured due to insufficient response time of probe. Higher values are estimated by extrapolating the trend from the range that could be reliably measured with the probe.

4.4.5. Measurement techniques

Details are given elsewhere for sample treatment and gravimetric determination of total (Section 3.3) and residual (Section 3.6) biomass, sample preparation for analysis of PHA and residual octanoic acid by GC-FID (Sections 3.4. and 3.5), and spectrophotometric determination of residual free ammonia (Section 3.9).

Assessment of performance metrics were done as previously described, including: specific growth rates, which were assessed at the target DO conditions as described in Section 3.6; specific and volumetric productivity (Section 3.7); and yield calculations (Section 3.8). Off-gas CO_2 measurement was done with the MIMS setup described in Section 3.11 for the purpose of carbon balancing (Section 3.12). Carbon dioxide measurements were not available for every experiment, so it was assumed that the left hand side of Equation 3.18 was equal to one, permitting CO_2 production to be back calculated.

4.5. Results and Discussion

4.5.1. Growth rate

Figure 4.1(a) shows sample growth curves for a representative O_2-excess condition, while an O_2-limited condition is represented in Figure 4.1(b). The target DO was typically reached about 6 h after inoculation in each trial, when the cells had grown to an average [X_t] of 0.7 g L^{-1} CDM. Figure 4.2 shows the change in μ at different DO conditions. Due to the lack of sensitivity of the bioreactor probe in conditions when the DO was not controlled (constant mixing at 250 rpm and constant aeration at either 3 LPM or 6 LPM), the MIMS was used to confirm the DO concentration in these two conditions (Table 4.1). The relationship between growth rate and DO concentration followed Monod kinetics (R^2 =0.99) and the fitted parameters indicated μ_{max} = 0.57 h^{-1} and the O_2 half saturation constant ($K_{s, O2}$) to be 0.19 mg L^{-1} (2.7% AS at 30 °C). This $K_{s, O2}$ value is relatively low compared to the values reported for other *Pseudomonas* species and strains and indicates a high affinity for O_2 (Beyenal et al. 2003; Alagappan and Cowan 2004). A possible explanation for this may be the presence of two putative subunits for a cytochrome bd complex (PPUTLS46_12918 and PPUTLS46_12923) in the genome annotation for the respiratory chains in *P. putida* LS46. Cytochrome bd is a terminal oxidoreductase with a high O_2 affinity (but lower ATP yield) and is expressed in several microorganisms in microaerophilic conditions (Bekker et al. 2009; Borisov et al. 2011). Another study showed that cytochrome bd expression increases dramatically when DO falls below 10%, and reached a maximum at 0% in *E. coli* cultures (Tseng et al. 1996). Based on the relatively steep reduction in growth rate at DO < 10% in *P. putida* LS46, it may be possible that this also occurs in LS46. Proteomic analysis would be necessary to confirm this. Overall, the data indicates that *P. putida* LS46 is capable of not only survival, but also growth in low DO environments (but not environments without O_2).

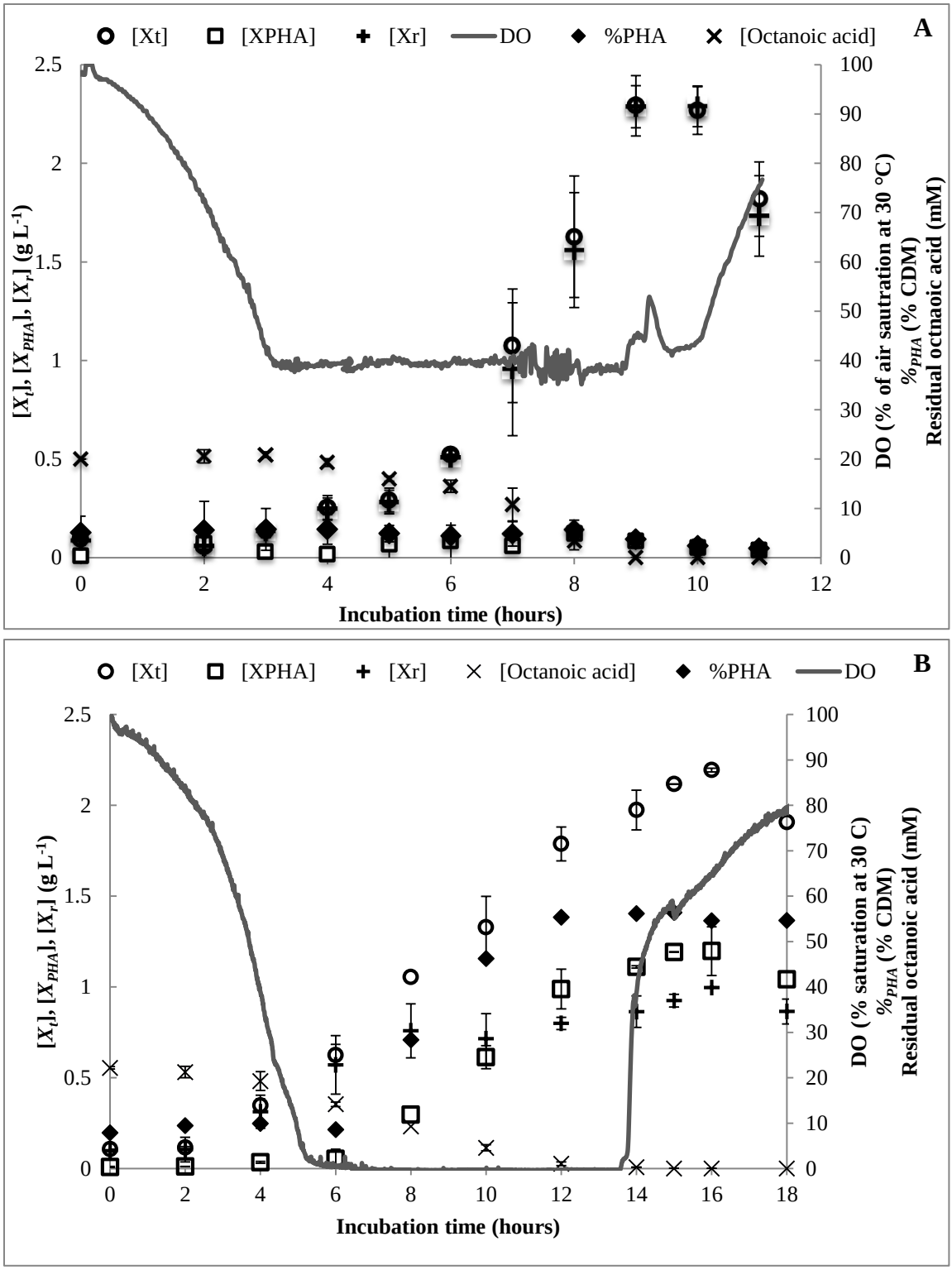

Figure 4.1. Representative growth and mcl-PHA synthesis curves from octanoic acid (C/N ratio of 7.05 C-mol N-mol^{-1}) at high and low DO conditions. a) DO was maintained at 40% and b) condition in which DO was below detectable limits with the bioreactor probe (k_La = 38 h^{-1}). Error bars represent standard deviations between biological replicates.

4.5.2. PHA synthesis characteristics

The maximum $\%_{PHA}$ data (Figure 4.2) shows that little PHA was detected for conditions in which DO was maintained at 10% or higher. A significant increase in $\%_{PHA}$ (up to 41.4% CDM) was first evident when DO was maintained at l%. At the lowest OTR tested (k_La = 38 h^{-1}), the maximum $\%_{PHA}$ was 57.3% CDM. The maximum $\%_{PHA}$ was somewhat variable at 5% DO, ranging from 23-38% CDM. This variability may suggest this condition could be close to a switching point from growth to PHA synthesis. Due to fluctuations in the PID-controlled DO measurement, further resolution was not possible. It appears that little PHA is accumulated when DO > 5% and whilst at DO ≤ 5%, cells begin to accumulate a significant amount of PHA. On the basis of final $\%_{PHA}$ these results indicate that growth in shaker flasks, with the same C/N ratio and low working volumes, is O_2 limited.

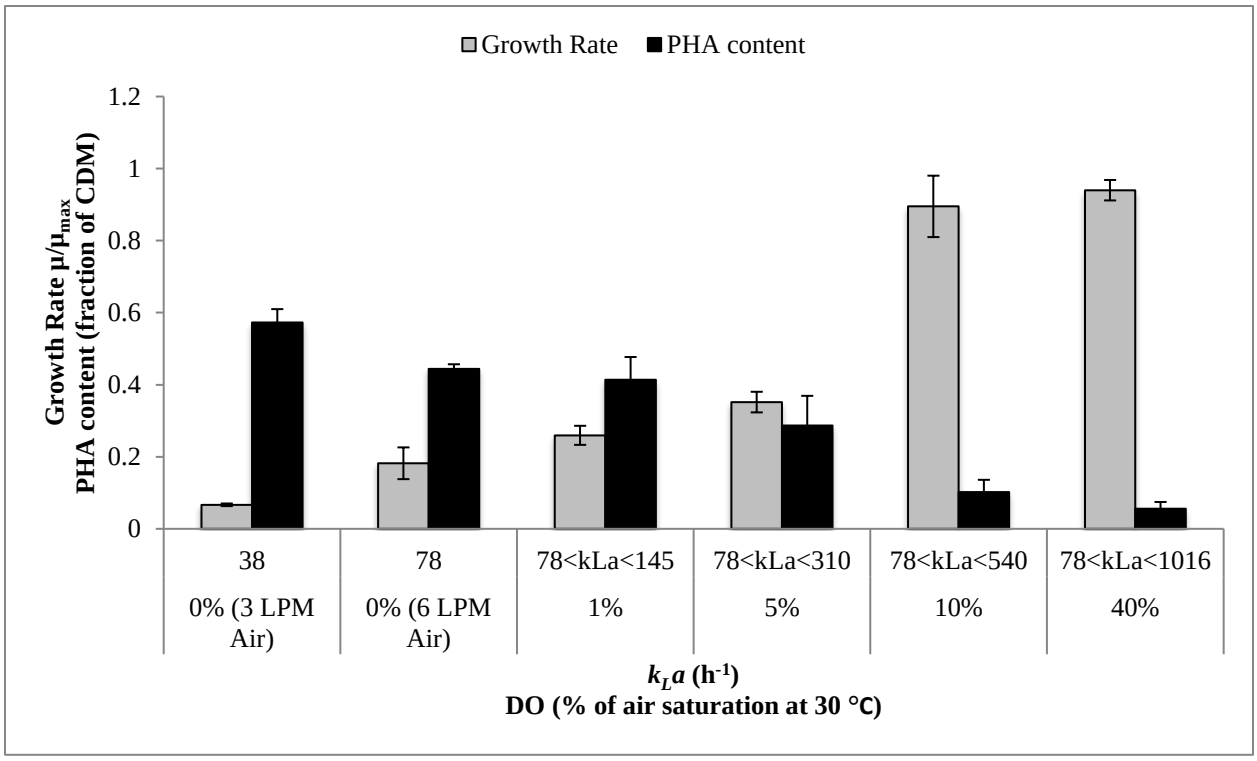

Figure 4.2. Specific growth rates and maximum $\%_{PHA}$ from octanoic acid at different OTRs. Values measured after 6 h of cultivation, or when DO had reached its intended steady state value. The dual label on the x-axis is because k_La more adequately describe conditions that were below the detectable limits of the bioreactor probe, whereas the DO measurement more adequately describes high mixing conditions where measurement of k_La may not be reliable due to mass the response time of the probe (k_La > 300 h^{-1}). Error bars represent standard deviations between biological replicates.

The relationship between O_2 limitation and PHA accumulation was first established as a way for disposal of excess reducing power during synthesis of PHB from glucose in *A. vinelandii* (Senior et al. 1972). Since there is no reductive step during synthesis of mcl-PHA from β-oxidation intermediates, this cannot explain observation of mcl-PHA synthesis from fatty acids in response to low DO. High NAD(P)H/$NAD(P)^+$ ratios have been linked to mcl-PHA synthesis from fatty acids (Ren et al. 2009; Escapa et al. 2012), as well as non-related substrates (Borrero-de Acuña et al. 2014). This redox imbalance would likely occur at low DO and cause inhibition of key enzymes in the TCA cycle (Senior and Dawes 1971). If PHA is produced from

intermediates of the β-oxidation cycle, conversion of either the enoyl-CoA monomers (via an R-specific enoyl-CoA hydratase, PhaJ) or (S)-3-hydroxyacyl-CoA monomers (via epimerase enzyme) to (R)-3-hydroxyacyl-CoA monomers requires only one oxidative step. In this step, the acyl-CoA dehydrogenase enzyme oxidizes acyl-CoA monomers to enoyl-CoA monomers using FAD as the electron acceptor (Madison and Huisman 1999; Sudesh et al. 2000; Magdouli et al. 2015; Prieto et al. 2016). Storage of these monomers as PHA (primarily C_8 and C_{10} in *P. putida*) would generate less reduced electron carriers compared to completion of the β-oxidation cycle. Further oxidation of 3-hydroxyacyl-CoA to 3-ketoacyl-CoA uses NAD^+ as the electron acceptor, and furthermore subsequent oxidation of acetyl-CoA to feed the TCA cycle, and each turn of the TCA cycle produces 3 NADH and 1 $FADH_2$ (Madison and Huisman 1999; Nelson et al. 2008). This would leave more carbon available for PHA synthesis that cannot be effectively further metabolized due to redox imbalance at low DO. Thus, mcl-PHA synthesis from fatty acids at low DO cannot be a 'sink' for electrons that has been previously described in PHB synthesis (Senior et al. 1972), but may be a mechanism for storing electrons as PHA (for subsequent oxidation when more O_2 becomes available) to maintain a balanced redox state. A similar assertion was also made for degradation of PHB to supply reducing power required to elicit an anti-oxidant stress response in *P. putida* 14-3 (Ayub et al. 2009).

This is not the case for synthesis of scl-PHA or mcl-PHA from carbohydrate substrates, since both pathways include reductive steps. Although improved scl-PHA production from carbohydrate substrates in low DO environments has been reported (Senior et al. 1972; Kshirsagar et al. 2012; Faccin et al. 2013), we did not observe any improvement in mcl-PHA production from *P. putida* LS46 cultured on crude glycerol using sequentially lower surface-area-to volume ratios in baffled shaker flasks (data not shown). Further investigation is required,

but this result is in agreement with other studies of mcl-PHA synthesis from non-related substrates via *de novo* fatty acid synthesis (Haywood et al. 1990; Diniz et al. 2004; Poblete-Castro et al. 2014a).

4.5.3. Monomer composition of the polymer

The monomer compositions of the polymer synthesized under the conditions tested are shown in Table 4.2. The monomer compositions were measured as the mean of all samples taken after the DO had reached its target concentration (generally after 6 h). For conditions in which PHA was accumulated the composition was not significantly different in any case. For these cases, the mean monomer composition was 5.9 ± 0.9% C_6, 92.3 ± 1.1% C_8, and 1.9 ± 0.6% C_{10}. However, after the exogenous carbon source was depleted, the C_8 monomers appeared to be consumed first, causing an enrichment of C_6 and C_{10} monomers and significantly different monomer distributions. This suggests that prolonged carbon limitation may cause inconsistent product quality, and the timing of harvest might be critical. Dissolved oxygen has been previously observed to play a role in altering the monomer composition in both scl-PHA and mcl-PHA production. Lefebvre et al. (1997) report that low DO (1-4%) caused more than a two-fold increase in yield of PHV from propionate during production of P(3-HB-co-3-HV) from glucose and propionate using *C. necator* as compared to conditions when the DO was maintained at 50-70% (Lefebvre et al. 1997). Fernández et al. (2005) report that during mcl-PHA production from crude oleic acid using *P. aeruginosa*, lowering the OTR caused significant increase of C_8, $C_{12:1}$ and the appearance of $C_{14:2}$ monomers, while C_{10}, C_{12}, and $C_{14:1}$ all decreased (Fernández et al. 2005). The major distinction between these two previous studies and this work is that we observed lower OTRs to significantly improve biopolymer productivity. Different substrates

produced less homogeneous polymers and should be tested in *P. putida* LS46 to broadly conclude whether or not OTR has an effect on monomer composition.

Table 4.2. Observed monomer compositions produced from octanoic acid at different OTRs.

DOC	k_La	**Monomer Composition (mol%)**		
% AS (30 °C)	h^{-1}	C_6	C_8	C_{10}
0 (3 LPM air)	38	6.0 ± 1.1	92.5 ± 0.8	1.4 ± 0.4
0 (6 LPM air)	78	6.0 ± 0.4	91.9 ± 0.5	2.0 ± 0.6
1	$78 < k_La < 145$	5.6 ± 1.2	92.4 ± 2.1	1.6 ± 0.3
5	$78 < k_La < 310$	4.8 ± 0.4	93.2 ± 0.1	2.0 ± 0.3
10	$78 < k_La < 540$	6.1 ± 1.2	92.3 ± 0.8	1.6 ± 0.4
40	$78 < k_La < 1016$	6.3 ± 0.3	91.6 ± 0.4	2.8 ± 0.9

Tolerances are standard deviations between biological replicates

4.5.4 PHA productivity and yield

Although low DO environments were shown to not only initiate synthesis but also incrementally improve maximum $\%_{PHA}$ in *P. putida* LS46, this is of little relevance unless the production rates and yields are taken into account. Figure 4.3 shows both Q_v (g L^{-1} h^{-1}) and Q_s (mg PHA g X_r^{-1} h^{-1}) obtained at the OTRs tested. As shown, Q_s improved significantly with lower OTRs, indicating an improved rate of polymer synthesis. The highest Q_s was 227.9 ± 9.8 mg PHA g X_r $^{-1}$ h^{-1} and was observed when the DO was below detectable limits (k_La = 38 h^{-1}). Further lowering the OTR by reducing aeration to 1 LPM (k_La = 12 h^{-1}) did not negatively affect Q_s, but reduced the overall Q_v because lower [X_t] was obtained. When aeration was replaced with N_2 gassing, both growth and PHA synthesis completely ceased (data not shown). This might be expected because initial activation of the fatty acid with coenzyme A consumes ATP, and subsequent oxidation of acyl-CoA to enoyl-CoA (the first suitable intermediate for the PHA

synthase) produces $FADH_2$ (Sudesh et al. 2000; Magdouli et al. 2015; Prieto et al. 2016). Consequently, in the complete absence of O_2, imbalance of redox couples would rapidly halt growth and PHA production.

The maximum obtained Q_s in this work (227.9 ± 9.8 mg PHA g X_r^{-1} h^{-1}) compares well with the value reported for *P. putida* KT2442 grown on decanoate under dual nitrogen and carbon limitation, but was lower than the value reported for strict nitrogen limitation (430 mg PHA g X_r^{-1} h^{-1}) (Poblete-Castro et al. 2012b). Interestingly, the maximum Q_s observed in low DO conditions was considerably higher than the value observed in several trials of NH_4-limited batch experiments in which DO was maintained at 40% and the C/N ratio was increased to 21.1 C-mol N-mol^{-1} (data not shown). In these experiments, the maximum Q_s was 140.7 ± 11.0 mg PHA g X_r^{-1} h^{-1}. It appears that a microaerophilic environment may be a stronger driver of PHA synthesis than strict NH_4 limitation in *P. putida* LS46 when cultured on octanoic acid.

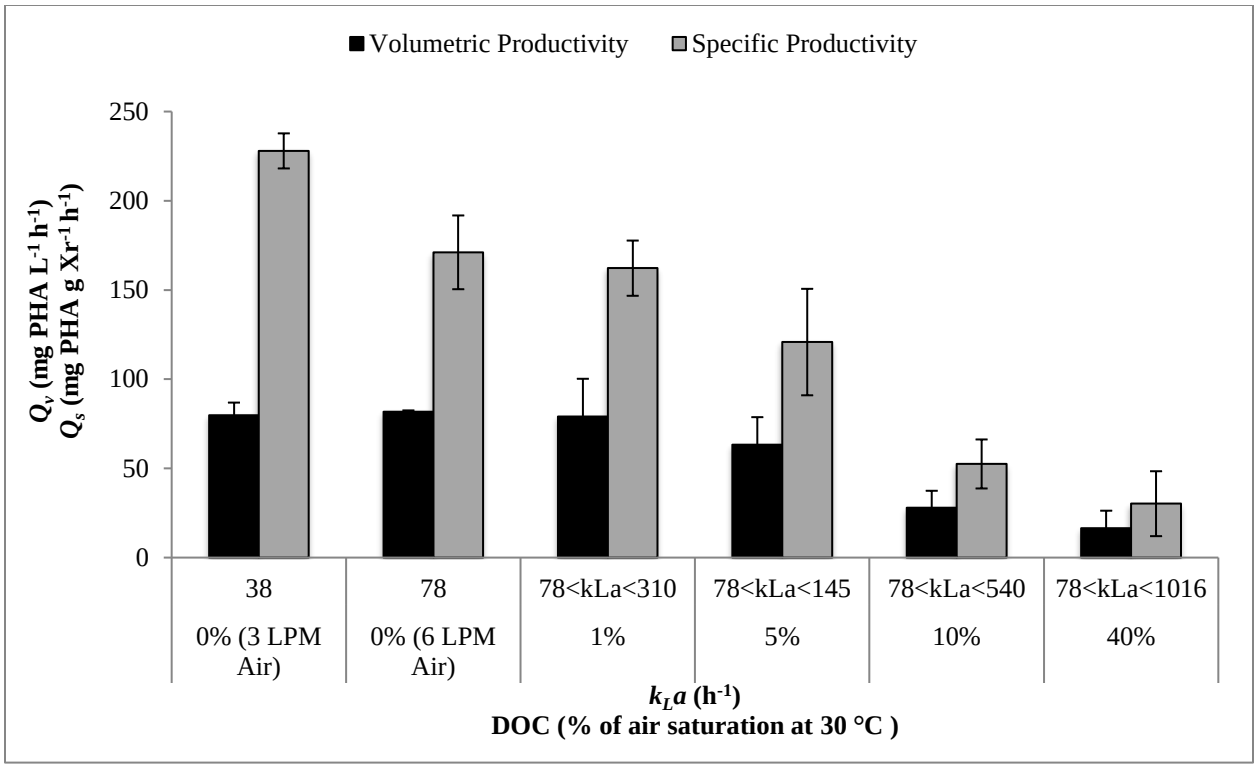

Figure 4.3. Maximum Q_s and Q_v of mcl-PHA synthesized from octanoic acid at indicated OTR. Error bars represent standard deviations between biological replicates.

Figure 4.4 shows that the highest carbon flux to PHA was observed when the DO was maintained below detectable limits, and the resulting $Y_{PHA/S}$ was 0.62 ± 0.06 g PHA g octanoic acid^{-1}. This was more than a ten-fold improvement in $Y_{PHA/S}$ compared with conditions in which DO was maintained at 10% or higher (0.04 ± 0.02 g g^{-1}), and higher than the theoretical yield of PHB from carbohydrate substrates (0.47-0.48 g g^{-1}) (Ackermann and Babel 1998). However, the result is still lower than the theoretical maximum yield of PHA from octanoic acid (0.98 g g^{-1}). Table 4.3 shows $Y_{PHA/S}$ for mcl-PHA production from various mcl-fatty acids using *P. putida*. Values ranging from 0.21-0.41 g g^{-1} have been reported for N-limited cultivations (Hori et al. 1994; Kellerhals et al. 2000; Durner et al. 2000; Elbahloul and Steinbüchel 2009). In this work, several N-limited batch trials of *P. putida* LS46 grown on octanoic acid were performed, and the average $Y_{PHA/S}$ obtained (0.53 ± 0.06 g g^{-1}) was not significantly different than those observed in

low DO conditions with excess NH_4. As shown in Table 4.3, high $Y_{PHA/S}$ values have recently been reported using carbon limitation (Sun et al. 2009a; Jiang et al. 2013; Gao et al. 2016), suggesting that it is possible to make further improvements.

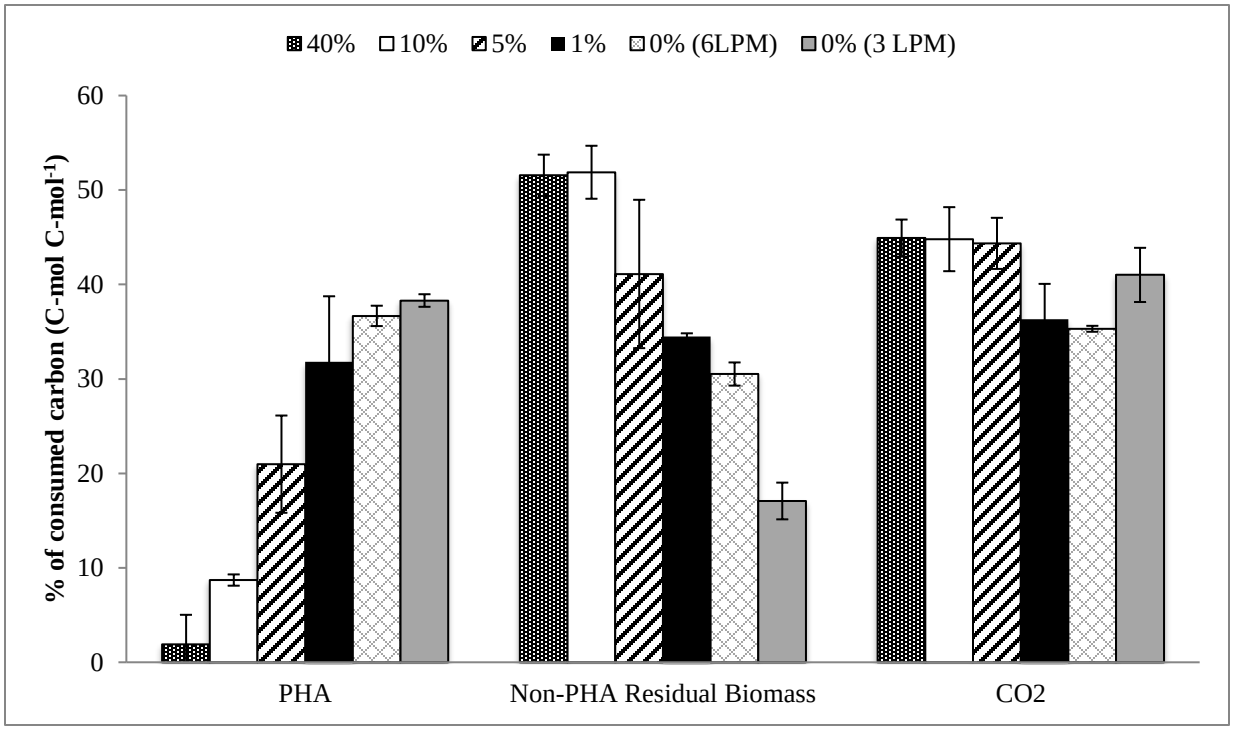

Figure 4.4. Distribution of carbon flux from octanoic acid at tested OTRs. Values measured after 6 h of cultivation or when DO had reached its intended steady-state value. Error bars represent standard deviations between biological replicates.

Table 4.3. Literature values for mcl-PHA yield from mcl-fatty acids using *P. putida* grown and various cultivation strategies.

Conditions	$[X_t]$	$\%_{PHA}$	Q_v	$Y_{PHA/S}$	Ref
	g L^{-1} CDM	% CDM	g L^{-1} h^{-1}	g g^{-1}	
N-limited fed batch using octanoic acid	53.0	55.4	0.76	0.41	(Elbahloul and Steinbüchel 2009)
N-limited fed batch using octanoic acid	51.5	35.8	0.41	0.21	(Kellerhals et al. 2000)
N-limited fed batch using octanoic acid	8	4	0.07	0.3	(Hori et al. 1994)
N-limited chemostat using octanoic acid (D = 0.1 h^{-1})	-	56.1	-	0.25	(Durner et al. 2000)
C-limited fed batch with decanoic acid	75	74	1.16	0.86	(Gao et al. 2016)
C-limited fed batch with nonanoic acid	71	56	1.4	0.66	(Sun et al. 2009)
C-limited chemostat with nonanoic acid	5.8	51.7	0.7	0.61	(Jiang et al. 2012)
C-limited fed batch with nonanoic acid	71.4	75.5	1.8	0.78	(Jiang et al. 2013)

4.5.5. Carbon dioxide and carbon balance

Since CO_2 measurements with the MIMS were not available in every experiment, results were back calculated by rearranging Equation 3.18. The efficacy of the back-calculated results was verified in experiments where CO_2 was measured with the MIMS and was found to be in good agreement. Figure 4.4 shows the distribution of consumed carbon at the indicated conditions. The main trade-off in carbon flux was between mass of PHA and X_r as DO became increasingly limited. Carbon balances for experiments where CO_2 was measured ranged from 0.94-1.07. This indicates that, within experimental error, the majority of the consumed carbon can be accounted for in PHA biomass, residual biomass, and CO_2.

4.5.6. Engineering applications

These results represent, to our knowledge, the first attempt to quantify how growth and mcl-PHA production from fatty acids are modulated in response to low DO environments. Since it was found that low DO environments strongly induce mcl-PHA synthesis from fatty acids, the bioreactor OTR can be adjusted to manipulate the process to maximize productivity without the need to manage C/N ratios. Many high-productivity mcl-PHA cultivation systems have been operated fed-batch mode with structurally related carbon sources like fatty acids. These studies have used various feeding strategies to achieve HCD cultures, before limiting carbon (Maclean et al. 2008; Sun et al. 2009a), phosphorus (Lee et al. 2000b), or nitrogen (Elbahloul and Steinbüchel 2009). An O_2-limited fed batch strategy could be employed, in which the DO is maintained as high as possible until the oxygen demand of the culture naturally drives DO to 1 % or lower. This would then divert carbon flux into PHA synthesis at a high rate. In a continuous system, it may be possible to use DO to tune the balance between growth and mcl-PHA synthesis to optimize productivity, without the need for a secondary PHA accumulation reactor. The maximum Q_s observed in this work using O_2 limitation indicates that, for a PHA accumulation step of a fed batch or multi-stage continuous production system, the residence time required could be significantly reduced using oxygen limitation compared to strict nitrogen limitation. Currently, mcl-PHA production under microaerophilic conditions has not been considered in detail, and could be a platform for improved rates and simultaneous cost reduction, especially at increased bioreactor scale.

4.6. Conclusions

The effect(s) of DO limitation has not been adequately addressed in mcl-PHA production and is usually blamed for early termination of production processes. These results show for the

first time that microaerophilic environments strongly induce mcl-PHA synthesis from fatty acids and the OTR can be manipulated to achieve higher productivity during the PHA accumulation phase than conventional nitrogen limitation. This provides valuable insight for bioreactor operation strategies in scaled-up mcl-PHA production processes, and suggests that the process responds well to inevitable oxygen transfer limitations that occur in HCD cultures and large-scale cultivations.

4.7. Acknowledgements

This work was funded by: 1) Genome Canada, through the Applied Genomics Research in Bioproducts or Crops (ABC) program for the grant titled, “Microbial Genomics for Biofuels and Co-Products from Biorefining Processes”; 2) the government of the Province of Manitoba through the Manitoba Research Innovation Fund (MRIF) and the Manitoba Rural Adaptation Council (MRAC); 3) the Natural Sciences and Engineering Research Council (NSERC); and 4) the University of Manitoba Sir Gordon Wu Graduate Student Scholarship. The authors disclose that no conflict of interest exists between them.

Chapter 5: Carbon flux to growth or polyhydroxyalkanoate synthesis under microaerophilic conditions is affected by fatty acid chain-length in *Pseudomonas putida* LS46

5.1. Preface

The results obtained in Chapter 4 (using octanoic acid as the carbon source) were compared with results obtained by Christopher Dartiailh (using LCFAs, primarily oleic) as the carbon source under similar conditions, and it was clear that key growth differences existed in a microaerophilic environment. These could have significant implications on further process development, so a set of experiments were designed to compare growth and mcl-PHA synthesis from the two substrates, building on the work done in Chapter 4. The main hypothesis of this work was that growth (i.e. production of X_r) is improved in a microaerophilic environment when LCFAs are used as the carbon source (this was based on observations made during bioreactor trials with the goal of producing mcl-PHA from waste LCFAs).

The work described in this chapter represents original research that has been published in *Applied Microbiology and Biotechnology* 2018 102(15): 6437-6449. The work is a formal co-authorship with Christopher Dartiailh. Several tasks were shared equally between us, including experimental design, taking samples, much of the bench assays, and preparation of the manuscript. My specific contributions were: 1) programming, automation, and on-line monitoring of fed-batch experiments; 2) performing fed-batch experiments using octanoic acid as the sole carbon source; and 3) mass balancing and yield analysis. Christopher Dartiailh's contributions were: 1) design co-feeding experiments and a process to hydrolyze canola oil and separate the fatty acids; 2) performing of co-feed and LCFA-based experiments; and 3) insights on monomer composition and product characteristics of the PHAs. The committee members

were also included as co-authors for their scientific guidance and for reviewing the manuscript prior to its publication.

5.2. Abstract

Economical production of mcl-PHA is dependent on efficient cultivation processes. This work describes growth and mcl-PHA synthesis characteristics of *Pseudomonas putida* LS46 when grown on mcl- fatty acids (octanoic acid) and lower-cost LCFAs (derived from hydrolyzed canola oil) in microaerophilic environments. Growth on octanoic acid ceased when the OUR was limited by the OTR and mcl-PHA accumulated to 61.9% CDM. From LCFAs, production of non-PHA cell mass continued at a rate of 0.36 g L^{-1} h^{-1} under oxygen-limited conditions, while mcl-PHA accumulated simultaneously to 31% CDM. The [X_r] from LCFAs at 14 h post inoculation was double that obtained from octanoic acid in bioreactors operated with identical feeding and aeration conditions. While the productivity for octanoic acid was higher by 14 h, prolonged cultivation on LCFAs achieved similar productivity but with twice the PHA titer. Simultaneous co-feeding of each substrate demonstrated the continued cell growth under microaerophilic conditions characteristic of LCFAs, and the resulting polymer was dominant in C8 monomers. Furthermore, co-feeding resulted in improved [X_{PHA}] titer and Q_v compared to either substrate individually. These results suggest that LCFAs improve growth of *P. putida* in oxygen-limited environments and could reduce production costs since more X_r, the cellular factories required to produce mcl-PHA and the most oxygen-intensive cellular process, can be produced for a given bioreactor OTR.

5.3. Introduction

Mcl-PHAs are bio-polyester polymers synthesized by primarily *Pseudomonas* species, under nutrient-limited conditions as a means of storing carbon and energy (Anderson and Dawes 1990; López et al. 2015; Anjum et al. 2016). While these polymers may have value as renewable and biodegradable alternatives to traditional petroleum-based polymers, current cost estimates range from three to fifteen-fold higher than polyethylene or polypropylene (Możejko-Ciesielska and Kiewisz 2016; Kourmentza et al. 2017), and must be reduced to facilitate widespread application.

Since the carbon source for PHA production has been reported to account for a significant proportion of the production costs (Choi and Lee 1997; Koller et al. 2017), it is imperative to find inexpensive and readily available feedstocks. Long-chain fatty acids (LCFAs) are a promising candidate for PHA production because the theoretical yield of polymer (3-hydroxydecanoate) from LCFAs (oleic acid) via β-oxidation is relatively high (Chanprateep 2010). There is a significant amount of waste LCFAs available as triacylglycerides (TAGs) or FFAs from the food-processing and biodiesel production industries (Chhetri et al. 2008; Du et al. 2012; Nikodinovic-Runic et al. 2013). Both LCFAs and TAGs are carbon-rich waste streams that create significant disposal challenges due to high biochemical oxygen demand and their hydrophobicity and insolubility in aqueous medium (Ravindran and Jaiswal 2016; Wallace et al. 2017). In North America and other temperate regions, waste sources of LCFAs (including biodiesel and hydrolyzed cooking oil wastes) are typically derived from plant oils like canola and soybean (Song et al. 2008; Nikodinovic-Runic et al. 2013). These contain a mixture of FFAs, predominantly C16:0, C18:0, C18:1 and C18:2 fatty acids (Fu et al. 2014). Fatty acids are degraded to acetyl-CoA and acyl-CoA intermediates using the β-oxidation cycle, producing

reduced electron carriers NADH and $FADH_2$. The PHA synthase has low substrate specificity, which allows incorporation of various acyl-CoA monomers into the polymer (Kim et al. 1997). The predominant mcl-PHA monomer units from fatty acids are eight and ten carbons in length, but LCFAs have been reported to produce PHA polymers containing longer as well as unsaturated monomer units (de Waard et al. 1993; Haba et al. 2007).

In addition to using low-cost carbon feedstocks, improving productivity through cultivation techniques or mode of bioreactor operation is crucial to the sustainability of PHAs (Kaur and Roy 2015; Koller et al. 2017). To date, the highest productivities for both scl- and mcl-PHA production have been achieved through fed-batch strategies, in which cells are grown to HCD with high $\%_{PHA}$ in short cultivation times (Wang and Lee 1997b; Lee et al. 2000b; Maclean et al. 2008). However, these HCD cultures are inevitably limited by the OTR from the introduced gas into the liquid phase resulting in environments with low DO. Previously, it was shown that in such microaerophilic environments with excess NH_4, *P. putida* LS46 accumulates mcl-PHA to 57.3% CDM in 14 h from 20 mM octanoic acid, and that the polymer synthesis rate was improved as k_La was reduced (Chapter 4). While that work showed that oxygen-limited mcl-PHA production could be a viable mcl-PHA production strategy, the results were limited to octanoic acid and productivity was limited by batch cultivation. This work aims to build on previous work by identifying if the previous response observed under oxygen limitation could be extended to other fatty acids, and specifically lower-cost LCFAs, or if it was a unique manifestation of mcl-PHA synthesis (primarily C8) from octanoic acid. The objectives of this work are therefore to: 1) compare growth and mcl-PHA synthesis characteristics between LCFAs and octanoic acid in simple fed-batch cultivations with low DO conditions (likely to persist in

HCD cultures and large-scale bioreactors); and 2) examine the effect of co-feeding both substrates to improve mcl-PHA productivities and/or yields.

5.4. Materials and Methods

5.4.1. Microorganism, medium, and substrates

The microorganism, strain maintenance practices, and medium used were all as described in Section 4.4.1. The carbon source was aseptically added post-autoclave. Octanoic acid (Sigma Chemical Co. (St. Louis, MO) was used as a representative mcl- fatty acids. When it was used as the sole carbon source (in inoculum flasks or bioreactors), it was added to an initial concentration of 20 mM (2.88 g L^{-1}). Hydrolyzed food-grade canola oil (No Name®, Superstore, Canada) was used as a representative LCFA. The hydrolysis of canola oil was carried out by saponification using 250 g of NaOH dissolved into 500 mL of H_2O per liter of canola oil. Once the reaction was complete, 200 mL of 98% H_2SO_4 was used to release the free fatty acids of canola oil. In all experiments the addition of LCFAs, whether adding an initial concentration to a flask or bioreactor, or during fed-batch experiments (described below) was carbon atom molar (C-mol) equivalent to the addition of octanoic acid (i.e. 160 C-mmol L^{-1}).

5.4.2. Reactor setup and preparation

The reactor setup, preparation, calibration, and sterilization procedures for this work are identical to those described in Section 3.10. It should be noted, however, that in this work, the Pyrex micro-bubblers described in Section 4.4.2 were not used. Instead aeration was simply delivered through the small holes in the bottom of the factor L-shaped sparging tube, located underneath the impeller. Because of this, k_La was re-evaluated in the bioreactor (containing 3 L of Ramsay's medium) in the absence of cells under operating flow rates (6 LPM) and agitation

rates (500 rpm). This was done using the dynamic method as described in Section 3.13. The corresponding k_La was determined to be 54 ± 3 h^{-1}.

The CO_2 in the off-gas was measured with both an HPR 40 dissolved species membrane inlet mass spectrometer (MIMS, Hiden Analytical, Warrington, UK) or a BlueInOne Cell O_2/CO_2 sensor (Bluesens Gas Sensor, GmbH, Germany), which are described in Section 3.11. Both instruments were verified against one another and found to be in good agreement.

The pH was maintained at 6.5 by addition of 4 M NaOH through automated peristaltic pumps for all single substrate experiments.

5.4.3. Feeding rates

During initial attempts at optimizing fed-batch cultivations, several trials on octanoic acid were conducted using a variety of exponential feeding rates and high k_La values resulting from use of a mixing cascade up to 1200 rpm. When those trials were compared to growth on LCFAs using a relatively fast feeding rate (μ = 0.5 h^{-1}), it was observed that under similar O_2-limited conditions, *P. putida* LS46 produced significantly higher total biomass and non-PHA residual cell mass (X_r). Because of this observation, the feeding of carbon and nitrogen sources was modeled for a specific growth rate (μ) of 0.25 h^{-1} (Equation 5.1). The rate of feeding for carbon and ammonium were calculated according to Equation 5.2 and Equation 5.3, respectively. In the case of LCFAs, the carbon feed rate was adjusted to be C-mol equivalent to the 0.25 h^{-1} feeding schedule developed for octanoic acid. Although the feeding schedule was based on maintaining a μ of 0.25 h^{-1}, this was not achieved in practice upon onset of O_2-limitation. The purpose of this model was to observe how each carbon source is utilized when fed at the same rate (i.e. C-mol h^{-1}) under O_2-limited conditions.

$$[X_r(t)] = [X_r|_{t_0}]e^{\mu(t-t_0)}$$ Equation 5.1

$$[C(t)] = \frac{[X_r|_t]e^t - [X_r|_{t_0}]e^{t_0}}{Y_{X_r/C}}$$ Equation 5.2

$$[N(t)] = \frac{[X_r|_t]e^t - [X_r|_{t_0}]e^{t_0}}{Y_{X_r/N}}$$ Equation 5.3

Where $X_r|_{to}$ is the amount of X_r present in the bioreactor at the beginning of the time interval (g); t_0, t the beginning and end of a given time interval (h), respectively. *C(t)* and *N(t)* are the required amounts (g) of carbon or NH_4, respectively, fed to the bioreactor in a given time interval; $Y_{Xr/C}$ and $Y_{Xr/N}$ are the yield coefficients of X_r from the carbon source and ammonium (g g^{-1}), respectively. The yield coefficients were derived from previous experimental values (Chapter 4). Square braces indicate concentration.

After an hour delay following inoculation, carbon (either LCFAs or octanoic acid) and a 200 g L^{-1} solution of $(NH_4)_2SO_4$ were continually supplied with two titration syringes adapted to three-way valves. The feeding program described above was automated in LabBoss software (Scion, Rotorua, New Zealand). Calibration and operation of this setup has been previously described in greater detail (Blunt et al. 2014). The initial value of $X_r|_{to}$ was set as 0.75 g to compare the cell mass production by *P. putida* LS46 cultured with LCFAs versus octanoic acid. All conditions were run in duplicate.

5.4.4. Co-feeding and prolonged LCFA cultivation experiments

To investigate further potential for production of X_r and/or mcl-PHA under microaerophilic conditions, experiments were conducted using co-feeding and LCFA feeding with prolonged cultivation under identical aeration conditions (k_La = 54 h^{-1}). To avoid

preferential uptake of octanoic acid or LCFAs, the co-feeding experiments were initiated with a 5% (vol vol^{-1}) inoculum from cells grown in LB medium, and washed in sterile PBS solution. Due to technical limitations, NH_4OH was used in place of $(NH_4)_2SO_4$ and NaOH for co-feeding experiments to maintain ammonium and pH levels. The co-feeding experiments were started with 10 mM of octanoic acid and C-mol equivalent LCFAs.

The feeding rates for prolonged co-feeding and LCFAs cultivations were identical (C-mol h^{-1}) to the aforementioned experimental rates (0.25 μ) up to 16 h post inoculation (pi). During co-feeding, each substrate was fed in a 1:1 ratio on a C-mol basis. As the exponential feeding program resulted in highly excess conditions by 16 h pi, feeding rates were decreased for further cultivation. Further cultivation with LCFAs provided substrate and $(NH_4)_2SO_4$ at linear rates of 1.43 g h^{-1} and 0.59 g h^{-1} respectively, while carbon feeding was ceased at 16 h pi in co-feeding experiments. In all experiments, the feeding after 16 h pi was determined to maintain carbon and NH_4 in excess without approaching toxic concentrations.

5.4.5. Sample treatment and analyses

After inoculation, 40 mL samples were periodically withdrawn from the reactor, typically in two-hour intervals. Samples were handled as described in Section 3.3, including gravimetric determination of total biomass. The sample preparation and GC-FID analysis for PHA in the biomass was performed as described in Sections 3.4 and 3.5, respectively. Contaminating oleic acid peaks (when LCFAs were used as the carbon source) detected in the PHA chromatograms were quantified and used to correct the measured [X_t]. Analysis of residual fatty acids in the supernatant was also performed by GC-FID following the same procedure described in Section 3.5.2. Residual free NH_4 in the culture supernatant was measured using the colorimetric indophenol blue method previously described (Section 3.9).

5.4.6. Carbon balance and yield analysis

Carbon balances were performed for both individual substrates following the approach and assumptions described in Section 3.12, in which the carbon moles of detected mcl-PHA monomers, NPCM, and CO_2 were compared to the carbon moles of substrate consumed. For the co-feeding experiments, the PHA obtained contained 8.2 C-mol mol^{-1}, and had molecular mass of 162.3 g mol^{-1}. These values were obtained as the weighted average of the detected monomers.

The experimental yield of PHA from carbon substrate was calculated as the slope of a plot between PHA titer (g L^{-1}) and substrate uptake (g L^{-1}). The maximum theoretical $Y_{PHA/S}$ from octanoic acid and LCFAs were assumed to be 0.98 and 0.72 g g^{-1}, respectively, which were derived in Section 3.8. Due to the mixed composition of LCFAs derived from canola oil, it was assumed to have a molecular mass of 271.5 g mol^{-1}. This value was obtained as the weighted average of the molecular masses of the individual fatty acid components detected by GC.

Due to problems determining the concentration of (insoluble) residual LCFAs in the culture medium, the carbon consumption was back calculated for LCFA cultures by assuming that all carbon could be accounted for through measurement of X_{PHA}, X_r, and CO_2. The efficacy of this assumption was verified in Chapter 4 (Section 4.5.5), where carbon recoveries ranging from 0.94-1.07 were obtained. The efficacy of the back-calculation method was verified using the results from octanoic acid (Chapter 4, Section 4.5.5), and it was found that octanoic acid uptake could be estimated within an average margin of error of 10%.

5.5. Results

On the basis of the results shown in Table 5.1, a feeding program of $\mu = 0.25$ h^{-1} was chosen for growth on octanoic acid since higher rates led to rapid accumulation of octanoic acid

to inhibitory levels. Stirring was kept constant at 500 rpm to provide consistent OTR throughout both conditions and avoid variations in the response of the DO controller. The following results describe the performance comparison between LCFA and octanoic acid feeds under identical exponential rates (C-mol h^{-1}) with DO as the only growth-limiting variable.

Table 5.1. Determination of appropriate specific growth rate for exponential feeding of octanoic acid to *P. putida* LS46.

Feeding program	Maximum $[X_t]$	Maximum $\%_{PHA}$	End of process	Reason for termination
	g L^{-1} CDM	% CDM	h pi	
μ=0.5 h^{-1} from 0 h pi with octanoic acid	2.6	13.6	10	Octanoic acid concentration ≥ 50 mM
μ=0.5 h^{-1} from 6 h pi with octanoic acid	3.9	30.3	9	Octanoic acid concentration ≥ 50 mM
μ=0.4 h^{-1} from 4 h pi with octanoic acid	12.4	39.1	16	Octanoic acid concentration ≥ 50 mM
μ=0.25 h^{-1} from 4 h pi with octanoic acid	21.5	41.5	33	Reduction in OD_{600} of culture
μ=0.5 h^{-1} from 4 h pi with LCFAs	46.7	32.8	35	Excess substrate

5.5.1. Dissolved oxygen

The measured DO profiles are shown in Figure 5.1(a). The reactor was saturated with air (DO = 100% or 6.77 mg L^{-1}) prior to inoculation, after which the culture consumed DO until the electrode read zero current at 4 h pi, despite constant mixing and aeration. After 4 h pi, the oxygen uptake rate should be equivalent to the OTR, which is in turn limited by k_La. Previous studies have confirmed that such conditions correspond to DO concentrations less than 0.05 mg L^{-1} (see Table 4.1). The DO remained below detectable limits until the experiment was terminated in the case of growth on LCFAs, or until octanoic acid accumulated to an inhibitory level, which is shown by the rapid rise in DO after 14 h pi.

5.5.2. Total biomass and PHA accumulation in single substrate comparison

Figure 5.1a shows the total biomass produced throughout the growth curves for each condition. The two conditions produced similar concentrations up to 4 h pi. After 6 h pi, when exponential growth was finished due to onset of O_2 limitation, the difference in $[X_t]$ became increasingly higher for the culture grown on LCFAs compared to octanoic acid. Accumulation of PHA is shown in Figure 5.1b. The mcl-PHA content of octanoic acid-grown cultures was initially 28.0 ± 6.1% CDM due to carry-over from the inoculum, and decreased to 19.2 ± 3.0% CDM at 4 h pi. The onset of O_2 limitation caused PHA to accumulate to 61.5 ± 1.4% CDM by 14 h pi, which is expected when the DO was maintained at 1-5% or less in the presence of excess carbon (Chapter 4). The maximum $[X_{PHA}]$ was 2.5 ± 0.3 g L^{-1}. When the substrate was LCFAs, the initial PHA content detected at 0 h pi was 8.5 ± 5.8% CDM and was similar at 4 h pi when the DO concentration dropped below detectable limits for the electrochemical probe (12.2 ± 6.8% CDM). Following onset of O_2 limitation, the $\%_{PHA}$ increased to 34.2 ± 6.1% CDM by 16 h

pi. The mcl-PHA titer in *P. putida* LS46 cultured with LCFAs reached 1.9 ± 0.6 g L^{-1} cells at 16 h pi.

5.5.3. Analysis of X_r and residual concentrations of carbon and NH_4

Shown in Figure 5.1c, a contrast in X_r production was observed for octanoic acid and LCFA cultures following the onset of O_2-limitation at 4 h pi. The [X_r] became relatively constant from 6 h pi in the octanoic acid-grown cultures, after which the majority increase in [X_t] was due to PHA accumulation. When grown on LCFAs, the [X_r] increased at a relatively constant rate (0.36 g L^{-1} h^{-1}) for 8 h past the onset of O_2 limitation, reaching 3.7 ± 0.1 g L^{-1}. This was more than double the highest value obtained by the culture grown on octanoic acid at 14 h pi (1.6 ± 0.1 g L^{-1}).

Figure 5.1d displays the residual octanoic acid and LCFA concentrations. Both substrates were slowly depleted for the first 8 h pi, after which the residual substrate levels began to accumulate. After 14 h pi, octanoic acid had accumulated to inhibitory levels (≥ 50 mM), and this toxicity likely led to the observed decrease in [X_r] for octanoic-acid fed cultures at 14-16 h pi. When in excess, the LCFAs were observed to form a layer on top of the medium after centrifugation, and the actual concentration of residual LCFAs was difficult to determine. No inhibitory or toxic effects were observed due to excess LCFAs, as was observed with excess octanoic acid. A similar trend was observed with residual NH_4 concentrations using either substrate, shown in Figure 5.1d. The residual concentrations of carbon substrate and free NH_4 being in excess for the entire cultivation period confirmed that O_2-limitation was the only growth-limiting factor.

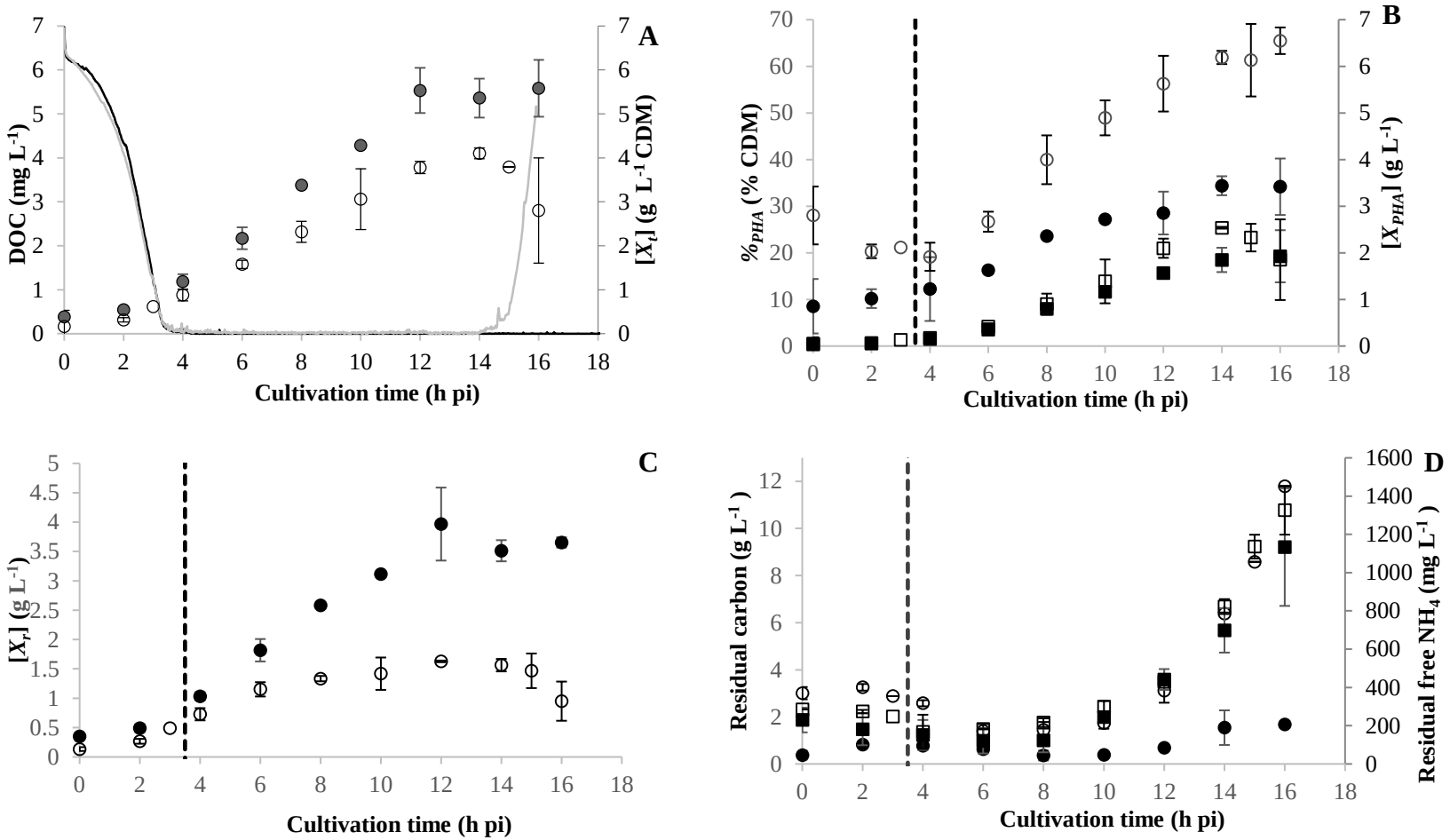

Figure 5. 1. Results from *P. putida* LS46 growth on either octanoic acid or LCFAs when grown in fed-batch at $\mu = 0.25\ h^{-1}$. a) DO profiles for octanoic acid (-) and LCFAs (-) and [X_t] (g L^{-1}) for octanoic acid (○) compared to LCFAs (●); b) $\%_{PHA}$ obtained from octanoic acid (○) and LCFAs (●) as well as [X_{PHA}] obtained from octanoic acid (□) compared to LCFAs (■); c) [X_r] obtained from octanoic acid (○) compared to LCFAs (●); d) residual concentrations of carbon (octanoic acid (○) and LCFAs (●)) as well as residual free NH_4 (octanoic acid (□) and LCFAs (■)). The dashed line indicates the onset of O_2-limiting conditions. Error bars represent standard deviations between biological replicates.

5.5.4. Co-feeding and prolonged LCFA cultivation experiments

Due to the higher biomass production and continued growth trends observed over the course of the previous experiments with LCFAs, the cultivations were prolonged with additional feeding to observe further potential capacity of both biomass and PHA production. The X_r production from these prolonged LCFA experiments is shown in Figure 5.2a. The [X_t], [X_r], and $\%_{PHA}$ continued to increase after 16 h pi and [X_r] finally stabilized near 7.1 ± 0.4 g L^{-1} (over four times the maximum [X_r] obtained from octanoic acid growth), while the final $\%_{PHA}$ reached 38.3 ± 2.8% CDM at 30 h pi ([X_{PHA}] = 4.4 ± 0.8 g L^{-1}, Table 5.2).

The results for the single substrate experiments indicate that for constant bioreactor conditions, the LCFAs have the potential to produce higher [X_t] and [X_r] under microaerophilic conditions, but the $\%_{PHA}$ was still lower in comparison to octanoic acid cultures. This led to querying the effect of co-feeding both substrates. The [X_t], [X_{PHA}], and $\%_{PHA}$ from the co-feed experiments are shown in Figure 5.2b. By 26 h pi, [X_t] reached 11.7 ± 0.1 g L^{-1}, containing 54.1 ± 2.2% PHA, resulting in a final [X_{PHA}] of 6.3 ± 0.3 g L^{-1}. The X_r for the co-feed experiment is shown in Figure 5.2a, and is overlaid with results from the single-substrate experiments for comparison. Over the course of the co-feed cultivation, the [X_r] was lower compared to when LCFAs were the sole carbon source and reached at final titer of 5.4 ± 0.4 g L^{-1} at 26 h pi (Table 5.2) This value is 3.3 times more than the maximum [X_r] obtained when octanoic acid was the sole substrate. Figure 5.3 also indicates simultaneous uptake of substrates during both growth and mcl-PHA synthesis phases of the cultivation. The specific carbon uptake rate shown in Figure 5.3b indicates that LCFAs were preferentially utilized while DO was in excess, and then following the onset of O_2-limited conditions, the specific uptake rate for either substrate appeared to be similar. Interstingly, the specific uptake rate in the case of octanoic acid showed

little change regardless of the DO or stage of the cultivation. At this point it is not clear if either substrate was preferentially taken up for mcl-PHA synthesis after 4 h, but the discussion of the obtained monomer compositions (below) can provide some insight.

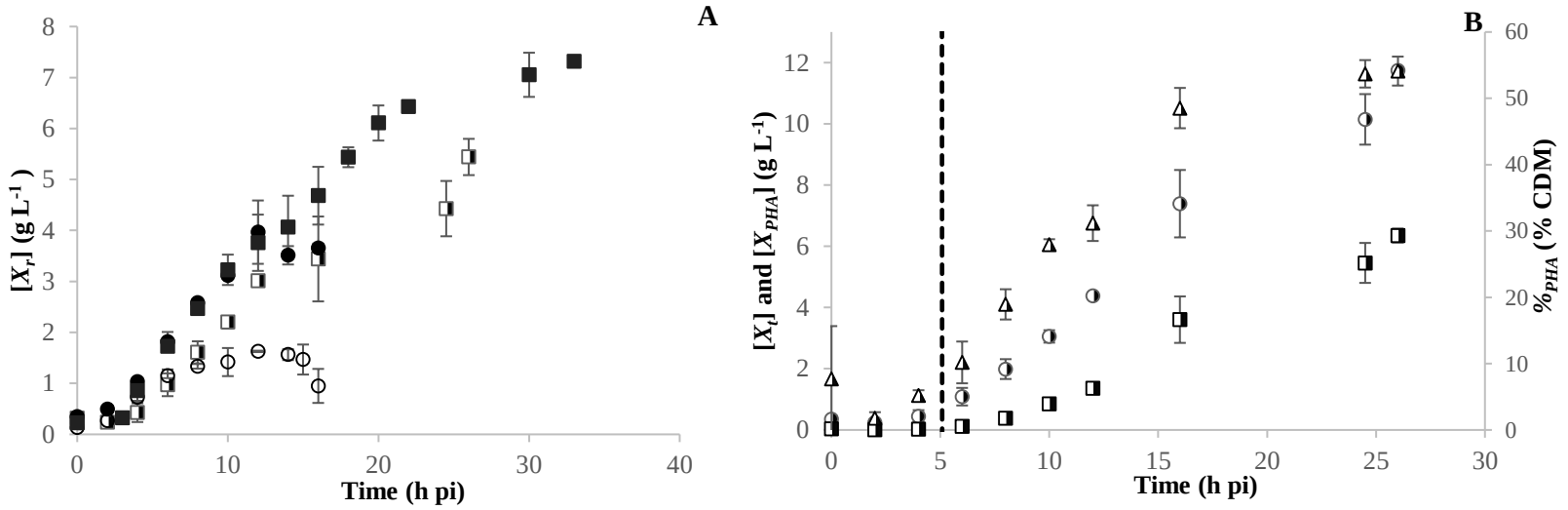

Figure 5.2. Results from cultivation of *P. putida* LS46 in prolonged LCFA and co-feed fed batch cultivations at 0.25µ. a) [X_r] observed during prolonged cultivations on either LCFAs (■) or when both substrates were co-fed at equivalent rates (◨) (i.e C-mol h^{-1}). Also shown for comparison is the [X_r] produced from previously discussed standard cultivations on either octanoic acid (○) or LCFAs (●); b) [X_t] (◑), [X_{PHA}] (◨), and $\%_{PHA}$ (Δ) obtained from co-feeding. The dashed line indicates the onset of O_2-limiting conditions. Error bars represent standard deviations between biological replicates.

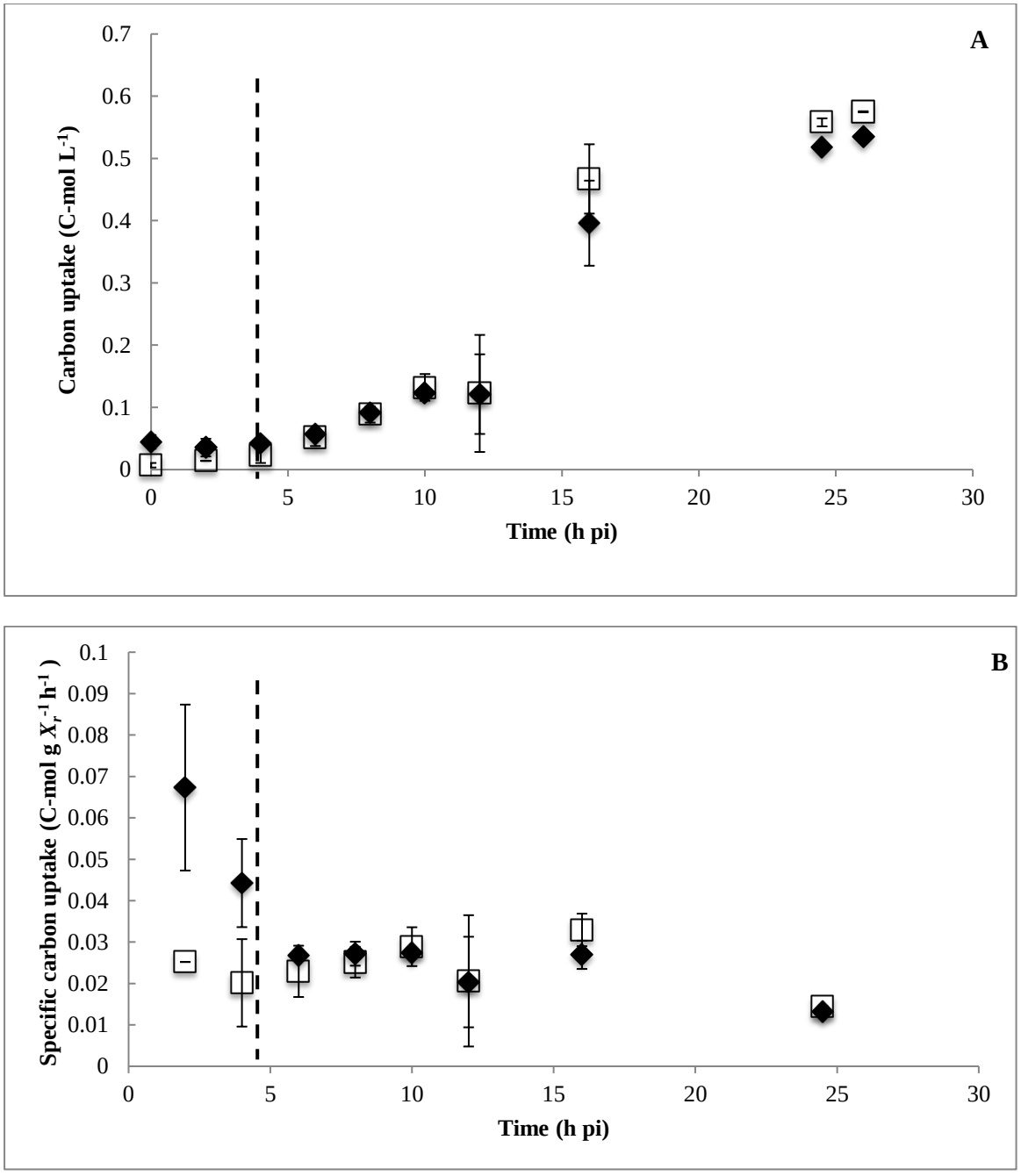

Figure 5.3. Uptake of each carbon source during the co-feed experiments. a) overall cumulative uptake C-mol L^{-1}) and b) specific uptake rate (C-mol g X_r^{-1} h^{-1}). Open squares (□) represent octanoic acid uptake, whereas the shaded diamonds (◆) represent LCFAs uptake. The dashed line indicates the onset of oxygen-limitation. Error bars represent standard deviations between biological replicates.

Table 5.2. Comparison of key process performance indicators during mcl-PHA production by *P. putida* LS46 from LCFAs or octanoic acid as the sole carbon source, or when co-fed in C-mol equivalent proportions.

	LCFAs		Octanoic	Co-Feed	
	16 h pi	30 h pi	14 h pi	16 h pi	26 h pi
$[X_t]$ (g L^{-1})	5.6 ± 0.6	11.5 ± 1.2	4.1 ± 0.1	7.4 ± 1.1	11.7 ± 0.1
$[X_r]$ (g L^{-1})	3.7 ± 0.1	7.1 ± 0.4	1.6 ± 0.1	3.8 ± 0.3	5.4 ± 0.3
$\%_{PHA}$ (% CDM)	34.1 ± 6.1	38.3 ± 2.8	61.9 ± 1.4	48.5 ± 3.0	54.1 ± 2.2
$[X_{PHA}]$ (g L^{-1})	1.9 ± 0.6	4.4 ± 0.8	2.5 ± 0.0	3.6 ± 0.8	6.4 ± 0.2
Q_v (g L^{-1} h^{-1})	0.12 ± 0.04	0.15 ± 0.03	0.18 ± 0.00	0.23 ± 0.05	0.24 ± 0.01

Tolerances indicate standard deviations between biological replicates.

5.5.5. Volumetric productivity

Overall Q_v for each process are summarized in Table 5.2. For the octanoic acid cultivation, Q_v reached a maximum value of 0.18 ± 0.00 g L^{-1} h^{-1} by 14 h pi. By comparison, lower Q_v was observed in the LCFA cultivation at 14 h (0.12 ± 0.01 g L^{-1} h^{-1}). With prolonged feeding, the LCFA cultures reached a maximum Q_v of 0.15 ± 0.02 g L^{-1} h^{-1} after 30 h pi. In the co-feed experiments, the maximum Q_v was 0.24 ± 0.01 g L^{-1} h^{-1} at 26 h pi.

5.5.6. Carbon balancing and yield analysis

Figure 5.4 shows the carbon flux under O_2-excess (0-4 h pi) and O_2-limiting conditions (6-12 h pi and onward) for octanoic acid in Figure 5.4a and LCFAs in Figure 5.4b. When octanoic acid was the substrate, the main tradeoff in carbon flux is between X_r and X_{PHA}. With the onset of O_2-limitation at 4 h pi, the yield of X_r decreased (0.48 to 0.08 C-mol C-mol^{-1}), while $Y_{PHA/S}$ increased (0.19 to 0.55 C-mol C-mol^{-1}). Little change was observed in CO_2 yield over time regardless of DO content, which is consistent with previous batch results (Chapter 4). When LCFAs were the substrate, the onset of O_2-limiting conditions increased the carbon flux to PHA (0.12 to 0.25 C-mol C-mol^{-1}), but the reduction in carbon flux to X_r (0.60 to 0.39 C-mol C-mol^{-1}) was not nearly as drastic as the six-fold reduction observed in the case of octanoic acid. Further incubation of the LCFA culture beyond 12 h pi resulted in similar carbon flux to PHA and a reduction in carbon flux to X_r (0.30 C-mol C-mol^{-1}) with increased CO_2 production. Since the obtained $Y_{PHA/S}$ from LCFA was well below the calculated theoretical value (0.72 g g^{-1}) it is possible that higher $\%_{PHA}$ was not obtained in the LCFA-grown culture during the first 16 h (Figure 5.1b) because of anabolic demand for X_r production. In fact, X_r accounted for a significant portion of the carbon consumed during this period. While the presence of some longer chain and unsaturated monomers suggested that a portion of the mcl-PHA was synthesized from

octanoic acid, the estimated maximum $Y_{PHA/S}$ from octanoic acid in the co-feed experiments was observed between 8 h pi and 26 h pi was 0.49 ± 0.05 C-mol C-mol^{-1} and was comparable to the yield obtained when octanoic acid was the sole carbon source.

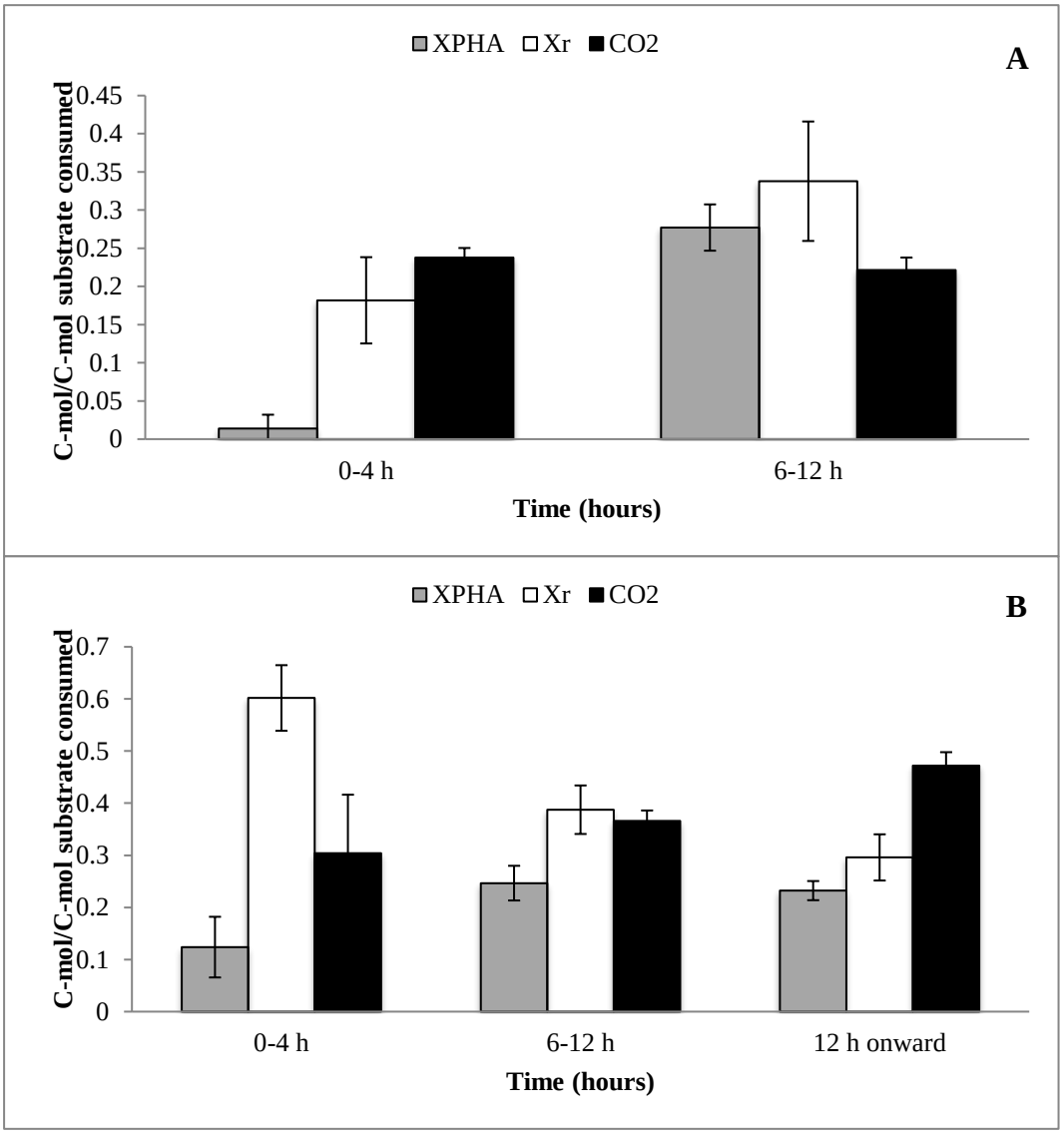

Figure 5.4. Yield analysis for a) octanoic acid and b) LCFA-grown cultures. Conditions shown are for O_2-excess (0-4 h) and O_2-limited conditions (6-12 h and 12 h onward). Error bars represent standard deviations between biological replicates.

5.5.7. Monomer composition of the polymer

Monomer composition of the PHAs produced from both octanoic acid and LCFAs are shown in Table 5.3. As indicated, the polymer produced from octanoic acid contained predominantly C8 monomers, which is consistent with the literature (Kellerhals et al. 2000; Elbahloul and Steinbüchel 2009; Fontaine et al. 2017). Previously, it was reported that O_2-limitation did not significantly affect the monomer composition of mcl-PHA polymers when octanoic acid was the substrate (Section 4.5.3 and Table 4.2). The polymer synthesized from LCFAs consists of a distribution of monomers ranging from C6 to C14, with C8 and C10 being the most predominant. Further, the LCFA-derived polymers also contained monomers with unsaturated carbon-carbon double-bonds (C12:1 and C14:1). Similar monomer compositions were reported for mcl-PHAs synthesized from LCFAs in other bacteria (Huijberts et al. 1992; Kellerhals et al. 2000; Fernández et al. 2005; Fontaine et al. 2017). The mcl-PHAs produced from LCFAs using *P. putida* LS46 remain amorphous, presumably because they contain longer and unsaturated monomers, and a broader distribution of monomers. In contrast, mcl-PHA polymers synthesized from octanoic acid crystallize (eventually) into elastomers. Similar observations have been previously reported (Kellerhals et al. 2000). Co-feeding of octanoic acid and LCFAs produced a polymer dominant in C8 monomers. Comparing the monomer compositions of co-feeding against single substrate feeding (Table 5.3), the C8 monomer content increased while longer monomer lengths (specifically C12:1 and C14:1, which are unique to LCFA PHA) were reduced by 90% in the co-feed experiment compared to the PHA purely from LCFAs. Since the polymer produced by co-feeding had monomer composition most similar to that synthesized from octanoic acid, it may have been preferentially taken up for mcl-PHA synthesis, implying that LCFAs primarily satisfied the growth and/or maintenance requirements.

Table 5.3. Final monomer compositions of mcl-PHA polymers synthesized from LCFAs and octanoic acid by *P. putida* LS46.

Substrate	mol% C_6	mol% C_8	mol% C_{10}	mol% C_{12}	mol% C_{14}	mol% $C_{12:1}$	mol% $C_{14:1}$
Octanoic	7.8 ± 0.3	89.3 ± 0.1	2.3 ± 0.2	0.6 ± 0.2	N. D.	N. D.	N. D.
LCFAs	5.4 ± 0.2	41.4 ± 0.6	26.7 ± 5.1	9.1 ± 1.2	9.3 ± 1.6	3.6 ± 0.9	8.6 ± 3.9
Co-feed	6.9 ± 0.2	80.7 ± 0.5	9.0 ± 3.4	1.7 ± 0.5	N.D.	0.5 ± 0.0	1.0 ± 0.2

Values are expressed as a molar percent of the total monomers detected by gas chromatography and measured at 16 h pi. N.D. - not detected. Tolerances indicate standard deviations between biological replicates.

5.6. Discussion

Fed-batch cultures are regarded as the best method for highly productive PHA production (Sun et al. 2007b), but producing high cell density cultures can be infeasible at larger scale due to power consumption for aeration, agitation, or use of purified O_2 (Lara et al. 2006a). In this study, growth on an equal C-mol basis and under identical, O_2-limited bioreactor operating conditions resulted in double the [X_r] obtained from LCFAs compared to cells grown on octanoic acid at 14 h pi. In addition, the $Y_{Xr/S}$ from LCFAs remained relatively high in low DO environment at 0.39 C-mol C-mol^{-1}, while the $Y_{Xr/S}$ from octanoic acid was almost negligible at 0.09 C-mol C-mol^{-1}. This suggests that LCFAs may be good substrate to efficiently produce X_r, or the cell chassis required to accumulate mcl-PHA, particularly under microaerophilic conditions. However, overall productivity is not only a function of high [X_t], but also requires obtaining a high $\%_{PHA}$ (Choi and Lee 1999). While lower Q_v was obtained at 14 h pi for LCFA compared to octanoic acid, similar productivity was obtained by extending the LCFA cultivation to 30 h pi. It is important to note that, despite lower $\%_{PHA}$, the [X_{PHA}] obtained from LCFAs at 30 h pi was more than double the maximum titer obtained from octanoic acid (Table 5.2). This

shows the potential value of sustained growth with simultaneous PHA production under low-DO conditions. A recent study of metabolic flux in N-limited fed batch culture of *P. putida* KT2440 grown on oleic acid has suggested that residual growth may also improve $Y_{PHA/S}$ by linking production of reduced cofactors of $FADH_2$ and NADH to anabolic demand (Andin et al. 2017). Cell growth simultaneous to PHB synthesis was reported not to affect PHB yield, but improved the PHB synthesis rate in P-limited fed batch cultures of *C. necator* grown on butyric acid (Grousseau et al. 2013).

The sustained growth rate on LCFAs and PHA synthesis from octanoic acid suggest an opportunity to maximize PHA titer and productivity in low-DO environments thereby reducing operating costs. The data obtained through co-feeding of octanoic acid and LCFAs indicates that both substrates were being consumed simultaneously with continued X_r production after onset of O_2-limitation. The obtained $\%_{PHA}$ (54.1% CDM) was improved over LCFA cultivations and the monomer composition was very similar to that obtained from octanoic acid in terms of C8 content (Table 5.3). Further optimization of the octanoic acid and LCFA feeding proportions and rates over time might further improve productivity, increase polymer uniformity, and improve $Y_{PHA/S}$ from octanoic acid. In a similar way, phase feeding strategies have used glucose or glycerol as an inexpensive carbon source for the growth phase followed by feeding fatty acids to improve $\%_{PHA}$ (Kim et al. 1997; Możejko and Ciesielski 2014; Davis et al. 2015; Fontaine et al. 2017) or to obtain novel monomer compositions (Dufresne et al. 2001; Kurth et al. 2002; Hartmann et al. 2006). The highest $Y_{PHA/S}$ from nonanoic acid was achieved by co-substrate growth with glucose in the presence of acrylic acid to prevent fatty acid degradation (Jiang et al. 2012).

Continued X_r production from LCFAs (compared to octanoic acid) under O_2-limited conditions is interesting from a redox perspective. Previously it was shown that in a microaerophilic environment, mcl-PHA is efficiently synthesized from octanoic acid and the polymer consists of predominantly C8 monomers (2 electron oxidation) (Chapter 4). This was thought to be a possible mechanism to maintain cellular redox through the reduction of a minimal amount of O_2, while providing some energy conservation through oxidative phosphorylation. When LCFAs are used as the substrate, the β-oxidation cycle needs to remain active to shorten oleic acid to C8-C10 (R)-3-hydroxyacyl-CoA monomers (4-5 complete cycles), which appear to be preferentially incorporated by the PHA synthase (Table 5.3). Because *P. putida* lacks any fermentative pathways, the resulting reduced electron carriers (NADH, $FADH_2$) must be oxidized via electron transport to O_2 (Sohn et al. 2010; Nikel and de Lorenzo 2013). This could create high $NADH/NAD^+$ ratios, a condition previously linked to PHA synthesis (Ren et al. 2009), and result in a major bottleneck for growth in a microaerophilic environment. However, contrary to this expectation, a consistent increase in X_r was observed in the current study when *P. putida* LS46 was cultured on LCFAs.

Examination of the available literature suggests several possible explanations for this observation: 1) Fatty acids are known to exert considerable toxicity on cells by disruption of the membrane potential and electron transport (Desbois and Smith 2010; Jarboe et al. 2013). When the substrate is octanoic acid, less carbon is available per proton translocated (compared to oleic acid), and this could cause greater uncoupling of proton-motive force and result in less ATP conserved, and hence less X_r produced; 2) Transport of fatty acids could be more limiting for one substrate depending on the hydrophobicity of the molecule (Jarboe et al. 2013); 3) LCFAs have been shown to bind to transcription factors (PsrA, FadR) and cause de-repression of genes

associated with fatty acid degradation and electron transport (DiRusso and Black 2004; Fujita et al. 2007; Kang et al. 2008). This would be expected to cause increased growth and less PHA production, which was recently demonstrated in a PsrA deficient mutant of *P. putida* KT2440 during growth on decanoate (Fonseca et al. 2014). These same observations occurred in this work when LCFAs were present, whether as the sole carbon source or when co-fed with octanoic acid. While the mechanism for the observed differences between the two substrates remains unclear, follow-up proteomic or transcriptomic analysis should be done to improve understanding of how the cell may respond at the molecular level to exogenous fatty acids of different chain lengths.

5.7. Conclusions

When grown on free fatty acids, carbon flux in *P. putida* LS46 appears to be greatly influenced by the length of the fatty acid carbon chain, particularly under microaerophilic conditions. In cells cultured with octanoic acid as the sole carbon source, we observed growth arrest and rapid mcl-PHA accumulation when the OUR was limited by the bioreactor OTR. In contrast, we observed continued cell division and lower mcl-PHA accumulation in cells cultured with LCFAs as the sole carbon source under identical conditions. This resulted in over twice the X_r when grown on LCFAs after 16 h pi of fed-batch cultivation, but with lower $\%_{PHA}$ compared to octanoic acid. With further incubation, the LCFA fed culture produced 4.4 times the maximum X_r measured in the octanoic acid culture, and achieved similar overall Q_v with much higher mcl-PHA titer, after 30 h pi. Similar behavior was also observed when the two substrates were co-fed, where X_r production continued after O_2-limitation resulting in 3.3 times the maximum [X_r] obtained from using octanoic acid as the sole carbon source. The $\%_{PHA}$ also improved from 38.4% to 54.1% CDM compared to using LCFA as the sole carbon source. The

[X_{PHA}] of 6.4 g L^{-1}, and Q_v of 0.24 g L^{-1} h^{-1} after 26 h pi of co-feeding were significantly higher than the single substrate conditions. Furthermore, the resulting mcl-PHA was 81% C8, suggesting preferential use of octanoic acid for mcl-PHA synthesis, with growth and maintenance requirements being supplied by LCFA. These data suggest that higher [X_r] for a given aeration input can be obtained when LCFAs are present. Further work on optimization of a fed-batch strategy by co-feeding mcl-fatty acids with LCFAs could reveal important information for future commercial applications by enhancing productivity and/or reducing costs.

5.8. Acknowledgements

This study was funded by Genome Canada, through the Genome Applications and Partnership Program (GAPP), and the Natural Sciences and Engineering Research Council (NSERC) of Canada through a Collaborative Research and Development (CRD) grant with Minto Bioproducts Ltd. as the industrial partner (grant number CRDPJ-490630-15). We are also thankful to Dennis Labossiere from the Department of Human Nutritional Sciences (University of Manitoba) for his assistance in analyzing the mixed composition of the LCFA substrate. The authors disclose they have no conflict of interest. This article does not contain any studies with human participants or animals performed by any of the authors.

Chapter 6: *De novo* fatty acid biosynthesis is not an effective route to medium chain-length polyhydroxyalkanoates

6.1. Preface

In Chapters 4 and 5, production of mcl-PHA under microaerophilic environments was found to exhibit favorable synthesis characteristics (i.e. yield and rate of formation) when the substrate was medium- and long-chain fatty acids, which are metabolized to mcl-PHA through intermediates of the β-oxidation pathway. However, there was a gap in both our own understanding and the literature about how similar environmental conditions would affect mcl-PHA synthesis from carbohydrates or short-chain VFAs using the *de novo* fatty acid biosynthetic pathway. This question was made more interesting when a colleague, Zimo Jin, reported synthesis of scl-*co*-mcl-PHA polymers from both butyric and valeric acid using *P. putida* LS46. If O_2-limitation could not induce mcl-PHA synthesis from the *de novo* pathway (which was the proposed hypothesis for this work on the basis of previous experiments producing mcl-PHA from biodiesel-derived glycerol), it may introduce an opportunity to use the bioreactor OTR to manipulate monomer composition in substrates that appear to utilize both pathways in mcl-PHA synthesis (on the basis of the obtained monomer composition). This work ultimately completes our understanding of how O_2-limited environments affect mcl-PHA synthesis characteristics in a spectrum of substrates with varying redox states, and the results provide guidelines in choosing appropriate carbon substrate in a large-scale process. This work was organized into a manuscript entitled "Efficacy of medium chain-length polyhydroxyalkanoate biosynthesis from different biochemical pathways under oxygen-limited conditions using *Pseudomonas putida* LS46" and was published online in *Process Biochemistry* on April 15, 2019. The contributions of the other

student co-authors are acknowledged in Section 6.8, and the supervising committee provided scientific guidance and reviewed the manuscript prior to its submission.

6.2. Abstract

The ability to synthesize PHAs under oxygen-limited conditions is a desirable characteristic for limiting aeration costs in large-scale bioreactors. Currently, little is known of how *de novo* biosynthesis of mcl-PHAs is impacted in low DO environments. To synthesize mcl-PHA via the *de novo* pathway, two reductive steps are required that use NADPH as the electron donor. This is similar to the reduction of acetoacetyl-CoA in organisms that produce scl-PHAs, which acts as an electron sink at low DO, allowing some conservation of energy through synthesis of PHB. In this study, we used fed-batch bioreactors with a 3 L working volume to examine mcl-PHA synthesis characteristics in *Pseudomonas putida* LS46 under oxygen-limited conditions from glucose, acetate, valerate, and hexanoate. All of these substrates require a *de novo* pathway, to varying degrees, to obtain monomers required for PHA synthesis. It was found that no significant amount of PHA was synthesized from glucose, acetic acid, or valeric acid using oxygen as the sole growth limitation (DO $\approx$ 0.15 mg L^{-1}), while PHA accumulated up to 19.5% of final CDM from hexanoic acid. The monomer composition of the mcl-PHA produced was 83% C6 (with the remainder being predominantly C8 and C10). This was 10% higher than that observed in an NH_4-limited (DO excess) control experiment, with less of the C10 monomers indicative of *de novo* synthesis. In all cases, the carbon-to-PHA yield was poor (< 0.1 C-mol C-mol^{-1}). From these results, we conclude that: 1) *de novo* biosynthesis of mcl-PHA is not effectively induced by oxygen limitation in *P. putida* LS46, perhaps indicating reductive synthesis of mcl-PHAs could be a challenge to implement at large scale; and 2) incorporation of β-oxidation intermediates appears to be favored at low DO conditions such that the bioreactor

oxygen transfer rate can be lowered to decrease the contribution of monomers incorporated using *de novo* synthesis.

6.3. Introduction

In PHA-synthesizing bacteria, the biochemical processes required for mcl-PHA synthesis is dependent on the carbon substrate being metabolized. This, in turn, plays a significant role in determining the monomer compositions and the physical and thermal characteristics of the product (Laycock et al. 2013). Synthesis of mcl-PHAs occurs via the incorporation of intermediates of the β-oxidation cycle or *de novo* fatty acid biosynthesis intermediates (see Figure 2.3). While the β-oxidation cycle can incorporate intermediates from mcl-fatty acid carbon substrates with high rate, yield, and titer (Sun et al. 2007a; Maclean et al. 2008; Gao et al. 2016), the *de novo* pathway can incorporate a number of potentially lower-cost carbon substrates, including simple sugars (Diniz et al. 2004), waste glycerol (Fu et al. 2014), and short-chain VFAs from fermented waste streams (Cerrone et al. 2014a; Cerrone et al. 2014b; Jin et al. 2019). Furthermore, the resulting polymers can contain different levels of unsaturated monomer subunits (Huijberts et al. 1992; Eggink et al. 1992), which may be suitable for further value-addition through functionalization (Ashby et al. 2000; Hazer et al. 2001; Tortajada et al. 2013). Both β-oxidation and *de novo* synthesis pathways can be active simultaneously (Huijberts et al. 1994). This appeared to be the case when Jin and coworkers found that *P. putida* LS46 produced copolymers of scl- and mcl-PHAs that contained 8.5% C4 from butyrate and 28% C5 from valerate when the cultures were grown on these respective scl- fatty acids. In either case, the remainder of the polymer was predominantly C10 and indicative of *de novo* synthesis (Jin et al. 2019)

In addition to cost of the carbon substrate, the energy requirements for mixing and aeration in highly-aerobic bioreactors for PHA production contributes significantly to the total cost and environmental impacts of PHA production (Akiyama et al. 2003; Koller et al. 2013). Therefore, oxygen-limited or microaerophilic PHA synthesis is desirable to reduce energy consumption and process costs for mcl-PHA production (Chen 2009; Wang et al. 2014; Chen and Jiang 2018). While the role of bioreactor OTR has been relatively well studied for scl-PHA production from both pure and mixed cultures, relatively little is known about how the OTR affects mcl-PHA production and polymer properties (Section 2.9.2).

It was previously shown that mcl-PHA is effectively synthesized (with high rate and yield) from β-oxidation intermediates using octanoic acid (Chapter 4) or LCFAs derived from vegetable oils (Chapter 5) under microaerophilic conditions. While synthesis of mcl-PHA from β-oxidation requires a minimum 2-electron oxidation, in *de novo* synthesis each successive elongation of a fatty-acyl-ACP molecule with acetyl-CoA (or propionyl-CoA as the case may be) requires two reductive steps that use NADPH as the electron donor. During synthesis of PHB from glucose a similar reductive step, catalyzed by acetoacetyl-CoA reductase, couples oxidation of NADPH to the reduction of $NADP^+$ by glucose 6-phosphate dehydrogenase in the Entner-Doudoroff pathway (Figure 2.2). This allows energy conservation via substrate-level phosphorylation with PHB synthesis, in low O_2 environments, while also repressing key enzymes of the TCA cycle (Senior and Dawes 1971; Senior et al. 1972; Jackson and Dawes 1976).

The role of O_2-limitation in mcl-PHA synthesis using the *de novo* pathway has not been studied in great detail. In previous studies, mcl-PHA was not synthesized from glucose or fructose with DO as low as 1% (of atmospheric air saturation at 30 °C) in *Pseudomonas* sp.

(Haywood et al. 1990; Diniz et al. 2004). However, with simultaneous NH_4, limitation, Haywood et al. (1990) reported a slight increase in the intracellular PHA content at low DO (4.4 to 7.0% CDM) in chemostat cultures. A more recent study cultured *P. oleovorans* on sugary cassava waste and reported that O_2-limitation was encountered below 13% DO and obtained 6.5% CDM as mcl-PHA under NH_4-excess conditions (Silva et al. 2014). However, details were minimal in these studies, and they were also limited to simple sugars.

Although the published literature suggests that incorporation of β-oxidation intermediates into mcl-PHA polymers is favorable in microaerophilic environments, but little comprehensive evidence is available to indicate if this may also be the case for *de novo* mcl-PHA synthesis. We hypothesized that, unlike synthesis of PHB from glucose, *de novo* mcl-PHA biosynthesis is not favorable in microaerophilic environments. This was due to previous observations during trials for production of mcl-PHA from waste glycerol. Furthermore, with carbon substrates like valeric or hexanoic acid (which appear to be metabolized to mcl-PHA via both pathways on the basis of the monomer compositions), the β-oxidation cycle could be favored in low-DO environments and cause a significant enrichment of those monomers (i.e. C5 for valeric acid and C6 for hexanoic acid). Therefore, the objectives of this study were to: 1) investigate whether mcl-PHAs can be synthesized from glucose and/or short-chain VFAs using O_2 as the sole growth-limiting nutrient in *P. putida* LS46; and 2) to identify if O_2 limitation causes significant shifts in the monomer distribution of the polymers synthesized primarily from *de novo* synthesis or a combination of *de novo* synthesis with β-oxidation.

6.4. Materials and Methods

6.4.1. Microorganism and medium

The strain used in this study was *Pseudomonas putida* LS46 and was maintained as described previously in Section 3.2. All bioreactor cultivations were carried out in Ramsay's medium with the initial concentration of $(NH_4)_2SO_4$ set to either 0.5 g L^{-1} or 2 g L^{-1}, depending on the conditions being tested (described below).

Several substrates were examined in this work, including glucose, acetic acid, valeric acid, and hexanoic acid. These were added to the bioreactor at an intial concentration of 160 C-mmol L^{-1}, which is equivalent to the carbon molar concentrations used in previous work with octanoic acid (Chapter 4). All chemicals were either purchased from Fisher Scientific (Toronto, ON) or Sigma-Aldrich (St. Louis, MO).

6.4.2. Bioreactor setup and experimental conditions

The bioreactor setup was for the most part identical to that described in Section 4.4.2. The only differences were that the DO was measured using a Visiferm optical DO sensor (Hamilton Company, Reno NV) and the pH was controlled with 2 N solutions of both H_2SO_4 and NaOH. The calibration, sterilization, and setup of the bioreactor system followed the approach described in Section 3.10. The trace elements, ferric ammonium citrate, $MgSO_4$, $CaCl_2$, and carbon source were introduced to the bioreactor through sterile 0.2 μm syringe filters after autoclaving. Each carbon source was dissolved in about 50 mL of distilled water, and in the case of the VFA solutions, the pH was adjusted to 7.0 with NaOH before being added to the bioreactor.

Experiments were initiated with addition of a variable inoculum volume such that the starting OD_{600} in all cases was approximately 0.1. The bioreactors were run as simple DO-stat fed-batch cultivations, in which a sudden rise in the DO signal indicated depletion of the carbon source. A second addition of 160 C-mmol L^{-1} (with pH adjusted to 7.0 to avoid significantly altering bioreactor pH) was added manually to the bioreactor through sterile 0.22 μm filters and monitoring was continued. Aeration was constant at 3 LPM in all experiments and was introduced to the liquid phase through two porous Pyrex spargers as described in 4.4.2. The procedure used for the measurement of k_La followed the approach described in Section 3.13.

Two conditions were evaluated for each substrate following a 4-6 h phase of unrestricted growth: 1) an O_2-limitation to test if *de novo* mcl-PHA synthesis can be induced by O_2-limitation; and 2) an O_2 excess (but NH_4-limited) condition to compare as a positive control for PHA synthesis. Parameters for these conditions are shown in Table 6.1. Depending on the consistency between biological replicates, each condition was replicated at least twice.

Table 6.1. Summary of experimental conditions used in the bioreactors.

	NH_4-limiting/O_2 excess	**O_2-limiting**
Total carbon (C-mmol L^{-1})	320	320
$(NH_4)_2SO_4$ (g L^{-1})	0.5	2.0
C/N ratio (C-mol/N-mol)	10.6	42.3
Aeration (LPM)	3	3
DO set-point (% saturation)	40	Not controlled
Mixing cascade (rpm)	350-900	250-400
k_La, (h^{-1})	49-500[a]	40-52

[a]high k_La values (k_La > 300 h^{-1}) are only estimates based on an extrapolated trend and could not be reliably measured due to insufficient response time of the DO probe.

6.4.3. Sample treatment and analyses

Samples (40 mL) were periodically taken (generally in two-hour intervals, but up to 24 h during extended PHA accumulation phases) and handled as described in Section 3.3 for gravimetric determination of [X_t], and the supernatant was stored at 4 °C until further analysis. Determination of $\%_{PHA}$ and monomer compositions were done by GC-FID following the sample preparation and GC protocol described in Sections 3.4 and 3.5, respectively. Since commercial standards were unavailable, the retention times for the unsaturated monomers were determined from a sample of purified mcl-PHA derived from flax fatty acids and the response factors were assumed to be the same as the corresponding saturated monomer. The [X_r] was determined as the difference between [X_t] and [X_{PHA}] as described in Section 3.6. All productivity calculations were performed as described in Section 3.7.

For analysis of the supernatant, residual free NH_4 was quantified using the indophenol blue method as described in Section 3.9. Residual hexanoic acid analysis was performed by GC-FID following the sample preparation and GC method described in Sections 3.4. and 3.5. Residual glucose, acetic acid, and valeric acid were measured by high-performance liquid chromatography (HPLC, Waters, Corp., Milford MA) equipped with a model 1515 pump, model 2707 autosampler, and model 2414 refractive index detector. The column used was an HPX-87H (Biorad Laboratories, Mississauga ON). The column was maintained at 60 °C and the detector at 45 °C. The eluent was 5 mM H_2SO_4 at a flow rate of 0.8 mL min^{-1}.

6.4.4. CO_2 measurement, carbon balancing, and yield analysis

Carbon dioxide was monitored in the condensed off-gas with a Bluesens Blue-in-One infrared CO_2/O_2 sensor (Bluesens Gas Sensor GmbH, Germany). Yield analysis followed the

balancing was performed approach previously described (Section 3.8), and in this work are expressed as C-mol product per C-mol of carbon substrate consumed for the products X_{PHA} ($Y_{PHA/S}$), X_r ($Y_{Xr/S}$) and CO_2 ($Y_{CO2/S}$). In Chapter 4, this approach produced carbon recoveries ranging from 0.94-1.07, verifying the validity of this assumption. The carbon balance was performed as described in Section 3.12.

6.5. Results

6.5.1. Growth and PHA synthesis

Growth and PHA synthesis from glucose, acetic acid, valeric acid, and hexanoic acid are shown in Figures 6.1 through 6.4, respectively, for both O_2-limited and the NH_4-limited (but DO excess) controls. In all O_2-limited experiments, the DO started at 100% (of saturation with atmospheric air at 30 °C) at the time of inoculuation, and decreased to 2% or less (i.e. less than 0.15 mg L^{-1} DO). Previously, the oxygen half saturation constant ($K_{s,\ O2}$) for *Pseudomonas putida* grown on glucose (Diniz et al. 2004) and octanoic acid (Chapter 4) were reported to be in this range of 1.5-2.7% of air saturation. The onset of O_2-limited conditions occurred around 6 h post-inoculation, and lasted until carbon was depleted. In the NH_4-limited experiments, NH_4 was depleted around 6-8 h post inoculation (indicated by the red line in Figures 6.1 through 6.4.), causing the onset of PHA accumulation for the remainder of the experiment. The second addition of carbon is indicated by the blue arrow in Figures 6.1 through 6.4, which also corresponded to a spike in the DO signal.

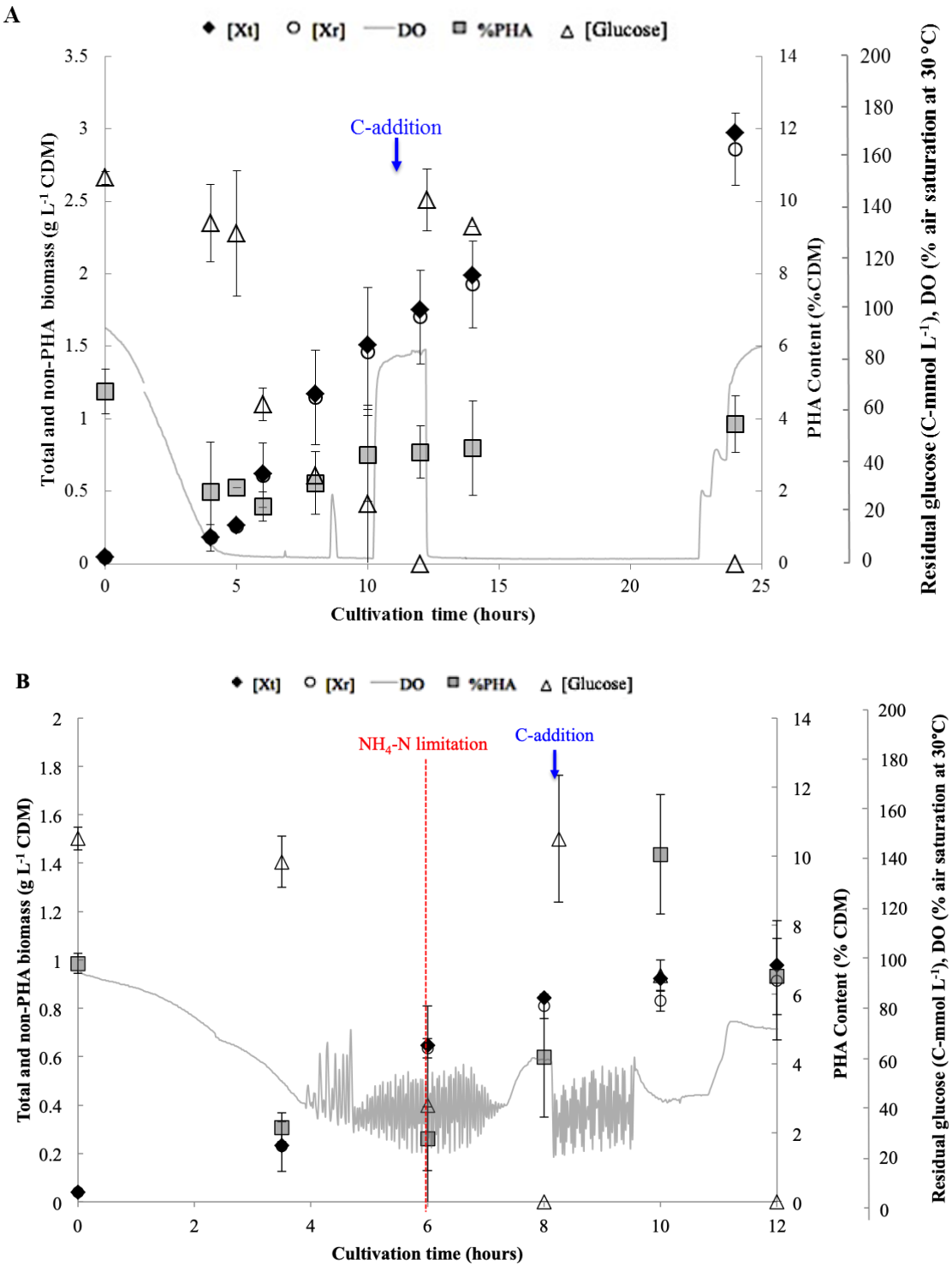

Figure 6.1. Growth and PHA synthesis from glucose using *P. putida* LS46 on under a) O_2-limited or b) NH_4-limited conditions. Error bars represent standard deviations between biological replicates.

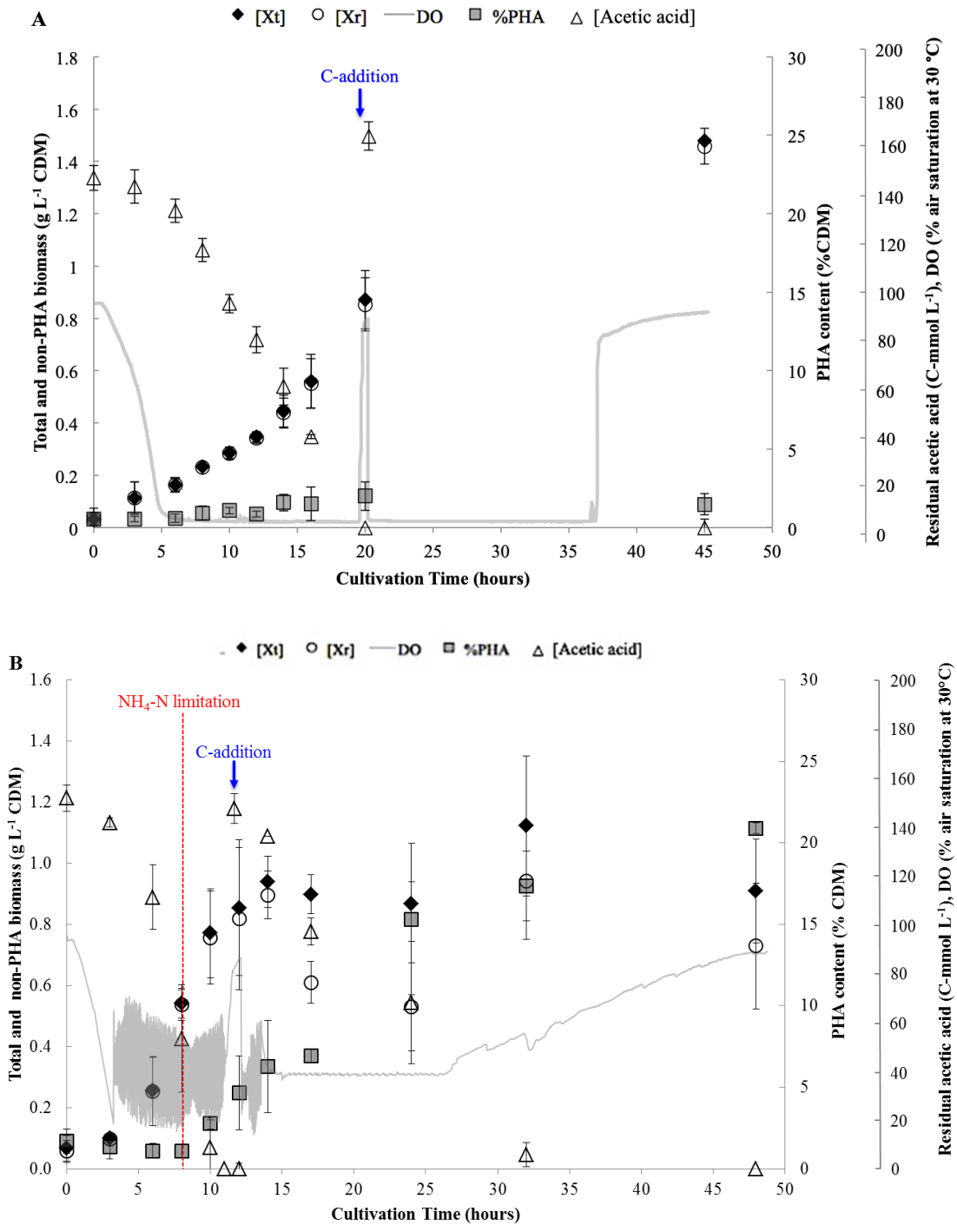

Figure 6.2. Growth and PHA synthesis from acetic acid using *P. putida* LS46 on under a) O_2-limited or b) NH_4-limited conditions. Error bars represent standard deviations between biological replicates.

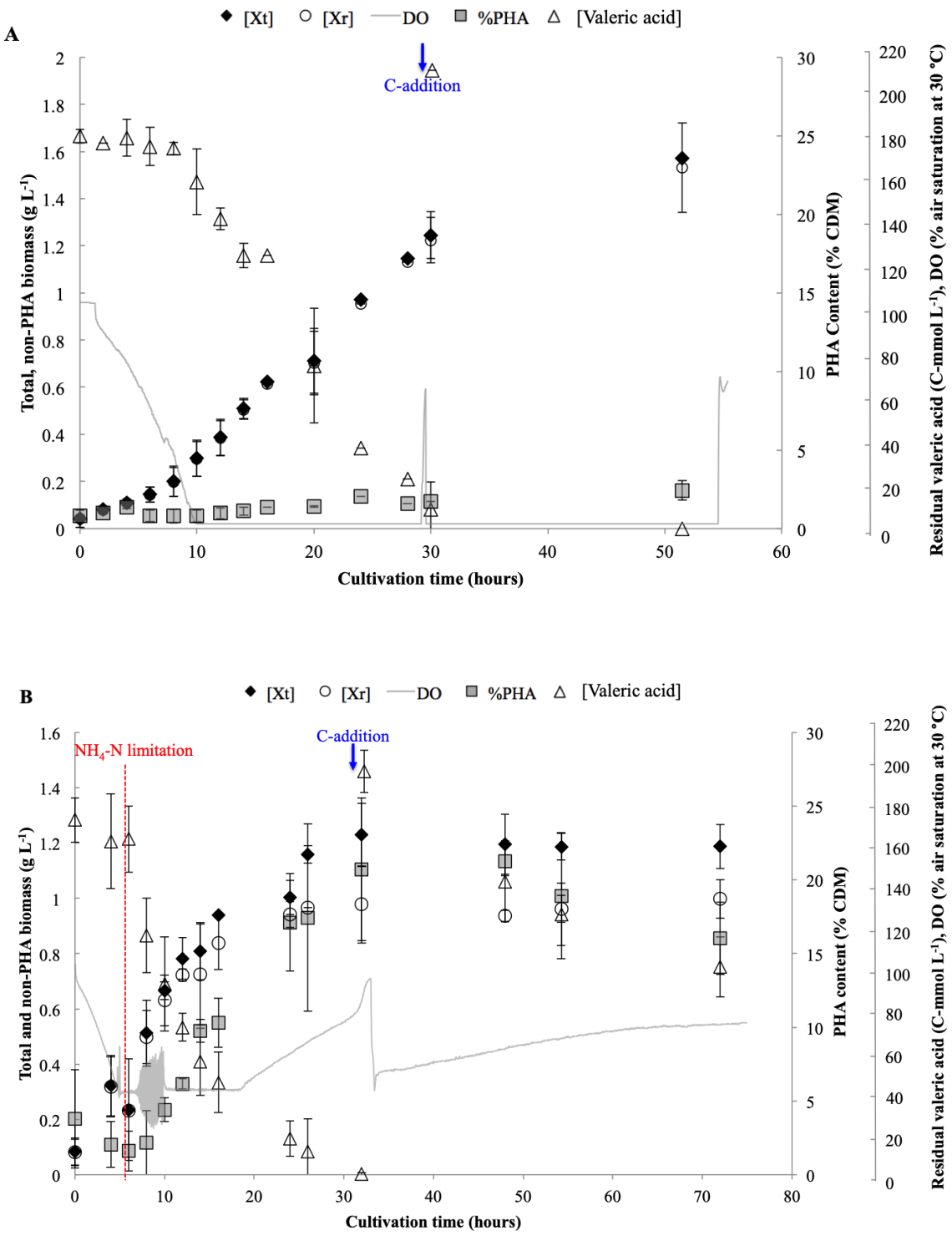

Figure 6.3. Growth and PHA synthesis from valeric acid using *P. putida* LS46 on under a) O_2-limited or b) NH_4-limited conditions. Error bars represent standard devaitions between biological replicates.

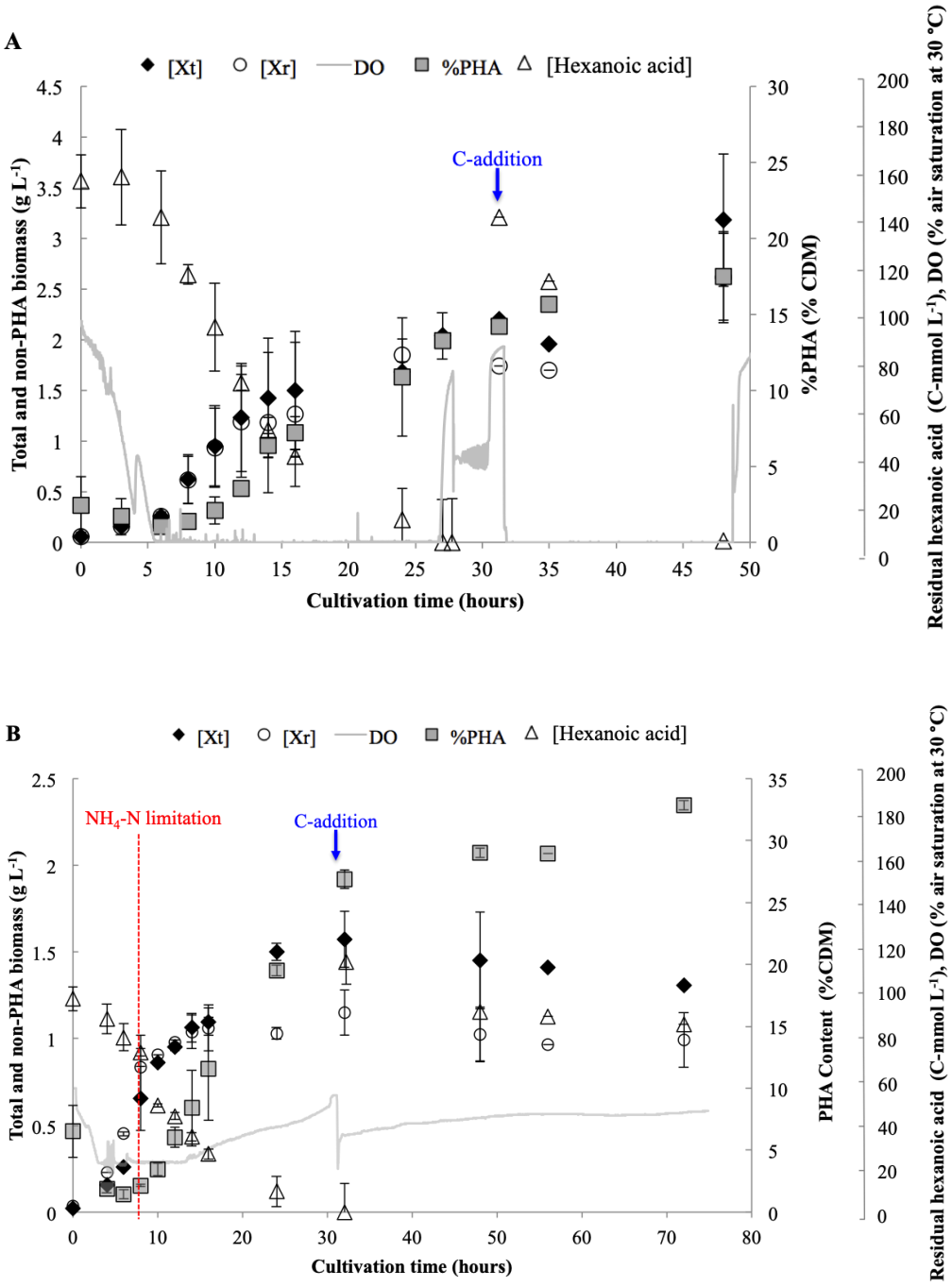

Figure 6.4. Growth and PHA synthesis from hexanoic acid using *P. putida* LS46 on under a) O_2-limited or b) NH_4-limited conditions. Error bars represent standard devaitions between biological replicates.

Table 6.2 shows some key parameters indicating the degree of limitation imposed by these conditions, including specific growth rate (μ, h^{-1}), carbon uptake rate (C-mmol g Xr^{-1} h^{-1}), and specific oxygen uptake rate (OUR, mmol O_2 g Xr^{-1} h^{-1}). As shown, under the O_2-limited conditions the specific growth rate was generally reduced to $0.25\mu_{max}$ or less. The O_2-limited specific OUR was also reduced to 25% of the values measured during the growth phase. The carbon uptake rates were (except for in the case of acetic acid) reduced more than 50% from the rates determined during the growth phase. Collectively, these results indicate that under the O_2-limited conditions, the organism was stressed from low DO, since no other known nutritional requirement was present in growth-limiting quantities. Other process performance metrics are shown in Table 6.3. These include biomass production (X_r and X_t) as well as PHA synthesis and productivity ($\%_{PHA}$, Q_s, Q_v, $Y_{PHA/S}$) characteristics for each of the four substrates tested in this work under each condition (both O_2- and NH_4-limiting).

Table 6.2. Specific growth rate, carbon uptake rate, and oxygen uptake rate observed during the growth phase, and under limiting (N or O_2) conditions.

	Glucose		**Acetic acid**		**Valeric acid**		**Hexanoic acid**	
Growth-phase								
μ_{max}[a]	0.54 ± 0.05		0.32 ± 0.11		0.28 ± 0.10		0.53 ± 0.04	
CUR_{max}[b]	29.3 ± 2.4		24.4 ± 2.6		13.4 ± 2.6		27.8 ± 10.1	
OUR_{max}[c]	34.4 ± 9.7		23.2 ± 9.8		23.7 ± 5.7		27.4 ± 12.0	
Limitation-phase (O_2 or N-limited)								
	O_2	**N**	**O_2**	**N**	**O_2**	**N**	**O_2**	**N**
μ_{avg}[d]	0.11 ± 0.00	-	0.08 ± 0.02	-	0.08 ± 0.02	-	0.04 ± 0.02	-
CUR_{avg}[e]	5.7 ± 2.4	22.3 ± 2.7	13.2 ± 3.3	17.8 ± 2.3	5.2 ± 0.5	6.7 ± 1.7	5.9 ± 1.1	6.9 ± 1.7
OUR_{avg}[f]	6.4 ± 1.9	19.5 ± 2.4	9.8 ± 1.3	8.6 ± 0.4	5.6 ± 0.6	2.8 ± 0.1	3.2 ± 0.1	3.0 ± 0.6

[a]μ_{max} – maximum specific growth rate measured during unlimited growth phase, units are h^{-1};[b]CUR_{max} – maximum carbon uptake rate measured during the growth phase, units are C-mmol g X_r^{-1} h^{-1};[c]OUR_{max} – maximum oxygen uptake rate measured during the growth phase, units are mmol O_2 g X_r^{-1} h^{-1}; [d]μ_{avg} – average specific growth rate measured during limiting phase, units are h^{-1}; [e]CUR_{avg} – average carbon uptake rate measured during the limiting phase, units are C-mmol g X_r^{-1} h^{-1}; [f]OUR_{avg} – average oxygen uptake rate measured during the limiting phase, units are mmol O_2 g X_r^{-1} h^{-1}. Tolerances indicate standard deviations between biological replicates.

Table 6.3. Biomass titer and PHA synthesis characteristics from 320 C-mmol L^{-1} of the indicated carbon substrates that utilize the *de novo* pathway to varying degrees, under conditions of strict NH_4-limitation or O_2-limitation.

	Glucose		**Acetic acid**		**Valeric acid**		**Hexanoic acid**		**Octanoic acid[g]**	
	O_2	**N**	**O_2**	**N**	**O_2**	**N**	**O_2**	**N**	**O_2**	**N**
$[X_t]$[a]	3.0 ± 0.3	1.0 ± 0.2	1.5 ± 0.1	1.1 ± 0.2	1.6 ± 0.2	1.3 ± 0.1	3.2 ± 0.7	1.7 ± 0.0	4.4 ± 0.4	3.5 ± 0.8
$\%_{PHA}$[b]	3.9 ± 0.8	10.1 ± 1.7	2.0 ± 0.9	17.4 ± 2.1	2.5 ± 0.6	21.4 ± 4.3	17.5 ± 2.9	32.8 ± 0.4	64.2 ± 0.5	51.6 ± 4.9
$[X_r]$[a]	2.9 ± 0.2	0.8 ± 0.0	1.5 ± 0.1	0.9 ± 0.2	1.5 ± 0.2	1.0 ± 0.1	2.5 ± 0.4	1.0 ± 0.1	2.2 ± 0.1	2.2 ± 0.3
Max. Q_s[c]	5.3 ± 0.9	18 ± 1.0	1.9 ± 0.9	24.8 ± 6.6	2.4 ± 0.01	33.5 ± 4.3	17.7 ± 5.2	31.2 ± 7.7	209 ± 48	141 ± 11
Max. Q_v[d]	6.1± 0.4	9.9 ± 0.2	0.9 ± 0.4	5.4 ± 1.2	0.9 ± 0.0	9.5 ± 2.4	11.7 ± 4.2	13.6 ± 1.5	97 ± 24	113 ± 45
Time[e]	22	12	45	32	55	48	48	72	24	12-16
Total carbon Consumed[f]	320	320	320	320	320	220	210	295	320	320

[a]$[X_t]$, $[X_r]$ – total and residual biomass concentrations, respectively, units are g L^{-1} CDM; [b]$\%_{PHA}$ measured as the final value at the time indicated, units are % of CDM; [c]Q_s – specific productivity, units are mg PHA g X_r^{-1} h^{-1}; [d]Q_v – volumetric productivity, units are mg PHA L culture^{-1} h^{-1}; [e]Total cultivation time, h post-inoculation; [f]units for consumed carbon are C-mmol L^{-1}; [g]results obtained from similar experiments using 320 C-mmol L^{-1} octanoic acid (C/N ratio = 21 C-mol N-mol^{-1}) that were conducted as unpublished supporting data from Chapter 4. Tolerances indicate standard deviations between biological replicates.

When grown on glucose, both μ_{max} (0.54 ± 0.05 h^{-1}) and the rate of carbon utilization under were the highest of the four substrates tested. All 320 C-mmol L^{-1} was utilized within 22 h under O_2-limited conditions (Figure 6.1a) and 12 h under NH_4-limited conditions (Figure 6.1b). During the O_2-excess phase (0-4 h), the $\%_{PHA}$ of the cells decreased from the amount carried over with the inoculum (4.7 ± 0.6% CDM) to a minimum value of 1.6 ± 0.4% CDM observed at 6 h. Following the onset of O_2-limitation, mcl-PHA accumulated up to 3.9 ± 0.8% CDM (observed at 22 h) while growth continued at μ = 0.11 ± 0.00 h^{-1} (see Tables 6.2 and 6.3). Although the amount accumulated after the onset of O_2-limitation was statistically significant (p = 0.004), the final $\%_{PHA}$ was still negligible from a commercial standpoint (de Koning et al. 1997; Choi and Lee 1999). Even under NH_4-limited conditions, the final $\%_{PHA}$ was only 10.1 ± 1.7 % CDM, which was the lowest amongst all substrates tested.

When grown on acetic acid (Figure 6.2), a negligible increase in $\%_{PHA}$ was detected following the onset of O_2-limited conditions (Figure 6.2a). In the O_2-limited condition, the $\%_{PHA}$ remained relatively constant from the amount initially added with the inoculum (0.5% CDM) while DO was in excess (0-5 h). After 5 h, the maximum $\%_{PHA}$ observed was 2.0 ± 0.9% CDM by 20 h. This was not statistically significant from the $\%_{PHA}$ measured before the onset of O_2-limited conditions (p = 0.052), and the $\%_{PHA}$ remained relatively constant until the cultivation was terminated at 48 h. Instead, growth was observed under O_2-limited conditions, albeit at a low (k_La-governed) rate of 0.10 ± 0.02 h^{-1}. This is roughly a third of the observed maximum specific growth rate (μ_{max}) of 0.34 ± 0.05 shown in Table 6.2. By contrast, in the NH_4-limited control experiment shown in Figure 6.2(b), the $\%_{PHA}$ increased up to 20.9 ± 0.3% CDM by 48 h.

Valeric acid and hexanoic acid were examined to observe if *P. putida* LS46 can effectively incorporate these into PHA under O_2-limited conditions, similar to the previous

observations (i.e. for high yields and synthesis rates) obtained from octanoic acid (Chapter 4). When grown on valeric acid (Figure 6.3), similar results were obtained as when acetic acid was the sole carbon source (Tables 6.2 and 6.3). While DO was in excess (0-10 h in Figure 6.3a), the $\%_{PHA}$ did not change tangibly from that carried over with the inoculum (≈1% CDM). When DO became limiting after 10 h, an increase in the $\%_{PHA}$ was detected (statistically significant $p < 0.005$), while growth continued at $\mu = 0.10 \pm 0.02$ h^{-1}. However, the final $\%_{PHA}$ was very low and reached only to 2.4 ± 0.6% CDM by 55 h. In contrast, under NH_4-limited conditions (Figure 6.3b) up to 21.4 ± 4.3% CDM was accumulated as PHA. When grown on hexanoic acid, μ_{max} was similar to that observed on glucose or octanoic acid, but declined to 0.04 ± 0.02 h^{-1} following the onset of O_2-limitation. This was accompanied by a significant ($p << 0.05$) increase in final $\%_{PHA}$ (17.5 ± 2.9% CDM) and rate of synthesis (Qs = 11.3 ± 5.1 mg PHA g X_r h^{-1}) compared to the other substrates (glucose, acetic acid, and valeric acid). Using NH_4-limitation, the final $\%_{PHA}$ was higher and reached 32.8 ± 0.4% CDM, which was the highest amongst all conditions tested in this work.

6.5.2. Monomer composition

The monomer compositions for each substrate tested under both O_2- and NH_4-limiting conditions are shown in Table 6.4. The composition of the obtained mcl-PHA was primarily C10 and was similar regardless of whether acetic acid or glucose was used as the substrate under NH_4-limited conditions. In the case of acetic acid, the monomer composition was for the most part consistent with those reported previously in *P. putida* LS46 cultured in flasks using strict NH_4-limitation (24.1% C8, 61.9% C10) (Jin et al. 2019). However, a shift toward smaller (particularly C6) monomers was observed in the polymer produced from acetic acid under O_2-limited conditions. Little change in monomer composition of the polymer was observed when

glucose was used as the carbon source regardless of the culture conditions. Small but detectable quantities of odd-chain-length monomers (C7 and C9) were observed in the polymers produced from both glucose and acetic acid. Although propionyl-CoA might be synthesized via the methylmalonyl-CoA pathway (Madison and Huisman 1999), Jin et al. (2019) could not find the required genes in the *P. putida* LS46 genome and suggested that propionyl-CoA might be produced via the 2-methylcitrate pathway or as an intermediate in the biosynthesis and degradation of amino acids.

In the case of valeric acid, the polymer obtained under NH_4-limited conditions was a copolymer of scl- and mcl-PHA, and the composition was generally consistent with the previously reported values of 27.7% C5, 46.5% C10 (Jin et al. 2019). Although very minor amounts of PHA were synthesized from valeric acid under O_2-limited conditions, a shift toward C5 monomers was observed, with lower amounts of longer-chain-length monomers (i.e. C10) associated with *de novo* synthesis. The C5/C10 ratio observed under the DO limited condition was 3.2, compared to the value of 0.7 obtained under NH_4-limiting (DO excess) conditions.

When hexanoic acid was used as the substrate, the resulting PHA was predominantly (73-82%) C6, and likely a result of direct incorporation as an intermediate of β-oxidation (Huijberts et al. 1994). The remainder of the monomers were C8 or longer, which indicates the *de novo* pathway was used (albeit to a lesser extent under O_2-limitation) simultaneously with β-oxidation (Huijberts et al. 1994). This C6 content is consistent with mcl-PHA produced from hexanoic acid in a previous study using *P. putida* KT2442 (Huijberts et al. 1994), but lower than that reported for *P. putida* GPo1 (formerly *P. oleovorans*) (Huisman et al. 1989). When O_2-limitation was used as the sole driving force for PHA synthesis, the C6 content was nearly 10% higher than when NH_4 limitation (where excess DO was used), and the C10 content was significantly

reduced. (Table 6.4). In fact, the C6.C10 ratio observed under NH4-limited (DO excess conditions) was 4.8, but the corrsponding value obtained under O_2-limitation was 82.2.

Table 6.4. Monomer composition of PHA obtained from carbon substrates that utilize the *de novo* pathway to varying degrees, under conditions of strict NH_4 limitation or O_2-limitation.

	Glucose		**Acetic acid**		**Valeric acid**		**Hexanoic acid**		**Octanoic acid[a]**	
	NH_4	**O_2**	**NH_4**	**O_2**	**NH_4**	**O_2**	**NH_4**	**O_2**	**NH_4**	**O_2**
C5	-	-	-	-	28.6 ± 1.3	47.4 ± 7.9	-	-	-	-
C6	7.0 ± 5.5	6.0 ± 0.7	6.3 ± 0.2	23.5 ± 1.2	1.1 ± 0.3	1.5 ± 0.3	72.7 ± 3.4	82.2 ± 1.1	7.1 ± 0.8	6.0 ± 1.1
C7	2.5 ± 0.6	1.6 ± 0.0	2.8 ± 0.8	2.0 ± 0.4	2.3 ± 0.5	1.4 ± 0.1	-	-	-	-
C8	22.3 ± 3.0	18.5 ± 5.6	23.4 ± 2.3	13.8 ± 2.2	10.5 ± 1.7	2.3 ± 0.0	7.1 ± 0.9	11.4 ± 0.4	90.9 ± 0.7	92.5 ± 0.8
C9	-	-	-	-	2.9 ± 0.4	2.1 ± 2.5	-	-	-	-
C10	57.2 ± 0.0	60.9 ± 8.1	56.7 ± 5.7	33.8 ± 3.6	40.1 ± 3.8	14.6 ± 2.5	15.1 ± 2.2	1.0 ± 0.4	1.3 ± 0.2	1.4 ± 0.4
C12	4.1 ± 0.1	7.2 ± 2.4	5.4 ± 1.7	8.8 ± 0.9	4.5 ± 2.1	9.4 ± 5.8	1.4 ± 0.4	0.6 ± 0.3	trace	trace
C12:1	2.7 ± 0.2	3.0 ± 1.6	1.0 ± 0.3	3.1 ± 0.7	1.0 ± 0.8	4.6 ± 0.8	0.9 ± 0.4	1.0 ± 0.8	-	-
C14	1.8 ± 0.1	6.4 ± 2.3	3.2 ± 1.9	11.2 ± 2.5	3.2 ± 0.8	13.7 ± 3.5	1.9 ± 1.6	1.7 ± 0.4	-	-
Other (<1%, trace)	C9, C12:2, C14:1, C14:2	C9, C12:2, C14:1, C14:2	C9, C12:2, C14:1, C14:2	C12:2, C14:1, C14:2	C12:2, C14:1, C14:2	C12:2, C14:1, C14:2	C14:1			C12

[d]O_2-limited results for octanoate obtained from experiments with 20 mM octanoic acid, 1.5 g L^{-1} $(NH_4)_2SO_4$ (C/N ratio = 7.05 C-mol N-mol^{-1}) and fixed OTR at k_La = 38 h^{-1} (Chapter 4); NH_4-limited experiments for octanoic acid obtained from unpublished supporting data from Chapter 4, as described in Table 6.3. Tolerances represent standard deviations between biological replicates.

6.5.4. Yield analysis

Table 6.5 shows a yield analysis for each substrate under both O_2-limited and NH_4-limited (DO excess) conditions, along with a comparison back to previous work undertaken with octanoic acid a (Chapter 4) and LCFAs (Chapter 5). These results show that none of these substrates are particularly effective candidates for mcl-PHA synthesis. In all cases, the $Y_{PHA/S}$ was less than 10% (C-mol C-mol^{-1}), even when PHA accumulated up to a relatively higher content in the NH_4-limited control conditions.

During the phase of unrestricted growth, the $Y_{Xr/S}$ from acetic acid and valeric acid (and to some extent, glucose) was also relatively low (0.33 C-mol C-mol^{-1}) compared to hexanoic acid and previous work with octanoic acid or LCFAs (0.5-0.6 C-mol C-mol^{-1}). This resulted in low overall [X_t] production and Q_v (Table 6.2) on these substrates compared to longer chain-length fatty acids. During either the growth or mcl-PHA synthesis phases of the cultivations on glucose, acetic acid, valeric acid, and hexanoic acid, the majority of the carbon was lost as CO_2. These substrates consistenly showed $Y_{CO2/S}$ values of 0.65 C-mol C-mol^{-1} and higher, whereas in previous work with octanoic acid (Chapter 4) or LCFAs (Chapter 5) generally the $Y_{CO2/S}$ coefficients were 0.4-0.55 C-mol^{-1} C-mol^{-1}.

The majority of carbon was accounted for as X_r, X_{PHA}, or CO_2, as indicated by the carbon recoveries, which generally ranged from 0.96 to 1.08 (Table 6.5). However, the obtained carbon balance for glucose under NH_4-limited conditions was poor (0.7 ± 0.14). This corroborated with a uniquely slimy and viscous appearance of the harvested culture, which could indicate the presence of extracellular polymeric material as a carbon sink. Although these substances were not accounted for in this work, further details are available in Chapter 8.

Table 6.5. Yield analysis for unrestricted growth conditions and growth-limited (NH_4 and O_2) conditions for each substrate.

	Growth-phase yield coefficient (% C-mol-C-mol^{-1})			Growth-limited yield coefficient (% C-mol-C-mol^{-1})				Carbon recovery	Ref
	$Y_{PHA/S}$	$Y_{Xr/S}$	$Y_{CO2/S}$	Growth Limitation	$Y_{PHA/S}$	$Y_{Xr/S}$	$Y_{CO2/S}$	C-mol-C-mol^{-1}	
Glc	0.7 ± 0.3	36.2 ± 10.6	51.1 ± 9.6	NH_4	4.1 ± 2.1	-	65.8 ± 11.2	0.7 ± 0.14	This work
				O_2	2.6 ± 1.3	46.1 ± 2.4	65.6 ± 0.6	0.96 ± 0.02	
Ac	0.2 ± 0.0	31.8 ± 8.3	71.3 ± 12.2	NH_4	4.7 ± 0.0*	-	91.0 ± 6.4	1.07 ± 0.1	This work
				O_2	0.3 ± 0.0*	17.8 ± 1.9	86.9 ± 5.3	1.08 ± 0.1	
Val	1.2 ± 0.9	33.9 ± 6.1	67.9 ± 14.6	NH_4	9.0 ± 6.4*	-	67.6 ± 20.6	1.05 ± 0.14	This work
				O_2	0.8 ± 0.3*	25.7 ± 2.3	56.9 ± 3.5	1.00 ± 0.10	
Hex	0.5 ± 0.0	58.6 ± 13.6	47.9 ± 6.0	NH_4	7.5 ± 5.6	-	71.8 ± 18.4	1.03 ± 0.00	This work
				O_2	9.2 ± 3.9	26.2 ± 13.0	65.6 ± 10.6	0.96 ± 0.07	
OA[a]	6.7 ± 2.3	50.7 ± 7.0	42.5 ± 6.6	O_2	63.4 ± 3.8	9.2 ± 5.1	36.5 ± 7.3	1.03 ± 0.01	Chapter 4
OA[b]	18.8 ± 9.7	48.0 ± 3.3	39.8 ± 6.0	O_2	55.5 ± 0.0	8.4 ± 3.1	40.6 ± 1.9	0.96 ± 0.08	Chapter 5
OA[c]	4.3 ± 0.9	40.0 ± 8.5	55.7 ± 11.1	NH_4	43.9 ± 14.5	-	56.4 ± 22.0	No data	Unpublished data
LCFAs[d]	12.4 ± 5.8	60.2 ± 6.3	30.4 ± 11.2	O_2	24.7 ± 3.3	38.7 ± 4.7	36.6 ± 2.0	No data	Chapter 5

[a]Yield values for O_2-limited batch experiments using octanoic acid derived from experiments with 20 mM octanoic acid, 1.5 g L^{-1} $(NH_4)_2SO_4$ (C/N ratio = 7.05 C-mol N-mol^{-1}) and fixed OTR at k_La = 38 h^{-1}, obtained from Chapter 4. [b]Yield values derived from fed-batch experiments (μ = 0.25 h^{-1}) using octanoic acid with excess NH_4 under O_2-limited conditions with fixed OTR (k_La = 54 h^{-1}). [c]Yield values for NH_4-limited experiments for octanoic acid obtained from unpublished supporting data from Chapter 4, as described in Table 6.2. [d]Yield values derived from fed-batch experiments (μ = 0.25 h^{-1}) using canola-derived LCFAs with excess NH_4 under O_2-limited conditions with fixed OTR (k_La = 54 h^{-1}) (Chapter 5). The dash indicates immeasurably small values, which are assumed to be zero. $Y_{PHA/S}$ values marked with an asterisk are statistically significant ($p < 0.05$) when the N-limited condition was compared to the O_2-limited experiment for the respective carbon source. Abbreviations not already defined: Ac – acetic acid; Val – valeric acid; Hex – hexanoic acid. Tolerances indicate standard deviations between biological replicates.

6.6. Discussion

Due to practical constraints on mixing equipment in large-scale bioreactors, overall mass transfer capability (and power consumption per unit volume) is generally reduced compared to lab-scale reactors (Byrom 1992; Lara et al. 2006a; Garcia-Ochoa et al. 2010). This, combined with the inherent low solubility of O_2 in aqueous medium, causes O_2 mass transfer limitations to become problematic in strictly aerobic bioprocesses. In large-scale bioreactors, chemical gradients can occur in the vertical and radial directions causing environments where DO is present in limiting concentrations (Bylund et al. 1998; Junker 2004). In this work, these environments were investigated in lab-scale bioreactors to observe how PHA production (primarily mcl-) in *P. putida* LS46 is affected when it is synthesized primarily by the *de novo* pathway under O_2-limitation. With respect to the NH_4-limited control experiments, low final $\%_{PHA}$ (<5% CDM) was obtained from both glucose and acetic acid using O_2-limitation. Under these conditions, a variable portion of the carbon consumed was used to maintain residual growth at a low rate ($\mu = 0.1\ h^{-1}$), whilst the majority was respired as CO_2. This may imply a high maintenance requirement or possible energy spilling through seemingly futile, energy-uncoupling cellular processes (Liu and Tay 2001; Russell 2007). Higher maintenance reqiurment might be due to the toxocity of the shorter chain VFAs; in these cases, the cell must spend more energy per C-mol consumed (compared to glucose or LCFAs) to remove protons from the cytoplasm to maintain both membrane potential and intracellular pH. This is supported by the highest CO_2 production coming from both acetic and valeric acids, whereas glucose produced less CO_2 with higher biomass yields (Table 6.5). The simultaneous biosynthesis and degradation of PHA has been suggested to play a role in energy metabolism, but is not currently understood very well (Ren et al. 2009; Escapa et al. 2012).

On this basis, it does not appear that the reductive steps in the *de novo* pathway act as an electron sink in O_2-limited environmental conditions, This is somewhat of a curiosity given that *P. putida* is generally known for low cellular energy demand for maintenance, and therefore maintains a relatively efficient metabolism with a higher net NAD(P)H generation capacity, which should be advantageous for redox-based biocatalysis (Ebert et al. 2011). It is also contrary to what is known of synthesis of PHB from glucose in low-DO environments (Senior et al. 1972; Faccin et al. 2013).

In synthesis of PHB from glucose, the $NADP^+$ produced from reduction of acetoacetyl-CoA to (R)-3-hydroxybutyryl-CoA is balanced by NADPH produced from oxidation of glucose-6-phosphate to 6-phosphogluconate in the Entner-Doudoroff pathway. By comparison, synthesis of a C10 mcl-PHA monomer from glucose via the *de novo* pathway would require eight NADPH, whereas only 2.5 $NADP^+$ would be reduced to catabolize the required amount of glucose via the Entner-Doudoroff pathway. In order to maintain cellular redox, the excess $NADP^+$ from mcl-PHA synthesis could conceivably be regenerated by several enzymes present in the LS46 genome (Sharma et al. 2013), shown in Table 6.6. Only a few of these are thought to make a significant contribution to meeting NADPH demand required for reductive biosynthetic reactions (Grousseau et al. 2013; Spaans et al. 2015; Andin et al. 2017). In fact, a previous study showed that over 75% of the NADPH demand during growth of *P. putida* KT2440 from fatty acids in fed-batch culture was met via transhydrogenase, malic enzyme, and the TCA cycle (Andin et al. 2017).

Table 6.6. Possible enzymes responsible for reactions that reduce $NADP^+$ in *P. putida* LS46.

Enzyme	Pathway(s)	Locus tag
G6PDH	ED, PP	PPUTLS46_012095
		PPUTLS46_016864
6-PGDH	PP	PPUTLS46_012100
GAPDH	EMP	PPUTLS46_004464
NADP-dependent GAPDH		PPUTLS46_018356
IDH	TCA	PPUTLS46_011965
NADP-dependent IDH		PPUTLS46_011960
NADP-dependent MDH	TCA	PPUTLS46_005216
$NADP^+$ TH (soluble)	Not associated with	PPUTLS46_004474
TH α-subunit (membrane-bound)	central carbon	PPUTLS46_016009
TH α-subunit (membrane-bound)	metabolism	PPUTLS46_016014
TH β-subunit (membrane-bound)		PPUTLS46_016019

Abbreviations: G6PDH – glucose 6-phosphate dehydrogenase; 6-PGDH – 6-phosphogluconate dehydrogenase; GAPDH – glyceraldehyde 3-phosphate dehydrogenase; IDH – isocitrate dehydrogenase; MDH – malate dehydrogenase; TH – transhydrogenase

The results in the present study, however, suggest that under microaerophlic conditions, the NADPH that is regenerated via these routes is used for biosynthesis and cellular functions other than mcl-PHA synthesis from glucose and short chain VFAs. Some of the aforementioned enzymes show reduced activity under O_2-limited conditions (Mitchell and Dawes 1982) or are inhibited by NADH, which would be expected to be in higher concentrations under O_2-limited conditions (Senior and Dawes 1971; Bae and Rittmann 1996). Transhydrogenase is inhibited by $NADP^+$ (Höjeberg et al. 1976) and has also been demonstrated to be transcriptionally up-regulated under O_2-limited conditions (Hanke et al. 2012). However, regeneration of NADPH via transhydrogenase consumes ATP and may not be thermodynamically favorable when the terminal electron acceptor, and hence ATP generation by oxidative phosphorylation, is limited.

It was interesting that when compared to acetic acid as the carbon source, glucose produced slightly higher $\%_{PHA}$, Q_s (Table 6.3) and $Y_{PHA/S}$ (Table 6.5), and more static monomer composition regardless of DO. This could suggest that the NADPH produced in the Entner-Doudoroff pathway during glucose catabolism does, to a small degree, help ease redox imbalance as a constraint on *de novo* mcl-PHA synthesis under low-DO conditions. However, in *P. putida* LS46, this certainly does not occur to the extent that was reported in previous studies with *A. beijerinckii* (Senior et al. 1972). It is doubtful that further stress from inadequate supply of DO could effectively stimulate mcl-PHA synthesis from glucose since no PHA was synthesized even in the complete absence of O_2 when the reactor was gassed with N_2 (data not shown).

Hexanoic acid accumulated comparatively high levels of mcl-PHA under O_2-limitation and appears to be the gateway to the efficient mcl-PHA synthesis from β-oxidation intermediates previously observed from octanoic acid (Chapter 4) or LCFAs (Chapter 5) at low DO. The polymer produced from hexanoic acid was predominantly (72.7 - 82.2%) C6 regardless of DO and indicates most of the monomers were obtained from β-oxidation intermediates rather than the longer monomers (C10, C12, C14, C12:1, and C14:1) that are generally characteristic of mcl-PHA synthesized *de novo* (Huijberts et al. 1992; Gillis et al. 2017). Interestingly, under O_2-limitation the content of the C6 increased by nearly 10% (from 72.7 to 82.2% of the polymer), while the C10 content was reduced by 14%. This corroborates the previous hypothesis that mcl-PHA synthesis from β-oxidation intermediates may be a way of storing electrons available in highly-reduced fatty acids when O_2 is not in sufficient supply to completely oxidize the substrate. Although further testing is needed, similar tests with canola-derived LCFAs (primarily oleic) showed that less C8 monomers, and a higher proporption of longer-chain monomers were

incorporated at lower DO (unpublished data). Therefore, if substrates with mixed composition were being used, O_2-limitation could be a way to tune polymers by enriching the content of monomers with the closest carbon chain-length to the (fatty acid) substrate being fed.

Despite a significant presence of C5 monomers in PHA synthesized from valeric acid, this substrate behaved more similarly to acetic acid (from which mcl-PHA is produced by *de novo* synthesis) than to hexanoic acid or octanoic acid (from which mcl-PHA is produced predominantly by β-oxidation) in terms of PHA synthesis under low-DO conditions. Interestingly, of the minimal amount of polymer that was synthesized, there was still a considerable enrichment of the C5 monomer under O_2-limited conditions. Further NMR studies using ^{13}C-labelled valeric acid would help to deduce if these monomers were a result of β-oxidation or *de novo* synthesis.

Although previous studies have indicated that mcl-PHA synthesis from glucose was not effective under O_2 limitation in *Pseudomonas* spp. (Haywood et al. 1990; Diniz et al. 2004), this study represents the first in-depth look at carbon flux when glucose and short-chain VFAs are metabolized by *P. putida* for mcl-PHA synthesis under O_2-limited conditions. Our main findings were that negligible amounts of PHA were synthesized from glucose and short chain VFAs (acetic acid, valeric acid) in low-DO conditions, and only a modest amount was synthesized from hexanoic acid. This could be problematic if large-scale PHA production were to be based on VFA- or carbohydrate-rich carbon feedstocks using *P. putida* LS46, or other strains of mcl-PHA-producing *Pseudomonas* spp., since large-scale bioreactors have inherently poor mass transfer capability (Lara et al. 2006; Byrom 1992). Furthermore, the low $Y_{PHA/S}$ coefficients obtained for all substrates examined in this work indicate that these carbon sources are not ideal for PHA

production using *P. putida* LS46, given that the carbon substrate can account for up to 60% of process costs (Wang et al. 2014).

Combined with Chapters 4 and 5, this completes a spectrum of work on mcl-PHA synthesis and yield characteristics in low-DO environments that now encompasses representative substrates for carbohydrates, VFAs, mcl-fatty acids, and LCFAs. In summary, medium and long-chain fatty acids (C8 and higher) are converted to mcl-PHA under microaerophlic conditions with high rate, yield, and reasonably high PHA contents. In contrast, volatile fatty acids (up to C6) and simple sugars like glucose do not allow any significant PHA synthesis to be induced solely by microaerophilic conditions. However, depending on the substrate, other interesting observations were noted. These include residual growth under microaerophilic conditions (i.e. from LCFAs) or different monomer compositions being obtained (i.e. from valeric acid, hexanoic acid, and LCFAs). This may have potential for future processes focusing on improving productivity or obtaining a particular monomer composition by manipulating bioreactor OTR. The combined results for growth, mcl-PHA synthesis characteristics, and monomer compositions are summarized in Figure 6.5 as a function of the biochemical pathways utilized as well as the redox value of the carbon substrate, which was adapted from a convention used previously (Blunt et al. 2014).

On the basis of the results, it seems that when *P. putida* LS46 is exposed to low-DO environments, favorable mcl-PHA synthesis characteristics are exhibited when the PHA is synthesized from oxidative processes (β-oxidation of fatty acids or alkanes) but not by reductive processes (*de novo* biosynthesis). This is somewhat counter-intuitive given that the reduced cofactors generated from operating the β-oxidation cycle must be regenerated through electron transport to O_2, and also contrary to the available literature on microaerophilic synthesis of PHB.

Ultimately, PHA synthesis in *P. putida* may be governed by different regulatory mechanisms than organisms that produce PHB through the reduction of acetoacetyl-CoA to 3-hydroxybutyryrl-CoA (in the process regenerating the reduced cofactor NADPH) at low DO (see Figure 2.2). Moving forward, a proteomic and/or transcriptomic study comparing oxygen-limited growth on glucose or acetate to oxygen-limited growth on octanoic acid (for example) may help to elucidate these mechanisms for mcl-PHA synthesis using *P. putida*.

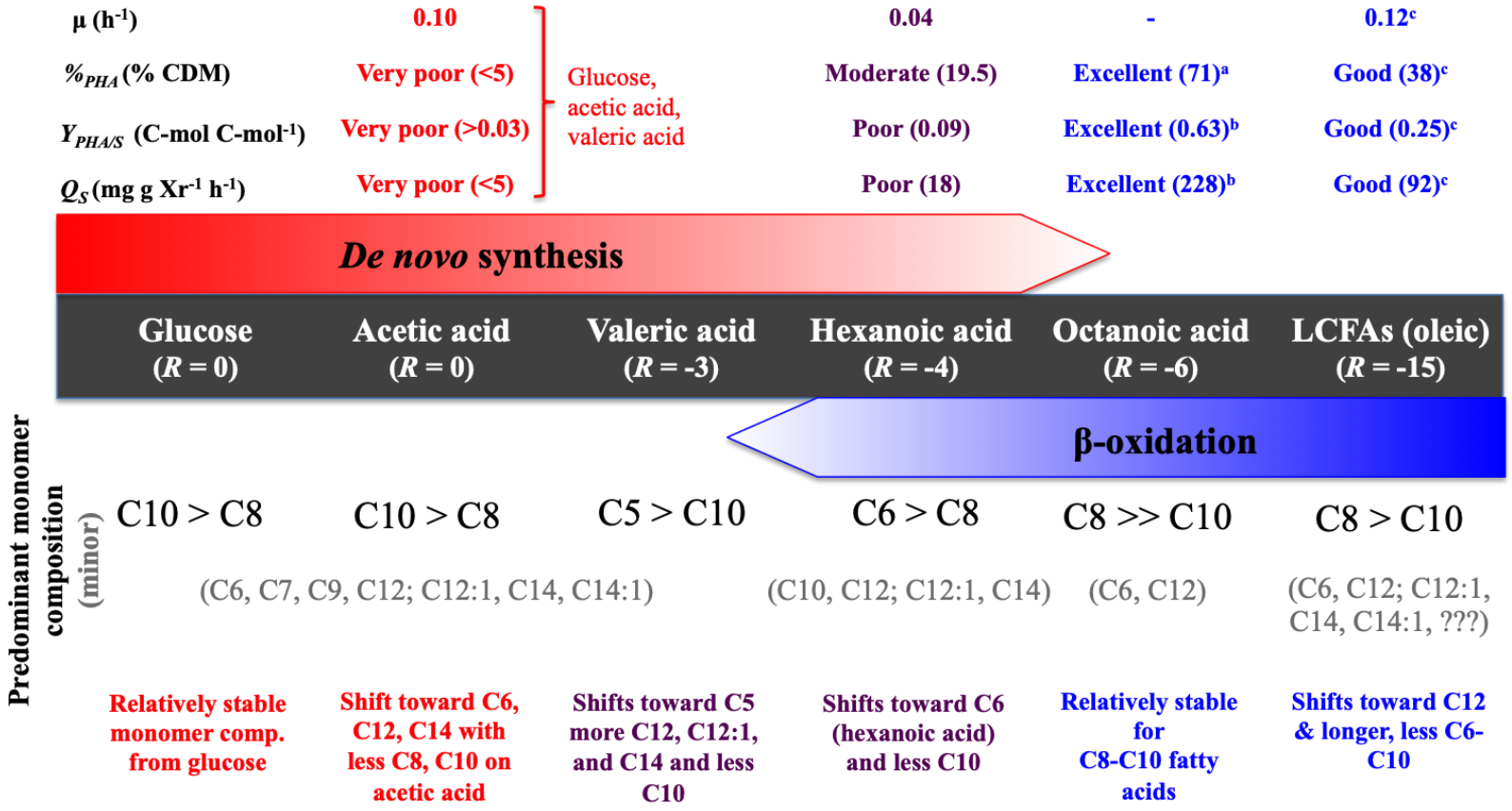

Figure 6.5. Mcl-PHA synthesis characteristics from a spectrum of substrates in low DO environments. [a]Results obtained from Chapter 4 for the conditions k_La = 12 h^{-1} with C/N ratio of 7.05 C-mol/N-mol. [b]results taken from Chapter 4 for conditions k_La = 38 h^{-1} with C/N ratio of 7.05 [c]results taken from O_2-limited fed-batch experiments (k_La = 54 h^{-1}) from Chapter 5. The redox value, *R*, of each carbon molecule in the susbtrate, is calculated as $x - 0.5y$, where x is the number of oxygens and y is the number of hydrogens in the molecule (Blunt et al. 2014).

6.7. Conclusions

In contrast to synthesis of mcl-PHA from intermediates of the β-oxidation cycle, no significant amount of mcl-PHA was synthesized from glucose and short-chain VFAs up to and including hexanoate. The monomer composition obtained from certain substrates (valeric acid, hexanoic acid) indicated that both β-oxidation and *de novo* synthesis contributed monomers to the polymer. When this was the case, lowering the DO appeared to enrich the dominant monomer formed by β-oxidation while decreasing the content of the monomers typical of *de novo* mcl-PHA synthesis.

Overall, it appears that glucose, acetic acid, valeric acid, and to a lesser degree, hexanoic acid are poor carbon sources on which to base an mcl-PHA-production platform using *P. putida* LS46 in a low DO environment due to low final PHA content, poor synthesis rate, low yields (most of the carbon was respired to CO_2), and poor productivity. This work does point toward an opportunity to enrich the content of certain monomers through co-feeding a particular substrate at low DO, which could produce polymers dinstinctive monomer compositions and unique properties. In this case, simultaneous NH_4-limitation should be applied to increase the PHA content to more desirable levels.

6.8. Acknowledgements

This work was funded by: 1) Genome Canada, through the Applied Genomics Research in Bioproducts or Crops (ABC) program for the grant titled, “Microbial Genomics for Biofuels and Co-Products from Biorefining Processes”; 2) the government of the Province of Manitoba through the Manitoba Research Innovation Fund (MRIF) and the Manitoba Rural Adaptation

Council (MRAC); 3) the Natural Sciences and Engineering Research Council (NSERC); and 4) the University of Manitoba Sir Gordon Wu Graduate Student Scholarship.

Special thanks to: 1) Zimo Jin, for his help in taking periodic samples and running the GC; 2) Alain Lagasse, also for his help in experimental setup, taking and preparing samples for GC analysis; and 3) Chris Dartiailh for his thoughts and inputs, for being around to bounce ideas off, and for reviewing the manuscript (along with the other co-authors).

Chapter 7: Development of an oxygen-limited fed-batch process for improved polyhydroxyalkanoate productivity using *Pseudomonas putida* LS46

7.1. Preface

In Chapter 4, it was found that low DO environments are favorable for mcl-PHA synthesis from octanoic acid, while in Chapter 5 (although not the sole focus of that work) it was found that control of fed batch strategies with such a toxic substrate was challenging. The objective of this work was to make a significant productivity advance over previous work by developing and applying a more optimal fed-batch strategy, based on real-time process feedback variables rather than the pre-determined feeding rates used in Chapter 5. This work has been organized into a manuscript, and the title and abstract were submitted to an upcoming special issue of the journal *Bioengineering* on "Advances in Polyhydroxyalkanoate Production, Volume 2."

7.2. Abstract

Application of HCD fed-batch cultures is widely perceived as a requisite for high-productivity PHA production processes. In this work, a CO_2-based pulse-feed strategy was used to control an O_2-limited fed-batch process targeting improved productivity of mcl-PHAs synthesized by *P. putida* LS46. The process reliably achieved [X_t] of 28.8 ± 3.9 g L^{-1} (with the average maximum $\%_{PHA}$ of 61 ± 8% CDM) using octanoic acid as the carbon source in a bench-scale (7 L) bioreactor. This resulted in a final Q_v of 0.66 ± 0.14 g L^{-1} h^{-1}, which was, on average, an eight-fold improvement over previous batch work (Chapter 4). Delivering carbon to the bioreactor as a continuous drip-feed process appeared to favor higher final [X_r], whereas pulse-feeding octanoic acid (in response to carbon depletion) produced lower final [X_r], but resulted in

higher $Y_{PHA/S}$ during the storage phase. Despite this difference, the two processes resulted in similar overall Q_v. Overall it was shown that the inherent O_2-limitation brought about by HCD cultures can be used to drive reasonably productive mcl-PHA synthesis from fatty acids, without the need to closely manage C/N or C/P ratios, which are considerably more difficult to measure in real time. Furthermore, the CO_2-based, pulse-feed strategy appears to be a relatively easy and reliable method for rapid optimization of fed-batch processes, particularly when using toxic substrates like octanoic acid.

7.3. Introduction

Microbial PHAs are a class of biopolymers with potential application as renewable, biodegradable materials that could displace petroleum-based plastics. Several factors have limited commercial applications of mcl-PHAs to certain niche markets, but the main factor is simply the cost of production, which has been estimated to be as much as fifteen-fold higher than polyethylene or polypropylene (Możejko-Ciesielska and Kiewisz 2016; Kourmentza et al. 2017).

Development of efficient bioprocesses is paramount to improving the economic viability and lessening the environmental impacts of PHA production (Kaur and Roy 2015; Koller et al. 2017). The overall Q_v of any bioprocess is a crucial performance metric, and is typically around 2 g L^{-1} h^{-1} for production of bulk bio-products (Heijnen et al. 1992). Employing HCD cultures is widely seen as the best cultivation strategy to achieve high Q_v and facilitate overall cost reduction (Ienczak et al. 2013). Several studies that have applied HCD fed-batch cultivation strategies have reported Q_v values close to 2 g L^{-1} h^{-1} for mcl-PHAs (Lee et al. 2000b; Maclean et al. 2008; Jiang et al. 2013; Cerrone et al. 2014b). For production of scl-PHAs, [X_t] in excess of 200 g L^{-1} and Q_v of 5.13 g L^{-1} h^{-1} have been reported (Ryu et al. 1997; Wang and Lee 1997b; Shang et al. 2003a).

There are several challenges that arise from HCD cultures. Firstly, monitoring and control of these processes is difficult because of the lack of real-time measurements of key process variables, such as substrate uptake (Riesenberg and Guthke 1999; Sun et al. 2006). This is particularly problematic when the substrate exhibits toxicity, and accumulation of substrate can have deleterious consequences (Kellerhals et al. 1999b). Previously it was found that a fine threshold exists between carbon-limited growth and substrate-induced inhibition when feeding octanoic acid at a predetermined exponential rate (i.e. the proactive feeding approach described in Chapter 5). However, in those experiments, it was observed that carbon-limitation was indicated by a rapid and sharp decrease in the off-gas CO_2 concentration, and subsequent rise in the DO signal, when feeding was briefly paused. Thus, a possible solution to the toxicity issue may be to use a reactive feeding approach; that is, to feed sub-inhibitory amounts of carbon when needed as indicated by real time signals, rather than feeding at a predetermined rate.

Similar strategies have been used in the past, using indicators such as pH, DO, and CO_2 production (Kim et al. 1997; Lee et al. 2000b; Kim 2002; Sun et al. 2006). As pointed out by Riesenberg and Guthke (1999), these strategies depend on carbon-limited growth, and thus may limit growth and product formation rates. While multiple studies have used predetermined feeding rates rather successfully (Sun et al. 2007a; Maclean et al. 2008; Gao et al. 2016), a reactive approach may be preferable during initial process optimization.

Collectivley, Chapters 4-6 indicated that when fatty acids are used as the carbon substrates, O_2-limitation induces favorable mcl-PHA synthesis characteristics. With that in mind, the key hypothesis of this work was that O_2-limitation (a condition naturally occurring at sufficiently HCD, and typically problematic in aerobic bioprocesses) could be as a simple and effective strategy to induce mcl-PHA synthesis in an aggressive, HCD fed batch cultivation

strategy. The objective of this work, therefore, was to build on previous work and develop robust and reliable cultivation processes for achieving HCD cultures of *P. putida* for improved Q_v.

7.4. Materials and Methods

7.4.1. Microorganism, medium, substrates

The microorganism (*P. putida* LS46) and strain maintenance practices in this work followed those described in Section 3.1. The medium used was similar to the minimal medium described in Section 3.2, except that the initial concentrations of $(NH_4)_2SO_4$, $MgSO_4$, $CaCl_2.2H_2O$, and trace element solution were increased to 2 g L^{-1}, 0.2 g L^{-1}, 20 mg L^{-1}, and 2 mL L^{-1}, respectively. Octanoic acid (Sigma-Aldrich, St Louis, MO) was added to an initial concentration of 20 mM (2.88 g L^{-1}). The $MgSO_4$, $CaCl_2.2H_2O$, ferric ammonium citrate, trace element solution, and octanoic acid were filter-sterilized into the bioreactor through a 0.2 μm filter after autoclaving.

7.4.2. Reactor setup and operation

The reactor setup, calibration, and sterilization procedures followed those described in Section 3.10. Experiments were initiated with the addition of a 5% (vol vol^{-1}) inoculum that was grown overnight as described in Section 3.2. Samples (20 to 40 mL) were periodically withdrawn from the bioreactor, generally in 1 to 3 h intervals. These were handled as described in Section 3.3 for gravimetric determination of total biomass. Quantification of PHA and residual octanoic acid in the culture supernatant was done by the GC-FID technique described in Sections 3.4 and 3.5, respectively.

The reactor pH was controlled at 6.5 through the addition of 4 M NaOH via automated peristaltic pumps. The DO was maintained at 40% (of relative saturation with atmospheric air at

30 °C), which was controlled through constant aeration at 6 LPM (atmospheric air only) with a mixing cascade operating from 350-1200 rpm using a single Rushton turbine. Air was delivered to the medium through the factory L-shaped sparging tube.

Feeding of octanoic acid and a 200 g L^{-1} solution of $(NH_4)_2SO_4$ was accomplished through automated injector syringes, previously described elsewhere (Blunt et al. 2014). These were used to feed pulses of octanoic acid in small concentrations (5-20 mM) along with sufficient $(NH_4)_2SO_4$ for balanced growth until 20 h, after which point $(NH_4)_2SO_4$ was no longer fed. Feeding was triggered manually immediately following observation of either a drop in the off-gas CO_2 concentration, or a sudden rise in the DO signal, which indicated depletion of the carbon source. The CO_2 signal was measured using a membrane-inlet mass spectrometer and quantified as described in Section 3.11. It was found that the off-gas CO_2 concentration was a more rapid indicator of carbon depletion during growth, while during PHA accumulation, changes in the CO_2 concentration became more difficult to detect and DO was a more reliable indicator. Experiments were generally completed by 27 h post inoculation and were terminated when either: 1) further addition of carbon had no effect on the (already declining) CO_2 production rates; or 2) the measured OD_{600} decreased; or 3) excessive and uncontrollable foaming was observed.

7.4.3. Yield coefficients

Yield coefficients were derived as described in Section 3.8. The yield coefficient of X_r from NH_4 ($Y_{Xr/N}$) was determined to be 6.1 g g^{-1} from previous data obtained in Chapter 4. This value is in reasonable agreement with the $Y_{Xr/N}$ of 5.44 g g^{-1} reported by Sun et al. (2006). Similarly, $Y_{Xr/C}$ and $Y_{PHA/S}$ (from octanoic acid) were derived from previous data obtained from batch experiments in Chapter 4 as 0.72 g g^{-1} and 0.62 g g^{-1}. While the $Y_{PHA/S}$ value was similar to

that reported previously for nonanoic acid, the $Y_{Xr/C}$ measured in this work is considerably higher than the 0.24 g g^{-1} previously reported (Sun et al. 2007a). Other medium components (PO_4^{3-}, Mg^{2+}, Fe^{3+}) were assumed to be in excess on the basis of the yield coefficients reported previously (Preusting et al. 1993a; Sun et al. 2006). The validity of this assumption was checked through measurement of residual trace metals in the culture supernatant (described below).

7.4.4. Measurement of residual carbon, NH_4-N, PO_4-P and trace medium components

Residual octanoic acid in the culture supernatants was determined using the sample preparation protocol outlined in Section 3.4.2, and the GC-FID method described in Section 3.5. Residual free NH_4 was measured spectrophotometrically as described in Section 3.9. Residual PO_4 was also measured spectrophotometrically in a flow injection system using the Quickchem® method 10-115-01-1-A. Briefly, PO_4^{3-} is reacts with ammonium molybdate and antimony tartarate to form a complex that produced a blue color when reduced with ascorbic acid. This color change is measured at 880 nm. Samples were filtered through a 0.45 μm filter and diluted 250X prior to measurement. The concentration of trace elements was measured via inductively coupled plasma optical emission spectrophotometer (ICP-OES) at select intervals over the cultivation time. Samples were prepared without dilution, although a 2% (vol vol^{-1}) nitric acid solution (also used as the eluent for ICP) was added to the samples, which were then filtered through a 0.2 μm filter.

7.5. Results

7.5.1. Pulse feed strategy

Figure 7.1a shows the results for growth and PHA production obtained from four independent pulse fed-batch experiments. Despite constant aeration set at 6 LPM and a cascading

stirrer reaching its maximal value, the DO could not be maintained at the intended set point of 40% (of air saturation at 30 °C implied throughout) beyond 11 h as shown in Figure 7.1b. By 14 h, the DO was consistently under 5% when carbon was in excess. These conditions are normally expected to cause a shift in carbon flux from growth to PHA synthesis, as described in Chapters 4 and 5. However, the $\%_{PHA}$ started increasing significantly from about 8 h onward, while DO was still maintained at relatively high levels. This may have been caused by either highly dynamic mixing conditions or growth being slowed by the rate of carbon (or NH_4) feeding. Low residual concentrations of both carbon and NH_4 were detected in the culture medium around 8 h, and carbon limitation has been shown to trigger storage of carbon as PHA (Sun et al. 2007a). The production of X_r continued until 14 h, and then declined to nearly negligible values due to DO limitation, which is consistent with previous work using octanoic acid (Chapter 5).

7.5.2. Residual concentrations of octanoic acid, NH_4-N and PO_4-P

Figure 7.1c shows the profiles of residual carbon, NH_4, and PO_4 detected in the culture medium. As shown, the initial 20 mM of carbon added to the reactor was depleted within 6 h. Subsequently, octanoic acid was fed in small, frequent pulses (5 to 20 mM) in response to either a drop in off-gas CO_2 concentration (or a rise in DO signal) and the residual concentration remained low until after 20 h, after which point slight excess was observed at the indicated sampling points. NH_4 appeared to be briefly limiting around 9-10 h, but began to accumulate after 10 h, likely due to cessation of growth from the onset of O_2-limitation. By 20 h, the residual NH_4 concentration reached a maximum value of 700 mg L^{-1}, and feeding of $(NH_4)_2SO_4$ was stopped (to prevent accumulation to toxic levels). The excess was consumed to 49 mg L^{-1} by 27 h, resulting in an uptake rate of 5.90 ± 0.25 mg NH_4 g X_r^{-1} h^{-1}. By comparison, the measured uptake rate of NH_4 during the growth phase (0-14h) was 286.5 ± 25.9 mg NH_4 g X_r^{-1} h^{-1}.

Phosphate was consumed most rapidly during the growth phase from 6 to 12 h and the slope of a plot between PO_4 consumption and X_r production (R^2 = 0.91) produced a yield coefficient of 13.48 g X_r g PO_4^{-1} (Table 7.1). This is similar to the value of 13.7 g g^{-1} reported by Sun et al. (2006) for *P. putida* KT2440. Consumption of PO_4 was also observed during the during PHA accumulation phase (14 h and onward) at the rate of 3.1 ± 1.0 mg PO_4 g X_r^{-1} h^{-1}. Prior to 14 h, the obtained growth-phase PO_4 uptake rate was 52.7 ± 11.1 mg PO_4 g X_r^{-1} h^{-1}.

7.5.3. Carbon flux and yield analysis

An overall yield analysis (on a C-mol basis) is shown in Figure 7.1d. There was little change in the CO_2 production (which accounted for approximately 50% of the consumed carbon) throughout the cultivation, which is consistent with previous results described in Chapters 4 and 5. However, the carbon flux to X_r was higher during the O_2-limited storage phase in comparison with previous work, which resulted lower PHA yield (see also Table 7.2, along with several other key indicators of process performance). The maximum observed Q_s and overall $Y_{PHA/S}$ were similar in either case, while the maximum yield during the O_2-limited PHA storage phase was somewhat lower than in previous batch experiments. The carbon recovery approached one (0.9 ± 0.15, Table 7.2) for the fed batch experiments, but was generally more variable than in previous batch experiments.

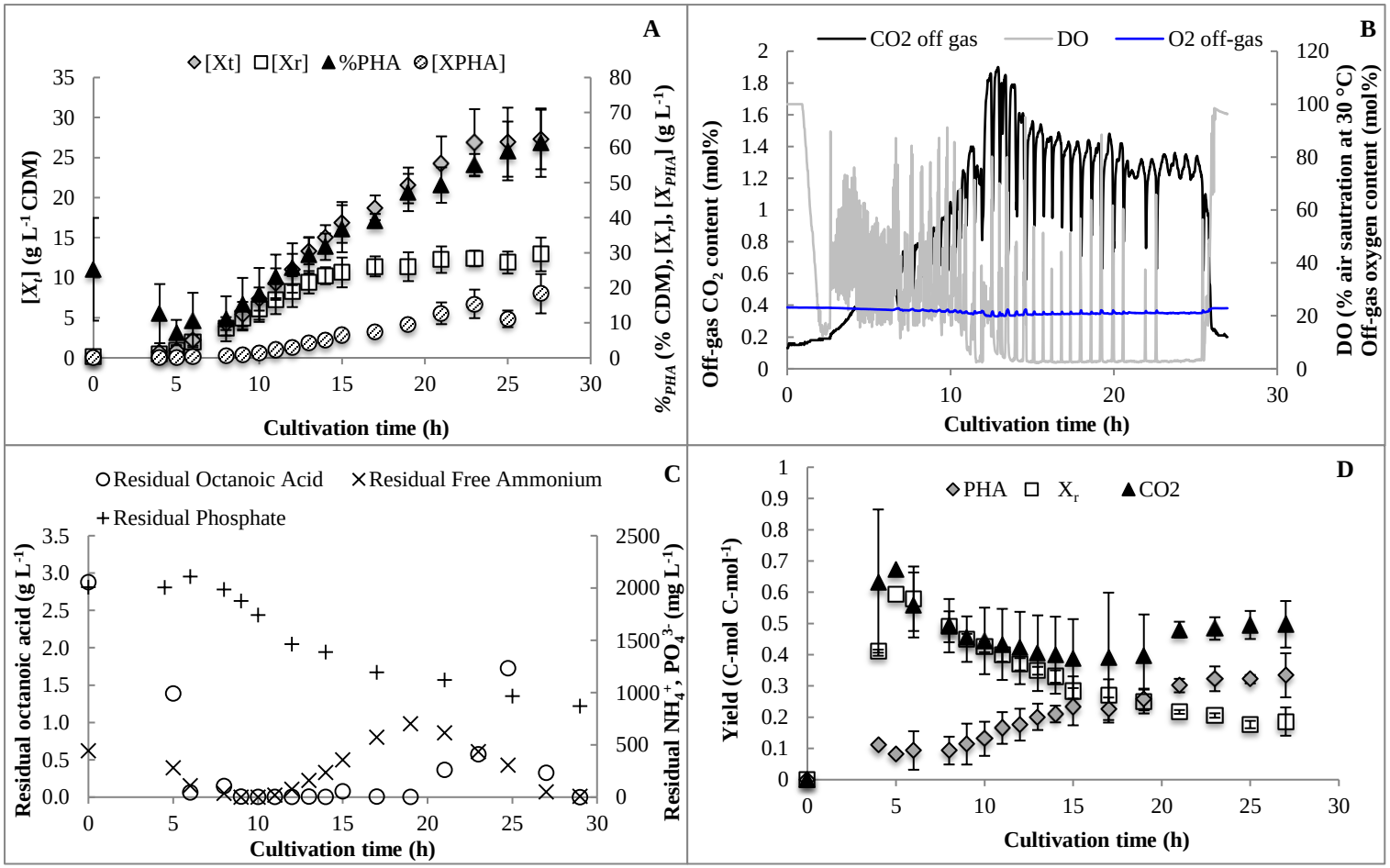

Figure 7.1. Supporting data obtained over the course of the pulse-feed experiments. a) Results for biomass and PHA production; b) Representative profile for DO and off-gas CO_2 and O_2 content (being a key control plot, a zoomed-in view of this figure is available in Appendix B); c) Representative profiles of residual concentrations of octanoic acid, free ammonium, and phosphate; d) Yield analysis expressed on a C-mol basis. Error bars represent standard deviations between biological replicates.

7.5.4. Residual trace elements

For measurement of trace residual metals with ICP-OES, satisfactory resolution was found for Fe^{3+}, Ca^{2+}, and Mg^{2+} (Figure 7.2a) but poorer resolution was obtained for Cu^{2+}, Mn^{2+} and Zn^{2+} (Figure 7.2b), which even initially were present in extremely low concentrations. The concentrations of Cu^{2+}, Mg^{2+}, and Mn^{2+} decreased until 14 h, and then concentrations began to slowly increase. The concentration of Fe^{3+} decreased rapidly until 6 h, and then remained relatively constant at a low concentration for the remainder of the cultivation. The concentration of Ca^{2+} decreased until 10 h and showed little change subsequently. Growth-phase yield coefficients (obtained prior to 12 h) for all detectable medium components are shown in Table 7.1. None of these trace metals reported zero concentration values at any time, and therefore were likely not limiting. However, for higher cell density cultivations, increasing the concentration would be advisable, particularly for Fe^{3+} and Mg^{2+}.

Table 7.1. Yield coefficients of residual, PHA-free biomass from C, N, P, and certain (detectable) trace elements.

Medium Component	**Yield Coefficient (g per g or mg X_r)**
Octanoic Acid (g g^{-1})	0.72[a]
NH_4^+ (g g^{-1})	6.1[a]
PO_4^{3-} (g g^{-1})	13.5
Ca^{2+} (g mg^{-1})	2.6
Cu^{2+} (g mg^{-1})	15.5
Fe^{3+} (g mg^{-1})	2.2
Mg^{2+} (g mg^{-1})	0.5

[a]results derived from growth phase (DO excess) data obtained from previous batch tests (Chapter 4).

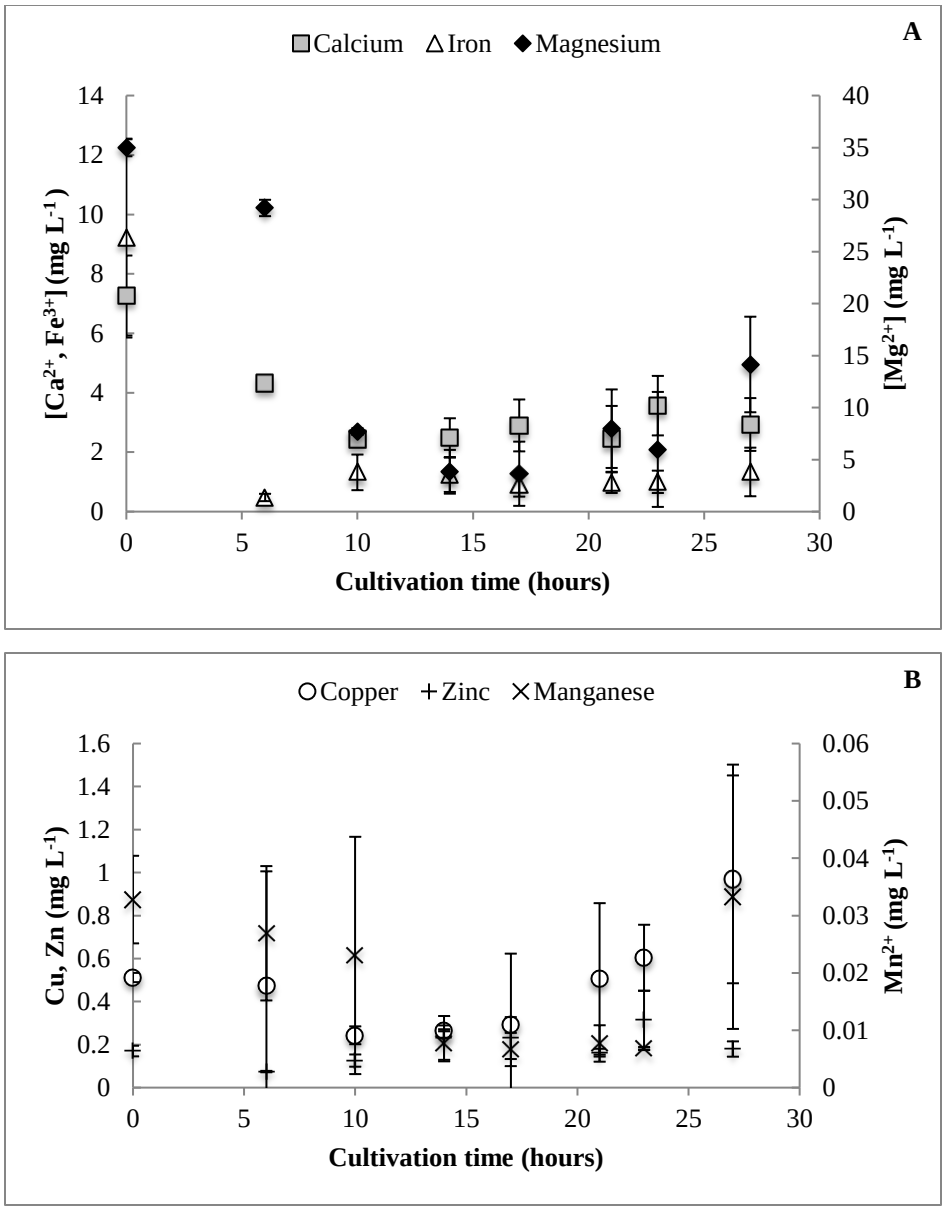

Figure 7.2. Uptake of trace metals in fed-batch culture of *P. putida* LS46. Analysis of residual concentrations of trace elements in the culture supernatant by ICP. a) calcium, iron, magnesium and b) copper, zinc, manganese. Error bars represent standard deviations between biological replicates.

7.5.5. Modeling of feeding rates – continuous drip feed strategy

Within the 27 h of fed-batch cultivation, a total of 185 mL octanoic acid and 235 mL of the 200 g L^{-1} $(NH_4)_2SO_4$ solution were fed. The total uptake of carbon and NH_4 were plotted over time and it was found that a satisfactory fit could be obtained with a piece-wise function in which the growth phase was fitted with an exponential function, whereas the PHA accumulation phase was fitted with a quadratic function (Figure 7.3). This trend is in agreement with what has been previously reported by Maclean et al. (2008), although in this study, a good linear fit (R^2 >0.99) was also obtained for carbon feeding during the accumulation phase.

$$C(t) = \begin{cases} 0.273e^{0.366t}, & t \leq 10\ h \\ -0.0293t^2 + 3.478t - 2.157, & t > 10\ h \end{cases} \quad \text{(Equation 7.1)}$$

$$N(t) = \begin{cases} 0.034e^{0.418t}, & t \leq 9\ h \\ -0.0151 + 0.628t - 3.0112, & t > 9\ h \\ 0, & t > 20\ h \end{cases} \quad \text{(Equation 7.2)}$$

The derivative of these equations was taken to obtain a time-based feeding rate. This rate was then related to speed of the injector syringe through a calibration curve of mass flow rate and motor output as the independent variable (i.e. syringe speed). This was programmed into LabBoss software to automate a continuous drip-feed process for comparison with the pulse-feed process. Several replicates were completed and the results for growth and mcl-PHA synthesis are shown in Figure 7.4a, as well as Table 7.2 with comparison to previous work (including the pulse-feed strategy). The concentration profile for DO was very similar to the pulse-feed experiments (Figure 7.1) while the concentration profiles for carbon and NH_4 (shown in Figure 7.4b) were also similar. The process was very reliable between replicates, but as shown in Table 7.2, the drip feed strategy appeared to favor production of X_r over X_{PHA}, as indicated by the slightly higher [X_t], but lower $\%_{PHA}$, $Y_{PHA/S}$, and Q_s during the accumulation phase.

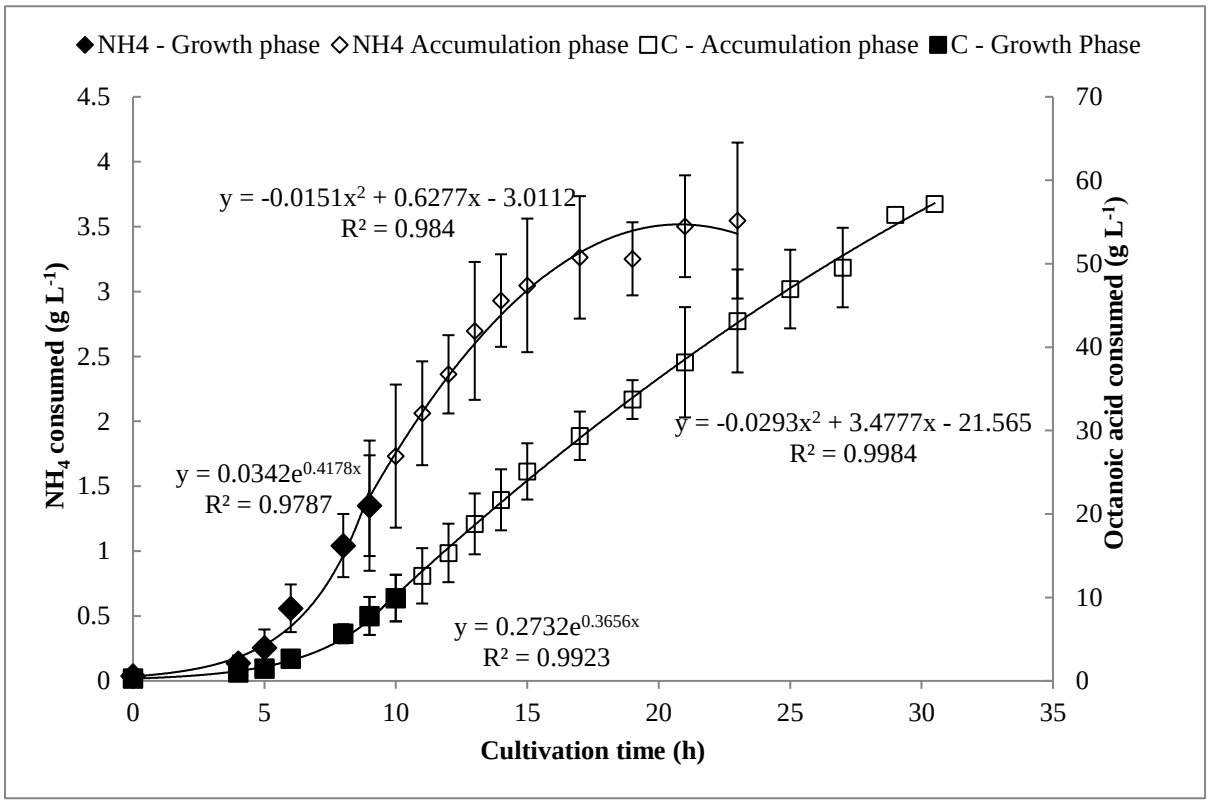

Figure 7.3. Modeled cumulative uptake of carbon and ammonium over the time course of the pulse-feed experiments. Error bars represent standard deviations between biological replicates.

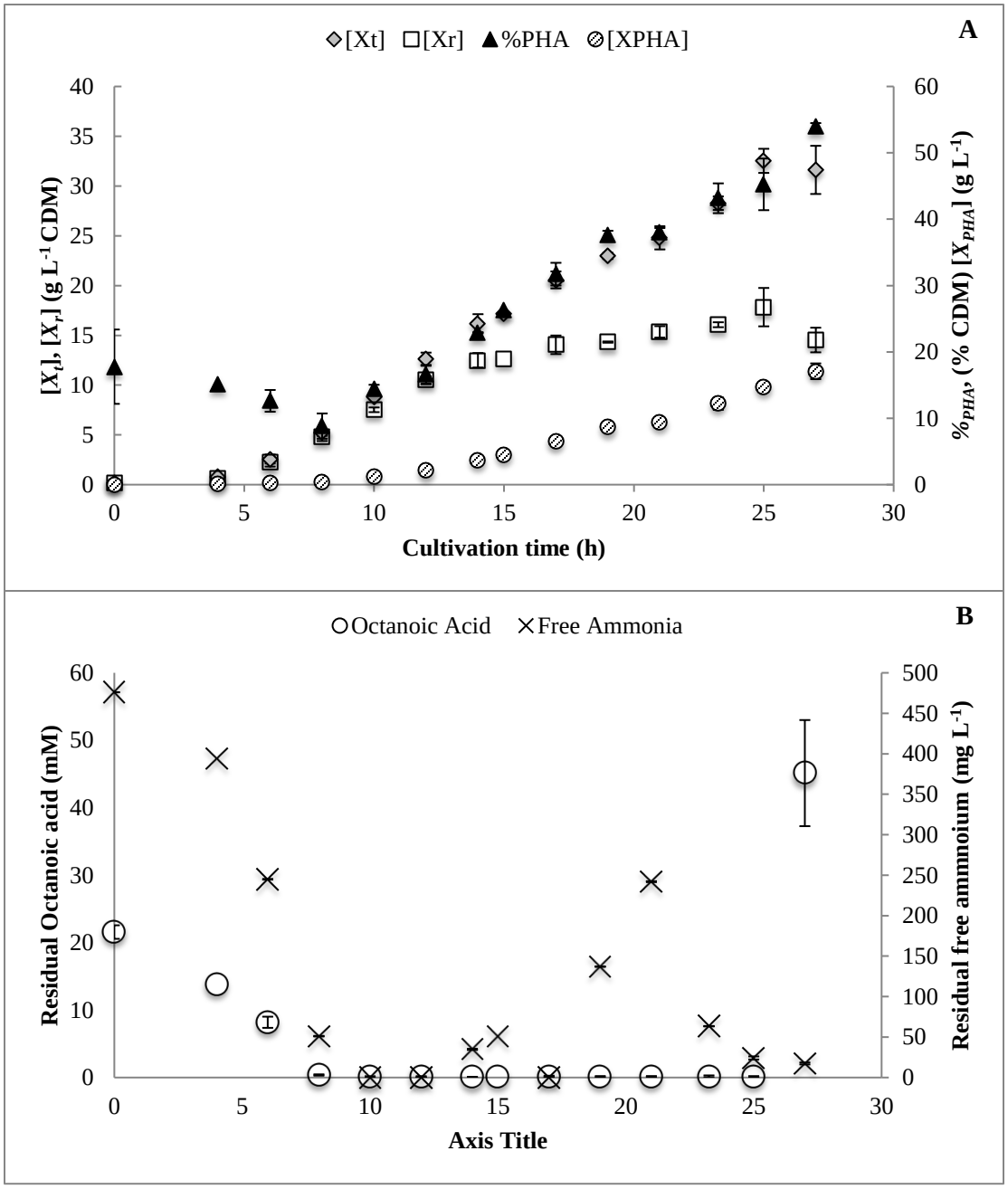

Figure 7.4. Results for the continuous, drip-feed fed-batch cultivation. a) Curves for growth and mcl-PHA synthesis shown for continuous drip fed-batch strategy; b) residual octanoic acid and free NH_4 detected in the supernatant over the cultivation. Error bars represent standard deviations between biological replicates.

Table 7.2. Comparing process performance of previous batch cultivations with the described fed batch processes.

	Previous batch results[a]	**Pulse feed strategy (at 27 h)**	**Continuous, drip feed strategy (at 27 h)**
n =	2	4	2
$[X_t]$ (g L^{-1})	2.37 ± 0.1	28.9 ± 4.0	32.4 ± 0.9
$\%_{PHA}$ (g g^{-1})	44.4 ± 1.3	60.6 ± 8.2	52.9 ± 2.5
$[X_r]$ (g L^{-1})	2.37 ± 0.5	11.2 ± 1.5	17.4 ± 2.1[b]
$[X_{PHA}]$ (g L^{-1})	1.01 ± 0.12	17.7 ± 4.8	15.4 ± 1.2
$\mu_{avg/Xr}$, growth phase (h^{-1})	0.29 ± 0.03	0.35 ± 0.11 (0-14 h)	0.31 ± 0.03 (0-14 h)
$\mu_{avg/Xr}$, storage phase (h^{-1})	0.11 ± 0.01	0.03 ± 0.01 (14-27 h)	0.03 ± 0.01 (14-27 h)
$Q_{v,\,final}$ (g L^{-1} h^{-1})	0.08 ± 0.00	0.61 ± 0.12	0.60 ± 0.04
$Q_{v,\,max}$ (g L^{-1} h^{-1})	0.08 ± 0.01	0.66 ± 0.14 (23-27 h)	0.60 ± 0.04 (27 h)
$Q_{s,\,max}$ (g PHA g X_r^{-1} h^{-1})	0.18 ± 0.03	0.18 ± 0.28 (15-19 h)	0.10 ± 0.03 (23-25 h)[b]
$Q_{s,\,avg}$ (g PHA g X_r^{-1} h^{-1})	0.11 ± 0.00	0.09 ± 0.01 (14-27 h)	0.06 ± 0.01 (14-27 h) [b]
$Y_{PHA/S}$, overall (C-mol C-mol^{-1})	0.35 ± 0.04	0.33 ± 0.05	0.26 ± 0.04
$Y_{PHA/S}$, storage phase (C-mol C-mol^{-1})	0.57 ± 0.05	0.52 ± 0.13 (14-27 h)	0.31 ± 0.06 (14-27 h)[b]
Carbon Recovery	1.04 ± 0.00	0.90 ± 0.15	0.89 ± 0.04

[a]results chosen for O_2-limited conditions with 6 LPM aeration and 250 rpm mixing (k_La = 78 h^{-1}), obtained from Chapter 4; [b]results that are compared for the two fed batch strategies that are statistically different using a two-tailed comparison of sample means ($p < 0.05$). Tolerances indicate standard deviations between biological replicates.

7.6. Discussion

This work has shown that: 1) oxygen limitation can be a viable strategy for inducing mcl-PHA accumulation from fatty acids using *P. putida* in HCD fed batch culture; and 2) this process can be rapidly optimized through simple pulse-feeding in response to DO and/or off-gas CO_2 signals. One advantage of this approach is that it eliminates the need to predict growth rates or feeding rates over time, which can lead to complicated automation and programming (Sun et al. 2006). In Chapter 5, a similar strategy proved to be a significant challenge to optimize when using with toxic substrates like octanoic acid. Furthermore, this approach can be implemented with standard bioreactor equipment (i.e. the setup could be as simple as a DO probe and a peristaltic pump), and should be independent of the bioreactor type, configuration, mass transfer capability, and to some extent scale. This is demonstrated in Appendix A, in which this strategy was implemented in a 150-L bioreactor with reasonably good results. Although O_2-limitation has been reported to cause excessive foaming and termination of fed-batch processes (Lee et al. 2000b; Sun et al. 2007a; Sun et al. 2009a), in this work we found that foam was manageable throughout the O_2-limited phase (except for at the very end of the process). In fact, foaming was observed upon carbon limitation in the pulse feed process, and was alleviated through further addition of ocatnoic acid.

During the storage phase consumption of both NH_4 and PO_4 was observed, albeit at a considerably slower rate than during growth. This may promote residual growth during the O_2-limited PHA storage phase, which could be advantageous compared to strict N or P limitation. Andin et al. (2017) examined the effect of maintaining a low residual growth rate on metabolic flux during synthesis of mcl-PHA from fatty acids in fed-batch culture using *P. putida* KT2440. Their analysis showed that when residual growth was present, the reduced co-factors from mcl-

PHA synthesis (NADH, $FADH_2$, see Figure 2.3) could be coupled to anabolic demand, and this improved the overall mcl-PHA yield from approximately 0.6 to 0.7 C-mol C-mol^{-1}. Another study reported a similar finding for PHB synthesis from butyrate using *C. necator* (Grousseau et al. 2013). In this work, the yield coefficient during the storage phase was lower at 0.52 ± 0.13 C-mol C-mol^{-1}, and the average residual growth rate during the storage phase was 0.03 ± 0.01 h^{-1} (Table 7.2). As suggested in Chapter 5, co-feeding LCFAs may help improve residual growth during the PHA storage phase, and perhaps even further improve overall $Y_{PHA/S}$.

Differences in the carbon feeding methods were also evaluated via a continuous drip-feed process developed using an empirical model of the pulse-feed data. Although the processes were largely similar, more favorable PHA storage characteristics (higher $Q_{s,\ max}$ and $Y_{PHA/S}$) were observed under pulse-feeding conditions, whereas the drip-feed process resulted in significantly higher [X_r], but lower $Y_{PHA/S}$ and $Q_{s,\ max}$. This may be due to the constant cycling between carbon excess and carbon limited conditions. A previous study indicated a significant improvement in $\%_{PHA}$ (from 25 to 44% of CDM) when *Pseudomonas* sp. G101 was pulse-fed waste canola oil, in comparison to a continuous drip feed (Możejko and Ciesielski 2014). The results of the present study do not suggest such a drastic difference between drip-feed and pulse-feed methodologies. However, the findings do imply that pulse feeding may help to maximize the yield and synthesis rate of mcl-PHA during the accumulation phase, whereas a continuous drip feed process may help boost biomass production during the growth phase. It should be noted that during the course of these drip-feed experiments, periodic carbon limitation was still imposed when the injector syringe was briefly paused to re-fill, which may have dampened the observed effect. Ultimately, a more optimized strategy could result from coupling a continuous, drip-feed strategy for growth with a pulse-feed strategy in the PHA accumulation phase.

This chapter has demonstrated a ten-fold improvement in [X_t], and an eight-fold improvement in Q_v compared to previous work. Interestingly, mcl-PHA synthesis characteristics were not improved over previous batch (Chapter 4) and/or simple fed-batch experiments (Chapter 5). This difference is somewhat interesting and might reveal that the kinetics of mcl-PHA synthesis and storage are perhaps more well suited to the simpler, more gradually changing chemical environment of a batch system. This implies that the main mode of advancing HCD fed-batch productivities, at least in this work, was solely through boosting [X_t] rather than improve mcl-PHA synthesis characteristics. The overall carbon recovery was also somewhat lower in the HCD fed-batch cultivations, which could indicate that carbon was used for end products other than X_{PHA}, X_r, and CO_2. These were not accounted for in this work, but some insight is given in Chapter 8.

Compared to other HCD fed-batch processes (Table 2.3), several previous bench-scale studies have demonstrated improved results over the fed-batch process described in this work (Lee et al. 2000b; Sun et al. 2007a; Maclean et al. 2008; Gao et al. 2016). Many of these studies have used an aeration medium with enriched oxygen content, which increases the driving force for oxygen transfer nearly five-fold, and has been shown to improve PHA productivity nearly four-fold in bench scale reactors (Shang et al. 2003b). Thus, using a technique to increase the driving force for oxygen transfer (enriched O_2, bioreactor pressurization) would help make this fed-batch process more competitive with previous studies documented in the literature. It is important to point out that the main contribution of this work was to show the effects of low-DO environments in HCD fed-batch cultivations, and not necessarily to maximize overall Q_v using techniques to keep DO in excess. Although those are worthwhile pursuits, they have been extensively explored in the literature (Table 2.3 and 2.4). Regardless of how much the k_La or

OTR might be improved, microaerophilic conditions will more than likely still prevail beyond a certain cell density.

7.7. Conclusions

A fed batch method was developed using a CO_2 and/or DO-based pulse feed strategy using atmospheric air as the aeration medium and O_2-limitation as the main driving force for mcl-PHA production. The process consistently produced 25-30 g L^{-1} total biomass and resulted in an overall Q_v of 0.66 ± 0.14 g L^{-1} h^{-1}, nearly an eight-fold improvement over previous batch experiments. Interestingly, the improvement was directly related to the total biomass improvement; no improvement to mcl-PHA synthesis characteristics (Q_s, $Y_{PHA/S}$) was observed when compared to previous oxygen-limited batch cultivations. Furthermore, the overall carbon recovery was lower, suggesting that carbon may be utilized less efficiently in HCD cultures. Finally, a continuous drip-feed strategy favored growth and production of X_r, a pulse feed strategy favored the production of mcl-PHA during the storage phase.

7.8. Acknowledgements

This work was funded by: 1) Genome Canada, through the Applied Genomics Research in Bioproducts or Crops (ABC) program for the grant titled, “Microbial Genomics for Biofuels and Co-Products from Biorefining Processes”; 2) the government of the Province of Manitoba through the Manitoba Research Innovation Fund (MRIF) and the Manitoba Rural Adaptation Council (MRAC); 3) the Natural Sciences and Engineering Research Council (NSERC); and 4) the University of Manitoba Sir Gordon Wu Graduate Student Scholarship. Special thanks to Elsie Jordaan, Dr. Joe Ackermann, and Dr. Tom Ward for their assistance with sample preparation and running the ICP-OES. Last but not least, thanks to Chris Dartiailh for his

assistance getting the bioreactors going and taking early samples, which helped immensely with the long days (and nights). The authors disclose that no conflict of interest exists between them.

Chapter 8: Rheological characterization of high-cell density cultures of *Pseudomonas putida* LS46

8.1. Preface

In Chapter 7, an O_2-limited fed batch strategy was described that significantly increased the productivity over results described in Chapters 4 and 5. However, some significant differences in the behavior of the samples were observed in this work, specifically in terms of viscosity, and difficulty involved in filtering or centrifuging the samples. This chapter delves into those issues through rheological characterization of the culture and the supernatants. The rheology aspect of this work was done using a pilot-scale (150 L) bioreactor system at Scion, whereas the supporting evidence (including measurements of DNA, sugars, proteins, and volatile solids, and k_La) and physiology was done in lab-scale reactors at the University of Manitoba. This work has been organized into a manuscript, and the title and abstract were submitted to an upcoming special issue of the journal *Bioengineering* on "Advances in Polyhydroxyalkanoate Production, Volume 2."

8.2. Abstract

Fed-batch cultures are widely perceived as a requisite for high-productivity PHA cultivations, but little is known about the rheological properties of HCD cultivation medium in PHA production. In this work, time-dependent rheological properties were monitored during fed-batch cultivation of *P. putida* LS46 for production of mcl-PHAs. It was found that as the cell density increased from 0 to 25 g L^{-1} CDM, the apparent viscosity increased nearly nine-fold (at a shearing rate of 10 rad s^{-1}). The viscosity was shear-dependent, and although the behavior was nearly Newtonian at lower cell densities, the medium became increasingly shear-thinning as the

cell density increased. At shearing rates of approximately 75 rad s^{-1} or higher, shear-thickening was observed in all samples, and its onset increased with viscosity of the sample. When the cells were removed from the sample (via centrifugation), it was found that the supernatant contributed more to the observed behavior than did the presence of cells. Up to 9 g L^{-1} volatile solids (VS) was detected in the supernatant, only half of which could be accounted for as extracellular (soluble) proteins, sugars, PHA, and DNA. This resulted in a 50% reduction in the k_La over time. Although a relatively small portion of the overall carbon balance (less than 10% on a C-mol basis) remains as organic material in the culture medium during fed-batch operations with *P. putida* LS46, this has a significant impact on the culture rheology, and also the oxygen transfer rate.

8.3. Introduction

Improving the productivity of processes involved in the production of value-added bio-products is a significant challenge facing bioprocess engineering. For production of PHAs, use of HCD fed batch cultures is widely perceived as the optimal process configuration to accomplish this, and reduce overall production costs (Ienczak et al. 2013). Some HCD cultures for PHA production have reached cell densities in excess of excess of 200 g L^{-1} CDM (Ryu et al. 1997; Wang and Lee 1997b; Shang et al. 2003a), but a common problem with HCD cultures in general is increasing medium viscosity (Riesenberg and Guthke 1999). This can lead to dead zones in the bioreactor and reduced heat and mass transfer capability - especially in large-scale bioreactors with inherently poor mixing capability (Gabelle et al. 2011).

Rheology is defined as the deformation of matter (in this case, the flow of liquid fermentation medium) under an applied stress. Little is currently known about how the rheological properties of the cultivation medium are affected by HCD cultures for PHA

production. Previous studies have examined the rheology of fermentation medium in viscous mycelial cultures of *Aspergillus awamori* (Badino et al. 2001), polyglutamic acid (PGA) production using *Bacillus subtilis* (Richard and Margaritis 2003), and production of extracellular polymeric substances (EPS) by *Pseudomonas* sp. (Freitas et al. 2009; Maalej et al. 2016), as well as mixtures of primary and secondary sewage sludge (Baroutian et al. 2013). In most cases, the fermentation media behaves as non-Newtonian, in which case the apparent viscosity is dependent on the shear rate (Goudar et al. 1999; Badino et al. 2001; Dhillon et al. 2013; Newton et al. 2017).

Since lack of adequate oxygen transfer to the liquid phase is the main limiting factor in most HCD cultivations for PHA production, the effect of changing viscosity may also be an important consideration. Several previous studies have demonstrated inversely proportional relationships between viscosity and oxygen transfer in both model Newtonian fluids (glycerol, glucose solutions) as well as non-Newtonian fluids (xanthan gum, carboxymethylcellulose solutions) (Buchholz et al. 1978; Herbst et al. 1992; García-Ochoa and Gómez 1998; Arjunwadkar et al. 1998; Puthli et al. 2005; Martín et al. 2010; Gabelle et al. 2011). Such model fluids are often preferred to actual biological cultures because they are cheaper and easier to use (Gabelle et al. 2011). A few studies have evaluated oxygen transfer characteristics in a biological medium (Badino et al. 2001; Richard and Margaritis 2003). In all cases, there is a strong consensus that k_La is inversely proportional to the medium viscosity.

Despite the numerous HCD fed-batch studies conducted for the purpose of PHA production, we can find no evidence that rheology of the culture medium has been studied to date. Considering PHA is a high molecular mass polymer that can occupy up to 75-88% CDM (Wang and Lee 1997b; Jiang et al. 2013), examination of culture rheology and its effects on

oxygen transfer is an important contribution to process development and scale-up of PHA production. Furthermore, this is likely to have significant impacts on downstream unit operations, including filtration or centrifugation.

The hypothesis driving this work was that even for moderately high cell density cultures for PHA production (such as those investigated in Chapter 7), the changes in viscosity of the culture have a significant and detrimental impact on process performance. This was accomplished by: 1) use of a rheometer to examine time-dependent rheological behavior of HCD fed-batch cultures of *P. putida* LS46; and 2) quantifying how viscosity impacts the oxygen transfer characteristics of the cultivation medium through off-line determinations of k_La. Given that most HCD cultivations in PHA production are limited by inadequate O_2 transfer, this is an important relationship to understand, and little information is available.

8.4. Materials and Methods

8.4.1. Micro-organism, medium and substrates

The microorganism (*P. putida* LS46) and strain maintenance practices in this work followed those described in Section 3.1. The minimal medium and substrate (octanoic acid) used was prepared as previously described in Section 7.4.1.

8.4.2. Reactor setup and operation

The bioreactor system used for generation of 1 L samples for rheological analysis was a stainless steel, sterilization in place (SIP) bioreactor with a 152 L total volume (Sartorius Stedim Biostat D-DCU, Göttingen, Germany). The bioreactor was equipped with three 160 mm diameter Rushton turbines, 4 wall-mounted baffles, pH and DO electrodes, and a ring-type sparger located underneath the impeller. The bioreactor was filled with an initial volume of 70 L medium, and

sterilized at 121 °C for 20 min before cooling to 30 °C. An initial concentration of 20 mM octanoic acid was then added aseptically following sterilization. Experiments were initiated with the addition of a 5% (vol vol^{-1}) inoculum, which was grown overnight in flask cultures.

The reactor was operated at pH 6.5, which was controlled through the addition of 10 M NaOH via automated peristaltic pumps. The DO was maintained at 40% (of air saturation at 30 °C). The cascade for DO was maintained through: 1) incremental increases in pressure from 200 mbar to 1000 mbar; 2) incremental increases in stirring rate from 100 rpm to 600 rpm; and 3) increasing aeration (atmospheric air only) from 10 LPM up to 30 LPM (maximum of approx. 0.4 VVM). At this scale, aeration was limited because of foaming and excessive gas holdup encountered at higher volumetric flow rates. Fed-batch experiments were carried out using a reactive DO-based pulse feeding method (Chapter 7). Using this strategy, sub-inhibitory concentrations of octanoic acid (5-20 mM) and a 200 g L^{-1} solution of $(NH_4)_2SO_4$ were fed via calibrated peristaltic pumps. Feeding of NH_4 was stopped around 16 h after O_2 became limiting and NH_4 was no longer being consumed rapidly.

Because of a variety of challenges, the other data generated in this work (described below) supporting the observations in the rheological assessment were investigated in a 7 L bench scale system with a 3 L working volume, which was operated as described in Section 7.4.2. The growth rates and total biomass obtained were similar to that observed in the 152 L bioreactor at the corresponding time – which indicated similar overall mass transfer capability (despite the 152 L bioreactor being operated with the headspace pressurized to 1 atm gauge). Furthermore, the DO was depleted at the same time (14 h) at either cultivation scale, so the total biomass and PHA content as a function of cultivation time were similar between the two scales.

8.4.3. Sample treatment and analyses

Samples (20-40 mL) were periodically withdrawn from the bioreactors, generally in 1-3 h intervals and handled as described in Section 3.3. Analysis of residual octanoic acid in the culture medium and PHA content and composition of the biomass was done by GC-FID as described in Sections 3.4. and 3.5. Residual free NH_4 was measured spectrophotometrically as described in Section 3.9.

8.4.4. Viscosity measurements

Periodic 1 L samples were withdrawn from the 150 L bioreactor for rheological analysis. For certain samples, a portion of the medium was centrifuged at 13,700 × g for 15 min (Sorvall RC-6 Plus with an F12-6 × 500 LEX rotor) to investigate the cell-free supernatants. The medium viscosity was assessed using a DHR-2 Rheometer (TA Instruments, New Castle, DE, USA) equipped with a cup-and-bob measurement system (30 mm cup diameter; 28 mm bob diameter). The samples were conditioned at 30 °C for 20 min prior to measuring. During this conditioning step, a constant shear of 1 s^{-1} was applied to avoid settlement of the samples. All samples were measured using a flow sweep between 2 and 1000 s^{-1}. All samples were measured in triplicate. The data analysis was done using TRIOS v4.1.0.31739 (TA Instruments).

The measured shear stress at different shear rates during rotational rheology can be described using a variety of established rheological models. In this work, the fit was best described using the Power law. A Power-law fluid is an idealized fluid, and its shear stress is a function of shear rate as described by:

$$\tau = \varphi * \omega^n \qquad \text{(Equation 8.1)}$$

where, τ is the shear stress (mPa), φ is the Power law viscosity constant (mPa.s); ω is the shear rate (s^{-1}) and *n* is the rate index (dimensionless).

8.4.5. Off-line k_La determination

The k_La, was measured using the dynamic method described in Section 3.11. However, instead of being measured in the production bioreactor, a small-scale cylindrical reactor was constructed from plexi-glass with height 7.9 cm and 5.4 cm in diameter to allow k_La determination (i.e. to observe trends under constant conditions) while using minimal sample volume (125 mL). The off-line measurement device was equipped with compression fitting ports for a DO probe, gas inlet, and gas outlet. The reactor was stirred magnetically with a 2.5 cm stir bar at 1000 rpm (all samples), and either air or N_2 was delivered to the reactor at flow rates of 200 or 500 mL min^{-1}, respectively. This was done using thermal mass flow controllers (Bronkhorst Hi-Tech, Ruurlo, the Netherlands), which were previously described (Blunt et al. 2014). A minimum of three determinations was done for each sample, and this was repeated for three biological replicate fed batch experiments. The unit was validated initially in trials using distilled water or Ramsay's medium, and k_La values of 34.3 ± 3.4 h^{-1} and 21.5 ± 2.1 h^{-1} were obtained, respectively. Not surprisingly, these were on the lower end of the values previously obtained in the 7 L bioreactor (Chapter 4, Table 4.1). This is probably because: 1) lack of baffles in the miniature device; 2) a stir bar was used instead of a proper impeller in the miniature device; and 3) the point of release of the bubbles was above the stir bar in the miniaturized reactor (as opposed to underneath the impeller in the 7 L bioreactor).

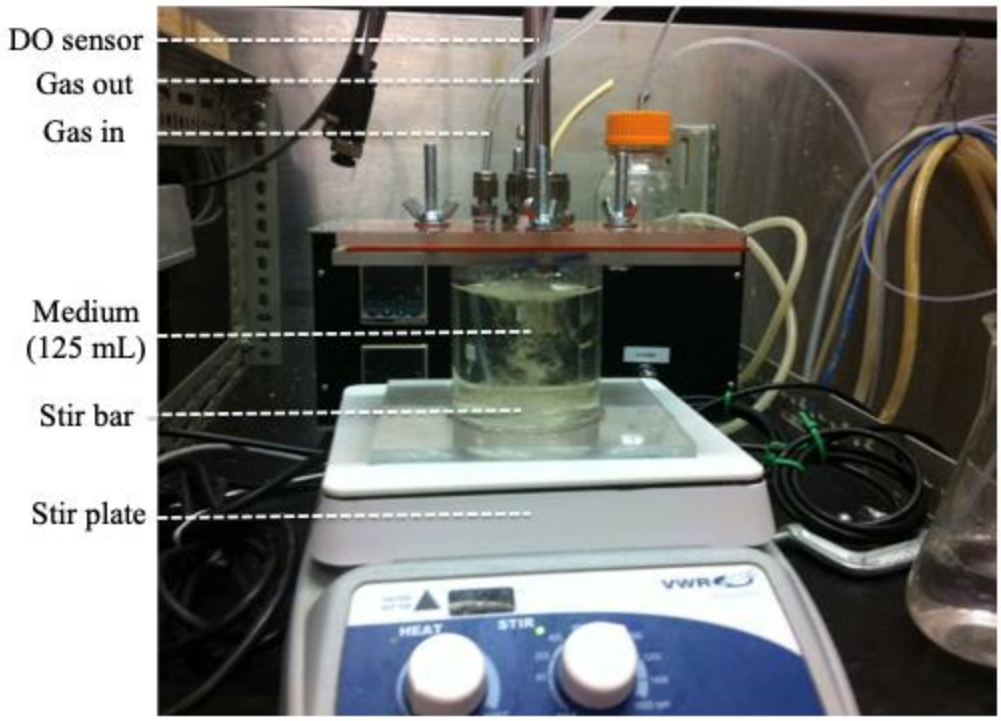

Figure 8.1. Plexi-glass reactor constructed for off-line determinations of k_La using a minimal amount of sample.

8.4.6. Analysis of organic products in the supernatant

Soluble protein in the supernatant was determined spectrophotometrically at 595 nm using a modified Bradford Assay (Bradford 1976). Briefly, 0.5 mL of supernatant was mixed with 0.5 mL of 0.4 M NaOH. The samples were boiled for 10 min, and centrifuged (12,500×g for 5 min). A 20 µL aliquot of each sample was then placed in triplicate wells of a 96-well plate with 200 µL of Bradford Reagent (obtained from Sigma-Aldrich, St Louis, MO). Standards were prepared using bovine serum albumin (Sigma-Aldrich, St Louis, MO) and diluted into 0.2 M NaOH at concentrations of 0-300 mg L^{-1}. Samples outside this concentration range were diluted appropriately in distilled water and the analysis was re-done.

Reducing sugars in the supernatant were determined by the Anthrone method adapted from a previous protocol (Viles and Silverman 1949). Briefly, 0.5 mL of supernatant was added

to glass reaction vials with sealed caps. Then 1 mL of 0.1% anthrone in concentrated H_2SO_4 was added to the vial (using filter tips) and sealed. Samples were placed in a water bath at 80 °C for 5 min, and then allowed to cool to room temperature. 200 uL of each sample was pipetted (again using filter tips) into triplicate wells in a 96-well plate and the color change (green-blue) was quantified spectrophotometrically at 620 nm. Standards were prepared using glucose at concentrations of 0-100 mg L^{-1}.

DNA in the supernatant was quantified using the Qubit Fluorometer. A 5 to 20 uL volume of sample was diluted into a 200 µL total volume of the working solution and sample (working solution was the fluorescence dye diluted 1:200 in buffer). If further dilutions were required, the samples were diluted in distilled water. The broad range DNA standards were used, which had a concentration range of 0 to 5 ng μL^{-1}.

Volatile solids in the supernatant were quantified using 50 mL crucibles. A known volume of supernatant was placed in pre-weighed crucibles that were kept in a desiccator. The crucibles were then oven-dried at 105 °C for 24 h and weighed again following an equilibration period in the desiccator, and then placed at 550 °C for at least 2 h. The final mass of the crucible was then measured following cooling and equilibration in a desiccator. Several tests confirmed that residual octanoic acid in the culture medium volatilized during oven drying at 105 °C and therefore did not contribute to VS measurements.

$$[VS] = \frac{[mass_{f,550°C} - mass_{f,105°C}\,(g)] \times 1000}{sample\ volume\ (mL)}\ (g\ L^{-1}) \qquad \text{Equation 8.2}$$

8.5. Results and Discussion

8.5.1. Rheological characterization of the cultivation medium

Data for [X_t], [X_r], [X_{PHA}], and $\%_{PHA}$ for the fed-batch cultivation process are shown in Figure 8.2a. Although the results shown are for the bench scale process, similar results (at the indicated points in time) were obtained in the pilot-scale bioreactor, although by the end of the process, the $\%_{PHA}$ obtained in the pilot scale bioreactor was somewhat lower. Further details on this process are given in Appendix A. Shown in Figure 8.2b the medium (even after centrifugation) became increasingly opaque and viscous over the time course of the cultivation. This appeared to significantly dampen the turbulence created for a given stirring input. The flow sweep curves for viscosity as a function of shear rate are shown for the cell suspensions (Figure 8.3a) and cell-free supernatants (Figure 8.3b) at various points in time. In both cases, the medium appeared to behave as a Newtonian fluid up until 12 h for shear rates of approximately 75 s^{-1} or less. By 14 h (which corresponded to the onset of O_2-limitation in the bioreactor), a significant increase in viscosity was observed and the samples also became increasingly shear thinning. This type of behavior has been described in previous studies of a variety of fermentation processes (Goudar et al. 1999; Newton et al. 2016; Newton et al. 2017). Similar shear rates were used in this study, but a unique attribute of this work is the viscosity of samples began to increase at a certain shear rate, which was consistent across the different measurements for the individual samples and increased with increasing sample viscosity (and hence cultivation time). This indicates a material property-related root cause rather than a measurement artifact.

In the initial (0 h) sample, this shear thickening behavior was observed at shear rate of 76.5 s^{-1}, and increased with increasing sample viscosity up to nearly 300 s^{-1} in the final sample (25.3 g L^{-1} CDM). Since similar shear rates can easily be encountered in a bioreactor, increasing

the agitation rate beyond this point might increase viscosity and reduce OTR (Martín et al. 2010).

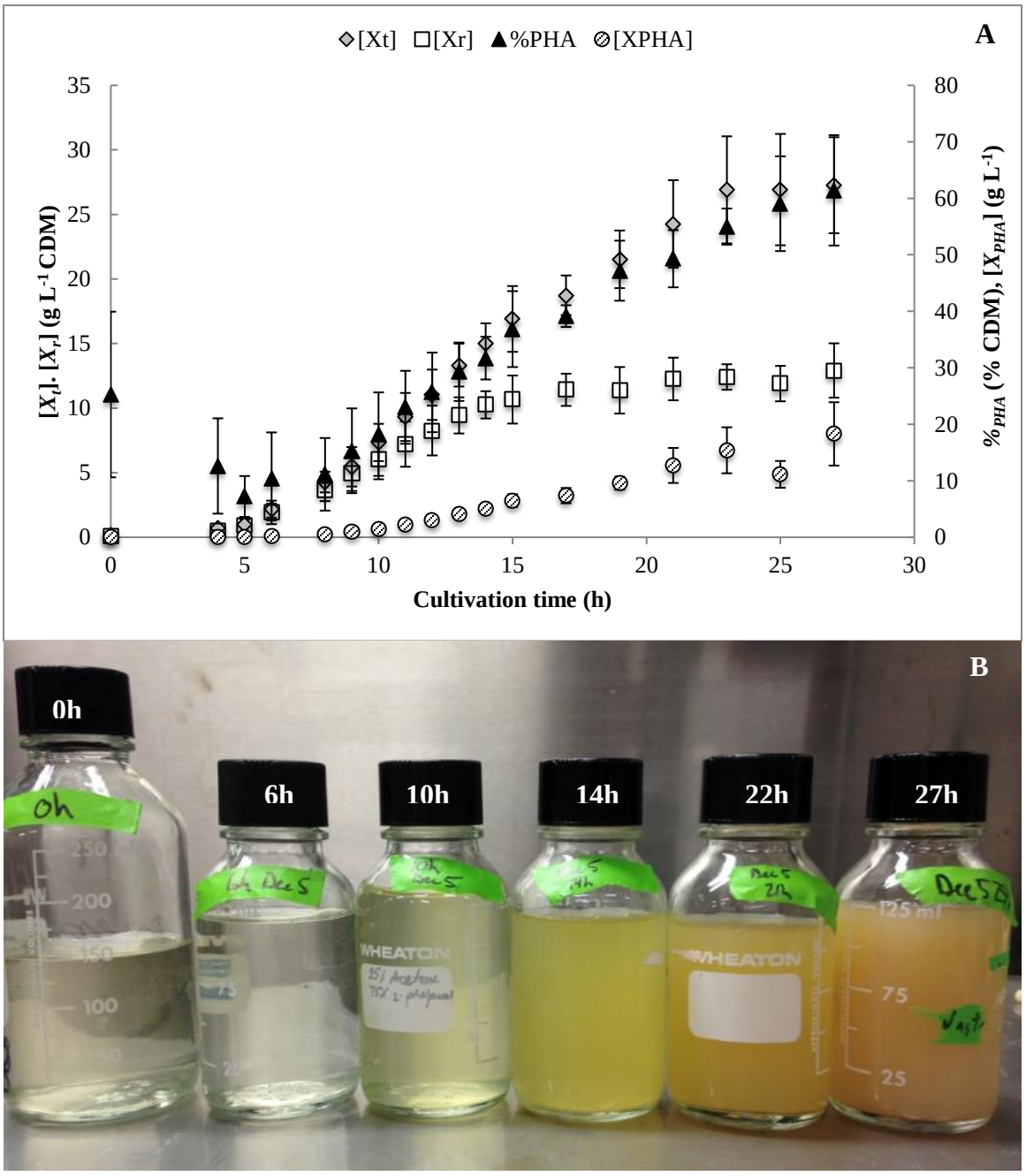

Figure 8.2. a) Growth and PHA synthesis curves and b) appearance of culture after centrifugation for fed-batch experiments at the cultivation time indicated. Error bars represent standard deviations between biological replicate experiments.

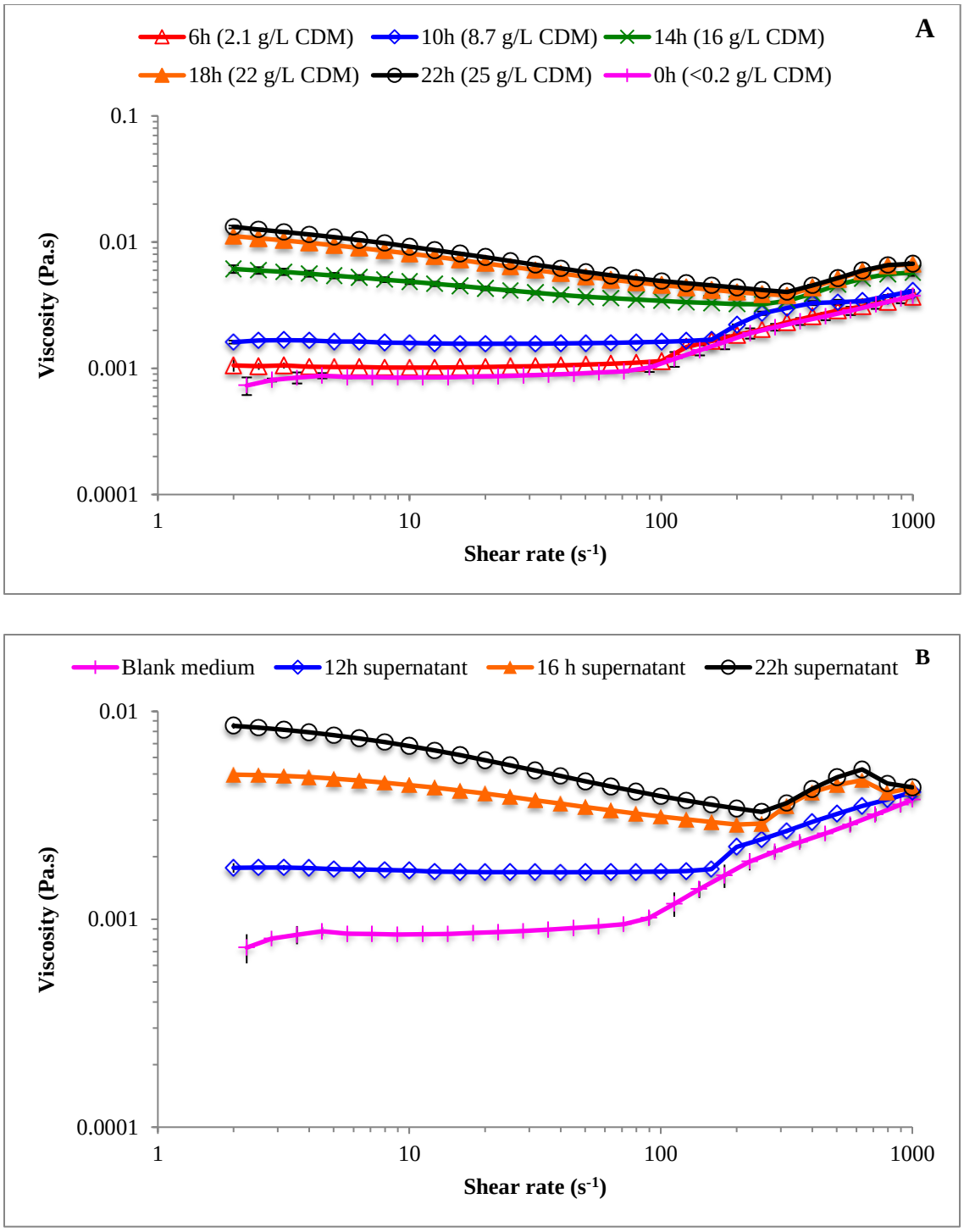

Figure 8.3. Flow sweep curves for growth medium from fed-batch cultures. a) *P. putida* LS46 cultures and b) supernatants from *P. putida* LS46 cultures.

The relationship between shear stress and shear rate was best described using the Power law (R^2 > 0.99 for all samples). A summary of model parameters for fitting the data from each sample with the Power Law are shown in Table 8.1. The Power Law constants derived for each sample are shown in Table 8.2, and in Figure 8.4 as a function of the total biomass. As shown in Figure 8.4, a strong linear relationship between the viscosity constant and the total biomass could be derived (R^2 = 0.96), and the slope was significantly different than zero (p = 0.028). However, the rate index was more or less constant throughout the cultivation, as slope was not significantly different than zero (p = 0.27). Only a weak relationship was obtained when the rate index data was fitted with a linear function (R^2 = 0.63).

The viscosity at a shear rate of 10 s^{-1} was used from the flow sweep results for comparison of the various samples over time. Using a Tukey's Range Test, statistically significant (95%) differences in the rotational viscosities and shear thickening onset across the different samples could be identified. These values are shown in Table 8.2, where it can be seen that over time, the apparent viscosity of the cell suspension increased from approximately 1.0 mPa.s to 9.2 mPa.s by 22 h. Interestingly, when the cells were removed by centrifugation, it was found that the viscosity of the 22 h supernatant was 6.8 mPa.s, which is nearly 75% of the value observed for the entire culture at 22 h. When a 25.3 g L^{-1} culture of *P. putida* LS46 (22 h) was centrifuged and then re-suspended in fresh medium at, the viscosity dropped to 1.7 mPa.s at shear rates of 10 s^{-1}, which was only slightly higher than the 0 h sample (1.01 mPa). Although the final CDM of the 22 h sample when re-suspended in fresh medium was reduced to 21.8 g L^{-1}) the reduction in viscosity was disproportional. Furthermore, when the 22 h sample was concentrated two-fold through centrifugation (final measured CDM of 50.1 g L^{-1}), the viscosity (at 10 s^{-1}) only increased from 9.2 to 12.3 mPa s. This indicates that most of the observed

rheological behavior appears to be explained by changes (through biological activity of *P. putida* LS46) in the medium that the cells are suspended in, rather than the presence of the cells themselves.

Table 8.1. Model parameters for fitting the rheological data with the Power Law. Tolerances indicate the standard deviations between technical replicates (n = 3).

Sample	**Power law constant: Viscosity (mPa.s)**	**Power law constant: Rate Index**	**Power law: Regression**
	Mean ± St. Dev.	**Mean ± St. Dev.**	**Mean ± St. Dev.**
0 h (< 0.2 g L^{-1})	0.156 ± 0.019	1.460 ± 0.019	1.000 ± 0.000
6 h (2.1 g L^{-1})	0.218 ± 0.013	1.410 ± 0.010	1.000 ± 0.000
10 h (8.7 g L^{-1})	0.448 ± 0.06	1.320 ± 0.021	0.998 ± 0.000
14 h (16.1 g L^{-1})	0.548 ± 0.146	1.345 ± 0.042	0.997 ± 0.002
18 h (22 g L^{-1})	0.62 ± 0.183	1.350 ± 0.047	0.995 ± 0.001
22 h (25.3 g L^{-1})	0.799 ± 0.171	1.312 ± 0.033	0.994 ± 0.000
12 h supernatant	0.323 ± 0.024	1.368 ± 0.012	1.000 ± 0.000
16 h supernatant	1.905 ± 0.028	1.120 ± 0.001	0.992 ± 0.002
22 h supernatant	3.151 ± 0.128	1.054 ± 0.007	0.986 ± 0.001

Table 8.2. Summary of average viscosity at a shearing rate of 10 rad s^{-1} and onset of shear thickening. Tolerances indicate the standard deviations between technical replicates (n = 3).

Sample	**Viscosity @ 10 s^{-1}, mPa.s**	**Shear thickening onset, s^{-1}**
	Mean ± St.Dev	**Mean ± St.Dev**
0 h (<0.2 g L^{-1})	1.009 ± 0.055	76.5 ± 13.0
6 h (2.1 g L^{-1})	1.014 ± 0.020	94.8 ± 0.6
10 h (8.7 g L^{-1})	1.588 ± 0.008	151.1 ± 0.6
14 h (16.1 g L^{-1})	4.860 ± 0.212	258.9 ± 18.1
18 h (22 g L^{-1})	8.101 ± 0.149	294.9 ± 9.1
22 h (25.3 g L^{-1})	9.223 ± 0.111	293.3 ± 12.5
12 h supernatant	1.713 ± 0.012	156.3 ± 2.2
16 h supernatant	4.422 ± 0.073	218.9 ± 2.6
22 h supernatant	6.813 ± 0.086	256.6 ± 8.3

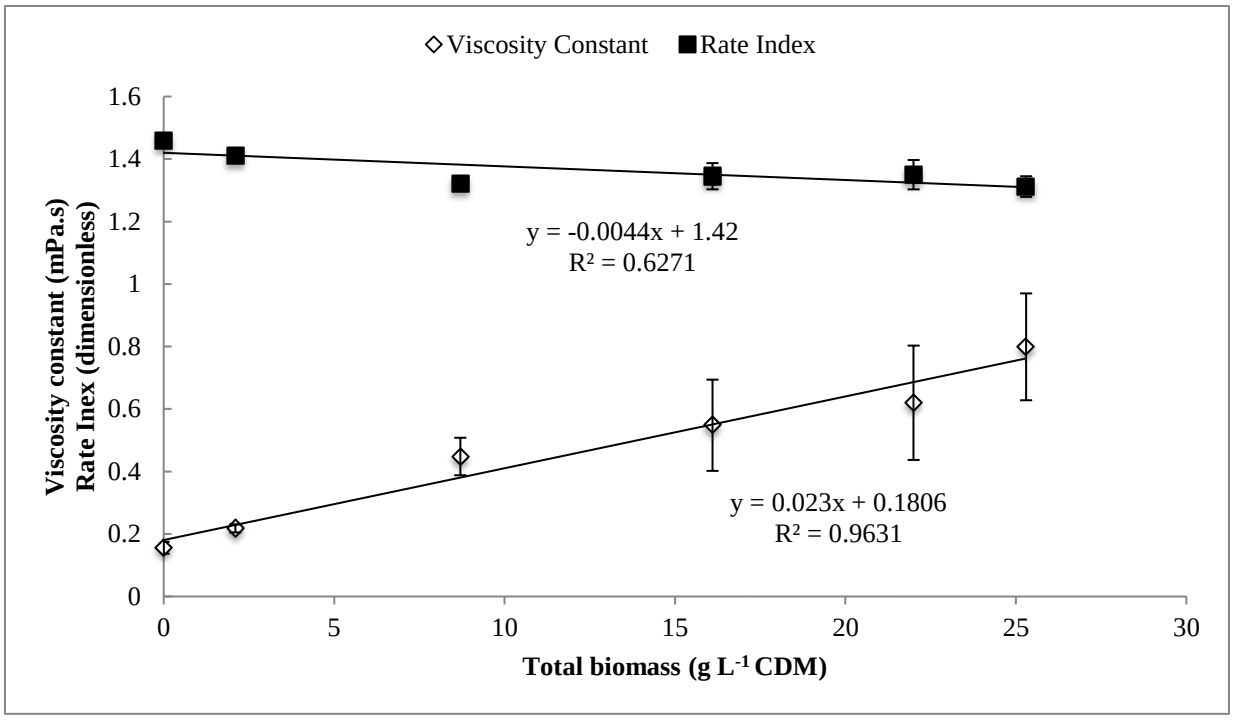

Figure 8.4. Changes in power-law constants describing culture rheology as a function of the total biomass in the fed batch cultivation at varying points over time. Error bars represent the standard deviations between technical replicate measurements (n = 3).

8.5.2. Quantifying extracellular components in the supernatant matrix

This data indicates that significant rheological changes to the culture medium occur over time (much of which is not simply explained by the presence of cells). According to Newton et al. (2016), in HCD *E. coli* cultures, this behavior is the result of structural interactions between cells and cellular debris (high molecular mass nucleic acids) resulting from lysed cells. *P. putida* and other *Pseudomonas* sp. have also been reported to produce significant quantities of extracellular polymeric substances (EPS), including alginate (Chang et al. 2007), DNA, proteins, and polysaccharides (Read and Costerton 1987; Jahn et al. 1999; Allesen-Holm et al. 2006; Celik et al. 2008). In several studies, the production of EPS not only increased viscosity but also had shear-thinning properties (Freitas et al. 2009; Maalej et al. 2016).

In this work, several of these putative EPS constituents and/or cell lysis products were monitored and quantified in the culture supernatant to better understand the observed rheological behavior. These include proteins, reducing sugars, DNA, and extracellular PHA, as well as bulk measurement of carbonaceous products in the supernatant by VS. These are shown over time in Figure 8.5.

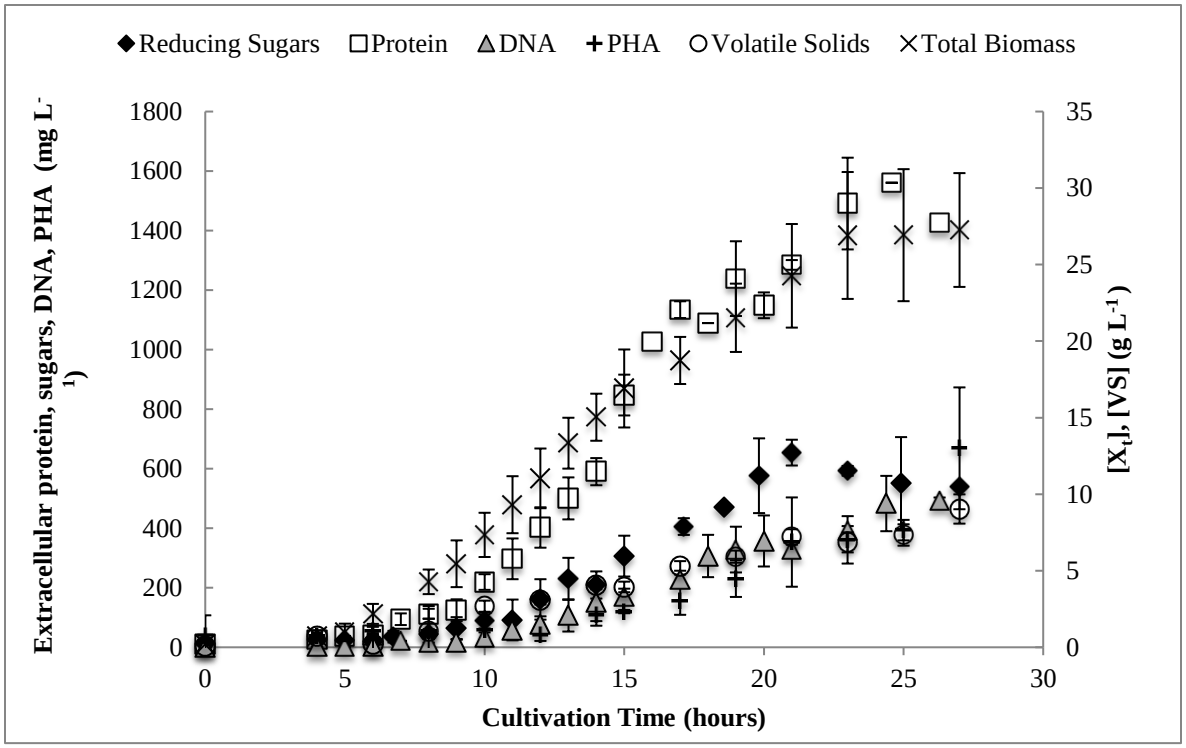

Figure 8.5. Carbonaceous products detected in the supernatant over time. Error bars represent standard deviations between biological replicates.

In general, the concentrations of these components increased as [X_t] increased, with the exception of reducing sugars, which reached a maximum concentration of 0.65 g L^{-1} at 21 h and then declined. The maximum concentrations (at 27 h) of proteins, PHA, and DNA in the medium were 1.56 g L^{-1}, 0.67 g L^{-1}, and 0.49 g L^{-1}, respectively. Collectively, the components could account for at most 48% of the total VS detected in the supernatant, which reached a maximum

of 9 g L^{-1} by 27 h. Newton et al. (2017) demonstrated that both protein (0-50 g L^{-1}) and DNA (0-4 g L^{-1}) contributed linearly to increased viscosity and the flow curves for solutions of protein and DNA exhibited shear thinning and Newtonian behavior, respectively. However, in that work a somewhat lesser increase in viscosity was noted (1.1 to 5.3 mPa s) for a 48 g L^{-1} *E. coli* culture, despite the presence of more extracellular DNA (typically 3 g L^{-1}) and protein (up to 40 g L^{-1}).

In Figure 8.6, the viscosity increase is expressed as a function of the individual components detected in the supernatant. Interestingly, the strongest correlations for the viscosity effect were between DNA (R^2 = 0.99) and sugars (R^2 = 0.98). Surprisingly, the extracellular PHA (R^2 = 0.86) did not correlate as strongly and correlation with the observed viscosity effect. Finally, the most abundant detected compound in the supernatant, protein, showed poor correlation (R^2 = 0.77).

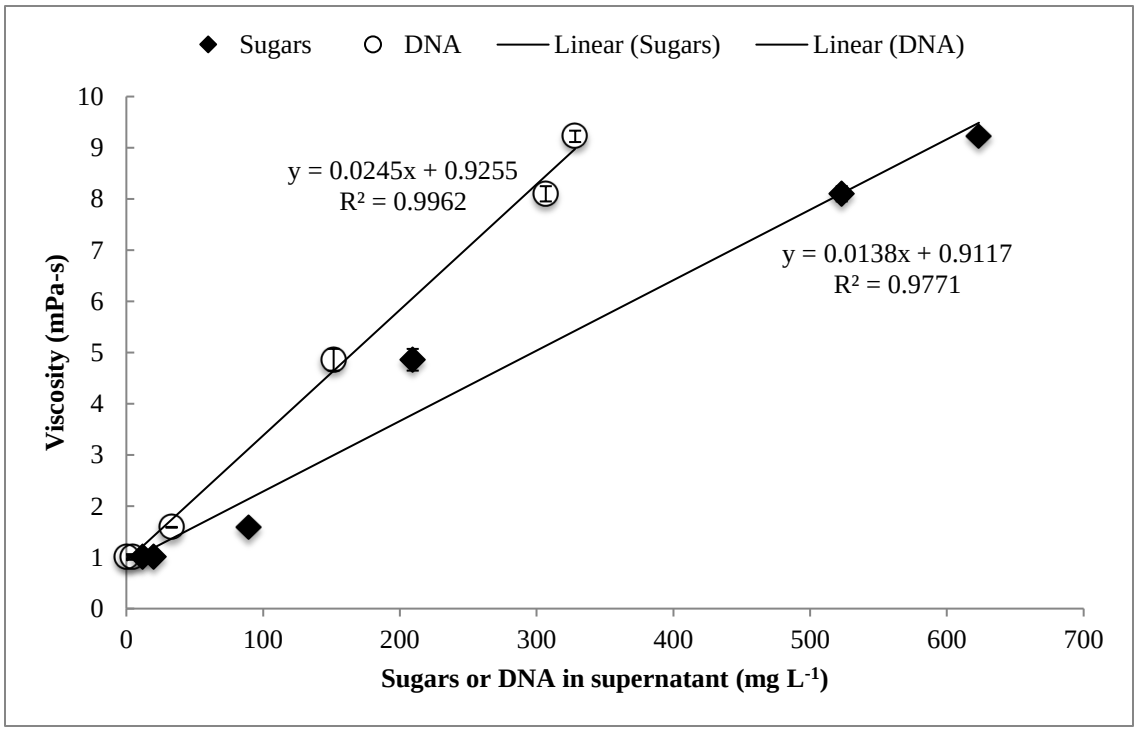

Figure 8.6. Relationship between select components of the VS with the observed viscosity. Error bars represent the standard deviations between biological replicates.

In this work, we do not attempt to differentiate whether these components of the supernatant are due to the production of EPS or are simply cell lysis products from cultivation in a high-shear environment. We can find evidence to make an argument in favor of either. Mg^{2+} is an intracellular metabolite that is known to leak from damaged membranes, which would precede cell lysis (Royce et al. 2013). In this work, the Mg^{2+} concentration monitored in the supernatant began to increase after 14 h, which corresponds to the onset of O_2 limitation and maximum agitation rates. However, when the ratios of protein-to-DNA of the culture supernatant was compared to that of *P. putida* cell lysate, it was found that the cell lysate contained only about half the DNA fraction that was observed in the supernatant. This could suggest DNA release as a possible EPS component, and would be supported by previous studies using *Pseudomonas* sp. (Jahn et al. 1999; Allesen-Holm et al. 2006). Furthermore, a similar experiment using lower shear rates using a maximum of 600 rpm mixing (compared to 1200 rpm) in the 7 L bioreactor, but with pure O_2 to increase driving force for oxygen transfer. Although this method produced less total biomass, statistically indifferent ($p < 0.05$) yields of extracellular organic content (protein, sugars, DNA) per unit [X_t] were observed in comparison with the normal mixing condition of 1200 rpm. While this does not disprove the occurrence of significant cell lysis, it does show that this behavior is difficult to avoid, even at impractically low bioreactor mixing rates.

8.5.3. Effects on k_La

Knowledge of viscosity in bioprocesses is important for process scale-up. Many empirical relationships (or dimensionless parameters like the Reynolds's number, *Re*) describing the k_La are inversely proportional to viscosity (Garcia-Ochoa and Gomez, 2009). According to Martin et al. (2010), this is due to: 1) reduced contact area between bubbles and a fluid because

bubbles are more stable in viscous fluids; and 2) decreased liquid diffusivity due to reduced velocity profile in the liquid layer surrounding the bubble.

The k_La of the various supernatant samples was assessed using the dynamic method. The final values (obtained at 27 h) showed a significant ($p << 0.05$) reduction of 45-52% from the values measured at 0 h or 6 h. The k_La of the cell suspensions could not be determined due to the high oxygen demand of the culture, preventing observable changes in DO as well as excessive foaming when air was bubbled through the cell suspensions in the miniature reactor. In Figure 8.7 this reduction in the k_La, and increase in viscosity, are expressed as a function of the VS detected in the supernatant.

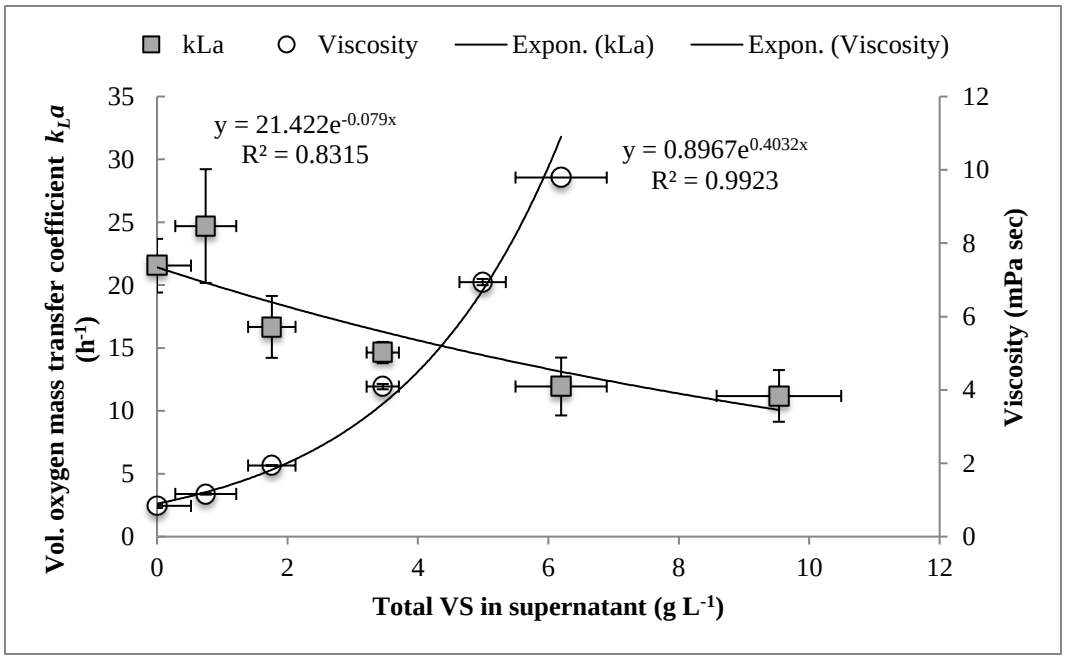

Figure 8.7. Correlating viscosity and to VS in the supernatant a) relationship between VS detected in the supernatant with k_La and viscosity and b) relationships between select components of the VS with the observed viscosity. Error bars represent the standard deviations between biological replicates.

The *Re* is an important parameter describing the hydrodynamic conditions within the bioreactor, and is used in many correlations to estimate k_La. Often, *Re* is related to the power consumption required to mix the reactor contents. Using the obtained constants shown in Table 8.2, we estimated that for a given (un-gassed) power input to the stirrer, *Re* decreased by 44-55% as [X_t] increased from 0 to 25 g L^{-1} following the approach of Gabelle et al. (2011). Not only does the power required to stir the bioreactor contents increase with viscosity, the OTR is generally reduced.

Considering that other fed-batch strategies have achieved 100 g L^{-1} CDM or more in PHA production (Ryu et al. 1997; Wang and Lee 1997b; Maclean et al. 2008; Cerrone et al. 2014b; Davis et al. 2015), the observed viscosity effect and reduction in k_La could be considerably more significant in those systems compared to that described in this work. This may be neglected in bench-scale high cell density PHA cultivations in which stirring and aeration are typically set as high as possible to maximize productivity. However, with increasing scale the required power consumption for mixing and aeration becomes significant (Koller et al. 2013), and so k_La must be carefully managed in order to save aeration costs. This aspect is emphasized in PHA production/waste treatment operations using enriched mixed cultures (Coats et al. 2016).

8.6. Conclusions

In moderately HCD fed-batch cultivations of *P. putida* LS46, significant changes in the rheological properties of the culture were observed. At lower shear rates the culture exhibited slight shear-thinning behavior while the onset of shear thickening was observed at shear rates that increased with sample viscosity (or increased [X_t]). An eight-fold increase in viscosity (at 10 s^{-1}) was measured throughout the course of the cultivation process, approximately 75% of which

was attributed to the supernatant rather than the presence of cells. Investigation of the culture supernatants revealed up to 9 g L^{-1} VS being present in the supernatant, of which half was accounted for as extracellular proteins, sugars, DNA, and PHA. The k_La of the supernatants was reduced by approximately 50% over the course of the cultivation process. Although difficulties in maintaining oxygen transfer are well known in HCD aerobic bioprocesses, this work has demonstrated that changes in the medium itself (through biological activity) also plays a large role, rather than just the oxygen uptake of the cells themselves.

8.7. Acknowledgements

This work was funded by: 1) Genome Canada, through the Applied Genomics Research in Bioproducts or Crops (ABC) program for the grant titled, "Microbial Genomics for Biofuels and Co-Products from Biorefining Processes"; 2) the government of the Province of Manitoba through the Manitoba Research Innovation Fund (MRIF) and the Manitoba Rural Adaptation Council (MRAC); 3) the Natural Sciences and Engineering Research Council (NSERC) through the CGS-D award and Michael Smith Foreign Study Supplement; and 4) the University of Manitoba Sir Gordon Wu Graduate Student Scholarship. On the technical side, thanks to the team at Scion for welcoming me as part of the Biotransformation lab, and their help in teaching me the workings of SIP pilot-scale bioreactors, continuous centrifugation, including Christophe Collet, Tracey Bowers, and Mark West. Special thanks also to Marc Gaugler for enthusiastically devoting his time, efforts, and insights in helping with the rheological analysis. Special thanks to those helping with off-hours supervision at Scion, including Dr. Daniel Gapes, Kim McGrouther, and Martin Cooke-Willis. Also thanks to Taylor Livingston for her help with protein, Anthrone, and DNA assays, as well as k_La measurements. The authors disclose that no conflict of interest exists between them.

Chapter 9: Towards continuous cultivation: tailoring selective conditions for mcl-PHA production in a non-sterile environment

9.1. Preface

This thesis has so far dealt extensively with batch (Chapter 4) and various fed-batch cultivation systems, with varying degrees of complexity (Chapters 5-8). Continuous production is an attractive bioprocessing platform for reduced costs through maintaining moderate but sustained productivity over time, but maintaining a stable axenic monoculture of the bio-catalyst of interest is a challenge. The objective of this chapter was to demonstrate feasibility of mcl-PHA production in a non-sterile environment, which, if successful, would allow considerable flexibility in the design of future process configurations.

9.2. Abstract

Production of mcl-PHAs from octanoic acid was investigated in non-sterile environments using *Pseudomonas putida* LS46. It was hypothesized that in such environments, the anti-microbial properties of the fatty acid carbon source would reduce or delay growth of microbial competitors and allow *P. putida* LS46 to dominate the population under non-sterile conditions. Non-sterile 24 h flask cultures produced similar final $\%_{PHA}$, Q_v, and monomer composition compared to sterile control cultures for initial octanoic acid concentrations 5-40 mM at an initial pH of 6.5. Similarly, a 27 h fed-batch process showed nearly identical mcl-PHA productivity under non-sterile conditions as compared to sterile controls. However, in the absence of *P. putida*, contaminants did grow in non-sterile medium (batch cultures) after a significant lag period of as much as 120 h, the length of which was concentration-dependent. This shows that given significant acclimation time, competitors could proliferate and may eventually out-

compete *P. putida* LS46. To test this, a semi continuous SBR was run over a prolonged period of 28 days using non-sterilized medium and equipment from an initial inoculum of an axenic *P. putida* LS46 culture. Although the $\%_{PHA}$ was somewhat variable throughout the first 240 h, at the end of 672 h of operation the $\%_{PHA}$ was 47% CDM. The monomer composition remained relatively stable at 87.0 ± 2.7% C8 and scl-PHA monomers were not detected. These results show that a non-sterile growth environment did not affect mcl-PHA productivity for short batch and fed-batch cultivation processes using octanoic acid as the carbon source. Furthermore, it may be possible to maintain mcl-PHA productivity on a long-term basis in a non-sterile environment. This could result in significant reduction in both fixed and operating costs for mcl-PHA production, and also suggests the possibility for open, continuous-feed cultivation.

9.3. Introduction

Microbial production of PHAs has been touted as a renewable and biodegradable alternative to petrochemical-based plastics (Anderson and Dawes 1990). Currently, PHA-based polymers are being produced commercially under several trade names (Dietrich et al. 2017), but despite this, applications are generally limited to niche markets. Further cost reduction is a requisite for large-scale PHA production to become competitive with petroleum-based plastics. While there are a number of factors that inflate the cost of PHAs, they may be broadly broken down into three main categories (in no particular order): 1) the cost of the carbon source combined with the relatively low product-to-carbon yield; 2) the energy requirement for bioreactor operation; and 3) downstream processing operations (Akiyama et al. 2003; Reis et al. 2003; Koller et al. 2013; Shahzad et al. 2013; Wang et al. 2014; Fernández-Dacosta et al. 2015; Koller et al. 2017). These factors also contribute to the questionable cradle-to-grave environmental impacts of PHA production compared to conventional materials, including non-

renewable energy use and global warming potential (Khoo and Tan 2010; Tabone et al. 2010). However, it is anticipated that as production technologies evolve, life-cycle studies will increasingly favor PHAs (Yates and Barlow 2013).

The main costs typically associated with bioreactor operation are the energy requirement for mixing and aeration as well as sterilization of substrates, medium, and equipment (the latter being necessary in pure culture PHA production) (Wang et al. 2014; Fernández-Dacosta et al. 2015). However, a relatively recent study pointed out that for mesophilic cultivation processes, up to 28% of the operating costs could be attributed to cooling requirement and use of a refrigerants (Levett et al. 2016), and should also merit consideration. The possibility of energy savings from the sterilization process has generated interest in non-sterile cultivations, as was highlighted in a recent review of non-sterile fermentation processes (Chen and Wan 2017). Non-sterile operation may well save costs for short-term batch and/or fed batch cultivation processes, it also allows the possibility for prolonged operation in open, continuous-feed processes if the process is resistant to contamination (Van Wegen et al. 1998; Chen 2012; Koller and Braunegg 2015). Typically in non-sterile fermentation processes, certain conditions (pH, temperature, salinity, substrate or product concentrations) are manipulated to maintain the selective pressure favoring organism of interest (Chen and Wan 2017). Previously, a variety of low-cost, high-volume bio-commodities have been produced under non-sterile conditions - including lactic acid (Abdel-Rahman et al. 2013), single-cell oils (Moustogianni et al. 2015), and H_2 (Chookaew et al. 2014). Production of PHB has been demonstrated under non-sterile (but highly saline) conditions using halophilic bacteria including *Halomonas bluephagenesis* TD01 (Tan et al. 2011) and a recombinant strain, *H. bluephagenesis* TD40 (Ye et al. 2018). Another study operated a 65-day non-sterile fed-batch process, without apparent infection, using *H. campaniensis*, cultivated at

pH 10 with 27 g L^{-1} NaCl (Yue et al. 2014). In another study, *Hfx. mediterranei* was cultivated in a chemostat for three months (Lillo and Rodriguez-Valera 1990). After 370 generations, the production strain was isolated and found to have similar PHB synthesis capability to the original cultures, although it is not clear to what extent other contaminants were present.

While these and others, including mixed microbial culture (MMC) PHA studies, have examined production of scl-PHAs, relatively few studies have looked at production on mcl-PHAs. Cisielska et al. (2008) found mcl-PHA synthases belonging to *Pseudomonas* spp., in activated sludge enriched on acetic acid and molasses under O_2-limited conditions (Ciesielski et al. 2008). A more recent studies indicated that a microbial population enriched from activated sludge using medium chain length alkanoic acids (octanoic, nonanoic, decanoic, dodecanoic acids) became dominated by *Pseudomonas aeruginosa* and accumulated mcl-PHA, although some strains accumulated scl- and mcl-PHA (Lee et al. 2011; Lee et al. 2018). This finding indeed suggests that *Pseudomonas* spp., including *P. putida* may also have a competitive advantage under non-sterile conditions when metabolizing free fatty acids, which are also converted to mcl-PHA with high yield (Chanprateep 2010). Since fatty acids exert considerable toxicity through disruption of cell membranes, leaking of intracellular metabolites, and uncoupling of the proton motive force (Desbois and Smith 2010; Jarboe et al. 2013), their presence may inhibit or delay growth and proliferation of microbial competitors.

The main hypothesis of this work is that due to the selection pressure applied by using sufficient concentrations of toxic alkanoic acids as the carbon source, mcl-PHA production could be accomplished under non-sterile conditions with *P. putida*. This was explored in a variety of cultivation platforms in this work and could be a significant cost saving measure for high-throughput PHA production. It could also demonstrate feasibility of further development toward

open, continuous-feed cultivation.

9.4. Materials and Methods

9.4.1. Microorganism, medium, and substrates

The microorganism (*P. putida* LS46) and strain maintenance practices in this work followed those described in Section 3.2. Ramsay's minimal medium was used for all studies and was prepared as described in Section 3.2. The initial pH of the medium was adjusted to 6.5 (using either HCl or NaOH) unless otherwise specified. In fed batch experiments, Ramsay's medium was modified as described in Section 7.4.1. Octanoic acid (Sigma Aldrich, St. Louis MO) was used as the carbon source in all studies.

9.4.2. Cultivation techniques/platforms

This work involved cultivations in multiple platforms. Initial conditions that could be tolerated by *P. putida* LS46 were examined in microplate experiments; however, the small cultivation scale did not allow proper assessment of biomass or mcl-PHA content of the biomass. Consequently, the conditions of interst identified by the microplate experiments were extended to the shake flask scale. Finally, the application was demonstrated at the bioreactor scale in a semi-continuously running SBR. This sequence of process development is illustrated in Figure 9.1

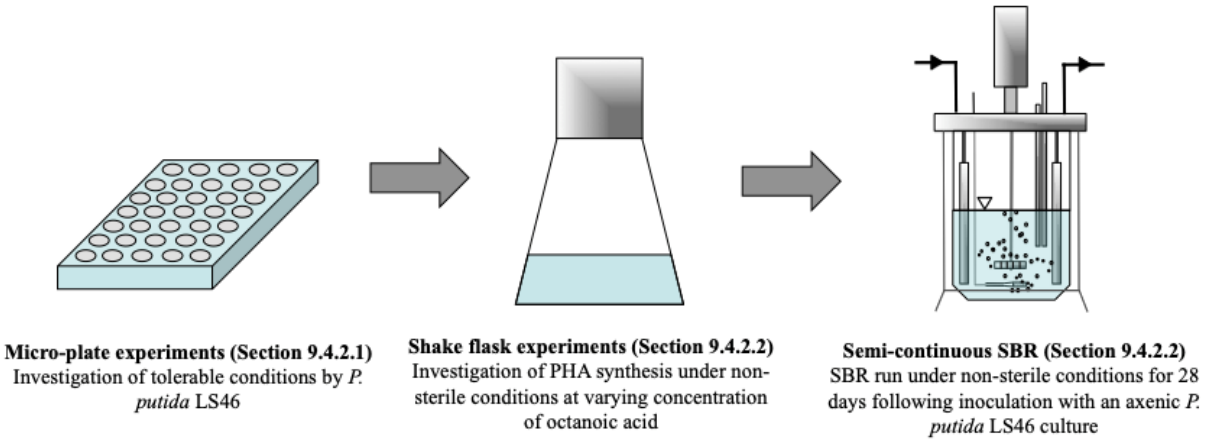

Figure 9.1. Sequential process development of the various cultivation scales used in this work.

9.4.2.1. Micro-plate experiments

Initial tests aimed at determining the limits for initial octanoic acid concentration and/or pH tolerated by *P. putida* LS46 were conducted in sterile 350 µL well plates. 200 µL of sterile medium (already containing the substrate and with pH adjusted to 7.0) was added to each well. A 1% (vol vol^{-1}) inoculum from an overnight culture as added to each well and this corresponded to a starting OD_{600} of 0.2. The well plate was then covered (not airtight to allow air exchange) and incubated at 30 °C for 24 h. The OD_{600} was monitored in 30-min intervals with continual shaking between intervals using a Synergy4 spectrophotometer (BioTek Instruments, Winooski VT). Each condition was assayed in four replicate wells, and each experiment was performed twice.

9.4.2.2. Flask experiments

The aim of the flask experiments was to evaluate how different concentrations of octanoic acid (optimized to a certain degree in the sterile micro-plate experiments described above) affected mcl-PHA production under non-sterile conditions, with comparison to sterile controls. All flask experiments employed 500 mL baffled shaker flasks with a 100 mL working

volume. Experiments were initiated with a 1% (vol vol^{-1}) addition of an overnight inoculum and incubated at 30 °C for 24 h with shaking at 150 rpm. For sterile control conditions, the flasks were autoclaved at 121 °C for an exposure time of 15 min. All conditions examined in flask cultures were performed in triplicate flasks in a minimum of two independent experiments.

9.4.2.3. Bioreactor experiments: semi-continuous SBR

The SBR experiment used the same bioreactor setup described above. However, mixing and aeration were kept constant at 350 rpm and 3 LPM of air. Using this strategy, the DO dropped to less than 4% (of saturation with atmospheric air at 30 °C), or < 0.3 mg L^{-1} O_2 assuming the solubility of O_2 in mineral salts medium at 30 °C is 6.77 mg L^{-1} (Vendruscolo et al. 2012). Because of this, O_2 limitation was the main factor controlling mcl-PHA synthesis, following a brief (4-6 h) period of growth while DO was at 10% or above. The initial octanoic acid concentration added with each batch was 40 mM (5.76 g L^{-1}) for the first 21 days (d), and was then reduced to 20 mM (2.88 g L^{-1}) from days 21 to 28 (504 h to 672 h). The reason for this change is discussed in the results. The glycol-based antifoaming agent was added at the beginning of each SBR cycle (15 μL L^{-1}). Both carbon and ammonium were in excess throughout the process. The pH was maintained at 6.5 via the addition of 2 N NaOH and 2 N H_2SO_4 as needed. The SBR was operated on a 24-h cycle that consisted of the following steps: 1) a 30-min fill phase; 2) a 23-h react phase for both growth (4-6 h) and storage (17-19 h); and 3) a 30-min decant phase, during which 94% of the contents of the bioreactor were removed and the remaining 6% was left as inoculum to re-seed the subsequent batch. The SBR experiment was initiated through the addition of a 1% vol vol^{-1} inoculum from an aseptic flask culture grown overnight (40 mM octanoic acid) as described above.

9.4.3. Contamination assessment

In the semi-continuous SBR experiments, samples were periodically plated on both LB and Ramsay's medium with 20 mM octanoic acid and 20 g L^{-1} agar to observe differences in colony morphologies over time. Several of the colonies that were suspected contaminants were re-grown in flasks under aseptic conditions (as described above) and compared to the mcl-PHA production of pure *P. putida* LS46. The colonies were also grown on LB medium and DNA was extracted and stored for future 16S amplification and sequencing.

9.4.4. Analytical methods

Total biomass from 40 mL samples (taken at 16-24 h for flask cultures, at 2-4 h intervals in fed-batch, and at 0 h and 24 h in the SBR study), were centrifuged, and the mass was determined gravimetrically as described in Section 3.3. The PHA content of the biomass was determined via the acid-catalyzed methanolysis procedure and subsequent GC-FID quantification as described in Section 3.4. Calculations of $\%_{PHA}$, X_r, Q_v, and $Y_{PHA/S}$ were done as described in Sections 3.7 and 3.8.

9.4.5. Statistical analyses

All statistical analysis was performed using StatPlus:mac LE v6 (AnalystSoft, Inc). The efficacy of the non-sterile treatments and challenge experiments were assessed by comparing the mean $\%_{PHA}$, $Y_{PHA/S}$, and/or Q_v of the test condition with that of the sterile control using a Student's t-test and assuming equal variances. A 95% confidence level was used for all tests ($\alpha = 0.05$).

9.5. Results

9.5.1. Micro-plate tests

These initial experiments determined the appropriate octanoic acid concentrations and/or medium pH that can be tolerated by *P. putida* LS46. Figure 9.2 shows the effect of different initial concentrations of octanoic acid in the medium at the initial pH of 7.0 on (on combined growth and/or mcl-PHA synthesis which unfortunately cannot be distinguished based on OD_{600} values alone). Following a brief lag of about 1 h, the rate of increase of OD_{600} for the first 8 h of growth indicated that total octanoic acid concentrations of up to 60 mM do not significantly impair *P. putida* LS46. Under these conditions, the time required to achieve the first doubling in OD_{600} was 3-4 h. The rate of increase in OD_{600} for the 50 mM condition began to slow after 8 h and reached lower final absorbance, suggesting a possible inhibitory effect as the cells entered stationary phase. This reduction in final OD_{600} was slightly more pronounced at concentrations of 60 mM. When the concentration was increased to 80 mM, the time required to achieve the first doubling was 14 h, and severe inhibition was observed throughout the 24 h growth period.

Since residual concentrations could not be measured in this scale, the estimated concentrations of octanoic acid are shown throughout the cultivation. This was done by assuming a 1.7:1 correlation factor (OD_{600}:[X_t], based on previous data) and that 50% of the carbon was lost as CO_2. Since the protonated form of the acid is known to be toxic (Jarboe et al. 2013), it is important to distinguish between octanoic acid and its ionized form, octanoate. In these tests, the initial pH of the medium was adjusted to 7.0. Since the ionization constant of octanoic acid (pKa) is 4.8, the initial concentration of un-ionized octanoic acid in the medium ranged from 0.15 mM (at 20 mM initial concentration) up to 0.77 mM at (100 mM initial concentration). Severe inhibition was observed at an initial concentration of 80 mM, where the concentration of

un-ionized octanoic acid was 0.62 mM. Ramsay et al. (1991) reported that *P. putida* ATCC 29347 (formerly *P. oleovorans*) was inhibited at 4.65 g L^{-1} sodium octanoate (this is equivalent to 28 mM total octanoic acid, of which 0.22 mM would remain in the un-ionized form at pH 7.0). In study, it was reported that total inhibition was observed at 6 g L^{-1} (this equivalent to 36 mM total octanoic acid, of which 0.28 mM would remain in the un-ionized form at pH 7.0) (Ramsay et al. 1991). Our results appear to indicate slightly higher tolerance to octanoic acid, since total concentrations of up to 40 mM showed no observable inhibition.

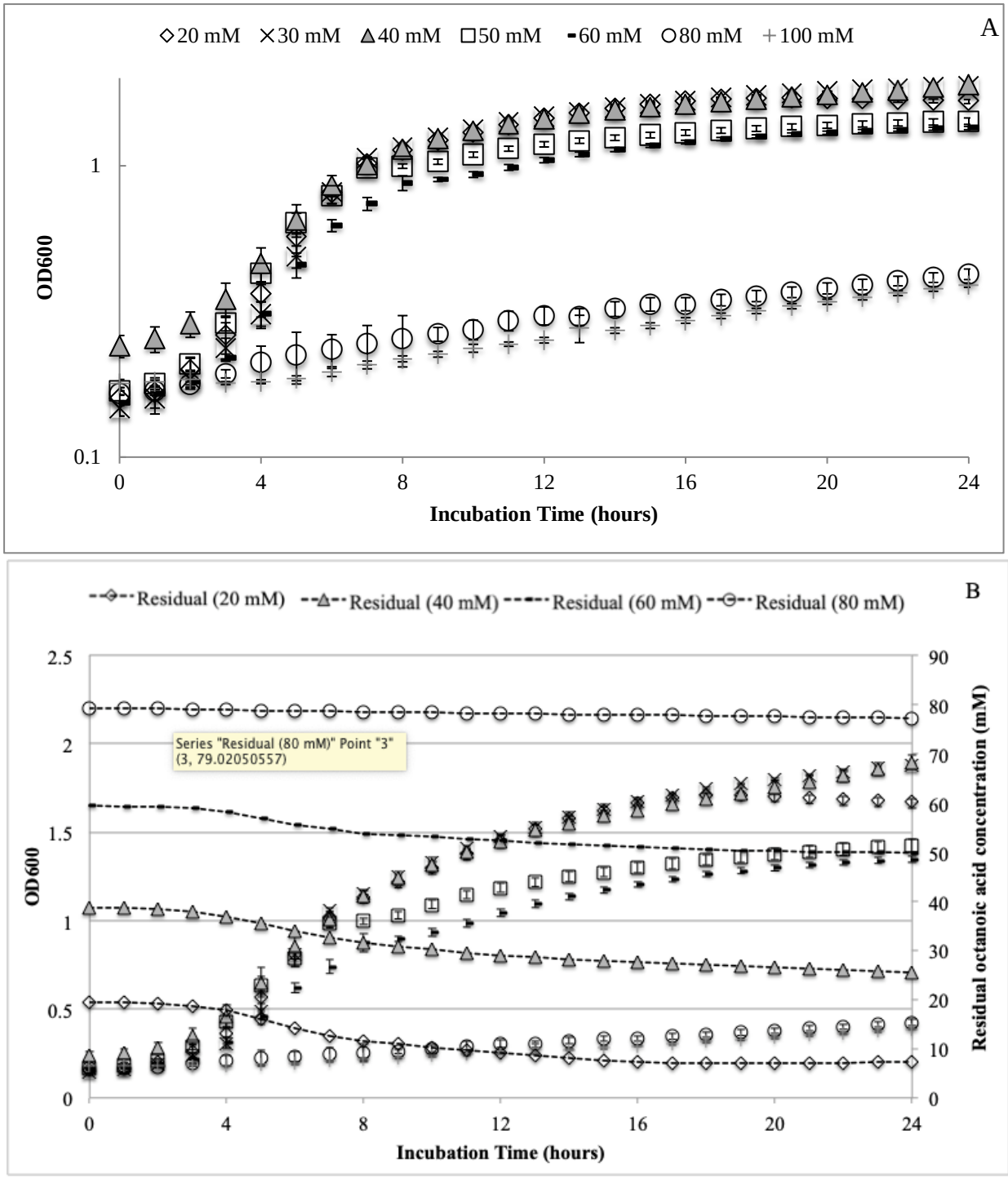

Figure 9.2. Effect of different initial total concentrations of octanoic acid (i.e. HA + A^-) in medium at pH 7.0 shown on a) a semi-log scale and b) a linear scale with estimated residual concentrations of total octanoic acid for select conditions. The corresponding levels of intial undissociated octanoic acid at pH 7 are expressed as [HA + A^-]:[HA] (in mM) as follows: 20:0.15; 30:0.23; 40:0.31; 50:0.39; 60:0.46; 80:0.62; 100:0.77. Error bars represent standard deviations between four replicate micro-plate wells.

The ionization of octanoic acid is dependent on the medium pH, and therefore the effects are complicated because medium pH has a separate effect on growth. The effect of pH was further investigated using an initial total concentration of 20 mM (0.15 mM of the un-ionized form at pH 7.0), which exhibited no observable inhibitory effect previously (Figure 9.2). As shown in Figure 9.3, there was little difference in the rate of increase in OD_{600} at pH 6.5-8.0 following a 1-2 h lag period. Under these conditions, the concentration of un-ionized octanoic acid remains at or below 0.5 mM. At pH 6.0 (1.44 mM un-ionized octanoic acid) a lag period of about 3 h was observed, but then the absorbance increased at a similar rate compared to a pH of 6.5 to 8.0. A significant (16 h) lag period was observed at pH 5.5 with a total concentration of 20 mM octanoic acid (3.94 mM of the un-ionized form), but then the OD_{600} increased at a similar rate to the other conditions at higher pH. Total inhibition was observed at pH 5.0 or less (8.74 mM un-ionized octanoic acid). When glucose was used as the sole carbon source, no noticeable inhibition was evident in batch tests with the pH as low as 4.7 (unpublished data). With this in mind, it appears that in the above tests, the concentration of un-ionized octanoic acid became inhibiting before pH was an issue, and therefore concentrations of 1.5 mM or more should be avoided. It is worth noting that at pH 5.5, the concentration of un-ionized octanoic acid (1.44 mM) was more than double that when inhibition was observed at 80 mM total concentration but neutral pH (0.62 mM). Although the un-ionized form passes through the cell membrane, this discrepancy could indicate that the ionized octanoic acid may also be inhibitory, even if to a lesser extent. While further tests are needed to more precisely differentiate these effects, it can be generally concluded that even for moderate total concentrations of octanoic acid (20 mM), pH values of 6.0 or lower should be avoided to prevent inhibition of *P. putida* itself. However, at near-neutral pH, total concentrations up to 40 mM can be tolerated. Thus, the maximum

allowable limits of concentration and pH for subsequent tests in a non-sterile environment were determined.

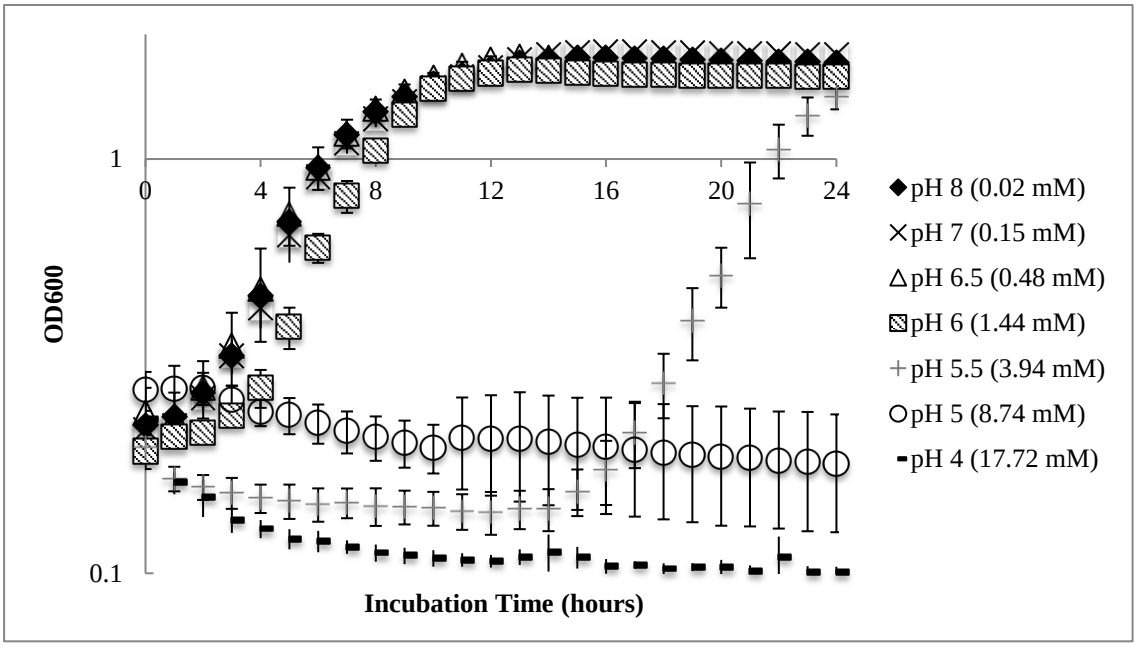

Figure 9.3. Effect of medium pH at 20 mM initial concentration of octanoic acid. Values in parentheses indicate the concentration of protonated octanoic acid in the medium at the indicated pH value. Error bars represent standard deviations between four replicate micro-plate wells.

9.5.2. Mcl-PHA production in non-sterile flask cultures

Knowing the combinations of both medium pH (6.5-8.0) and octanoic acid (up to 40 mM) that can be tolerated by *P. putida* LS46 without noticeable inhibition, growth in flasks under non-sterile conditions was examined using different concentrations of octanoic acid at pH 6.5. The observed [X_t] and [X_r] are not shown but were very similar for sterile and non-sterile conditions within each concentration ($p > 0.05$). The final $\%_{PHA}$ and Q_v (observed at 24 h) for sterile and non-sterile conditions are shown in Figure 9.4, and were generally not significantly different (Table 9.1). The monomer composition of the polymer also remained relatively stable at 87% C8, 11% C6, 2% C10, and trace amounts of C12 regardless of initial octanoic acid

concentration or cultivation under non-sterile conditions (Table 9.2). Short chain-length monomers (C4, C5) were not detected.

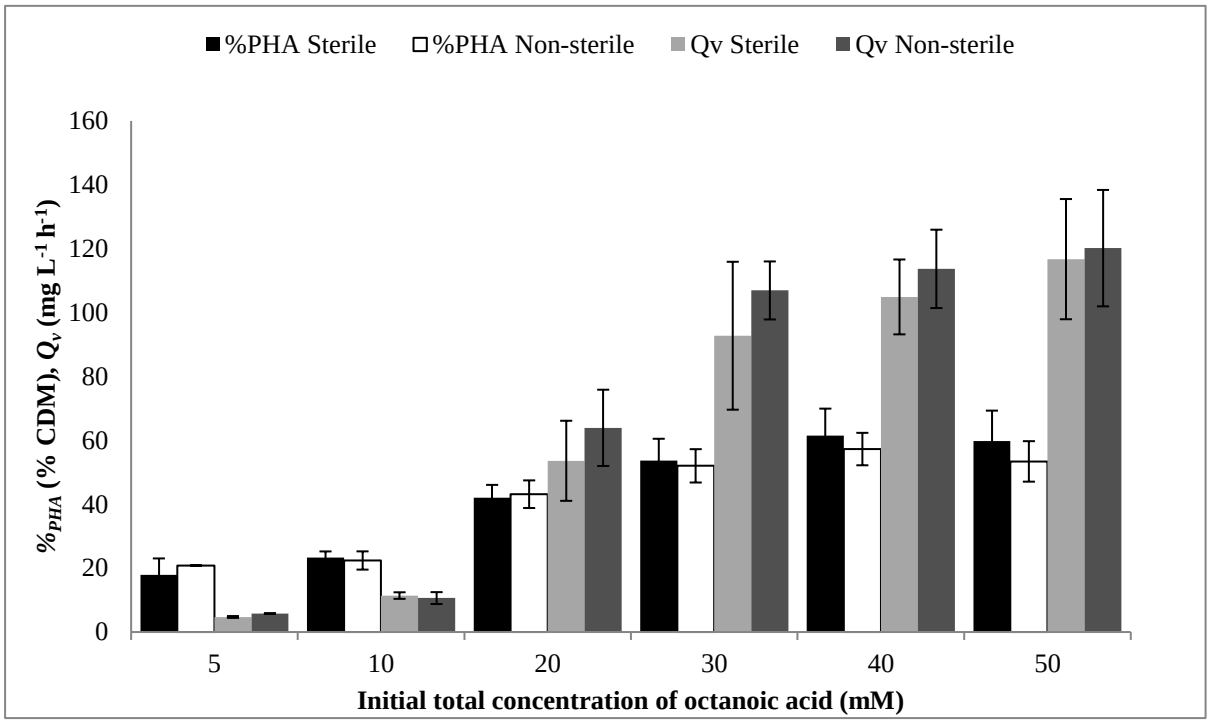

Figure 9.4. Final $\%_{PHA}$ and Q_v observed at 24 h when *P. putida* LS46 was grown in flasks under sterile and non-sterile conditions. The corresponding levels of intial undissociated octanoic acid at pH 7 are expressed as [HA + A^-]:[HA] (in mM) as follows: 5:0.12; 10:0.24; 20:0.48; 30:0.72; 40:0.96; 50:1.20. Error bars represent standard deviations between biological replicates (minimum of six replicates).

Table 9.1. Statistical analysis of $\%_{PHA}$ and Q_v using a two-tailed comparison of means ($\alpha = 0.05$) between sterile and non-sterile flasks cultures of *P. putida* LS46 using different concentrations of octanoic acid. Tolerances indicate standard deviations between biological replicates.

Conc.	**Sterile**	**Non-sterile**	**Comparison**	
	Mean $\%_{PHA}$ ± St.Dev (g L^{-1} CDM)	Mean $\%_{PHA}$ ± St.Dev (g L^{-1} CDM)	*p*-value	Significant?
5 mM	22.5 ± 5.1	22.5 ± 5.1	0.60	No
10 mM	23.3± 2.0	23.3± 2.0	0.69	No
20 mM	37.0 ± 8.1	37.0 ± 8.1	0.31	No
30 mM	47.6 ± 11.6	47.6 ± 11.6	0.76	No
40 mM	50.3 ± 12.0	50.3 ± 12.0	0.53	No
50 mM	59.8 ± 9.5	59.8 ± 9.5	0.02	Yes
	Mean Q_v ± St.Dev (mg L^{-1} h^{-1})	Mean Q_v ± St.Dev (mg L^{-1} h^{-1})	*p*-value	Significant?
5 mM	4.7 ± 0.3	5.8 ± 0.04	0.08	No
10 mM	11.4 ± 1.0	10.6 ± 1.9	0.87	No
20 mM	53.6 ± 12.5	63.9 ± 11.9	0.32	No
30 mM	92.8 ± 23.1	106.9 ± 9.1	0.37	No
40 mM	104.9 ± 11.7	113.7 ± 12.3	0.33	No
50 mM	116.7 ± 18.8	120.2 ± 18.2	0.24	No

Table 9.2. Monomer composition of mcl-PHA obtained for sterile and non-sterile flask cultures. Tolerances indicate standard deviations between biological replicates.

Conc.	**Sterile**			**Non-sterile**		
mM	%C6	%C8	%C10	%C6	%C8	%C10
5	12.2 ± 0.4	85.4 ± 1.7	2.4 ± 1.3	11.5 ± 0.4	86 ± 0.8	2.5 ± 0.6
10	11.6 ± 0.6	85.8 ± 1.9	2.5 ± 1.5	11.7 ± 0.5	86.1 ± 0.8	2.3 ± 0.7
20	9.6 ± 0.3	87.8 ± 0.1	2.6 ± 0.1	9.5 ± 0.3	88.2 ± 0.3	2.3 ± 0.0
30	10.3 ± 0.6	85.5 ± 0.5	4.2 ± 0.9	10.4 ± 0.5	86.4 ± 1.2	3.2 ± 1.0
40	10.5 ± 0.5	87.6 ± 0.5	1.9 ± 0.2	9.9 ± 0.6	88 ± 0.5	2.1 ± 0.2
50	9.5 ± 2.2	88.7 ± 0.2	1.8 ± 0.5	10.3 ± 0.2	87.1 ± 0.2	2.7 ± 0.4

Despite generally insignificant differences in $\%_{PHA}$ and Q_v at 24 h in flask cultures, Figure 9.5 shows that when non-sterile control flasks (with no inoculum) were incubated for a sufficiently long time period, contaminating organisms did eventually adapt and grow. Lag times were greatly influenced by the concentration of octanoic acid in the medium. At a total initial octanoic acid concentration of 5-10 mM, the OD_{600} of this culture did not increase until after 18 h. When the concentration was increased to 40 mM, the OD_{600} did not increase significantly until after 40 h of incubation, and nearly 60 h in the 50 mM condition. By comparison, when *P. putida* was added (using the standard inoculum size for flask work done in flasks throughout this thesis of 1% vol/vol from an overnight culture, resulting in a typical initial OD_{600} of about 0.08) carbon was depleted within 20 h in all conditions, which was apparently not enough time to allow detrimental contaminants to adapt and grow even at the lowest concentrations of octanoic acid (5-10 mM). Depending on the concentration, the observed final $[X_t]$ in the non-sterile controls ranged from 0.32 - 3.67 g L^{-1} CDM and contained low mcl-PHA content in all cases (16.5% CDM was the maximum observed at 50 mM). This shows that while other organisms may have been present, they were consistently out-competed in the presence of a healthy *P. putida* inoculum during short batch cultivations.

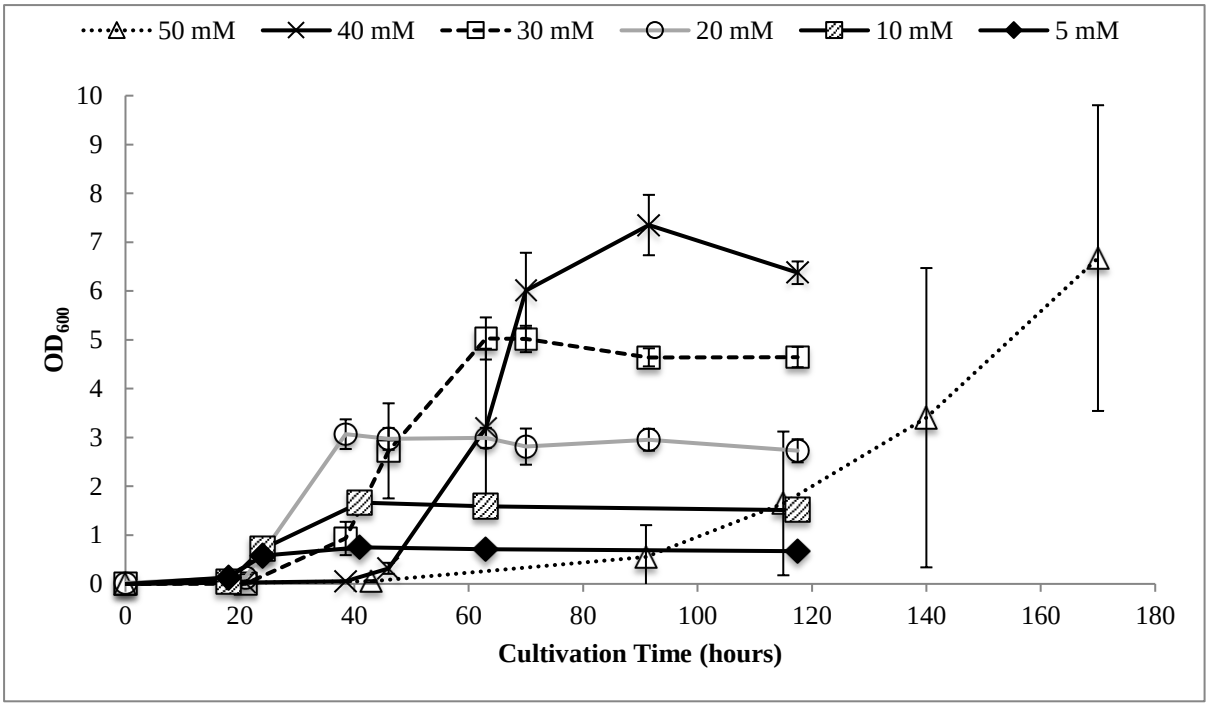

Figure 9.5. Growth of non-sterile control cultures (no inoculum) at different initial concentrations of octanoic acid. Error bars represent the standard deviations between biological replicates.

9.5.3. Prolonged mcl-PHA production in non-sterile (semi-continuous) SBR

Due to the eventual appearance of contaminating organisms (which produced little mcl-PHA) in flask cultures, we queried what would result if the competing organisms were given sufficient time to acclimate and grow. This hypothesis was tested by running a semi-continuous SBR for 28 days (d) or 672 h under non-sterile conditions from an axenic *P. putida* LS46 inoculum. The results for [X_t] and $\%_{PHA}$ for the non-sterile SBR are shown in Figure 9.6. Both [X_t] and $\%_{PHA}$ were somewhat variable within the first 10 d (240 h), but the SBR appeared to establish a pseudo-steady state afterward (264-672 h), with average [X_t] of 1.7 ± 0.2 g L^{-1} and average $\%_{PHA}$ of 46.2 ± 4.5% CDM. The highest $\%_{PHA}$ was recorded at 67% CDM at 2 d (48 h), and the lowest was recorded was 36.2% CDM at 20 d (480 h). In comparison, the final [X_t] and

$\%_{PHA}$ multiple sterile (batch) control bioreactors operated under otherwise similar conditions were 1.7 ± 0.4 g L^{-1} CDM and 54.9 ± 7.6% CDM, respectively. While the [X_t] after 10 d (240 h) was similar to that of the control, (p = 0.79), the $\%_{PHA}$ of the SBR at pseudo-steady state was slightly lower than the sterile control bioreactors (p = 0.0005) (Table 9.3). After 21 d, the initial concentration of ocatnoic acid was reduced to 20 mM (2.88 g L^{-1}) in order to prevent wasting of carbon (which was in excess after each cycle at an intital concentration of 40 mM), and to further evaluate the robustness of the system toward depletion of the carbon source, and the selective pressure.

Overall evaluation of the performance of the SBR system can be assessed by the Q_v and $Y_{PHA/S}$. These parameters are shown over time in Figure 9.7. Again, both Q_v and $Y_{PHA/S}$ were quite variable within the first 10 d (240 h) but stabilized afterward with mean values of 32.7 ± 5.7 mg L^{-1} h^{-1} and 0.24 ± 0.07 g g^{-1}, respectively. These values were lower than those obtained for the sterile control cultures, which were 51.7 ± 18.2 mg L^{-1} h^{-1} ($p << 0.05$) for Q_v and 0.33 ± 0.05 g g^{-1} ($p << 0.05$) for $Y_{PHA/S}$. It should be noted that these yield values include carbon consumed for the growth phase, which generally lasted 4-6 h while DO was 10% or higher. If only the carbon consumed during the PHA accumulation phase is considered in the yield analysis, the average $Y_{PHA/S}$ of the non-sterile SBR (after 10 d or 240 h) was 0.38 ± 0.8 g g^{-1} (see Table 9.3). The composition of the PHA was similar throughout the entire duration of the run as 87.4 ± 2.5% C8, 7.2 ± 0.9% C6, and 7.2 ± 0.9% C6, 4.9 ± 1.7% C10, and trace amounts of C12 (0.5 ± 0.3%). At no point during the run were scl-PHA peaks detected in the analysis.

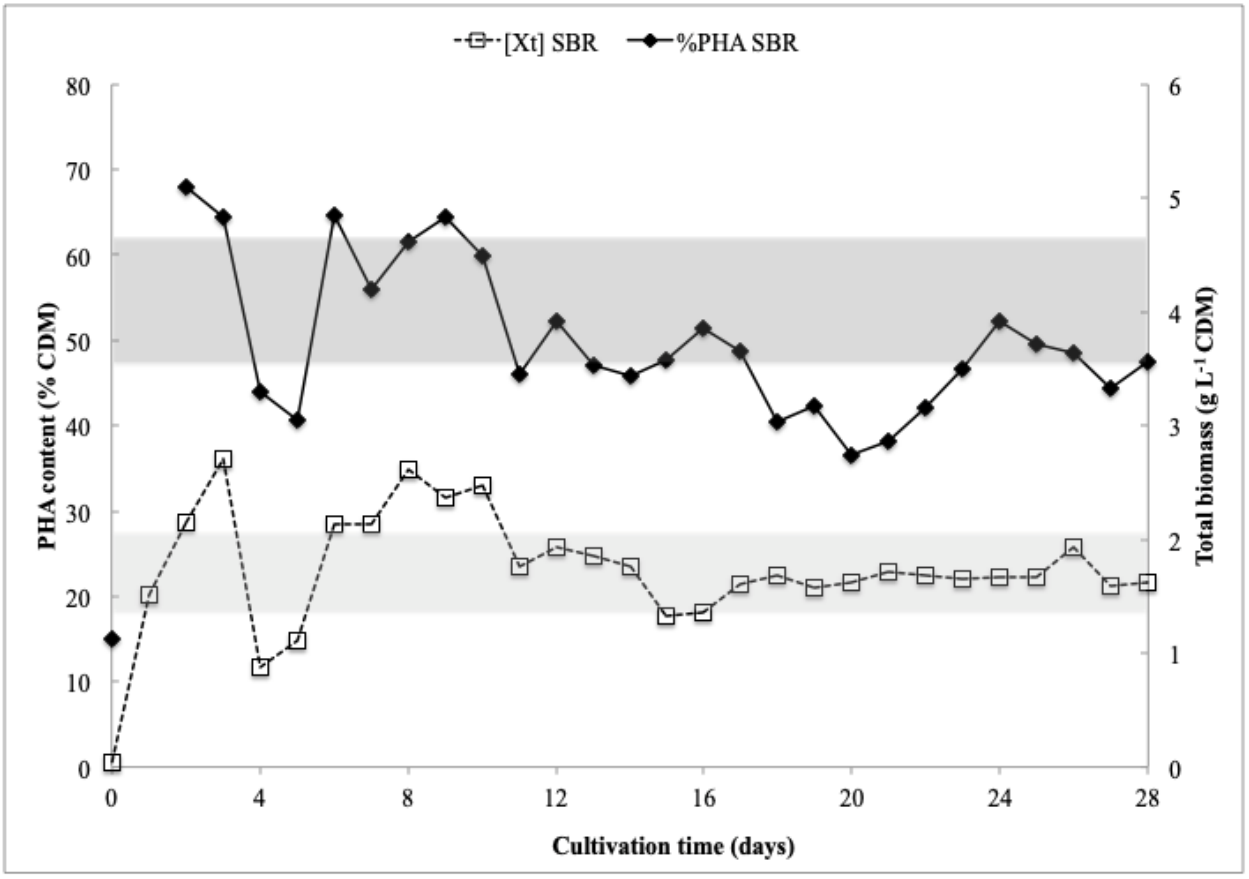

Figure 9.6. Long term performance of [X_t] and $\%_{PHA}$ during the 28-day non-sterile SBR cultivation. Values measured at the end of each 24-h cycle. The shaded bars represent the range of values obtained in multiple sterile batch experiments performed under otherwise similar conditions.

Table 9.3. Summary of mcl-PHA production in a non-sterile environment during a 28-day SBR cultivation. Tolerances indicate the standard deviations between biological replicates.

	SBR		**Sterile control**	**Significance?**
	0-10 d (0-240 h)	10-28 d (240-672 h)	24 h batch culture	Two-tailed comparison ($\alpha = 0.05$)
$[X_t]$ (g L^{-1})	2.00 ± 0.63	1.70 ± 0.20	1.73 ± 0.35	Not significantly different
$\%_{PHA}$ (% CDM)	58.2 ± 9.6	46.2 ± 4.6	54.9 ± 7.5	240-672 h, $p = 0.001$
Q_v (mg L^{-1} h^{-1})	52.0 ± 20.5	32.7 ± 5.7	51.7 ± 18.2	240-672 h, $p = 0.001$
Overall $Y_{PHA/S}$[a] (g g^{-1})	0.34 ± 0.10	0.24 ± 0.07	0.33 ± 0.05	240-672 h, $p = 0.004$
$Y_{PHA/S}$[b] (g g^{-1})	0.46 ± 0.11	0.38 ± 0.08	0.57 ± 0.13	240-672 h, $p = 0.004$

[a]Yield measured as PHA titer (g L^{-1}) per total octanoic acid consumed, including the growth phase. [b]yield measurement calculated as the PHA titer (g L^{-1}) produced per octanoic acid consumed during the PHA accumulation phase only (from approximately 5 h to 23.5 h).

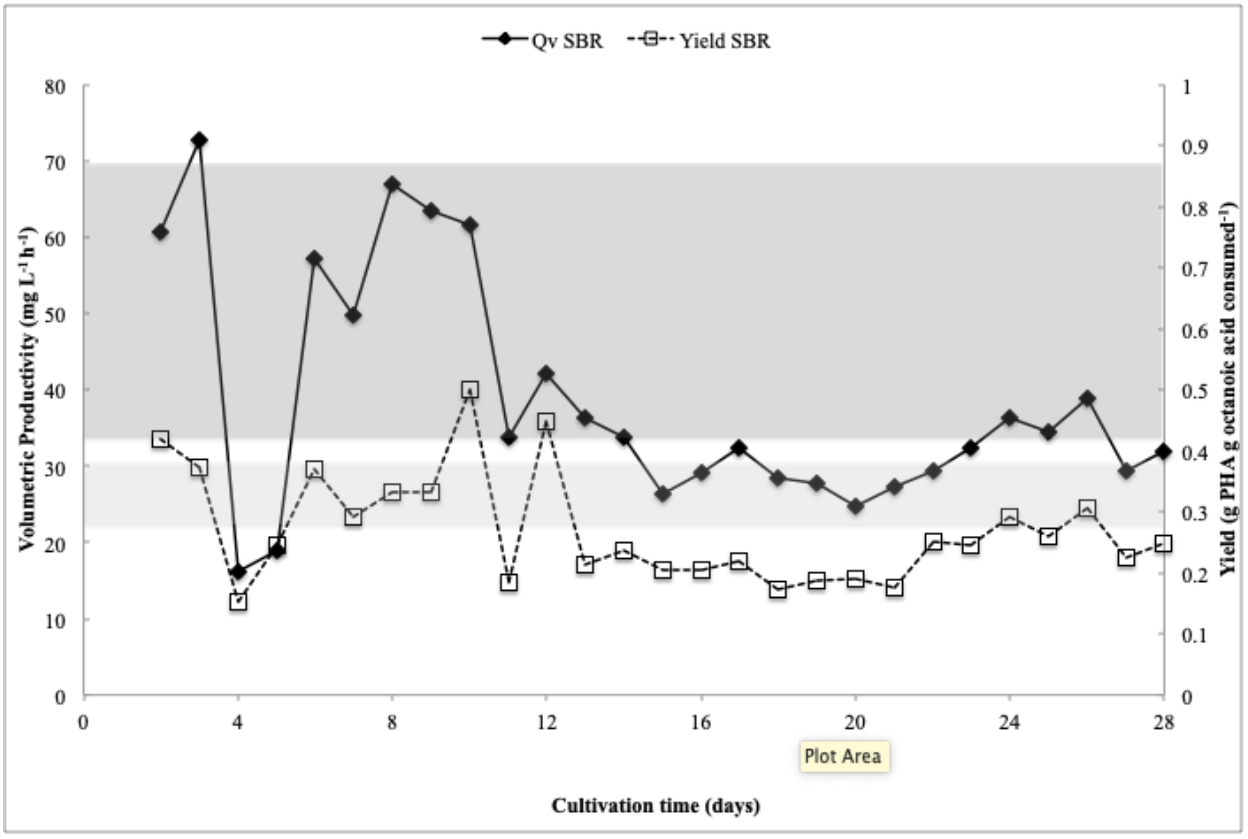

Figure 9.7. Long-term performance of Q_v and $Y_{PHA/S}$ during the 28-day non-sterile SBR cultivation. Values measured at the end of each 24-h cycle. The shaded bars represent the range of values obtained in multiple sterile batch experiments performed under otherwise similar conditions.

A crude assessment of the microbial community was done by plating. Colonies that were visually distinct and poorly produced mcl-PHA (< 5% CDM) when grown side-by-side with pure LS46 were first observed by 7 d (168 h) when plated on LB medium and by 15 d (360 h) when plated on Ramsay medium. Despite relatively high $\%_{PHA}$ of the SBR by 28 d or 672 h (47.4% CDM), more than half of the colonies that grew on the minimal medium plates were visually distinct from LS46. These colonies appeared darker when compared with LS46 (matching the progressively darker color of the culture in the SBR over time). When these putative contaminants were re-grown in a side-by-side comparison with LS46 in flask cultures (sterile conditions using 20 mM octanoic acid, pH 6.5 as per the methods above), it was found that these colonies produced little mcl-PHA. Although the growth environment on a plate is by no means representative of the microbial community structure inside the bioreactor, it does give evidence that at the end of the 28-day cultivation process, the SBR was likely behaving more as a mixed microbial community rather than a pure culture of LS46. Further investigation through sequencing and/or meta-genomic analysis is required to elucidate and understand the population dynamic.

9.6. Discussion and engineering significance

The need to maintain axenic cultures and sterile cultivation environments adds significant expense and environmental impact to PHA production with pure cultures (Fernández-Dacosta et al. 2015; Morgan-Sagastume et al. 2016). Moustogianni et al. (2015) report that lack of medium sterilization could result in a 4.6 fold reduction in utility cost in microbial oil production with oleaginous yeast. Moreover, fixed costs could also be reduced because the bioreactor could be constructed with less robust isolation from the external environment (Chen and Wan 2017). Harding et al. (2007) have estimated that to produce 1000 kg PHB (from sugar cane-based

sucrose) required 18,800 MJ of energy, and 12,700 MJ was attributable to steam requirement for sterilization. Steam generation and electricity usage reportedly had the greatest contribution to nearly every environmental impact category evaluated, except eutrophication; steam requirement made the greatest contribution to abiotic depletion, global warming potential, petrochemical oxidation, and acidification; whereas, electricity usage made the greatest contribution to ozone depletion, human toxicity, as well as ecotoxicity of marine, freshwater, and terrestrial environments (Harding et al. 2007).

As with any bioprocess, contamination is a possibility regardless of whether the cultivation takes place in a pre-sterilized environment. For 'pure culture' cultivations in non-sterile medium, the risk of contamination must be weighed against the potential benefit of savings in terms of both cost (capital investment and operating expenses) and time, as well as the final intended application. In the present study, we have shown that short-term batch (or HCD fed-batch as shown in Appendix D) cultivations can be performed under non-sterile conditions using octanoic acid as the sole carbon source with no significant detriment to $\%_{PHA}$, Q_v, and $Y_{PHA/S}$, all of which are important factors in overall process economics (Choi and Lee 1999; Akiyama et al. 2003). This is a contrast to a previous study that investigated non-sterile mcl-PHA production from biodiesel-waste glycerol in concentrations up to 30 g L^{-1} using *P. putida* LS46. In that work, negligible mcl-PHA was observed in the resulting cell mass when compared to sterile control cultures suggesting that *P. putida* was not able to compete with other organisms prevalent in a lab environment (Sharma et al. 2014). Therefore, this result appears to be somewhat specific to mcl-fatty acids amongst the range of substrates that *P. putida* LS46 can metabolize. Although such carbon sources may be infeasible for high-volume applications due to the associated cost and environmental impact (Crank et al. 2004), the demonstrated lack of

sterilization in short-batch and fed-batch cultivations could help to offset some of those costs. It may also be possible to use other lower-cost fatty-acid feedstocks to achieve a similar effect. Long-chain fatty acids (LCFAs) are available as a waste product from biodiesel production and food-processing industries (Fu et al. 2014; Cruz et al. 2016; Wallace et al. 2017). These are reportedly more inhibitory than shorter chain-length fatty acids due to increased ability to insert into the cell membrane and cause disruption of membrane fluidity and transport activities (Desbois and Smith 2010). These may also delay growth of microbial competitors and allow mcl-PHA production from *P. putida* LS46 under non-sterile conditions. LCFAs are indeed a good substrate for both growth and mcl-PHA synthesis (Chapter 5) and one of the highest Q_v values yet obtained in fed-batch culture for mcl-PHA production used oleic acid as the substrate (Lee et al. 2000b). A preliminary analysis of biodiesel-waste LCFAs in flask cultures has indicated little difference in productivity with respect to sterile conditions (data not shown).

Ultimately, the main benefit of non-sterile operation may be that it would alleviate one of the main challenges in continuous cultivation (Koller and Muhr 2014). In this study, a semi-continuous SBR was run for 28 days in order to address the question of whether prolonged operation is possible under non-sterile conditions. Despite variable operation for the first 10 d (240 h), the Q_v and $Y_{PHA/S}$ became statistically lower with respect to the expected values derived from multiple sterile batch cultivations under otherwise similar conditions after 240 h. However, overall $\%_{PHA}$ remained relatively high throughout the run (average value of 49.8 ± 5.1 % CDM throughout the 28-day process). This suggests that octanoic acid does provide a strong selective pressure for mcl-PHA accumulating organisms (again, PHB was not detected in the analysis), and that non-sterile continuous cultivation for mcl-PHA production may have potential, even if as a mixed microbial community. This selective pressure applied using octanoic acid as the

carbon source was further confirmed when flasks that had been inoculated from activated sludge produced 43.9% mcl-PHA (87.3% C8 without contamination of PHB) after a relatively short acclimation time of only 24 h (data not shown). One recent study has also exploited this selective pressure to obtain a mixed culture mostly dominant in *P. aeruginosa* and other *Pseudomonas* sp. by adding octanoic, nonanoic, and decanoic acid to activated sludge samples (Lee et al. 2011; Lee et al. 2018). This suggests mixed-culture mcl-PHA production is a possibility under certain conditions. This was briefly explored in Appendix E of this thesis.

Despite phenotypically acceptable performance in the present SBR study over the 28-day period, several questions remain as challenges for future work at the genotypic level. These are important to answer before the potential of such continuous, non-sterile operation can be truly evaluated, and include: 1) addressing if *P. putida* LS46 was in fact the organism mostly responsible for mcl-PHA production at the end of the 672 h SBR cultivation, or if it was washed out and replaced by a different mcl-PHA accumulating organism; and 2) addressing if the *P. putida* LS46 (if still the dominant organism) was genetically similar after 672 h to the *P. putida* LS46 originally added with the inoculum.

9.7. Conclusions

This work has demonstrated that mcl-PHA production from mcl-fatty acids is feasible under non-sterile conditions, in short-term batch or fed batch cultivations, and may also have potential in prolonged semi-continuous or continuous applications. Presumably this is due to the relative toxicity of fatty acids, and the affinity of *P. putida* (or other *Pseudomonas* sp.) for fatty acids. During numerous batch and fed-batch operations in non-sterile environments, no detrimental effect on overall productivity or composition of the polymer was observed, compared to sterile controls. However, when semi-continuous production was evaluated in an

SBR run over a 28-day period, mcl-PHA productivity and yield began to drop slightly after 10 days, but overall mcl-PHA content of the biomass (46.2 ± 5.1% CDM) and productivity remained relatively high during that time. Furthermore, the monomer composition of the polymer was 87.0 ± 2.7% C8 and solely mcl-PHAs were detected. The main conclusions are that fatty acid carbon substrates appear to apply a high selective pressure for mcl-PHA producing organisms, such that significant mcl-PHA storage capacity can be maintained in a non-sterile environment. This may suggest an opportunity for mcl-PHA production in fully continuous-feed bioreactors under open-atmosphere conditions. Although this may not be realistic in an industrial setting (depending on the final application), at the very least it suggests that mcl-PHA production from fatty acids may be a robust bioprocess for application in environments that are traditionally difficult to maintain sterile (i.e. continuous bioreactors). This finding lends considerable process flexibility to mcl-PHA production from fatty acids.

9.8. Acknowledgements

This work was funded by Genome Canada, through the Genome Applications and Partnership Program (GAPP), and the Natural Sciences and Engineering Research Council (NSERC) of Canada through a Canada Graduate Scholarship, and the University of Manitoba through the Graduate Fellowship and Sir Gordon Wu Scholarship. Thanks to Alain Lagasse for his time and efforts spent running the semi-continuous SBR preparing samples for analysis. We are also thankful for the help of research assistants Carolina Gutiérrez Cisneros, Taylor Livingston, Zimo Jin, and Jacob Harvey.

Chapter 10: Discussion, engineering significance, and future work

10.1 Overview and discussion of findings

Despite the fact that microbial PHAs have been studied for over 40 years, they remain a promising alternative to petroleum-derived materials that are both renewable and completely biodegradable. A number of issues continue to hinder their widespread use. These include: 1) the cost of production, including both cultivation and downstream processing costs; 2) inconsistent material properties; and 3) lack of demonstrated high-value applications (Wang et al. 2014). This thesis has focused primarily on addressing the former; that is, understanding and anticipating engineering challenges involved with bioreactor-scale mcl-PHA production processes for subsequent process design (scale-up, high cell density cultivations, continuous setups). This was done with the motivation of improving the cultivation process while reducing production costs at the bioreactor level.

The literature review (Chapter 2, section 2.7) indicated that most studies have targeted high PHA productivities using HCD fed-batch cultivations and that the productivities achieved in lab-scale processes are much higher than those reported in the available literature on pilot or industrial-scale PHA production. A common theme in both HCD fed-batch processes and large-scale bioreactors is inadequate gas-to-liquid transfer of oxygen. Section 2.9 of the literature review indicated that very little was known about how DO gradients influence mcl-PHA biosynthesis. Investigating the role of low-DO microenvironments was therefore a necessary pursuit in anticipation of complications with HCD cultivations and/or large-scale operations in a bioreactor environment (see Figure 2.6). The main contributions of this chapter include: 1) a general literature review of how microaerophilic environments modulate PHA metabolism,

which was previously missing from the literature; and 2) a current summary of literature regarding various bioreactor operating strategies and how they affect PHA productivity.

10.1.1. Microaerophilic mcl-PHA synthesis in P. putida LS46 (Chapters 4-6)

In Chapter 4, the hypothesis that oxygen-limited environments cause fatty acids to be stored as mcl-PHA was explored. It was found that octanoic acid is effectively incorporated into mcl-PHA when the DO was reduced to 0.2 mg L^{-1} or less. Further reduction in the OTR resulted in further improvement to PHA content, synthesis rate, and yield. Interestingly, at some of the lowest OTRs tested, the $\%_{PHA}$ obtained in the bioreactor matched that of shake-flask cultures using the same C/N ratio. This indicated that baffled flasks are O_2-limited at cell densities as low as 0.5 g L^{-1} CDM, and was likely the driving force for mcl-PHA synthesis from fatty acids in previous flask studies (Sharma et al. 2012; Fu et al. 2014). This can lead to inaccurate presumptions (i.e. mcl-PHA synthesis from fatty acids being growth-associated) and underscores the importance of measuring process parameters like DO, oxygen uptake rate, and the oxygen half saturation constant, even in flask cultures if possible (Zimmermann et al. 2006).

Previous studies have shown that the reduction of acetoacetyl-CoA is known to act as an electron sink and allow synthesis of PHB from glucose in low DO environments (Senior and Dawes 1971; Senior et al. 1972). This reasoning does not apply to mcl-PHA from fatty acids because incorporation of β-oxidation intermediates is an oxidative process. In this thesis, the assertion was made for the first time that storage of β-oxidation intermediates as mcl-PHA is a way to store electrons when the terminal electron acceptor, O_2, is not in sufficient supply to completely oxidize the carbon substrate to meet anabolic demand. Although similar studies have been undertaken with organisms that produce PHB (Faccin et al. 2013), this work represents the first known in-depth investigation of O_2-limitation and its effects on carbon flux and mcl-PHA

synthesis from fatty acids. The findings represent a substantial contribution that not only improves fundamental understanding of how microaerophilic environments affect carbon flux through central metabolic pathways, but also for anticipating and understanding potential scale-up challenges.

In Chapter 5, the findings in Chapter 4 were built upon by exploring the role that O_2-limitation plays when lower cost canola-derived LCFAs (primarily oleic acid) were used as the carbon source. Since each carbon atom in oleic acid is accompanied by a higher degree of reduction, it seemed logical that there may be more of a bottleneck for growth and/or mcl-PHA synthesis in a microaerophilic environment. This is owing to the need to oxidize a C18 fatty acid to C8 or C10 using the β-oxidation cycle for polymerization by the PHA synthase. Yet, during experiments conducted to produce mcl-PHA from waste LCFAs, we hypothesized that this was in fact, not the case. This ended up being supported by the experimental observations. Although mcl-PHA synthesis was still induced from LCFAs by O_2-limitation (although not to the extent observed in Chapter 4 with octanoic acid), carbon flux toward growth was higher compared to octanoic acid under similar conditions. Previous studies have shown that maintaining residual growth during PHA storage has important consequences on overall PHA yield (Grousseau et al. 2013; Andin et al. 2017). These results suggest that co-feeding LCFAs might be a way to achieve this when oxygen is limiting. When the two substrates were co-fed, the highest PHA titer and overall productivity were achieved. While the growth profile appeared closer to that observed when LCFAs were used as the sole carbon substrate, the yield of PHA from octanoic acid was unaffected and the monomer composition suggested the majority of the mcl-PHA was synthesized from octanoic acid.

LCFAs have been previously explored for mcl-PHA production in batch cultures (Fernández et al. 2005; Fu et al. 2014; Fontaine et al. 2017), HCD fed-batch cultivations (Lee et al. 2000b; Kellerhals et al. 2000) and even continuous systems (Huijberts and Eggink 1996). However, this study has shown for the first time that feeding LCFAs causes higher residual growth under microaerophilic conditions compared to octanoic acid. This chapter made contribution to the literature by: 1) examining carbon fluxes in microaerophilic environments between LCFAs and mcl-fatty acids for the purpose of mcl-PHA production; 2) suggesting simultaneous uptake of LCFAs and octanoic acid, where octanoic acid appears to be used for PHA synthesis (on the basis of monomer composition) while LCFAs presumably satisfy the anabolic demand or maintenance requirement; and 3) pointing toward how a co-feed strategy of LCFAs and octanoic acid could be designed to achieve a high-productivity cultivation strategy, particularly in an oxygen-limited environment.

Whereas the previous chapters examined oxidative mcl-PHA biosynthesis, Chapter 6 explores the effect of microaerophilic environments when mcl-PHA is synthesized reductively from acetyl-CoA via the *de novo* biosynthetic pathway. Despite the fact that the *de novo* pathway has reductive steps similar to PHB synthesis, no significant amount of mcl-PHA was synthesized under O_2-limiting conditions from glucose, acetic acid, or valeric acid. Furthermore, the yield was poor and most of the carbon was lost as CO_2, while a lesser portion was spent on residual growth. When hexanoic acid was used as the substrate, some mcl-PHA storage was observed under O_2-limiting conditions, but not to the extent observed in Chapters 4 and 5. Interestingly, when valeric or hexanoic acids were used as the carbon substrate (which appear to utilize both β-oxidation and *de novo* pathways for PHA synthesis on the basis of monomer compositions), O_2-limited conditions increased the proportion of monomers incorporated by β-oxidation relative to

monomers typically indicative of *de novo* synthesis. Previous works have reported little effect of O_2-limitation on mcl-PHA synthesis from carbohydrates (Haywood et al. 1990; Diniz et al. 2004; Silva et al. 2014). This study not only confirmed those results but also provided complete data on bioreactor oxygen transfer rates, yield analysis, and monomer compositions, while also investigating a variety of substrates (with different redox states) that produce mcl-PHA via the *de novo* pathway to varying extents. This work completed our understanding of how the carbon source, mcl-PHA synthesis pathways, and carbon flux are influenced when environmental conditions turn microaerophilic.

The results were all somewhat counter-intuitive on the basis of what is known about synthesis of PHB, what might be predicted from the redox state of the carbon substrate, or whether the pathway required is oxidative (i.e. producing reduced electron carriers) or reductive (i.e. producing oxidized electron carriers). This is further confounded by the well-known fact that *P. putida* is known for high net NAD(P)H generation capacity, which should favor *de novo* PHA synthesis (Ebert et al. 2011). It may be that *P. putida* LS46 (and likely other strains of *P. putida*) has evolved intricate and complex regulatory networks, which may or may not involve high PHA storage capacity as the phenotype, in order to remain competitive in natural microaerophilic environments. After all, these environments are extremely pervasive on the earth's surface despite the atmosphere containing 21% O_2 (Stolper et al. 2010), mostly owing to the low solubility of O_2 in aqueous medium.

Further study is needed to clarify the observations from a molecular point of view. From a thermodynamic perspective, it appears that under microaerophilic conditions, the objective of *P. putida* LS46 is to maximize storage of energy-dense molecules (fatty acids) when available, while minimizing the amount of energetically expensive molecules that must be synthesized

from acetyl-CoA when supply of the terminal electron acceptor (O_2) becomes limiting. Although this thesis may have contributed some understanding of what can be expected on a phenotypic level, further proteomic and/or metabolomics studies may be a valuable pursuit to help elucidate the molecular mechanisms.

Despite the low yields and productivities reported in Chapter 6 the contributions of this are several-fold: 1) this is the first known in-depth study of *de novo* mcl-PHA under O_2-limitation and completes understanding of how mcl-PHA synthesis responds to low DO when the pathway is oxidative vs. reductive (i.e. for a variety of carbon substrates); 2) it shows for the first time how monomer compositions of mcl-PHA (and perhaps thermal and/or physical characteristics of the polymer) can be impacted by the bioreactor oxygen transfer rate; and 3) the study suggests that, due to poor yield, carbon susbtrates requiring the *de novo* pathways may not be a good candidates on which to base full-scale production of mcl-PHAs using *P. putida* LS46.

10.1.2. Process optimization under oxygen-limited conditions (Chapters 7-9)

The remaining chapters of this thesis focus on investigating process configurations for improved bioreactor productivities. In Chapter 7, a HCD fed-batch cultivation platform was developed by maximizing the bioreactor OTR for the growth phase before letting DO fall below detectable limits to induce PHA accumulation from fatty acids. Feeding of a toxic substrate like octanoic acid proved tricky (Chapter 5), but it was found that carbon limitation was indicated by sharp rises in the DO signal and also a rapid drop in CO_2 content in the reactor off-gas. These signals were then used to rapidly optimize feeding for a HCD fed-batch process. This resulted in a final [X_t] of 28.9 ± 4.0 g L^{-1} and an overall Q_v of 0.66 ± 0.14 g L^{-1} h^{-1}. Multiple studies have demonstrated much higher mcl-PHA productivities (Lee et al. 2000b; Maclean et al. 2008; Gao et al. 2016). Those studies have focused on advancing productivity while maintaining O_2 in

excess (often through aeration enriched with purified O_2, which can be costly). The contribution of this chapter, in contrast, was to demonstrate potential viability of a HCD fed-batch process coupled to an O_2-limited accumulation phase. When the literature is surveyed (Table 2.3), little information is available on this type of process. Kellerhals et al. (1999a) reported an O_2-limited HCD fed batch cultivation using octane, but achieved poor PHA content and overall productivity. Kim et al. (1997) used simultaneous N and O_2 limitation on a co-feed process using glucose and octanoate with good productivity, but few details were given on the effects of O_2-limitation.

As part of the work described above, significant changes to the rheological properties of the culture medium were noticed over time, and these were further investigated and quantified in Chapter 8. The main hypothesis of this work was that these rheological changes result in significant reduction in the oxygen mass transfer coefficient of the medium. It was found that a nine-fold increase in apparent viscosity occurred during the course of a fed-batch cultivation and this reduced the k_La of the medium by as much as 50%. Interestingly, a large part of this effect seemed to have more to do with the medium the cells were suspended in, rather than the presence of the cells themselves. Although in Chapters 4 and 5, O_2-limitation was shown to be beneficial for mcl-PHA synthesis, the onset of microaerophilic conditions was likely triggered sooner because of the effect of viscosity on oxygen transfer, thus reducing $[X_r]$ and overall productivity.

Multiple works have investigated culture rheology in other applications ranging from wastewater treatment to production of food and pharmaceutical-grade commodities (Richard and Margaritis 2003; Freitas et al. 2009; Baroutian et al. 2013; Maalej et al. 2016). However, Chapter 8 has made a contribution in being the first known attempt to investigate and quantify rheological properties of PHA cultivation medium using pure cultures, for mcl- or scl-PHA

production. Further investigation is required, but the effect on the oxygen transfer of the medium does indeed add relevance to having an O_2-limited PHA accumulation strategy, such as that described in Chapter 7.

Chapter 9 moves away from investigation of HCD production of mcl-PHAs and towards maintaining a mcl-PHA producing culture over more prolonged operation. Although continuous-based production should in theory be able to achieve the highest productivity of any cultivation platform, its application appears be limited by technical challenges (Koller and Muhr 2014; Koller and Braunegg 2015). One of those challenges is the increased risk of contamination. Since fatty acids exert considerable toxicity to cells (Desbois and Smith 2010; Jarboe et al. 2013; Royce et al. 2013) and are also a good substrate for mcl-PHA synthesis, it was hypothesized that a sufficient concentration of fatty acids in a minimal medium could maintain a selection pressure for *P. putida* (or other mcl-PHA producers) and allow mcl-PHA production under non-sterile conditions. In terms of $\%_{PHA}$ and Q_v, this was found to be a highly effective strategy in short-term batch and fed-batch cultivations. In fact, little statistical difference was found between the non-sterile conditions and sterile control cultures. The efficacy of such a non-sterile was evaluated over prolonged operation using a long-term SBR study. Despite the clear presence of contaminants, the $\%_{PHA}$ (although somewhat variable) remained relatively high throughout 28 days of operation. The $\%_{PHA}$ of the final sample on day 28 was 48% CDM, and throughout the run the $\%_{PHA}$ was never less than 36% CDM. The PHA composition was consistently 88-90% C8 and never showed any detectable contamination with PHB. A few similar studies have investigated PHB production under non-sterile conditions using halophilic microorganisms (Lillo and Rodriguez-Valera 1990; Tan et al. 2011; Yue et al. 2014). This work represents the first time that a similar approach was applied to mcl-PHA production using the fatty acid carbon source to

maintain the selection pressure. Furthermore, after nearly 28 days (672 h) of operation, this study represents one of the longer-running cultivation processes for mcl-PHA production. Although chemostat studies do not often explicitly report duration of the cultivation, only one study was found that was run for longer (an octane-fed chemostat culture of *P. oleovorans* that was run for 760 h) (Preusting et al. 1993a). However, a promising and relatively recent development is mcl-PHA production using a mixed culture that was enriched by feeding mcl-fatty acids (Lee et al. 2011; Lee et al. 2018). This approach was applied in Appendix E of this thesis, and the results were indeed intriguing.

This work suggests that non-sterile mcl-PHA production could be viable given the right selective pressure. Further work is needed to demonstrate how reliable this is and also elucidate the population dynamic during longer durations of operation under non-sterile conditions. It also suggests that mcl-PHA production from fatty acids using *P. putida* is a relatively robust process against contamination (at least contamination detrimental enough to significantly reduce productivity). This should give considerable flexibility to bioreactor or process configurations, even if the growth environment is not left intentionally non-sterile.

10.2 Engineering Significance

This body of work represents a guideline for consideration of certain engineering challenges likely to be encountered during scale-up of mcl-PHA production. This work could have several implications on process engineering and design and would enable a bioprocess engineer to design for scalability from the early stages of process development. If a company was interested in large-scale production of mcl-PHAs, helpful information could be gleaned from this thesis. From the results in the first half of this thesis (Chapters 4-6), this includes: 1) management strategies for DO and/or bioreactor oxygen transfer rate; 2) for which carbon

substrates O_2-limitation is beneficial; and 3) co-feeding certain substrates to improve growth, PHA yield, or for adjusting monomer compositions under microaerophilic conditions. The results from these chapters have implications reaching further back in bioprocess development than the engineering phase. For instance, consideration of how a strain performs when subject to microaerophilic conditions should be a target in selection of a robust industrial production strain. Often during this phase of bioprocess development, the 'optimization' is done in flasks and the effect(s) of DO and/or oxygen uptake rate are not considered until a later stage of process development (Zimmermann et al. 2006). This exact scenario played out during the course of this work, in which the results of Chapter 4 contradicted some previous assumptions made from observations that were based on flask cultures.

Whereas the first half of this thesis sought fundamental understanding how *P. putida* LS46 responds to its environment, the latter half of the thesis investigated other aspects of scale-up concerning process design. These include: 1) operating regime and some of the advantages and challenges of fed-batch or semi-continuous operation; 2) fluid viscosity, rheology of the culture, and consequent effects on oxygen transfer in an HCD, high-shear environment; and 3) resilience of the process against contamination by maintaining a selection pressure (concentration of toxic free fatty acids) for mcl-PHA producing organisms. The latter apparently allows the possibility of non-sterile mcl-PHA production and gives considerable flexibility to process configurations for future studies.

Cost is a significant factor detracting from widespread commercial production of PHAs (Wang et al. 2014; Levett et al. 2016; Dietrich et al. 2017), and is also a crucial engineering constraint. The underlying motivation for the above scientific outcomes essentially had to do with finding ways to make mcl-PHA production more cost effective. Specifically, this work has

focused on two ways to reduce both cost and environmental impact associated with bioreactor operations. The first pertains to the need for highly aerobic conditions, which requires high-intensity aeration and mixing and becomes less feasible in larger-scale bioreactors due to power consumption and practical limits for mixing equipment (Akiyama et al. 2003; Koller et al. 2013). Depending on the carbon substrate, it was found in this thesis that an O_2-limited, low-aeration strategy could be employed during the PHA accumulation phase because *P. putida* accumulates mcl-PHAs from medium and long-chain fatty acids effectively under those conditions. Secondly, the requirement for a sterile production environment can add significant fixed costs, operating costs (energy consumption), and process complexity (Chen and Wan 2017). Chapter 9 in this work has shown that this can be at least minimized, if conditions are created that apply a selective pressure favoring *P. putida* LS46 or other mcl-PHA producing organisms. Implementation of this type of process would, however, be highly dependent on the final application of the product.

10.3 Future Research

Future work from this thesis could go in a number of directions. From Chapters 4-6, a proteomic and/or metabolomic study comparing microaerophilic metabolism of glucose vs. octanoic acid vs. long-chain fatty acids could be of value for elucidating some of the molecular/regulatory mechanisms of *P. putida* under microaerophilic conditions. This could perhaps also suggest targets for genetic engineering strategies. Furthermore, a robust analysis of how the conditions tested in thest chapters might affect important product characteristics, including M, T_g, T_m, crystallinity, and tensile properties (for example) would represent a novel and substantial contribution to the literature. Secondly, In Chapter 2, it was indicated that fully continuous bioreactor systems in PHA production has been under-developed in the last eight

years. The promising results from co-feeding of LCFAs and octanoic acid explored in Chapter 5 could be adapted to a fully continuous system to sustain high mcl-PHA productivity over time, with help from some of the feeding strategies high-cell density insights obtained in Chapter 7.

Future directions could also pick up on Chapter 9. In that context, the first task would be to demonstrate long-term reliability of the SBR process under non-sterile conditions. This could continue to investigate non-sterile production from an axenic *P. putida* inoculum, but we feel that a more viable option would be to start with a mixed culture enriched for mcl-PHA producers. Subsequently, (if reliable) the process could be improved to be more commercially attractive by increasing productivity, perhaps by running sequencing fed-batch bioreactors or even in a full continuous system.

Finally, this thesis has focused on what happens to mcl-PHA production when mass transfer limitations cause conditions to inevitably turn microaerophilic. However, investigation of viable, cost-effective ways to actually improve gas-to-liquid mass transfer would significantly improve productivities and be a considerable advancement for PHA production in general. As discussed in Section 2.8, microfluidic bubblers have facilitated nearly ideal mass transfer, and are a very promising development. However, little if any information is available on how this type of device would perform in a high cell density process for PHA production. Application of this (or similar) technology would indeed be a worthy engineering challenge for future research.

References

Abdel-Rahman MA, Tashiro Y, Zendo T, Sonomoto K (2013) Improved lactic acid productivity by an open repeated batch fermentation system using *Enterococcus mundtii* QU 25. RSC Adv 3:8437. doi: 10.1039/c3ra00078h

Ackermann J-U, Babel W (1998) Approaches to increase the economy of the PHB production. Polym Degrad Stab 59:183–186. doi: 10.1016/S0141-3910(97)00154-7

Aeschelmann F, Carus M (2015) Biobased Building Blocks and Polymers in the World: Capacities, Production, and Applications–Status Quo and Trends Towards 2020. Ind Biotechnol 11:154–159. doi: 10.1089/ind.2015.28999.fae

Ahn WS, Park SJ, Lee SY (2001) Production of poly(3-hydroxybutyrate) from whey by cell recycle fed-batch culture of recombinant *Escherichia coli*. Biotechnol Lett 23:235–240.

Akaraonye E, Keshavarz T, Roy I (2010) Production of polyhydroxyalkanoates: the future green materials of choice. J Chem Technol Biotechnol 85:732–743. doi: 10.1002/jctb.2392

Akiyama M, Tsuge T, Doi Y (2003) Environmental life cycle comparison of polyhydroxyalkanoates produced from renewable carbon resources by bacterial fermentation. Polym Degrad Stab 80:183–194. doi: 10.1016/S0141-3910(02)00400-7

Alagappan G, Cowan RM (2004) Effect of temperature and dissolved oxygen on the growth kinetics of *Pseudomonas putida* F1 growing on benzene and toluene. Chemosphere 54:1255–1265. doi: 10.1016/j.chemosphere.2003.09.013

Allesen-Holm M, Barken KB, Yang L, Klausen M, Webb JS, Kjelleberg S, Molin S, Givskov M, Tolker-Nielsen T (2006) A characterization of DNA release in *Pseudomonas aeruginosa* cultures and biofilms. Mol Microbiol 59:1114–1128. doi: 10.1111/j.1365-2958.2005.05008.x

Amulya K, Reddy MV, Rohit MV, Mohan SV (2016) Wastewater as renewable feedstock for bioplastics production: understanding the role of reactor microenvironment and system pH. J Clean Prod 112:4618–4627. doi: 10.1016/j.jclepro.2015.08.009

Anderson AJ, Dawes EA (1990) Occurrence, metabolism, metabolic role, and industrial uses of bacterial polyhydroxyalkanoates. Microbiol Mol Biol Rev MMBR 54:450–472.

Andin N, Longieras A, Veronese T, Marcato F, Molina-Jouve C, Uribelarrea J-L (2017) Improving carbon and energy distribution by coupling growth and medium chain length polyhydroxyalkanoate production from fatty acids by *Pseudomonas putida* KT2440. Biotechnol Bioprocess Eng 22:308–318. doi: 10.1007/s12257-016-0449-1

Anjum A, Zuber M, Zia KM, Noreen A, Anjum MN, Tabasum S (2016) Microbial production of polyhydroxyalkanoates (PHAs) and its copolymers: A review of recent advancements. Int J Biol Macromol 89:161–174. doi: 10.1016/j.ijbiomac.2016.04.069

Arjunwadkar SJ, Sarvanan K, Kulkarni PR, Pandit AB (1998) Gas-liquid mass transfer in dual impeller bioreactor. Biochem Eng J 1:99–106. doi: 10.1016/S1385-8947(97)00083-1

Asciano G, Castro B, Galindo E (2004) Meaurement of power consumption in stirred vessels - a review. Chem Eng Res Des 82:1282–1290.

Ashby RD, Foglia TA, Solaiman DKY, Liu C-K, Nuñez A, Eggink G (2000) Viscoelastic properties of linseed oil-based medium chain length poly(hydroxyalkanoate) films: effects of epoxidation and curing. Int J Biol Macromol 27:355–361. doi: 10.1016/S0141-8130(00)00140-9

Atlić A, Koller M, Scherzer D, Kutschera C, Grillo-Fernandes E, Horvat P, Chiellini E, Braunegg G (2011) Continuous production of poly([R]-3-hydroxybutyrate) by *Cupriavidus necator* in a multistage bioreactor cascade. Appl Microbiol Biotechnol 91:295–304. doi: 10.1007/s00253-011-3260-0

Ayub ND, Tribelli PM, López NI (2009) Polyhydroxyalkanoates are essential for maintenance of redox state in the Antarctic bacterium *Pseudomonas sp.* 14-3 during low temperature adaptation. Extremophiles 13:59–66. doi: 10.1007/s00792-008-0197-z

Badino AC, Facciotti MCR, Schmidell W (2001) Volumetric oxygen transfer coefficients (k_La) in batch cultivations involving non-Newtonian broths. Biochem Eng J 8:111–119. doi: 10.1016/S1369-703X(01)00092-4

Bae W, Rittmann BE (1996) Responses of intracellular cofactors to single and dual substrate limitations. Biotechnol Bioeng 49:690–699. doi: 10.1002/(SICI)1097-0290(19960320)49:6<690::AID-BIT11>3.0.CO;2-A

Baker JJ, Crivellari F, Gagnon Z, Betenbaugh MJ (2016) Microfluidic bubbler facilitates near complete mass transfer for sustainable multiphase and microbial processing: Microfluidic Bubbler Facilitates Mass Transfer. Biotechnol Bioeng 113:1924–1933. doi: 10.1002/bit.25972

Barnes DKA, Galgani F, Thompson RC, Barlaz M (2009) Accumulation and fragmentation of plastic debris in global environments. Philos Trans R Soc B Biol Sci 364:1985–1998. doi: 10.1098/rstb.2008.0205

Baroutian S, Eshtiaghi N, Gapes DJ (2013) Rheology of a primary and secondary sewage sludge mixture: Dependency on temperature and solid concentration. Bioresour Technol 140:227–233. doi: 10.1016/j.biortech.2013.04.114

Bejgarn S, MacLeod M, Bogdal C, Breitholtz M (2015) Toxicity of leachate from weathering plastics: An exploratory screening study with Nitocra spinipes. Chemosphere 132:114–119. doi: 10.1016/j.chemosphere.2015.03.010

Bekker M, de Vries S, Ter Beek A, Hellingwerf KJ, de Mattos MJT (2009) Respiration of *Escherichia coli* can be fully uncoupled via the nonelectrogenic terminal cytochrome bd-II oxidase. J Bacteriol 191:5510–5517. doi: 10.1128/JB.00562-09

Berezina N (2013) Novel approach for productivity enhancement of polyhydroxyalkanoates (PHA) production by *Cupriavidus necator* DSM 545. New Biotechnol 30:192–195. doi: 10.1016/j.nbt.2012.05.002

Bergmann M, Gutow L, Klages M, Alfred-Wegener-Institut, Göteborgs Universitet (eds) (2015) Marine anthropogenic litter. Springer, Cham Heidelberg New York Dordrecht London

Besseling E, Wegner A, Foekema EM, van den Heuvel-Greve MJ, Koelmans AA (2013) Effects of Microplastic on Fitness and PCB Bioaccumulation by the Lugworm *Arenicola marina* (L.). Environ Sci Technol 47:593–600. doi: 10.1021/es302763x

Beyenal H, Chen SN, Lewandowski Z (2003) The double substrate growth kinetics of *Pseudomonas aeruginosa*. Enzyme Microb Technol 32:92–98. doi: 10.1016/S0141-0229(02)00246-6

Blunt W (2013) On-line monitoring of microbial fermentation end-products synthesized by *Clostridium thermocellum* using Titrimetric Off-Gas Analysis (TOGA). M.Sc., University of Manitoba.

Blunt W, Hossain MdE, Gapes DJ, Sparling R, Levin DavidB, Cicek N (2014) Real-Time Monitoring of Microbial Fermentation End-Products in Biofuel Production with Titrimetric Off-Gas Analysis (TOGA). Biol Eng Trans 6:203–219. doi: 10.13031/bet.6.10496

Borisov VB, Gennis RB, Hemp J, Verkhovsky MI (2011) The cytochrome bd respiratory oxygen reductases. Biochim Biophys Acta BBA - Bioenerg 1807:1398–1413. doi: 10.1016/j.bbabio.2011.06.016

Borrero-de Acuña J, Bielecka A, Häussler S, Schobert M, Jahn M, Wittmann C, Jahn D, Poblete-Castro I (2014) Production of medium chain length polyhydroxyalkanoate in metabolic flux optimized *Pseudomonas putida*. Microb Cell Factories 13:88. doi: 10.1186/1475-2859-13-88

Bourque D, Pomerleau Y, Groleau D (1995) High-cell-density production of poly-β-hydroxybutyrate (PHB) from methanol by *Methylobacterium extorquens*: production of high-molecular-mass PHB. Appl Microbiol Biotechnol 44:367–376. doi: 10.1007/BF00169931

Bradford MM (1976) A rapid and sensitive method for the quantitation of microgram quantities of protein utilizing the principle of protein-dye binding. Anal Biochem 72:248–254. doi: 10.1016/0003-2697(76)90527-3

Brandl H, Gross RA, Lenz RW, Fuller RC (1988) *Pseudomonas oleovorans* as a source of poly(β-hydroxyalkanoates) for potential applications as biodegradable polyesters. Appl Environ Microbiol 54:1977–1982.

Braunegg G, Bona R, Koller M (2004) Sustainable Polymer Production. Polym-Plast Technol Eng 43:1779–1793. doi: 10.1081/PPT-200040130

Braunegg G, Lefebvre G, Genser KF (1998) Polyhydroxyalkanoates, biopolyesters from renewable resources: Physiological and engineering aspects. J Biotechnol 65:127–161. doi: 10.1016/S0168-1656(98)00126-6

Braunegg G, Lefebvre G, Renner G, Zeiser A, Haage G, Loidl-Lanthaler K (1995) Kinetics as a tool for polyhydroxyalkanoate production optimization. Can J Microbiol 41:239–248. doi: 10.1139/m95-192

Buchholz H, Buchholz R, Niebeschütz H, Schügerl K (1978) Absorption of oxygen in highly viscous newtonian and non-Newtonian fermentation model media in bubble column bioreactors. Eur J Appl Microbiol Biotechnol 6:115–126.

Budde CF, Mahan AE, Lu J, Rha C, Sinskey AJ (2010) Roles of Multiple Acetoacetyl Coenzyme A Reductases in Polyhydroxybutyrate Biosynthesis in *Ralstonia eutropha* H16. J Bacteriol 192:5319–5328. doi: 10.1128/JB.00207-10

Bylund F, Collet E, Enfors S-O, Larsson G (1998) Substrate gradient formation in the large-scale bioreactor lowers cell yield and increases by-product formation. Bioprocess Eng 18:171. doi: 10.1007/s004490050427

Byrom D (1992) Production of poly-β-hydroxybutyrate: poly-β-hydroxyvalerate copolymers. FEMS Microbiol Lett 103:247–250. doi: 10.1016/0378-1097(92)90316-G

Carey J (2017) News Feature: On the brink of a recycling revolution? Proc Natl Acad Sci 114:612–616. doi: 10.1073/pnas.1620655114

Castillo T, Heinzle E, Peifer S, Schneider K, Peña M CF (2013) Oxygen supply strongly influences metabolic fluxes, the production of poly(3-hydroxybutyrate) and alginate, and the degree of acetylation of alginate in *Azotobacter vinelandii*. Process Biochem 48:995–1003. doi: 10.1016/j.procbio.2013.04.014

Cavalheiro JMBT, de Almeida MCMD, Grandfils C, da Fonseca MMR (2009) Poly(3-hydroxybutyrate) production by *Cupriavidus necator* using waste glycerol. Process Biochem 44:509–515. doi: 10.1016/j.procbio.2009.01.008

Cavalheiro JMBT, Raposo RS, de Almeida MCMD, Teresa Cesário M, Sevrin C, Grandfils C, da Fonseca MMR (2012) Effect of cultivation parameters on the production of poly(3-hydroxybutyrate-co-4-hydroxybutyrate) and poly(3-hydroxybutyrate-4-hydroxybutyrate-3-hydroxyvalerate) by *Cupriavidus necator* using waste glycerol. Bioresour Technol 111:391–397. doi: 10.1016/j.biortech.2012.01.176

Celik GY, Aslim B, Beyatli Y (2008) Characterization and production of the exopolysaccharide (EPS) from *Pseudomonas aeruginosa* G1 and *Pseudomonas putida* G12 strains. Carbohydr Polym 73:178–182. doi: 10.1016/j.carbpol.2007.11.021

Cerrone F, Choudhari SK, Davis R, Cysneiros D, O'Flaherty V, Duane G, Casey E, Guzik MW, Kenny ST, Babu RP, O'Connor K (2014a) Medium chain length polyhydroxyalkanoate (mcl-PHA) production from volatile fatty acids derived from the anaerobic digestion of grass. Appl Microbiol Biotechnol 98:611–620. doi: 10.1007/s00253-013-5323-x

Cerrone F, Duane G, Casey E, Davis R, Belton I, Kenny ST, Guzik MW, Woods T, Babu RP, O'Connor K (2014b) Fed-batch strategies using butyrate for high cell density cultivation of *Pseudomonas putida* and its use as a biocatalyst. Appl Microbiol Biotechnol 98:9217–9228. doi: 10.1007/s00253-014-5989-8

Cesário MT, Raposo RS, de Almeida MCMD, van Keulen F, Ferreira BS, da Fonseca MMR (2014) Enhanced bioproduction of poly-3-hydroxybutyrate from wheat straw lignocellulosic hydrolysates. New Biotechnol 31:104–113. doi: 10.1016/j.nbt.2013.10.004

Chang W-S, van de Mortel M, Nielsen L, Nino de Guzman G, Li X, Halverson LJ (2007) Alginate production by *Pseudomonas putida* creates a hydrated microenvironment and contributes to biofilm architecture and stress tolerance under water-limiting conditions. J Bacteriol 189:8290–8299. doi: 10.1128/JB.00727-07

Chanprateep S (2010) Current trends in biodegradable polyhydroxyalkanoates. J Biosci Bioeng 110:621–632. doi: 10.1016/j.jbiosc.2010.07.014

Chanprateep S, Buasri K, Muangwong A, Utiswannakul P (2010) Biosynthesis and biocompatibility of biodegradable poly(3-hydroxybutyrate-co-4-hydroxybutyrate). Polym Degrad Stab 95:2003–2012. doi: 10.1016/j.polymdegradstab.2010.07.014

Chen GQ (2009) A microbial polyhydroxyalkanoates (PHA) based bio- and materials industry. Chem Soc Rev 38:2434. doi: 10.1039/b812677c

Chen GQ (2012) New challenges and opportunities for industrial biotechnology. Microb Cell Factories 11:111. doi: 10.1186/1475-2859-11-111

Chen GQ, Jiang XR (2018) Engineering microorganisms for improving polyhydroxyalkanoate biosynthesis. Curr Opin Biotechnol 53:20–25. doi: 10.1016/j.copbio.2017.10.008

Chen GQ, Page WJ (1994) The effect of substrate on the molecular weight of poly-β-hydroxybutyrate produced by *Azotobacter vinelandii* UWD. Biotechnol Lett 16:155–160. doi: 10.1007/BF01021663

Chen GQ, Zhang G, Park S, Lee SY (2001) Industrial scale production of poly(3-hydroxybutyrate-co-3-hydroxyhexanoate). Appl Microbiol Biotechnol 57:50–55. doi: 10.1007/s002530100755

Chen Z, Wan C (2017) Non-sterile fermentations for the economical biochemical conversion of renewable feedstocks. Biotechnol Lett 39:1765–1777. doi: 10.1007/s10529-017-2429-8

Chhetri A, Watts K, Islam M (2008) Waste Cooking Oil as an Alternate Feedstock for Biodiesel Production. Energies 1:3–18. doi: 10.3390/en1010003

Choi J, Lee SY (1999) Factors affecting the economics of polyhydroxyalkanoate production by bacterial fermentation. Appl Microbiol Biotechnol 51:13–21. doi: 10.1007/s002530051357

Choi J, Lee SY (1997) Process analysis and economic evaluation for poly(3-hydroxybutyrate) production by fermentation. Bioprocess Eng 17:335. doi: 10.1007/s004490050394

Choi J, Lee SY, Han K (1998) Cloning of the *Alcaligenes latus* polyhydroxyalkanoate biosynthesis genes and use of these genes for enhanced production of poly(3-hydroxybutyrate) in *Escherichia coli*. Appl Environ Microbiol 64:4987–4903.

Choi J, Lee SY, Shin K, Lee WG, Park SJ, Chang HN, Chang YK (2002) Pilot scale production of poly(3-hydroxybutyrate-co-3-hydroxyvalerate) by fed-batch culture of recombinant *Escherichia coli*. Biotechnol Bioprocess Eng 7:371–374. doi: 10.1007/BF02933524

Chookaew T, O-Thong S, Prasertsan P (2014) Biohydrogen production from crude glycerol by immobilized *Klebsiella sp.* TR17 in a UASB reactor and bacterial quantification under non-sterile conditions. Int J Hydrog Energy 39:9580–9587. doi: 10.1016/j.ijhydene.2014.04.083

Ciesielski S, Pokoj T, Klimiuk E (2008) Molecular insight into activated sludge producing polyhydroxyalkanoates under aerobic–anaerobic conditions. J Ind Microbiol Biotechnol 35:805–814. doi: 10.1007/s10295-008-0352-7

Coats ER, Watson BS, Brinkman CK (2016) Polyhydroxyalkanoate synthesis by mixed microbial consortia cultured on fermented dairy manure: Effect of aeration on process rates/yields and the associated microbial ecology. Water Res 106:26–40. doi: 10.1016/j.watres.2016.09.039

Crank M, Patel MK, Marscheider-Weidemann F, Schleich J, Huesing B, Angerer G (2004) Techno-economic feasibility of large-scale production of bio-based polymers in Europe (PRO-BIP) Final report. European Commission Joint Research Center, Netherlands

Cruz MV, Freitas F, Paiva A, Mano F, Dionísio M, Ramos AM, Reis MAM (2016) Valorization of fatty acids-containing wastes and byproducts into short- and medium-chain length polyhydroxyalkanoates. New Biotechnol 33:206–215. doi: 10.1016/j.nbt.2015.05.005

Danckwertz PV (1951) Significance of Liquid-Film Coefficients in Gas Absorption. Ind Eng Chem 43:1460.

Davis R, Duane G, Kenny ST, Cerrone F, Guzik MW, Babu RP, Casey E, O'Connor KE (2015) High cell density cultivation of *Pseudomonas putida* KT2440 using glucose without the

need for oxygen enriched air supply. Biotechnol Bioeng 112:725–733. doi: 10.1002/bit.25474

de Almeida A, Giordano AM, Nikel PI, Pettinari MJ (2010) Effects of aeration on the synthesis of poly(3-hydroxybutyrate) from glycerol and glucose in recombinant *Escherichia coli*. Appl Environ Microbiol 76:2036–2040. doi: 10.1128/AEM.02706-09

de Jong E, Higson A, Walsh P, Wellisch M (2012) Bio-based chemicals: value added products from biorefineries. IEA Bioenergy - Task 42 Biorefinery.

de Koning GJM, Kellerhals M, van Meurs C, Witholt B (1997) A process for the recovery of poly(hydroxyalkanoates) from *Pseudomonads* Part 2: Process development and economic evaluation. Bioprocess Eng 17:15. doi: 10.1007/s004490050346

de las Heras AM, Portugal-Nunes DJ, Rizza N, Sandström AG, Gorwa-Grauslund MF (2016) Anaerobic poly-3-hydroxybutyrate production from xylose in recombinant *Saccharomyces cerevisiae* using a NADH-dependent acetoacetyl-CoA reductase. Microb Cell Factories 15. doi: 10.1186/s12934-016-0598-0

de Smet MJ, Eggink G, Kingma J, Wynberg H (1983) Characterization of intracellular inclusions formed by *Pseudomonas oleovorans* during growth on octane. J Bacteriol 154:870–878.

de Waard P, van der Wal H, Huijberts GNM, Eggink G (1993) Heteronuclear NMR analysis of unsaturated fatty acids in poly(3-hydroxyalkanoates. J Biol Chem 268:315–319.

Desbois AP, Smith VJ (2010) Antibacterial free fatty acids: activities, mechanisms of action and biotechnological potential. Appl Microbiol Biotechnol 85:1629–1642. doi: 10.1007/s00253-009-2355-3

Dhillon GS, Brar SK, Kaur S, Verma M (2013) Rheological studies during submerged citric acid fermentation by *Aspergillus niger* in stirred fermentor using apple pomace ultrafiltration sludge. Food Bioprocess Technol 6:1240–1250. doi: 10.1007/s11947-011-0771-8

Dietrich K, Dumont M-J, Del Rio LF, Orsat V (2017) Producing PHAs in the bioeconomy — Towards a sustainable bioplastic. Sustain Prod Consum 9:58–70. doi: 10.1016/j.spc.2016.09.001

Dilkes-Hoffman LS, Lane JL, Grant T, Pratt S, Lant PA, Laycock B (2018) Environmental impact of biodegradable food packaging when considering food waste. J Clean Prod 180:325–334. doi: 10.1016/j.jclepro.2018.01.169

Diniz SC, Taciro MK, Gomez JGC, Pradella JG da C (2004) High cell density cultivation of *Pseudomonas putida* IPT 046 and medium chain-length polyhydroxyalkanoate production from sugarcane carbohydrates. Appl Biochem Biotechnol 119:51–70. doi: 10.1385/ABAB:119:1:51

DiRusso CC, Black PN (2004) Bacterial Long Chain Fatty Acid Transport: Gateway to a Fatty Acid-responsive Signaling System. J Biol Chem 279:49563–49566. doi: 10.1074/jbc.R400026200

Doran PM (2013) Bioprocess engineering principles, 2nd ed. Elsevier/Academic Press, Amsterdam; Boston.

Du C, Sabirova J, Soetaert W, Ki Carol Lin S (2012) Polyhydroxyalkanoates production from low-cost sustainable raw materials. Curr Chem Biol 6:14–25. doi: 10.2174/187231312799984394

Du G-C, Chen J, Gao H-J, Chen Y-G, Lun S-Y (2000) Effects of environmental conditions on cell growth and poly-β-hydroxybutyrate accumulation in *Alcaligenes eutrophus*. World J Microbiol Biotechnol 16:9–13.

Du G-C, Chen J, Yu J, Lun S (2001) Continuous production of poly-3-hydroxybutyrate by *Ralstonia eutropha* in a two-stage culture system. J Biotechnol 88:59–65. doi: 10.1016/S0168-1656(01)00266-8

Dufresne A, Reche L, Marchessault RH, Lacroix M (2001) Gamma-ray crosslinking of poly(3-hydroxyoctanoate-co-undecenoate). Int J Biol Macromol 29:73–82. doi: 10.1016/S0141-8130(01)00152-0

Dufresne A, Samain E (1998) Preparation and characterization of a poly(β-hydroxyoctanoate) latex produced by *Pseudomonas oleovorans*. Macromolecules 31:6426–6433. doi: 10.1021/ma980508a

Dumont E, Andrès Y, Le Cloirec P (2006) Effect of organic solvents on oxygen mass transfer in multiphase systems: Application to bioreactors in environmental protection. Biochem Eng J 30:245–252. doi: 10.1016/j.bej.2006.05.003

Dumont E, Delmas H (2003) Mass transfer enhancement of gas absorption in oil-in-water systems: a review. Chem Eng Process Process Intensif 42:419–438. doi: 10.1016/S0255-2701(02)00067-3

Durner R, Witholt B, Egli T (2000) Accumulation of poly[(R)-3-hydroxyalkanoates] in *Pseudomonas oleovorans* during growth with octanoate in continuous culture at different dilution rates. Appl Environ Microbiol 66:3408–3414

Ebert BE, Kurth F, Grund M, Blank LM, Schmid A (2011) Response of *Pseudomonas putida* KT2440 to increased NADH and ATP demand. Appl Environ Microbiol 77:6597–6605. doi: 10.1128/AEM.05588-11

Eggink G, Waard P, Huijberts GNM (1992) The role of fatty acid biosynthesis and degradation in the supply of substrates for poly(3-hydroxyalkanoate) formation in *Pseudomonas putida*. FEMS Microbiol Lett 103:159–163. doi: 10.1111/j.1574-6968.1992.tb05833.x

Elbahloul Y, Steinbüchel A (2009) Large-scale production of poly(3-hydroxyoctanoic acid) by *Pseudomonas putida* GPo1 and a simplified downstream process. Appl Environ Microbiol 75:643–651. doi: 10.1128/AEM.01869-08

Enfors S-O, Jahic M, Rozkov A, Xu B, Hecker M, Jürgen B, Krüger E, Schweder T, Hamer G, O'Beirne D, Noisommit-Rizzi N, Reuss M, Boone L, Hewitt C, McFarlane C, Nienow A, Kovacs T, Trägårdh C, Fuchs L, Revstedt J, Friberg PC, Hjertager B, Blomsten G, Skogman H, Hjort S, Hoeks F, Lin H-Y, Neubauer P, van der Lans R, Luyben K, Vrabel P, Manelius å. (2001) Physiological responses to mixing in large scale bioreactors. J Biotechnol 85:175–185. doi: 10.1016/S0168-1656(00)00365-5

Escapa IF, García JL, Bühler B, Blank LM, Prieto MA (2012) The polyhydroxyalkanoate metabolism controls carbon and energy spillage in *Pseudomonas putida*. Environ Microbiol 14:1049–1063. doi: 10.1111/j.1462-2920.2011.02684.x

Faccin DJL, Rech R, Secchi AR, Cardozo NSM, Ayub MAZ (2013) Influence of oxygen transfer rate on the accumulation of poly(3-hydroxybutyrate) by *Bacillus megaterium*. Process Biochem 48:420–425. doi: 10.1016/j.procbio.2013.02.004

Fernández D, Rodríguez E, Bassas M, Viñas M, Solanas AM, Llorens J, Marqués AM, Manresa A (2005) Agro-industrial oily wastes as substrates for PHA production by the new strain *Pseudomonas aeruginosa* NCIB 40045: Effect of culture conditions. Biochem Eng J 26:159–167. doi: 10.1016/j.bej.2005.04.022

Fernández-Dacosta C, Posada JA, Kleerebezem R, Cuellar MC, Ramirez A (2015) Microbial community-based polyhydroxyalkanoates (PHAs) production from wastewater: Techno-economic analysis and ex-ante environmental assessment. Bioresour Technol 185:368–377. doi: 10.1016/j.biortech.2015.03.025

Follonier S, Henes B, Panke S, Zinn M (2012) Putting cells under pressure: A simple and efficient way to enhance the productivity of medium-chain-length polyhydroxyalkanoate in processes with *Pseudomonas putida* KT2440. Biotechnol Bioeng 109:451–461. doi: 10.1002/bit.23312

Follonier S, Riesen R, Zinn M (2015) Pilot-scale production of functionalized mcl-PHA from grape pomace supplemented with fatty acids. Chem Biochem Eng Q 29:113–121. doi: 10.15255/CABEQ.2014.2251

Fonseca P, de la Peña F, Prieto MA (2014) A role for the regulator PsrA in the polyhydroxyalkanoate metabolism of *Pseudomonas putida* KT2440. Int J Biol Macromol 71:14–20. doi: 10.1016/j.ijbiomac.2014.04.014

Fontaine P, Mosrati R, Corroler D (2017) Medium chain length polyhydroxyalkanoates biosynthesis in *Pseudomonas putida* mt-2 is enhanced by co-metabolism of glycerol/octanoate or fatty acids mixtures. Int J Biol Macromol 98:430–435. doi: 10.1016/j.ijbiomac.2017.01.115

Freitas F, Alves VD, Pais J, Costa N, Oliveira C, Mafra L, Hilliou L, Oliveira R, Reis MAM (2009) Characterization of an extracellular polysaccharide produced by a *Pseudomonas* strain grown on glycerol. Bioresour Technol 100:859–865. doi: 10.1016/j.biortech.2008.07.002

Fu J, Sharma U, Sparling R, Cicek N, Levin DB (2014) Evaluation of medium-chain-length polyhydroxyalkanoate production by *Pseudomonas putida* LS46 using biodiesel by-product streams. Can J Microbiol 60:461–468. doi: 10.1139/cjm-2014-0108

Fujita Y, Matsuoka H, Hirooka K (2007) Regulation of fatty acid metabolism in bacteria. Mol Microbiol 66:829–839. doi: 10.1111/j.1365-2958.2007.05947.x

Gabelle J-C, Augier F, Carvalho A, Rousset R, Morchain J (2011) Effect of tank size on kLa and mixing time in aerated stirred reactors with non-newtonian fluids. Can J Chem Eng 89:1139–1153. doi: 10.1002/cjce.20571

Gahlawat G (2018) Enhancing the production of polyhydroxyalkanoate biopolymer by *Azohydromonas australica* using a simple empty and fill bioreactor cultivation strategy. Chem Biochem Eng Q 31:479–485. doi: 10.15255/CABEQ.2017.1148

Gao J, Ramsay JA, Ramsay BA (2016) Fed-batch production of poly-3-hydroxydecanoate from decanoic acid. J Biotechnol 218:102–107. doi: 10.1016/j.jbiotec.2015.12.012

Gapes DJ (2002) External and internal mass transfer in biological wastewater treatment systems. Ph.D., The University of Queensland.

Garcia-Ochoa F, Gomez E (2009) Bioreactor scale-up and oxygen transfer rate in microbial processes: An overview. Biotechnol Adv 27:153–176. doi: 10.1016/j.biotechadv.2008.10.006

García-Ochoa F, Gómez E (1998) Mass transfer coefficient in stirred tank reactors for xanthan gum solutions. Biochem Eng J 1:1–10. doi: 10.1016/S1369-703X(97)00002-8

Garcia-Ochoa F, Gomez E, Santos VE, Merchuk JC (2010) Oxygen uptake rate in microbial processes: An overview. Biochem Eng J 49:289–307. doi: 10.1016/j.bej.2010.01.011

Gasperi J, Wright SL, Dris R, Collard F, Mandin C, Guerrouache M, Langlois V, Kelly FJ, Tassin B (2018) Microplastics in air: Are we breathing it in? Curr Opin Environ Sci Health 1:1–5. doi: 10.1016/j.coesh.2017.10.002

Germanov ES, Marshall AD, Bejder L, Fossi MC, Loneragan NR (2018) Microplastics: No Small Problem for Filter-Feeding Megafauna. Trends Ecol Evol. doi: 10.1016/j.tree.2018.01.005

Gillis J, Ko K, Ramsay JA, Ramsay BA (2017) Potential for mcl-PHA production from nonanoic and azelaic acids. Can J Microbiol 1–9. doi: 10.1139/cjm-2017-0554

Goldberg RN, Kishore N, Lennen RM (2002) Thermodynamic Quantities for the Ionization Reactions of Buffers. J Phys Chem Ref Data 31:231–370. doi: 10.1063/1.1416902

Gomes N, Aguedo M, Teixeira J, Belo I (2007) Oxygen mass transfer in a biphasic medium: Influence on the biotransformation of methyl ricinoleate into γ-decalactone by the yeast Yarrowia lipolytica. Biochem Eng J 35:380–386. doi: 10.1016/j.bej.2007.02.002

Gorenflo V, Schmack G, Vogel R, Steinbüchel A (2001) Development of a process for the biotechnological large-scale production of 4-hydroxyvalerate-containing polyesters and characterization of their physical and mechanical properties. Biomacromolecules 2:45–57. doi: 10.1021/bm0000992

Goudar CT, Strevett KA, Shah SN (1999) Influence of microbial concentration on the rheology of non-Newtonian fermentation broths. Appl Microbiol Biotechnol 51:310–315. doi: 10.1007/s002530051396

Gourmelon G (2015) Global Plastic Production Rises, Recycling Lags. Worldwatch Institute, Washington, DC.

Grousseau E, Blanchet E, Déléris S, Albuquerque MGE, Paul E, Uribelarrea J-L (2013) Impact of sustaining a controlled residual growth on polyhydroxybutyrate yield and production kinetics in *Cupriavidus necator*. Bioresour Technol 148:30–38. doi: 10.1016/j.biortech.2013.08.120

Guedon E, Payot S, Desvaux M, Petitdemange H (1999) Carbon and electron flow in *Clostridium cellulolyticum* grown in chemostat culture on synthetic medium. J Bacteriol 181:3262–3269.

Gurieff N, Lant P (2007) Comparative life cycle assessment and financial analysis of mixed culture polyhydroxyalkanoate production. Bioresour Technol 98:3393–3403. doi: 10.1016/j.biortech.2006.10.046

Haas C, El-Najjar T, Virgolini N, Smerilli M, Neureiter M (2017) High cell-density production of poly(3-hydroxybutyrate) in a membrane bioreactor. New Biotechnol 37:117–122. doi: 10.1016/j.nbt.2016.06.1461

Haba E, Vidal-Mas J, Bassas M, Espuny MJ, Llorens J, Manresa A (2007) Poly 3-(hydroxyalkanoates) produced from oily substrates by *Pseudomonas aeruginosa* 47T2 (NCBIM 40044): Effect of nutrients and incubation temperature on polymer composition. Biochem Eng J 35:99–106. doi: 10.1016/j.bej.2006.11.021

Hale RC (2018) Are the Risks from Microplastics Truly Trivial? Environ Sci Technol 52:931–931. doi: 10.1021/acs.est.7b06615

Hammer J, Kraak MHS, Parsons JR (2012) Plastics in the Marine Environment: The Dark Side of a Modern Gift. In: Whitacre DM (ed) Reviews of Environmental Contamination and Toxicology. Springer New York, New York, NY, pp 1–44.

Hanke T, Richhardt J, Polen T, Sahm H, Bringer S, Bott M (2012) Influence of oxygen limitation, absence of the cytochrome bc1 complex and low pH on global gene expression in *Gluconobacter oxydans* 621H using DNA microarray technology. J Biotechnol 157:359–372. doi: 10.1016/j.jbiotec.2011.12.020

Harding K, Dennis J, Vonblottnitz H, Harrison S (2007) Environmental analysis of plastic production processes: Comparing petroleum-based polypropylene and polyethylene with biologically-based poly-β-hydroxybutyric acid using life cycle analysis. J Biotechnol 130:57–66. doi: 10.1016/j.jbiotec.2007.02.012

Harms P, Kostov Y, Rao G (2002) Bioprocess monitoring. Curr Opin Biotechnol 13:124–127. doi: 10.1016/S0958-1669(02)00295-1

Hartmann R, Hany R, Pletscher E, Ritter A, Witholt B, Zinn M (2006) Tailor-made olefinic medium-chain-length poly[(R)-3-hydroxyalkanoates] by *Pseudomonas putida* GPo1: Batch versus chemostat production. Biotechnol Bioeng 93:737–746. doi: 10.1002/bit.20756

Hartmann R, Hany R, Witholt B, Zinn M (2010) Simultaneous Biosynthesis of two copolymers in *Pseudomonas putida* GPo1 using a two-stage continuous culture system. Biomacromolecules 11:1488–1493. doi: 10.1021/bm100118t

Haywood GW, Anderson AJ, Chu L, Dawes EA (1988) The role of NADH- and NADPH-linked acetoacetyl-CoA reductases in the poly-3-hydroxybutyrate synthesizing organism *Alcaligenes eutrophus*. FEMS 52:259–264.

Haywood GW, Anderson AJ, Ewing DF, Dawes EA (1990) Accumulation of a polyhydroxyalkanoate containing primarily 3-hydroxydecanoate from simple carbohydrate substrates by *Pseudomonas* sp. strain NCIMB 40135. Appl Environ Microbiol 45:3354–3359.

Hazenberg W, Witholt B (1997) Efficient production of medium-chain-length poly(3-hydroxyalkanoates) from octane by *Pseudomonas oleovorans*: economic considerations. Appl Microbiol Biotechnol 48:588–596. doi: 10.1007/s002530051100

Hazer B, Demirel SI, Borcakli M, Eroglu MS, Cakmak M, Erman B (2001) Free radical crosslinking of unsaturated bacterial polyesters obtained from soybean oily acids. Polym Bull 46:389–394. doi: 10.1007/s002890170047

Heijnen JJ, Terwisscha van Scheltinga AH, Straathof AJ (1992) Fundamental bottlenecks in the application of continuous bioprocesses. J Biotechnol 22:3–20. doi: 10.1016/0168-1656(92)90128-V

Heinrich D, Madkour MH, Al-Ghamdi MA, Shabbaj II, Steinbüchel A (2012) Large scale extraction of poly(3-hydroxybutyrate) from *Ralstonia eutropha* H16 using sodium hypochlorite. AMB Express 2:59. doi: 10.1186/2191-0855-2-59

Herbst H, Schumpe A, Deckwer W-D (1992) Xanthan production in stirred tank fermenters: Oxygen transfer and scale-up. Chem Eng Technol 15:425–434. doi: 10.1002/ceat.270150610

Higbie R (1935) The Rate of Absorption of a Pure Gas into a Still Liquid During Short Periods of Exposure. Am Inst Chem Eng 365–389.

Höjeberg B, Brodelius P, Rydström J, Mosbach K (1976) Affinity chromatography and binding studies on immobilized adenosine 5′-monophosphate and adenosine 2′, 5′-bisphosphate of nicotinamide nucleotide transhydrogenase from *Pseudomonas aeruginosa*. Eur J Biochem 66:467–475.

Hori K, Soga K, Doi Y (1994) Effects of culture conditions on molecular weights of poly(3-hydroxyalkanoates) produced by *Pseudomonas putida* from octanoate. Biotechnol Lett 16:709–714. doi: 10.1007/BF00136476

Huang T-Y, Duan K-J, Huang S-Y, Chen CW (2006) Production of polyhydroxyalkanoates from inexpensive extruded rice bran and starch by *Haloferax mediterranei*. J Ind Microbiol Biotechnol 33:701–706. doi: 10.1007/s10295-006-0098-z

Huijberts GNM, de Rijk TC, de Waard P, Eggink G (1994) 13C Nuclear magnetic resonance studies of *Pseudomonas putida* fatty acid metabolic routes involved in poly(3-hydroxyalkanoate) synthesis. J Bacteriol 176:1661–1666.

Huijberts GNM, Eggink G (1996) Production of poly(3-hydroxyalkanoates) by *Pseudomonas putida* KT2442 in continuous cultures. Appl Microbiol Biotechnol 46:233–239. doi: 10.1007/s002530050810

Huijberts GNM, Eggink G, de Waard P, Huisman GW, Witholt B (1992) *Pseudomonas putida* KT2442 cultivated on glucose accumulates poly(3-hydroxyalkanoates) consisting of saturated and unsaturated monomers. Appl Microbiol Biotechnol 58:536–544.

Huisman GW, de Leeuw O, Eggink G, Witholt B (1989) Synthesis of poly-3-hydroxyalkanoates is a common feature of fluorescent *Pseudomonads*. Appl Environ Microbiol 55:1949–1954.

Huschner F, Grousseau E, Brigham CJ, Plassmeier J, Popovic M, Rha C, Sinskey AJ (2015) Development of a feeding strategy for high cell and PHA density fed-batch fermentation of Ralstonia eutropha H16 from organic acids and their salts. Process Biochem 50:165–172. doi: 10.1016/j.procbio.2014.12.004

Ibrahim MHA, Steinbüchel A (2009) Poly(3-hydroxybutyrate) production from glycerol by *Zobellella denitrificans* MW1 via high-cell-density fed-batch fermentation and simplified solvent extraction. Appl Environ Microbiol 75:6222–6231. doi: 10.1128/AEM.01162-09

Ibrahim MHA, Steinbüchel A (2010) High-cell-density cyclic fed-batch fermentation of a poly(3-hydroxybutyrate)-accumulating thermophile, *Chelatococcus* sp. Strain MW10. Appl Environ Microbiol 76:7890–7895. doi: 10.1128/AEM.01488-10

Ienczak JL, Schmidell W, de Aragão GMF (2013) High-cell-density culture strategies for polyhydroxyalkanoate production: a review. J Ind Microbiol Biotechnol 40:275–286. doi: 10.1007/s10295-013-1236-z

Ienczak JL, Schmidt M, Quines LK, Zanfonato K, da Cruz Pradella JG, Schmidell W, de Aragao GMF (2016) Poly(3-hydroxybutyrate) production in repeated fed-batch with cell recycle using a medium with low carbon source concentration. Appl Biochem Biotechnol 178:408–417. doi: 10.1007/s12010-015-1883-9

Inan K, Sal FA, Rahman A, Putman RJ, Agblevor FA, Miller CD (2016) Microbubble assisted polyhydroxybutyrate production in *Escherichia coli*. BMC Res Notes 9. doi: 10.1186/s13104-016-2145-9

Iwata T (2015) Biodegradable and bio-based polymers: future prospects of eco-friendly plastics. Angew Chem Int Ed 54:3210–3215. doi: 10.1002/anie.201410770

Jackson FA, Dawes EA (1976) Regulation of the tricarboxylic acid cycle and polyhydroxybutyrate metabolism in *Azotobacter beijerinckii* grown under nitrogen or oxygen limitation. J Gen Microbiol 97:303–312. doi: 10.1099/00221287-97-2-303

Jahn A, Griebe T, Nielsen PH (1999) Composition of *Pseudomonas putida* biofilms: Accumulation of protein in the biofilm matrix. Biofouling 14:49–57. doi: 10.1080/08927019909378396

Janes B, Hollar J, Dennis D (1990) Molecular Characterization of the Poly-ß-Hydroxybutyrate Biosynthetic Pathway of *Alcaligenes eutrophus* H16. In: Dawes EA (ed) Novel Biodegradable Microbial Polymers. Springer Netherlands, Dordrecht, pp 175–190.

Jarboe LR, Royce LA, Liu P (2013) Understanding biocatalyst inhibition by carboxylic acids. Front Microbiol 4. doi: 10.3389/fmicb.2013.00272

Jia S, Chen G, Kahar P, Choi DB, Okabe M (1999) Effect of soybean oil on oxygen transfer in the production of tetracycline with an airlift bioreactor. J Biosci Bioeng 87:825–827. doi: 10.1016/S1389-1723(99)80162-5

Jiang G, Hill D, Kowalczuk M, Johnston B, Adamus G, Irorere V, Radecka I (2016) Carbon sources for polyhydroxyalkanoates and an integrated biorefinery. Int J Mol Sci 17:1157. doi: 10.3390/ijms17071157

Jiang X, Sun Z, Marchessault RH, Ramsay JA, Ramsay BA (2012) Biosynthesis and properties of medium-chain-length polyhydroxyalkanoates with enriched content of the dominant monomer. Biomacromolecules 13:2926–2932. doi: 10.1021/bm3009507

Jiang X, Sun Z, Ramsay JA, Ramsay BA (2013) Fed-batch production of MCL-PHA with elevated 3-hydroxynonanoate content. AMB Express 3:50. doi: 10.1186/2191-0855-3-50

Jin Z, Wushke S, Blunt W, Dartiailh C, Sharma PK, Levin DavidB, Sparling R (2019) Production of complex medium-chain-length polyhydroxyalkanoates from volatile fatty

acids and potential application to wastewater treatment. Appl Microbiol Biotechnol Accepted.

Johnson K, Jiang Y, Kleerebezem R, Muyzer G, van Loosdrecht MCM (2009) Enrichment of a mixed bacterial culture with a high polyhydroxyalkanoate storage capacity. Biomacromolecules 10:670–676. doi: 10.1021/bm8013796

Jung K, Hazenberg W, Prieto M, Witholt B (2001) Two-stage continuous process development for the production of medium-chain-length poly(3-hydroxyalkanoates). Biotechnol Bioeng 72:19–24. doi: 10.1002/1097-0290(20010105)72:1<19::AID-BIT3>3.0.CO;2-B

Junker BH (2004) Scale-up methodologies for *Escherichia coli* and yeast fermentation processes. J Biosci Bioeng 97:347–364. doi: 10.1016/S1389-1723(04)70218-2

Kachrimanidou V, Kopsahelis N, Papanikolaou S, Kookos IK, De Bruyn M, Clark JH, Koutinas AA (2014) Sunflower-based biorefinery: Poly(3-hydroxybutyrate) and poly(3-hydroxybutyrate- co -3-hydroxyvalerate) production from crude glycerol, sunflower meal and levulinic acid. Bioresour Technol 172:121–130. doi: 10.1016/j.biortech.2014.08.044

Kang Y, Nguyen DT, Son MS, Hoang TT (2008) The *Pseudomonas aeruginosa* PsrA responds to long-chain fatty acid signals to regulate the fadBA5 -oxidation operon. Microbiology 154:1584–1598. doi: 10.1099/mic.0.2008/018135-0

Kanjanachumpol P, Kulpreecha S, Tolieng V, Thongchul N (2013) Enhancing polyhydroxybutyrate production from high cell density fed-batch fermentation of *Bacillus megaterium* BA-019. Bioprocess Biosyst Eng 36:1463–1474. doi: 10.1007/s00449-013-0885-7

Kaur G, Roy I (2015) Strategies for large-scale production of polyhydroxyalkanoates. Chem Biochem Eng Q 29:157–172. doi: 10.15255/CABEQ.2014.2255

Kellerhals MB, Hazenberg W, Witholt B (1999a) High cell density fermentations of *Pseudomonas oleovorans* for the production of mcl-PHAs in two-liquid phase media. Enzyme Microb Technol 24:111–116. doi: 10.1016/S0141-0229(98)00113-6

Kellerhals MB, Kessler B, Witholt B (1999b) Closed-loop control of bacterial high-cell-density fed-batch cultures: Production of mcl-PHAs by *Pseudomonas putida* KT2442 under single-substrate and cofeeding conditions. Biotechnol Bioeng 65:306–315. doi: 10.1002/(SICI)1097-0290(19991105)65:3<306::AID-BIT8>3.0.CO;2-0

Kellerhals MB, Kessler B, Witholt B, Tchouboukov A, Brandl H (2000) Renewable long-chain fatty acids for production of biodegradable medium-chain-length polyhydroxyalkanoates (mcl-PHAs) at laboratory and pilot plant scales. Macromolecules 33:4690–4698. doi: 10.1021/ma000655k

Kendall A (2012) A life cycle assessment of biopolymer production from material recovery facility residuals. Resour Conserv Recycl 61:69–74. doi: 10.1016/j.resconrec.2012.01.008

Keshavarz T, Roy I (2010) Polyhydroxyalkanoates: bioplastics with a green agenda. Curr Opin Microbiol 13:321–326. doi: 10.1016/j.mib.2010.02.006

Khanna S, Srivastava AK (2005a) Recent advances in microbial polyhydroxyalkanoates. Process Biochem 40:607–619. doi: 10.1016/j.procbio.2004.01.053

Khanna S, Srivastava AK (2005b) Repeated batch cultivation of *Ralstonia eutropha* for poly (β-hydroxybutyrate) production. Biotechnol Lett 27:1401–1403. doi: 10.1007/s10529-005-0689-1

Khoo HH, Tan RBH (2010) Environmental impacts of conventional plastic and bio-based carrier bags: Part 2: end-of-life options. Int J Life Cycle Assess 15:338–345. doi: 10.1007/s11367-010-0163-8

Kim BS (2002) Production of medium chain length polyhydroxyalkanoates by fed-batch culture of *Pseudomonas oleovorans*. Biotechnol Lett 24:125–130

Kim BS, Lee SC, Lee SY, Chang HN, Chang YK, Woo SI (1994) Production of poly(3-hydroxybutyric acid) by fed-batch culture of *Alcaligenes eutrophus* with glucose concentration control. Biotechnol Bioeng 43:892–898. doi: 10.1002/bit.260430908

Kim BS, Lee SY, Chang HN (1992) Production of poly-β-hydroxybutyrate by fed-batch culture of recombinant *Escherichia coli*. Biotechnol Lett 14:811–816. doi: 10.1007/BF01029144

Kim GJ, Lee IY, Yoon SC, Shin YC, Park YH (1997) Enhanced yield and a high production of medium-chain-length poly(3-hydroxyalkanoates) in a two-step fed-batch cultivation of *Pseudomonas putida* by combined use of glucose and octanoate. Enzyme Microb Technol 20:500–505. doi: 10.1016/S0141-0229(96)00179-2

Kim SW, Kim P, Lee HS, Kim JH (1996) High production of poly-β-hydroxybutyrate (PHB) from *Methylobacterium organophilum* under potassium limitation. Biotechnol Lett 18:25–30. doi: 10.1007/BF00137805

Koller M, Braunegg G (2015) Potential and prospects of continuous polyhydroxyalkanoate (PHA) production. Bioengineering 2:94–121. doi: 10.3390/bioengineering2020094

Koller M, Braunegg G (2018) Advanced approaches to produce polyhydroxyalkanoate (PHA) biopolyesters in a sustainable and economic fashion. EuroBiotech J 2:89–103. doi: 10.2478/ebtj-2018-0013

Koller M, Maršálek L, de Sousa Dias MM, Braunegg G (2017) Producing microbial polyhydroxyalkanoate (PHA) biopolyesters in a sustainable manner. New Biotechnol 37:24–38. doi: 10.1016/j.nbt.2016.05.001

Koller M, Muhr A (2014) Continuous production mode as a viable process-engineering tool for efficient poly(hydroxyalkanoate) (PHA) bio-production. Chem Biochem Eng Q 28:65–77.

Koller M, Sandholzer D, Salerno A, Braunegg G, Narodoslawsky M (2013) Biopolymer from industrial residues: Life cycle assessment of poly(hydroxyalkanoates) from whey. Resour Conserv Recycl 73:64–71. doi: 10.1016/j.resconrec.2013.01.017

Kourmentza C, Ntaikou I, Lyberatos G, Kornaros M (2015) Polyhydroxyalkanoates from *Pseudomonas sp.* using synthetic and olive mill wastewater under limiting conditions. Int J Biol Macromol 74:202–210. doi: 10.1016/j.ijbiomac.2014.12.032

Kourmentza C, Plácido J, Venetsaneas N, Burniol-Figols A, Varrone C, Gavala HN, Reis MAM (2017) Recent advances and challenges towards sustainable polyhydroxyalkanoate (PHA) production. Bioengineering 4:55. doi: 10.3390/bioengineering4020055

Koyama N, Doi Y (1995) Continuous production of poly(3-hydroxybutyrate-co-3-hyhroxyvalerate) by *Alcaligenes eutrophus*. Biotechnol Lett 17:281–284. doi: 10.1007/BF01190637

Kshirsagar P, Suttar R, Nilegaonkar S, Kulkarni S, Kanekar P (2012) Scale up production of polyhydroxyalkanoate (PHA) at different aeration, agitation and controlled dissolved oxygen levels in fermenter using *Halomonas campisalis* MCM B-1027. J Biochem Technol 4:512–517.

Kundu A, Dumont E, Duquenne A-M, Delmas H (2008) Mass Transfer Characteristics in Gas-liquid-liquid System. Can J Chem Eng 81:640–646. doi: 10.1002/cjce.5450810341

Kurth N, Renard E, Brachet F, Robic D, Guerin P, Bourbouze R (2002) Poly(3-hydroxyoctanoate) containing pendant carboxylic groups for the preparation of nanoparticles aimed at drug transport and release. Polymer 43:1095–1101. doi: 10.1016/S0032-3861(01)00692-9

Lageveen RG, Huisman GW, Preusting H, Ketelaar P, Eggink G, Witholt B (1988) Formation of polyesters by *Pseudomonas oleovorans*: effect of substrates on formation and composition of poly-(R)-3-hydroxyalkanoates and poly-(R)-3-hydroxyalkenoates. Appl Environ Microbiol 54:2924–2932.

Lara AR, Galindo E, Ramírez OT, Palomares LA (2006a) Living with heterogeneities in bioreactors. Mol Biotechnol 34:355–381.

Lara AR, Leal L, Flores N, Gosset G, Bolívar F, Ramírez OT (2006b) Transcriptional and metabolic response of recombinant *Escherichia coli* to spatial dissolved oxygen tension gradients simulated in a scale-down system. Biotechnol Bioeng 93:372–385. doi: 10.1002/bit.20704

Lavers JL, Bond AL (2017) Exceptional and rapid accumulation of anthropogenic debris on one of the world's most remote and pristine islands. Proc Natl Acad Sci 114:6052–6055. doi: 10.1073/pnas.1619818114

Laycock B, Halley P, Pratt S, Werker A, Lant P (2013) The chemomechanical properties of microbial polyhydroxyalkanoates. Prog Polym Sci 38:536–583. doi: 10.1016/j.progpolymsci.2012.06.003

Lee I, Kim M, Chang HN, Park YH (1995) Regulation of poly-β-hydroxybutyrate biosynthesis by nicotinamide nucleotide in *Alcaligenes eutrophus*. FEMS Microbiol Lett 131:35–39. doi: 10.1016/0378-1097(95)00231-S

Lee J, Lee SY, Park S, Middelberg APJ (1999) Control of fed-batch fermentations. Biotechnol Adv 17:29–48. doi: 10.1016/S0734-9750(98)00015-9

Lee SH, Kim JH, Chung C-W, Kim DY, Rhee YH (2018) Analysis of Medium-Chain-Length Polyhydroxyalkanoate-Producing Bacteria in Activated Sludge Samples Enriched by Aerobic Periodic Feeding. Microb Ecol 75:720–728. doi: 10.1007/s00248-017-1084-x

Lee SH, Kim JH, Mishra D, Ni Y-Y, Rhee YH (2011) Production of medium-chain-length polyhydroxyalkanoates by activated sludge enriched under periodic feeding with nonanoic acid. Bioresour Technol 102:6159–6166. doi: 10.1016/j.biortech.2011.03.025

Lee SH, Oh DH, Ahn WS, Lee Y, Choi J, Lee SY (2000a) Production of poly(3-hydroxybutyrate-co-3-hydroxyhexanoate) by high-cell-density cultivation of *Aeromonas hydrophila*. Biotechnol Bioeng 67:240–244 . doi: 10.1002/(SICI)1097-0290(20000120)67:2<240::AID-BIT14>3.0.CO;2-F

Lee SY (1996) Plastic bacteria? Progress and prospects for polyhydroxyalkanoate production in bacteria. Trends Biotechnol 14:431–438. doi: 10.1016/0167-7799(96)10061-5

Lee SY, Wong HH, Choi J, Lee SH, Lee SC, Han CS (2000b) Production of medium-chain-length polyhydroxyalkanoates by high-cell-density cultivation of *Pseudomonas putida* under phosphorus limitation. Biotechnol Bioeng 68:466–470. doi: 10.1002/(SICI)1097-0290(20000520)68:4<466::AID-BIT12>3.0.CO;2-T

Lee W-H, Azizan MNM, Sudesh K (2004) Effects of culture conditions on the composition of poly(3-hydroxybutyrate-co-4-hydroxybutyrate) synthesized by *Comamonas acidovorans*. Polym Degrad Stab 84:129–134. doi: 10.1016/j.polymdegradstab.2003.10.003

Lefebvre G, Rocher M, Braunegg G (1997) Effects of low dissolved-oxygen concentrations on poly-(3-hydroxybutyrate-co-3-hydroxyvalerate) production by *Alcaligenes eutrophus*. Appl Environ Microbiol 63:827–833.

Levett I, Birkett G, Davies N, Bell A, Langford A, Laycock B, Lant P, Pratt S (2016) Techno-economic assessment of poly-3-hydroxybutyrate (PHB) production from methane—The case for thermophilic bioprocessing. J Environ Chem Eng 4:3724–3733. doi: 10.1016/j.jece.2016.07.033

Li T, Chen X, Chen J, Wu Q, Chen G-Q (2014) Open and continuous fermentation: Products, conditions and bioprocess economy. Biotechnol J 9:1503–1511. doi: 10.1002/biot.201400084

Li W, Cicek N, Levin DB, Liu S (2018) Enabling electrospinning of medium-chain length polyhydroxyalkanoates (PHAs) by blending with short-chain length PHAs. Int J Polym Mater Polym Biomater 1–11. doi: 10.1080/00914037.2018.1466136

Li X, Li P, Zu L, Yang C (2016) Gas-Liquid Mass Transfer Characteristics with Microbubble Aeration - I. Standard Stirred Tank. Chem Eng Technol 39:945–952. doi: 10.1002/ceat.201500644

Liebergesell M, Steinbüchel A (1992) Cloning and nucleotide sequences of genes relevant for biosynthesis of poly(3-hydroxybutyric acid) in *Chromatium vinosum* strain D. Eur J Biochem 209:135–150. doi: 10.1111/j.1432-1033.1992.tb17270.x

Lillo JG, Rodriguez-Valera F (1990) Effects of Culture Conditions on Poly(β-Hydroxybutyric Acid) Production by *Haloferax mediterranei*. Appl Environ Microbiol 56:2517–2521.

Lithner D, Larsson Å, Dave G (2011) Environmental and health hazard ranking and assessment of plastic polymers based on chemical composition. Sci Total Environ 409:3309–3324. doi: 10.1016/j.scitotenv.2011.04.038

Liu C, Tanaka H, Zhang L, Zhang J, Huang X, Ma J, Matsuzawa Y (2012) Fouling and structural changes of Shirasu porous glass (SPG) membrane used in aerobic wastewater treatment process for microbubble aeration. J Membr Sci 421–422:225–231. doi: 10.1016/j.memsci.2012.07.023

Liu W, Chen G-Q (2007) Production and characterization of medium-chain-length polyhydroxyalkanoate with high 3-hydroxytetradecanoate monomer content by fadB and fadA knockout mutant of *Pseudomonas putida* KT2442. Appl Microbiol Biotechnol 76:1153–1159. doi: 10.1007/s00253-007-1092-8

Liu Y, Tay J-H (2001) Strategy for minimization of excess sludge production from the activated sludge process. Biotechnol Adv 19:97–107 . doi: 10.1016/S0734-9750(00)00066-5

Lopes M, Belo I, Mota M (2014) Over-pressurized bioreactors: Application to microbial cell cultures. Biotechnol Prog 30:767–775. doi: 10.1002/btpr.1917

Lopes M, Mota M, Belo I (2013) Oxygen mass transfer rate in a pressurized lab-scale stirred bioreactor. Chem Eng Technol 36:1779–1784. doi: 10.1002/ceat.201300082

López NI, Pettinari MJ, Nikel PI, Méndez BS (2015) Polyhydroxyalkanoates: Much More than Biodegradable Plastics. Adv Appl Microbiol 93:73–106. doi: 10.1016/bs.aambs.2015.06.001

Lynd LR, Wang MQ (2003) A Product-Nonspecific Framework for Evaluating the Potential of Biomass-Based Products to Displace Fossil Fuels. J Ind Ecol 7:17–32. doi: 10.1162/108819803323059370

Maalej H, Hmidet N, Boisset C, Bayma E, Heyraud A, Nasri M (2016) Rheological and emulsifying properties of a gel-like exopolysaccharide produced by *Pseudomonas stutzeri* AS22. Food Hydrocoll 52:634–647. doi: 10.1016/j.foodhyd.2015.07.010

Maclean H, Sun Z, Ramsay JA, Ramsay A. B (2008) Decaying exponential feeding of nonanoic acid for the production of medium-chain-length poly(3-hydroxyalkanoates) by *Pseudomonas putida* KT2440. Can J Chem 86:564–569. doi: 10.1139/v08-062

Madison LL, Huisman GW (1999) Metabolic engineering of poly(3-hydroxyalkanoates): from DNA to plastic. Microbiol Mol Biol Rev MMBR 63:21–53.

Magdouli S, Brar SK, Blais JF, Tyagi RD (2015) How to direct the fatty acid biosynthesis towards polyhydroxyalkanoates production? Biomass Bioenergy 74:268–279. doi: 10.1016/j.biombioe.2014.12.017

Majone M, Massanisso P, Carucci A, Lindrea K, Tandoi V (1996) Influence of storage on kinetic selection to control aerobic filamentous bulking. Water Sci Technol 34:223–232.

Martín M, Montes FJ, Galán MA (2010) Mass transfer rates from bubbles in stirred tanks operating with viscous fluids. Chem Eng Sci 65:3814–3824 . doi: 10.1016/j.ces.2010.03.015

Masood F, Yasin T, Hameed A (2015) Polyhydroxyalkanoates – what are the uses? Current challenges and perspectives. Crit Rev Biotechnol 35:514–521. doi: 10.3109/07388551.2014.913548

Mato Y, Isobe T, Takada H, Kanehiro H, Ohtake C, Kaminuma T (2001) Plastic Resin Pellets as a Transport Medium for Toxic Chemicals in the Marine Environment. Environ Sci Technol 35:318–324. doi: 10.1021/es0010498

Merchuk JC, Yona S, Siegel MH, Zvi AB (1990) On the first-order approximation to the response of dissolved oxygen electrodes for dynamic kLa estimation. Biotechnol Bioeng 35:1161–1163. doi: 10.1002/bit.260351113

Millán M, Segura D, Galindo E, Peña C (2016) Molecular mass of poly-3-hydroxybutyrate (P3HB) produced by *Azotobacter vinelandii* is determined by the ratio of synthesis and degradation under fixed dissolved oxygen tension. Process Biochem 51:950–958. doi: 10.1016/j.procbio.2016.04.013

Miranda De Sousa Dias M, Koller M, Puppi D, Morelli A, Chiellini F, Braunegg G (2017) Fed-batch synthesis of poly(3-hydroxybutyrate) and poly(3-hydroxybutyrate-co-4-hydroxybutyrate) from sucrose and 4-hydroxybutyrate precursors by *Burkholderia sacchari* strain DSM 17165. Bioengineering 4:36. doi: 10.3390/bioengineering4020036

Mitchell CG, Dawes EA (1982) The role of oxygen in the regulation of glucose metabolism, transport and the tricarboxylic acid cycle in *Pseudomonas aeruginosa*. Microbiology 128:49–59. doi: 10.1099/00221287-128-1-49

Modi S, Koelling K, Vodovotz Y (2011) Assessment of PHB with varying hydroxyvalerate content for potential packaging applications. Eur Polym J 47:179–186. doi: 10.1016/j.eurpolymj.2010.11.010

Morgan-Sagastume F, Heimersson S, Laera G, Werker A, Svanström M (2016) Techno-environmental assessment of integrating polyhydroxyalkanoate (PHA) production with services of municipal wastewater treatment. J Clean Prod 137:1368–1381. doi: 10.1016/j.jclepro.2016.08.008

Moustogianni A, Bellou S, Triantaphyllidou I-E, Aggelis G (2015) Feasibility of raw glycerol conversion into single cell oil by *Zygomycetes* under non-aseptic conditions: Glycerol conversion into single cell oil. Biotechnol Bioeng 112:827–831. doi: 10.1002/bit.25482

Możejko J, Ciesielski S (2014) Pulsed feeding strategy is more favorable to medium-chain-length polyhydroxyalkanoates production from waste rapeseed oil. Biotechnol Prog 30:1243–1246. doi: 10.1002/btpr.1914

Możejko-Ciesielska J, Kiewisz R (2016) Bacterial polyhydroxyalkanoates: Still fabulous? Microbiol Res 192:271–282. doi: 10.1016/j.micres.2016.07.010

Mozumder MdSI, De Wever H, Volcke EIP, Garcia-Gonzalez L (2014) A robust fed-batch feeding strategy independent of the carbon source for optimal polyhydroxybutyrate production. Process Biochem 49:365–373. doi: 10.1016/j.procbio.2013.12.004

Mumtaz T, Rahman NA, Yee PL, Shirai Y, Hassan MA (2009) Fed-batch production of P(3HB-co-3HV) copolymer by *Comamonas* sp. EB 172 using mixed organic acids under dual nutrient limitation. Eur J Sci Res 33:374–384.

Myshkina VL, Nikolaeva DA, Makhina TK, Bonartsev AP, Bonartseva GA (2008) Effect of growth conditions on the molecular weight of poly-3-hydroxybutyrate produced by *Azotobacter chroococcum* 7B. Appl Biochem Microbiol 44:482–486. doi: 10.1134/S0003683808050050

Nakazawa T (2002) Travels of a *Pseudomonas*, from Japan around the world. Environ Microbiol 4:782–786. doi: 10.1046/j.1462-2920.2002.00310.x

Nath A, Dixit M, Bandiya A, Chavda S, Desai AJ (2008) Enhanced PHB production and scale up studies using cheese whey in fed batch culture of *Methylobacterium* sp. ZP24. Bioresour Technol 99:5749–5755. doi: 10.1016/j.biortech.2007.10.017

Nelson DL, Lehninger AL, Cox MM (2008) Lehninger Principles of Biochemistry, 5th edn. W.H. Freeman and Company, New York

Nerkar M, Ramsay JA, Ramsay BA, Kontopoulou M (2014) Melt Compounded Blends of Short and Medium Chain-Length Poly-3-hydroxyalkanoates. J Polym Environ 22:236–243. doi: 10.1007/s10924-013-0635-6

Newton JM, Schofield D, Vlahopoulou J, Zhou Y (2016) Detecting cell lysis using viscosity monitoring in *E. coli* fermentation to prevent product loss. Biotechnol Prog 32:1069–1076. doi: 10.1002/btpr.2292

Newton JM, Vlahopoulou J, Zhou Y (2017) Investigating and modelling the effects of cell lysis on the rheological properties of fermentation broths. Biochem Eng J 121:38–48. doi: 10.1016/j.bej.2017.01.009

Nikel PI, de Lorenzo V (2013) Engineering an anaerobic metabolic regime in *Pseudomonas putida* KT2440 for the anoxic biodegradation of 1,3-dichloroprop-1-ene. Metab Eng 15:98–112. doi: 10.1016/j.ymben.2012.09.006

Nikodinovic-Runic J, Guzik M, Kenny ST, Babu R, Werker A, O Connor KE (2013) Carbon-rich wastes as feedstocks for biodegradable polymer (polyhydroxyalkanoate) production using bacteria. In: Advances in Applied Microbiology. Elsevier, pp 139–200

Noda I, Lindsey SB, Caraway D (2010) Nodax™ Class PHA Copolymers: Their Properties and Applications. In: Chen GG-Q (ed) Plastics from Bacteria. Springer Berlin Heidelberg, Berlin, Heidelberg, pp 237–255.

Oldshue JY (1997) Heed this advice in scaling up mixers. Chem Eng Prog 93:70–74.

Olle B, Bucak S, Holmes TC, Bromberg L, Hatton TA, Wang DIC (2006) Enhancement of Oxygen Mass Transfer Using Functionalized Magnetic Nanoparticles. Ind Eng Chem Res 45:4355–4363. doi: 10.1021/ie051348b

Park SJ, Park JP, Lee SY (2002) Production of poly(3-hydroxybutyrate) from whey by fed-batch culture of recombinant *Escherichia coli* in a pilot-scale fermenter. Biotechnol Lett 24:185–189. doi: 10.1023/A:1014196906095

Peña C, López S, García A, Espín G, Romo-Uribe A, Segura D (2014) Biosynthesis of poly-β-hydroxybutyrate (PHB) with a high molecular mass by a mutant strain of *Azotobacter vinelandii* (OPN). Ann Microbiol 64:39–47. doi: 10.1007/s13213-013-0630-0

Philp JC, Ritchie RJ, Guy K (2013) Biobased plastics in a bioeconomy. Trends Biotechnol 31:65–67. doi: 10.1016/j.tibtech.2012.11.009

Poblete-Castro I, Becker J, Dohnt K, dos Santos VM, Wittmann C (2012a) Industrial biotechnology of *Pseudomonas putida* and related species. Appl Microbiol Biotechnol 93:2279–2290. doi: 10.1007/s00253-012-3928-0

Poblete-Castro I, Binger D, Oehlert R, Rohde M (2014a) Comparison of mcl-poly(3-hydroxyalkanoates) synthesis by different *Pseudomonas putida* strains from crude glycerol: citrate accumulates at high titer under PHA-producing conditions. BMC Biotechnol 14. doi: 10.1186/s12896-014-0110-z

Poblete-Castro I, Escapa IF, Jäger C, Puchalka J, Chi Lam C, Schomburg D, Prieto M, Martins dos Santos VA (2012b) The metabolic response of *P. putida* KT2442 producing high

levels of polyhydroxyalkanoate under single- and multiple-nutrient-limited growth: Highlights from a multi-level omics approach. Microb Cell Factories 11:34. doi: 10.1186/1475-2859-11-34

Poblete-Castro I, Rodriguez AL, Lam CMC, Kessler W (2014b) Improved production of medium-chain-length polyhydroxyalkanoates in glucose-based fed-batch cultivations of metabolically engineered *Pseudomonas putida* strains. J Microbiol Biotechnol 24:59–69. doi: 10.4014/jmb.1308.08052

Poli A, Di Donato P, Abbamondi GR, Nicolaus B (2011) Synthesis, Production, and Biotechnological Applications of Exopolysaccharides and Polyhydroxyalkanoates by Archaea. Archaea 2011:1–13. doi: 10.1155/2011/693253

Pozo C, Martínez-Toledo MV, Rodelas B, González-López J (2002) Effects of culture conditions on the production of polyhydroxyalkanoates by *Azotobacter chroococcum* H23 in media containing a high concentration of alpechín (wastewater from olive oil mills) as primary carbon source. J Biotechnol 97:125–131. doi: 10.1016/S0168-1656(02)00056-1

Pradella JG da C, Ienczak JL, Delgado CR, Taciro MK (2012) Carbon source pulsed feeding to attain high yield and high productivity in poly(3-hydroxybutyrate) (PHB) production from soybean oil using *Cupriavidus necator*. Biotechnol Lett 34:1003–1007. doi: 10.1007/s10529-012-0863-1

Pradella JG da C, Taciro MK, Mateus AYP (2010) High-cell-density poly (3-hydroxybutyrate) production from sucrose using *Burkholderia sacchari* culture in airlift bioreactor. Bioresour Technol 101:8355–8360. doi: 10.1016/j.biortech.2010.05.046

Pratt S, Werker A, Morgan-Sagastume F, Lant P (2012) Microaerophilic conditions support elevated mixed culture polyhydroxyalkanoate (PHA) yields, but result in decreased PHA production rates. Water Sci Technol 65:243. doi: 10.2166/wst.2012.086

Pratt S, Yuan Z, Gapes D, Dorigo M, Zeng RJ, Keller J (2003) Development of a novel titration and off-gas analysis (TOGA) sensor for study of biological processes in wastewater treatment systems. Biotechnol Bioeng 81:482–495. doi: 10.1002/bit.10490

Preusting H, Hazenberg W, Witholt B (1993a) Continuous production of poly(3-hydroxyalkanoates) by *Pseudomonas oleovorans* in a high-cell-density, two-liquid-phase chemostat. Enzyme Microb Technol 15:311–316. doi: 10.1016/0141-0229(93)90156-V

Preusting H, van Houten R, Hoefs A, van Langenberghe EK, Favre-Bulle O, Witholt B (1993b) High cell density cultivation of *Pseudomonas oleovorans*: Growth and production of poly (3-hydroxyalkanoates) in two-liquid phase batch and fed-batch systems. Biotechnol Bioeng 41:550–556. doi: 10.1002/bit.260410507

Prieto A, Escapa IF, Martínez V, Dinjaski N, Herencias C, de la Peña F, Tarazona N, Revelles O (2016) A holistic view of polyhydroxyalkanoate metabolism in *Pseudomonas putida*. Environ Microbiol 18:341–357. doi: 10.1111/1462-2920.12760

Puthli MS, Rathod VK, Pandit AB (2005) Gas–liquid mass transfer studies with triple impeller system on a laboratory scale bioreactor. Biochem Eng J 23:25–30. doi: 10.1016/j.bej.2004.10.006

Quillaguamán J, Doan-Van T, Guzmán H, Guzmán D, Martín J, Everest A, Hatti-Kaul R (2008) Poly(3-hydroxybutyrate) production by *Halomonas boliviensis* in fed-batch culture. Appl Microbiol Biotechnol 78:227–232. doi: 10.1007/s00253-007-1297-x

Quillaguamán J, Hashim S, Bento F, Mattiasson B, Hatti-Kaul R (2005) Poly(β-hydroxybutyrate) production by a moderate halophile, *Halomonas boliviensis* LC1 using starch hydrolysate as substrate. J Appl Microbiol 99:151–157. doi: 10.1111/j.1365-2672.2005.02589.x

Ramsay BA, Lomaliza K, Chavarie C, Dubé B, Ramsay JA (1990) Production of poly-(beta-hydroxybutyric-co-beta-hydroxyvaleric) acids. Appl Environ Microbiol 56:2093–2098

Ramsay BA, Saracovan I, Ramsay JA, Marchessault RH (1991) Continuous production of long-side-chain poly-3-hydroxyalkanoates by *Pseudomonas oleovorans*. Appl Environ Microbiol 57:625–629.

Ravindran R, Jaiswal AK (2016) Exploitation of food industry waste for high-value products. Trends Biotechnol 34:58–69. doi: 10.1016/j.tibtech.2015.10.008

Raza ZA, Abid S, Banat IM (2018) Polyhydroxyalkanoates: Characteristics, production, recent developments and applications. Int Biodeterior Biodegrad 126:45–56. doi: 10.1016/j.ibiod.2017.10.001

Read RR, Costerton JW (1987) Purification and characterization of adhesive exopolysaccharides from *Pseudomonas putida* and *Pseudomonas fluorescens*. Can J Microbiol 33:1080–1090. doi: 10.1139/m87-189

Reddy CSK, Ghai R, Rashmi, Kalia VC (2003) Polyhydroxyalkanoates: an overview. Bioresour Technol 87:137–146. doi: 10.1016/S0960-8524(02)00212-2

Regenhardt D, Heuer H, Heim S, Fernandez DU, Strompl C, Moore ERB, Timmis KN (2002) Pedigree and taxonomic credentials of *Pseudomonas putida* strain KT2440. Environ Microbiol 4:912–915. doi: 10.1046/j.1462-2920.2002.00368.x

Reis MAM, Serafim LS, Lemos PC, Ramos AM, Aguiar FR, Van Loosdrecht MCM (2003) Production of polyhydroxyalkanoates by mixed microbial cultures. Bioprocess Biosyst Eng 25:377–385. doi: 10.1007/s00449-003-0322-4

Ren Q, de Roo G, Ruth K, Witholt B, Zinn M, Thöny-Meyer L (2009) Simultaneous accumulation and degradation of polyhydroxyalkanoates: Futile cycle or clever regulation? Biomacromolecules 10:916–922. doi: 10.1021/bm801431c

Reusch RN, Hiske TW, Sadoff HL (1986) Poly-ß-hydroxybutyrate membrane structure and its relationship to genetic transformability in *Escherichia coli*. J Bacteriol 168:553–562.

Richard A, Margaritis A (2003) Rheology, oxygen transfer, and molecular weight characteristics of poly(glutamic acid) fermentation by *Bacillus subtilis*. Biotechnol Bioeng 82:299–305. doi: 10.1002/bit.10568

Riedel SL, Bader J, Brigham CJ, Budde CF, Yusof ZAM, Rha C, Sinskey AJ (2012) Production of poly(3-hydroxybutyrate-co-3-hydroxyhexanoate) by *Ralstonia eutropha* in high cell density palm oil fermentations. Biotechnol Bioeng 109:74–83. doi: 10.1002/bit.23283

Riesenberg D, Guthke R (1999) High-cell-density cultivation of microorganisms. Appl Microbiol Biotechnol 51:422–430. doi: 10.1007/s002530051412

Rischbieter E, Schumpe A, Wunder V (1996) Gas Solubilities in Aqueous Solutions of Organic Substances. J Chem Eng Data 41:809–812. doi: 10.1021/je960039c

Rochman CM, Browne MA, Halpern BS, Hentschel BT, Hoh E, Karapanagioti HK, Rios-Mendoza LM, Takada H, Teh S, Thompson RC (2013) Policy: Classify plastic waste as hazardous. Nature 494:169–171. doi: 10.1038/494169a

Rodriguez-Perez S, Serrano A, Pantión AA, Alonso-Fariñas B (2018) Challenges of scaling-up PHA production from waste streams. A review. J Environ Manage 205:215–230. doi: 10.1016/j.jenvman.2017.09.083

Rols JL, Goma G (1991) Enhanced oxygen transfer rates in fermentation using soybean oil-in-water dispersions. Biotechnol Lett 13:7–12. doi: 10.1007/BF01033508

Royce LA, Liu P, Stebbins MJ, Hanson BC, Jarboe LR (2013) The damaging effects of short chain fatty acids on *Escherichia coli* membranes. Appl Microbiol Biotechnol 97:8317–8327. doi: 10.1007/s00253-013-5113-5

Russell JB (2007) The Energy Spilling Reactions of Bacteria and Other Organisms. J Mol Microbiol Biotechnol 13:1–11. doi: 10.1159/000103591

Ryu HW, Hahn SK, Chang YK, Chang HN (1997) Production of poly(3-hydroxybutyrate) by high cell density fed-batch culture of *Alcaligenes eutrophus* with phospate limitation. Biotechnol Bioeng 55:28–32. doi: 10.1002/(SICI)1097-0290(19970705)55:1<28::AID-BIT4>3.0.CO;2-Z

Salehizadeh H, Van Loosdrecht MCM (2004) Production of polyhydroxyalkanoates by mixed culture: recent trends and biotechnological importance. Biotechnol Adv 22:261–279. doi: 10.1016/j.biotechadv.2003.09.003

Sander R (1999) Compilation of Henry's Law Constants for Inorganic and Organic Species of Potential Importance in Environmental Chemistry. Max-Planck Institute of Chemstiry, Mainz, Germany.

Satoh H, Iwanmoto Y, Mino T, Matsuo T (1998) Activated sludge as a possible source of biodegradable plastic. Water Sci Technol 38:103–109.

Schmidt FR (2005) Optimization and scale up of industrial fermentation processes. Appl Microbiol Biotechnol 68:425–435. doi: 10.1007/s00253-005-0003-0

Schmidt M, Ienczak JL, Quines LK, Zanfonato K, Schmidell W, de Aragão GMF (2016) Poly(3-hydroxybutyrate-co-3-hydroxyvalerate) production in a system with external cell recycle and limited nitrogen feeding during the production phase. Biochem Eng J 112:130–135. doi: 10.1016/j.bej.2016.04.013

Schumpe A (1993) The estimation of gas solubilities in salt solutions. Chem Eng Sci 48:153–158. doi: 10.1016/0009-2509(93)80291-W

Schumpe A, Quicker G, Deckwer W-D (1982) Gas solubilities in microbial culture media. In: Reaction Engineering. Springer Berlin Heidelberg, Berlin, Heidelberg, pp 1–38.

Senior PJ, Beech GA, Ritchie GAF, Dawes EA (1972) The role of oxygen limitation in the formation of poly-β-hydroxybutyrate during batch and continuous culture of *Azotobacter beijerinckii*. Biochem J 128:1193–1201. doi: 10.1042/bj1281193

Senior PJ, Dawes EA (1971) Poly-β-hydroxybutyrate biosynthesis and the regulation of glucose metabolism in *Azotobacter beijerinckii*. Biochem J 125:55–66. doi: 10.1042/bj1250055

Senior PJ, Dawes EA (1973) The regulation of poly-β-hydroxybutyrate metabolism in *Azotobacter beijerinckii*. Biochem J 134:225–238. doi: 10.1042/bj1340225

Serafim LS, Lemos PC, Albuquerque MGE, Reis MAM (2008) Strategies for PHA production by mixed cultures and renewable waste materials. Appl Microbiol Biotechnol 81:615–628. doi: 10.1007/s00253-008-1757-y

Shahzad K, Kettl K-H, Titz M, Koller M, Schnitzer H, Narodoslawsky M (2013) Comparison of ecological footprint for biobased PHA production from animal residues utilizing different energy resources. Clean Technol Environ Policy 15:525–536. doi: 10.1007/s10098-013-0608-4

Shang L, Jiang M, Chang HN (2003a) Poly(3-hydroxybutyrate) synthesis in fed-batch culture of *Ralstonia eutropha* with phosphate limitation under different glucose concentrations. Biotechnol Lett 25:1415–1419.

Shang L, Jiang M, Ryu CH, Chang HN, Cho SH, Lee JW (2003b) Inhibitory effect of carbon dioxide on the fed-batch culture of *Ralstonia eutropha*: Evaluation by CO_2 pulse injection and autogenous CO_2 methods. Biotechnol Bioeng 83:312–320. doi: 10.1002/bit.10670

Shang L, Jiang M, Yun Z, Yan H-Q, Chang H-N (2008) Mass production of medium-chain-length poly(3-hydroxyalkanoates) from hydrolyzed corn oil by fed-batch culture of *Pseudomonas putida*. World J Microbiol Biotechnol 24:2783–2787. doi: 10.1007/s11274-008-9808-1

Shantini K, Yahya ARM, Amirul AA (2015) Influence of feeding and controlled dissolved oxygen level on the production of poly(3-hydroxybutyrate-co-3-hydroxyvalerate)

copolymer by *Cupriavidus* sp. USMAA2-4 and its characterization. Appl Biochem Biotechnol 176:1315–1334. doi: 10.1007/s12010-015-1648-5

Sharma PK, Fu J, Cicek N, Sparling R, Levin DB (2012) Kinetics of medium-chain-length polyhydroxyalkanoate production by a novel isolate of *Pseudomonas putida* LS46. Can J Microbiol 58:982–989. doi: 10.1139/w2012-074

Sharma PK, Fu J, Zhang X, Fristensky BW, Davenport K, Chain PSG, Sparling R, Levin DB (2013) Draft Genome Sequence of Medium-Chain-Length Polyhydroxyalkanoate-Producing *Pseudomonas putida* Strain LS46. Genome Announc 1. doi: 10.1128/genomeA.00151-13

Sharma U, Cicek N, Fu J, Sparling R, Levin DB (2014) Effects of media sterilization and variable carbon-loading on medium-chain length PHA (bio-plastics) production by *Pseudomonas putida* LS46 using biodiesel derived glycerol. American Society of Agricultural and Biological Engineers, pp 1–13.

Shi H, Shiraishi M, Shimizu K (1997) Metabolic flux analysis for biosynthesis of poly(β-hydroxybutyric acid) in *Alcaligenes eutrophus* from various carbon sources. J Ferment Bioeng 84:579–587. doi: 10.1016/S0922-338X(97)81915-0

Silva DA da, Antonio RV, Rossi JM, Pena R da S (2014) Production of medium-chain-length polyhydroxyalkanoate by *Pseudomonas oleovorans* grown in sugary cassava extract supplemented with andiroba oil. Food Sci Technol Camp 34:738–745. doi: 10.1590/1678-457X.6465

Singhaboot P, Kaewkannetra P (2015) A higher in value biopolymer product of polyhydroxyalkanoates (PHAs) synthesized by *Alcaligenes latus* in batch/repeated batch fermentation processes of sugar cane juice. Ann Microbiol 65:2081–2089. doi: 10.1007/s13213-015-1046-9

Sohn SB, Kim TY, Park JM, Lee SY (2010) *In silico* genome-scale metabolic analysis of *Pseudomonas putida* KT2440 for polyhydroxyalkanoate synthesis, degradation of aromatics and anaerobic survival. Biotechnol J 5:739–750. doi: 10.1002/biot.201000124

Song JH, Jeon CO, Choi MH, Yoon SC, Park W (2008) Polyhydroxyalkanoate (PHA) production using waste vegetable oil by *Pseudomonas* sp. strain DR2. J Microbiol Biotechnol 18:1408–1415.

Spaans SK, Weusthuis RA, van der Oost J, Kengen SWM (2015) NADPH-generating systems in bacteria and archaea. Front Microbiol 6. doi: 10.3389/fmicb.2015.00742

Stolper DA, Revsbech NP, Canfield DE (2010) Aerobic growth at nanomolar oxygen concentrations. Proc Natl Acad Sci 107:18755–18760. doi: 10.1073/pnas.1013435107

Stumm W, Morgan JJ (1995) Chapter 4: Dissolved carbon dioxide. In: Aquatic Chemistry: Chemical Equilibria and Rates in Natural Waters, 3rd edn. p 1040.

Sudesh K, Abe H, Doi Y (2000) Synthesis, structure and properties of polyhydroxyalkanoates: biological polyesters. Prog Polym Sci 25:1503–1555. doi: 10.1016/S0079-6700(00)00035-6

Sun Z, Ramsay JA, Guay M, Ramsay BA (2009a) Enhanced yield of medium-chain-length polyhydroxyalkanoates from nonanoic acid by co-feeding glucose in carbon-limited, fed-batch culture. J Biotechnol 143:262–267. doi: 10.1016/j.jbiotec.2009.07.014

Sun Z, Ramsay JA, Guay M, Ramsay BA (2007a) Carbon-limited fed-batch production of medium-chain-length polyhydroxyalkanoates from nonanoic acid by *Pseudomonas putida* KT2440. Appl Microbiol Biotechnol 74:69–77. doi: 10.1007/s00253-006-0655-4

Sun Z, Ramsay JA, Guay M, Ramsay BA (2009b) Fed-batch production of unsaturated medium-chain-length polyhydroxyalkanoates with controlled composition by *Pseudomonas putida* KT2440. Appl Microbiol Biotechnol 82:657–662. doi: 10.1007/s00253-008-1785-7

Sun Z, Ramsay JA, Guay M, Ramsay BA (2006) Automated feeding strategies for high-cell-density fed-batch cultivation of *Pseudomonas putida* KT2440. Appl Microbiol Biotechnol 71:423–431. doi: 10.1007/s00253-005-0191-7

Sun Z, Ramsay JA, Guay M, Ramsay BA (2007b) Fermentation process development for the production of medium-chain-length poly-3-hyroxyalkanoates. Appl Microbiol Biotechnol 75:475–485. doi: 10.1007/s00253-007-0857-4

Suzuki T, Yamane T, Shimizu S (1986) Mass production of poly-β-hydroxybutyric acid by fed-batch culture with controlled carbon/nitrogen feeding. Appl Microbiol Biotechnol 24:370–374. doi: 10.1007/BF00294592

Tabone MD, Cregg JJ, Beckman EJ, Landis AE (2010) Sustainability Metrics: Life Cycle Assessment and Green Design in Polymers. Environ Sci Technol 44:8264–8269. doi: 10.1021/es101640n

Takabatake H, Satoh H, Mino T, Matsuo T (2000) Recovery of biodegradable plastics from activated sludge process. Water Sci Technol 42:351–356.

Tan D, Xue Y-S, Aibaidula G, Chen G-Q (2011) Unsterile and continuous production of polyhydroxybutyrate by *Halomonas* TD01. Bioresour Technol 102:8130–8136. doi: 10.1016/j.biortech.2011.05.068

Teuten EL, Saquing JM, Knappe DRU, Barlaz MA, Jonsson S, Bjorn A, Rowland SJ, Thompson RC, Galloway TS, Yamashita R, Ochi D, Watanuki Y, Moore C, Viet PH, Tana TS, Prudente M, Boonyatumanond R, Zakaria MP, Akkhavong K, Ogata Y, Hirai H, Iwasa S, Mizukawa K, Hagino Y, Imamura A, Saha M, Takada H (2009) Transport and release of chemicals from plastics to the environment and to wildlife. Philos Trans R Soc B Biol Sci 364:2027–2045. doi: 10.1098/rstb.2008.0284

Thinagaran L, Sudesh K (2017) Evaluation of sludge palm oil as feedstock and development of efficient method for its utilization to produce polyhydroxyalkanoate. Waste Biomass Valorization. doi: 10.1007/s12649-017-0078-8

Third KA, Newland M, Cord-Ruwisch R (2003) The effect of dissolved oxygen on PHB accumulation in activated sludge cultures. Biotechnol Bioeng 82:238–250. doi: 10.1002/bit.10564

Thompson RC, Moore CJ, vom Saal FS, Swan SH (2009a) Plastics, the environment and human health: current consensus and future trends. Philos Trans R Soc B Biol Sci 364:2153–2166. doi: 10.1098/rstb.2009.0053

Thompson RC, Swan SH, Moore CJ, vom Saal FS (2009b) Our plastic age. Philos Trans R Soc B Biol Sci 364:1973–1976. doi: 10.1098/rstb.2009.0054

Tortajada M, Ferreira da Silva L, Auxiliadora Prieto M (2013) Second-generation functionalized medium chain-length polyhydroxyalkanoates: the gateway to high-value bioplastic applications. Int Microbiol 1–15. doi: 10.2436/20.1501.01.175

Tripathi L, Wu L-P, Dechuan M, Chen J, Wu Q, Chen G-Q (2013) *Pseudomonas putida* KT2442 as a platform for the biosynthesis of polyhydroxyalkanoates with adjustable monomer contents and compositions. Bioresour Technol 142:225–231. doi: 10.1016/j.biortech.2013.05.027

Tseng CP, Albrecht J, Gunsalus RP (1996) Effect of microaerophilic cell growth conditions on expression of the aerobic (cyoABCDE and cydAB) and anaerobic (narGHJI, frdABCD, and dmsABC) respiratory pathway genes in *Escherichia coli*. J Bacteriol 178:1094–1098.

Van Loosdrecht MCM, Pot MA, Heijnen JJ (1997) Importance of bacterial storage polymers in bioprocesses. Water Sci Technol 35. doi: 10.1016/S0273-1223(96)00877-3

van Wegen RJ, Lee S-Y, Middelberg APJ (2001) Metabolic and kinetic analysis of poly(3-hydroxybutyrate) production by recombinant *Escherichia coli*. Biotechnol Bioeng 74:70–81. doi: 10.1002/bit.1096

Van Wegen RJ, Ling Y, Middelberg APJ (1998) Industrial production of polyhydroxyalkanoates using *Escherichia coli*: An economic analysis. Chem Eng Res Des 76:417–426. doi: 10.1205/026387698524848

Vendruscolo F, Rossi MJ, Schmidell W, Ninow JL (2012) Determination of oxygen solubility in liquid media. ISRN Chem Eng 2012:1–5. doi: 10.5402/2012/601458

Viles FJ, Silverman L (1949) Determination of Starch and Cellulose with Anthrone. Anal Chem 21:950–953. doi: 10.1021/ac60032a019

Vjayan T, Vadivelu VM (2017) Effect of famine-phase reduced aeration on polyhydroxyalkanoate accumulation in aerobic granules. Bioresour Technol 245:970–976. doi: 10.1016/j.biortech.2017.09.038

Wallace T, Gibbons D, O'Dwyer M, Curran TP (2017) International evolution of fat, oil and grease (FOG) waste management – A review. J Environ Manage 187:424–435. doi: 10.1016/j.jenvman.2016.11.003

Wallen LL, Rohwedder WK (1974) Poly-beta-hydroxyalkanoate from activated sludge. Environ Sci Technol 8:576–579

Wang F, Lee SY (1997a) Production of poly(3-hydroxybutyrate) by fed-batch culture of filamentation-suppressed recombinant *Escherichia coli*. Appl Environ Microbiol 63:4765–4769.

Wang F, Lee SY (1998) High cell density culture of metabolically engineered *Escherichia coli* for the production of poly(3-hydroxybutyrate) in a defined medium. Biotechnol Bioeng 58:325–328. doi: 10.1002/(SICI)1097-0290(19980420)58:2/3<325::AID-BIT33>3.0.CO;2-8

Wang F, Lee SY (1997b) Poly(3-hydroxybutyrate) production with high productivity and high polymer content by a fed-batch culture of *Alcaligenes latus* under nitrogen limitation. Appl Environ Microbiol 63:3703–3706.

Wang X, Oehmen A, Freitas EB, Carvalho G, Reis MAM (2017) The link of feast-phase dissolved oxygen (DO) with substrate competition and microbial selection in PHA production. Water Res 112:269–278. doi: 10.1016/j.watres.2017.01.064

Wang Y, Yin J, Chen G-Q (2014) Polyhydroxyalkanoates, challenges and opportunities. Curr Opin Biotechnol 30:59–65. doi: 10.1016/j.copbio.2014.06.001

Ward AC, Rowley BI, Dawes EA (1977) Effect of oxygen and nitrogen limitation on poly-hydroxybutyrate biosynthesis in ammonium-grown *Azotobacter beijerinckii*. J Gen Microbiol 102:61–68. doi: 10.1099/00221287-102-1-61

Weisenberger S, Schumpe A (1996) Estimation of gas solubilities in salt solutions at temperatures from 273 K to 363 K. AIChE J 42:298–300. doi: 10.1002/aic.690420130

Wendlandt K-D, Jechorek M, Helm J, Stottmeister U (2001) Producing poly-3-hydroxybutyrate with a high molecular mass from methane. J Biotechnol 86:127–133. doi: 10.1016/S0168-1656(00)00408-9

Weusthuis RA, Huijberts GNM, Eggink G (1997) Production of mcl-poly (hydroxyalkanoates) (review). In: 1996 International Symposium on Bacterial Polyhydroxyalkanoates. NRC Research Press, Ottawa, pp 102–109.

Whitman WG (1962) The two-film theory of gas absorption. Int J Heat Mass Transf 5:429–433.

Wong HH, Lee SY (1998) Poly-(3-hydroxybutyrate) production from whey by high-density cultivation of recombinant *Escherichia coli*. Appl Microbiol Biotechnol 50:30–33. doi: 10.1007/s002530051252

Woo S-H, Kim J-H, Ni Y-Y, Rhee Y-H (2012) Biosynthesis of Copolyesters Consisting of 3-Hydroxyvalerate and Medium-chain-length 3-hydroxyalkanoates by the *Pseudomonas aeruginosa* P-5 Strain. Korean J Microbiol 48:200–206. doi: 10.7845/kjm.2012.031

Worm B, Lotze HK, Jubinville I, Wilcox C, Jambeck J (2017) Plastic as a Persistent Marine Pollutant. Annu Rev Environ Resour 42:1–26. doi: 10.1146/annurev-environ-102016-060700

Yamane T, Fukunaga M, Lee YW (1996) Increased PHB productivity by high-cell-density fed-batch culture of *Alcaligenes latus*, a growth-associated PHB producer. Biotechnol Bioeng 50:197–202. doi: 10.1002/(SICI)1097-0290(19960420)50:2<197::AID-BIT8>3.0.CO;2-H

Yang TH, Wittmann C, Heinzle E (2003) Dynamic calibration and dissolved gas analysis using membrane inlet mass spectrometry for the quantification of cell respiration. Rapid Commun Mass Spectrom 17:2721–2731. doi: 10.1002/rcm.1251

Yarsley E, Couzens EG (1945) Plastics. Penguin Books, London.

Yates MR, Barlow CY (2013) Life cycle assessments of biodegradable, commercial biopolymers—A critical review. Resour Conserv Recycl 78:54–66. doi: 10.1016/j.resconrec.2013.06.010

Ye J, Huang W, Wang D, Chen F, Yin J, Li T, Zhang H, Chen G-Q (2018) Pilot scale-up of poly(3-hydroxybutyrate- *co* -4-hydroxybutyrate) production by *Halomonas bluephagenesis* via cell growth adapted optimization process. Biotechnol J 13:1800074. doi: 10.1002/biot.201800074

Yue H, Ling C, Yang T, Chen X, Chen Y, Deng H, Wu Q, Chen J, Chen G-Q (2014) A seawater-based open and continuous process for polyhydroxyalkanoates production by recombinant *Halomonas campaniensis* LS21 grown in mixed substrates. Biotechnol Biofuels 7:108. doi: 10.1186/1754-6834-7-108

Zafar Mohd, Kumar S, Kumar S, Dhiman AK (2012) Modeling and optimization of poly(3hydroxybutyrate-co-3hydroxyvalerate) production from cane molasses by *Azohydromonas lata* MTCC 2311 in a stirred-tank reactor: effect of agitation and aeration regimes. J Ind Microbiol Biotechnol 39:987–1001. doi: 10.1007/s10295-012-1102-4

Zheng Y, Yanful EK, Bassi AS (2005) A Review of Plastic Waste Biodegradation. Crit Rev Biotechnol 25:243–250. doi: 10.1080/07388550500346359

Zhu C, Nomura CT, Perrotta JA, Stipanovic AJ, Nakas JP (2009) Production and characterization of poly-3-hydroxybutyrate from biodiesel-glycerol by *Burkholderia cepacia* ATCC 17759. Biotechnol Prog NA-NA. doi: 10.1002/btpr.355

Zimmermann HF, Anderlei T, Büchs J, Binder M (2006) Oxygen limitation is a pitfall during screening for industrial strains. Appl Microbiol Biotechnol 72:1157–1160. doi: 10.1007/s00253-006-0414-6

Zinn M, Durner R, Zinn H, Ren Q, Egli T, Witholt B (2011) Growth and accumulation dynamics of poly(3-hydroxyalkanoate) (PHA) in *Pseudomonas putida* GPo1 cultivated in continuous culture under transient feed conditions. Biotechnol J 6:1240–1252. doi: 10.1002/biot.201100219

Zinn M, Weilenmann H-U, Hany R, Schmid M, Egli Th (2003) Tailored synthesis of poly([R]-3-hydroxybutyrate-co-3-hydroxyvalerate) (PHB/HV) in *Ralstonia eutropha* DSM 428. Acta Biotechnol 23:309–316. doi: 10.1002/abio.200390039

Zinn M, Witholt B, Egli T (2001) Occurrence, synthesis and medical application of bacterial polyhydroxyalkanoate. Adv Drug Deliv Rev 53:5–21. doi: 10.1016/S0169-409X(01)00218-6

Appendix A: Scaling up production of mcl-PHA to pilot-scale bioreactors

A.1. Preface

This work was done in the Biotransformation lab at Scion Research in Rotorua, New Zealand under the supervision of Dr. Daniel Gapes and Dr. Christophe Collet. I was invited to conduct research in their labs for a four-month period after receiving funding through an NSERC Michael Smith Foreign Study Supplement.

In this work, the pulse-feed fed batch process (described in Chapter 7) was evaluated for its robustness using larger-scale bioreactors, and a new strain (*Pseudomonas putida* mt-2) was introduced for comparison. The objectives of this work were therefore several-fold: 1) to determine if the developed methodologies could be scaled up by an order of magnitude; and 2) evaluate if the observed effect with O_2 limitation and PHA synthesis described in Chapters 4 and 5 could be extended to other *Pseudomonas* sp. or if they are a unique manifestation of LS46.

A.2. Methods

A.2.1. Medium, strains, and culturing practices

The medium and culturing practices were as defined in Chapter 7. *P. putida* mt-2 was used as a comparative strain in these studies. This strain is nearly identical to *P. putida* KT2440, except that it contains the *tol* plasmid.

A.2.2. Bioreactor setup

The efficacy of process scale-up was tested in stainless steel, sterilization in place (SIP) bioreactors with total volumes of 14 L and 152 L (Sartorius Stedim Biostat D-DCU, Göttingen, Germany). These bioreactors were equipped with three Rushton turbines (two were submersed initially and the third became submersed with feeding), 4 baffles, pH and DO electrodes, and a

ring-type sparger located underneath the impeller. The 14 L bioreactor was operated with a 7 L initial working volume, up to 1000 mbar of pressure, aeration up to 1 VVM, and agitation up to 1000 rpm. The 152 L bioreactor was operated with under similar conditions, but with an initial working volume of 70 L, maximum aeration of 0.375 VVM, and 600 rpm agitation. At this scale, aeration was limited because of excessive foaming and gas holdup encountered at higher volumetric flow rates.

Experiments were initiated with the addition of a 5% (vol vol^{-1}) inoculum, which was grown overnight in 2 L flasks with The bioreactor inoculum was prepared in 2 L flasks with 750 mL working volumes. Dissolved oxygen (DO) was maintained at 40% (for as long as possible) with a cascading mixer and by incrementing bioreactor pressure, and pH was maintained with 4 M H_2SO_4 and 4 M NaOH (10 M in the case of the 152 L bioreactor) via automated peristaltic pumps. Octanoic acid and ammonium sulfate were dosed with peristaltic pumps following the same pulse-feed procedure described above, except that pulses were fed on the basis of rising DO signals, since CO_2 measurements were not available with this bioreactor system. Due to technical constraints, octanoic acid was fed during the PHA accumulation phase using automated peristaltic pumps (replacing 4 M H_2SO_4) in response to increasing pH, typically observed during stationary phase.

A.2.3. Measurement of CDM, PHA, and residual octanoic acid

Sample treatment and determination of CDM followed the procedure outlined in Section 3.3. The PHA content was determined using the same method described in Sections 3.4 and 3.5, except that the GC used as an Agilent 6890N with a 7683 Series autosampler and an HP-5 column (30 m x 0.32 mm x 0.25 μm). Octanoic acid was determined by HPLC. Supernatants were mixed 50/50 with 75% acetonitrile, and filtered through a 0.2 μm filter, and run on an

HPLC equipped with an Agilent ZORBAX Eclipse Plus C18 column 2.1 x 50 mm, 1.8 µm. The injection volume was 2 µL and the column was maintained at a flow rate of 0.5 mL min^{-1} and temperature of 40 °C. The mobile phase consisting of eluent A (65%): water with 0.1% formic acid; and eluent B (35%) acetonitrile + 0.1% formic acid. A UV detector was used and peaks were integrated at 210 nm.

A.3. Results

A.3.1. HCD scale-up using P. putida LS46

The results for LS46 at the 14 L scale are shown in Figure A.1(a). DO dropped below detectable limits around 14 h, which is similar to the bench-scale results reported in Chapter 7. By 14 h, [X_t] and [X_r] were achieved in this reactor setup compared to previous results (Table A.1) in a non-pressurized system. This might be attributed to increased driving force for oxygen transfer by pressurization. By restricting the agitation rate to 1000 rpm in the 14 L bioreactor, the impeller tip speed (a common scale-up criterion) remained constant at 3.8 m s^{-1} in comparison with previous results reported in Chapter 7.

The $\%_{PHA}$ by 14 h was poor at only 20.6% CDM, compared to the average content of 36.9% CDM achieved in the 7 L bench-scale bioreactor. Interestingly, amongst several replicates, carbon was not readily consumed in the 14 L pressurized system after 16-18 h, either by pH-stat feeding or continued pulse feeding. The DO remained high, and further addition of carbon did not appear to increase oxygen demand. Since this state could not be recovered, the final $\%_{PHA}$ was poor at only 25.4 ± 6.4 CDM and Q_v was low (0.33 ± 0.11 g L^{-1} h^{-1}). This behavior may be due to three reasons: 1) cells must be transitioned into stationary phase gradually from a rapid growth phase; 2) DO may not be an optimal monitoring and control parameter when increased driving force is used; or 3) fundamental limitation of an essential

growth nutrient like Fe^{3+}, which was shown to be present in low concentrations at the end of the growth phase in Chapter 7.

Slightly improved results were actually noticed when the system was scaled up to the 152 L bioreactor, shown in Figure A.1(b). In this system, the DO was depleted below detectable limits by 13 h, and the culture continued to uptake carbon until 22 h, after which point DO rose and further addition of carbon had no effect. Although the growth rates and final [X_r] was somewhat lower than the 14 L scale, $\%_{PHA}$ was higher, reaching 39% CDM and resulting in Q_v of 0.46 g L^{-1} h^{-1}. From these results, the most notable difference was that the time taken to achieve maximum [X_r] was about 33% longer in the 152 L bioreactor, and growth was more linear.

A.3.2. HCD scale-up using P. putida mt-2

Interestingly, better results were achieved using *P. putida* mt-2, which are shown in Figure A.1(c). During the growth phase prior to the onset of oxygen limitation (14 h), behavior was similar in terms of non-PHA biomass production, but the PHA content was higher than the LS46 trials, resulting in higher total biomass (Table A.2). However, the main difference between the mt-2 and LS46 scale up was that after O_2-limitation, the mt-2 cultivations were both characterized by long PHA accumulation phases of up to 32 h at the 14 L scale and 47 h at the 152 L scale (total cultivation time), the via pH-based feeding method. In both cultivations, the final mcl-PHA content was more than 70% CDM. Interestingly, at both scales, the maximum volumetric productivity was observed around 21-23 h, and despite higher PHA content, appeared to decrease after this point – although the decrease was greater at the 152 L scale. Significant reductions in the non-PHA biomass were also observed after the onset of oxygen limitation (Table A.2). Although very similar final results were achieved at both scales, the 152 L bioreactor took 47 h, whereas the 14 L took 32 h – roughly a 33% increase in time.

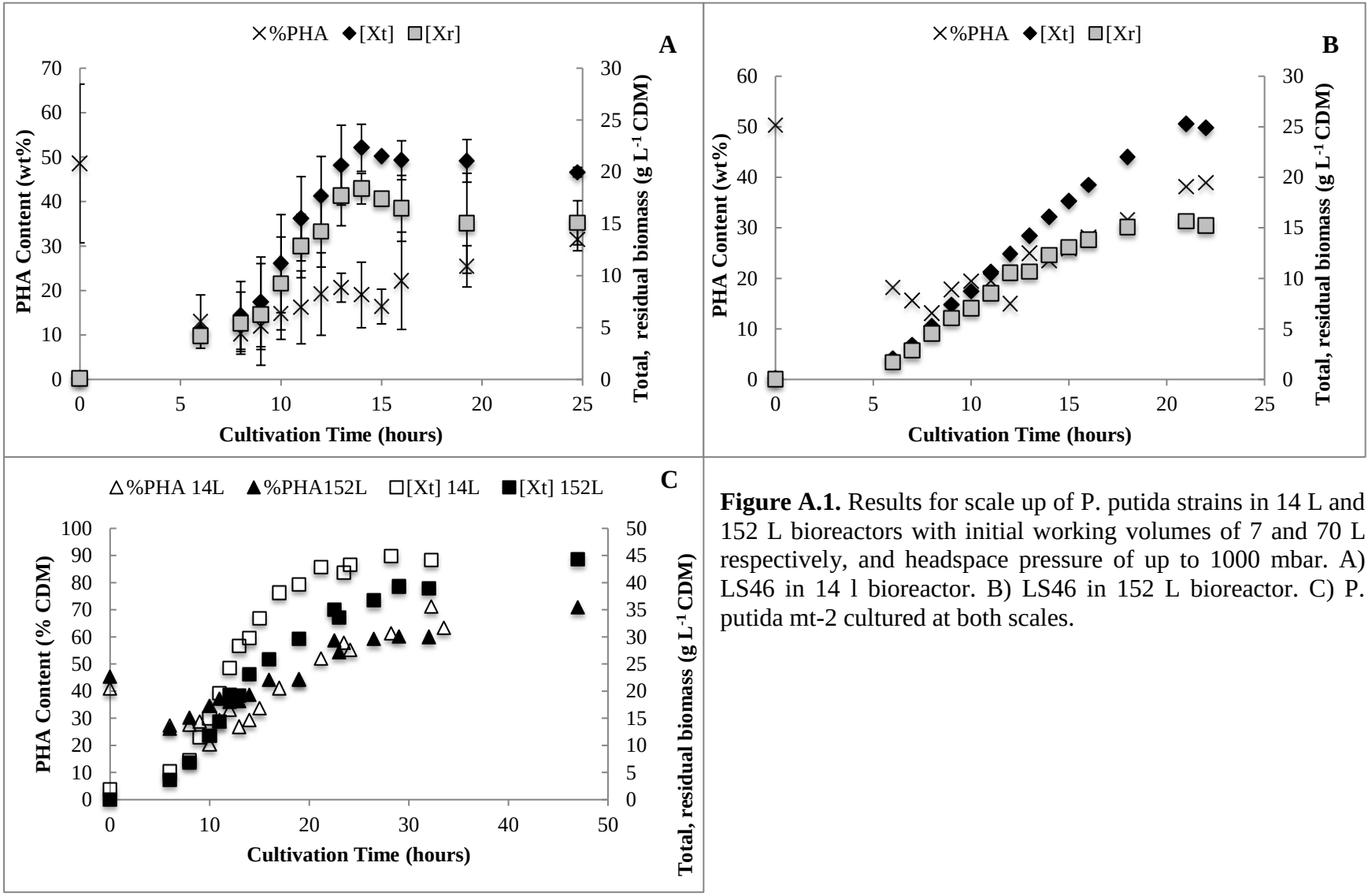

Figure A.1. Results for scale up of P. putida strains in 14 L and 152 L bioreactors with initial working volumes of 7 and 70 L respectively, and headspace pressure of up to 1000 mbar. A) LS46 in 14 l bioreactor. B) LS46 in 152 L bioreactor. C) P. putida mt-2 cultured at both scales.

Table A.1. Scale up using *P. putida* LS46.

	7L Bench-scale (Chapter 7)	14 L bioreactor	152 L bioreactor
μ_{max}	0.66	0.71	0.61
μ_{avg} (growth phase)	0.33	0.29	0.29
[X_t] at O_2 limitation (g L^{-1})	15.0 ± 2.3 (14 h)	22.3 ± 2.3 (14 h)	19.2 (13 h)
$\%_{PHA}$ at O_2 limitation (% CDM)	31.7 ± 3.8 (14 h)	19 ± 7.4 (14 h)	28.1 (13 h)
[X_r] at O_2 limitation (g L^{-1})	10.3 ± 1.1 (14 h)	18.4 ± 1.5 (14 h)	13.8 (13 h)
Final [X_t] (g L^{-1})	28.8 ± 3.9 (27 h)	21.1 ± 2.1 (19 h)	24.9 (22 h)
Final $\%_{PHA}$ (% CDM)	60.6 ± 8.2 (27 h)	25.4 ± 6.4 (19 h)	39 (22 h)
Final [X_r] (g L^{-1})	11.2 ± 1.5 (27 h)	15.1 ± 4.8 (19 h)	15.2 (22 h)
Max. [X_{PHA}] (g L^{-1})	17.7 ± 4.8 (27 h)	8.2 ± 1.4 (19 h)	9.7 (22 h)
Max Q_v (g L^{-1} h^{-1})	0.66 ± 0.14 (23 -27 h)	0.31 ± 0.09	0.46 (21 h)

Table A.2. Scale up using *P. putida* mt-2.

	14 L	**152 L**
μ_{max}	0.83	0.51
μ_{avg} (growth phase)	0.34 (0-14 h)	0.33 (0-14 h)
[X_t] at O_2 limitation (g L^{-1})	28.3 (14 h)	23.1 (14 h)
$\%_{PHA}$ at O_2 limitation (% CDM)	29.3 (14 h)	38.7 (14 h)
[X_r] at O_2 limitation (g L^{-1})	20.0 (14 h)	14.2 (14 h)
Final [X_t] (g L^{-1})	44.9 (14 h)	44.4 (47 h)
Final $\%_{PHA}$ (% CDM)	71.3 (32 h)	70.9 (47 h)
Final [X_r] (g L^{-1})	12.9 (32 h)	12.9 (47 h)
Final Q_v (g L^{-1} h^{-1})	0.99 (32h)	0.66 (47 h)
Max. [X_{PHA}] (g L^{-1})	32.0 (32 h)	31.5 (22.5 h)
Max Q_v (g L^{-1} h^{-1})	1.05 (21 h)	0.91 (21 h)

A.3.4. Characteristics uniquely distinguishing LS46 and mt-2

It should be noted that *P. putida* mt-2 also displayed some interesting characteristics compared to LS46. Most notably, the organism appeared to form granules or flocs that would rapidly settle out of suspension. *P. putida* LS46 did not display any visible settling, even after being left for 12 h. This is shown in Figure A.2, and quantified via the sludge volume index (SVI) in Figure A.3. The SVI is defined as the settled sludge volume (mL L^{-1}) normalized to the total suspended solids (in this case total biomass). The SVI after 30 minutes was initially very high and then stabilized around 20-25 before 14 h. After 14 h, the SVI decreased such that values less than 10 were obtained by 19 h.

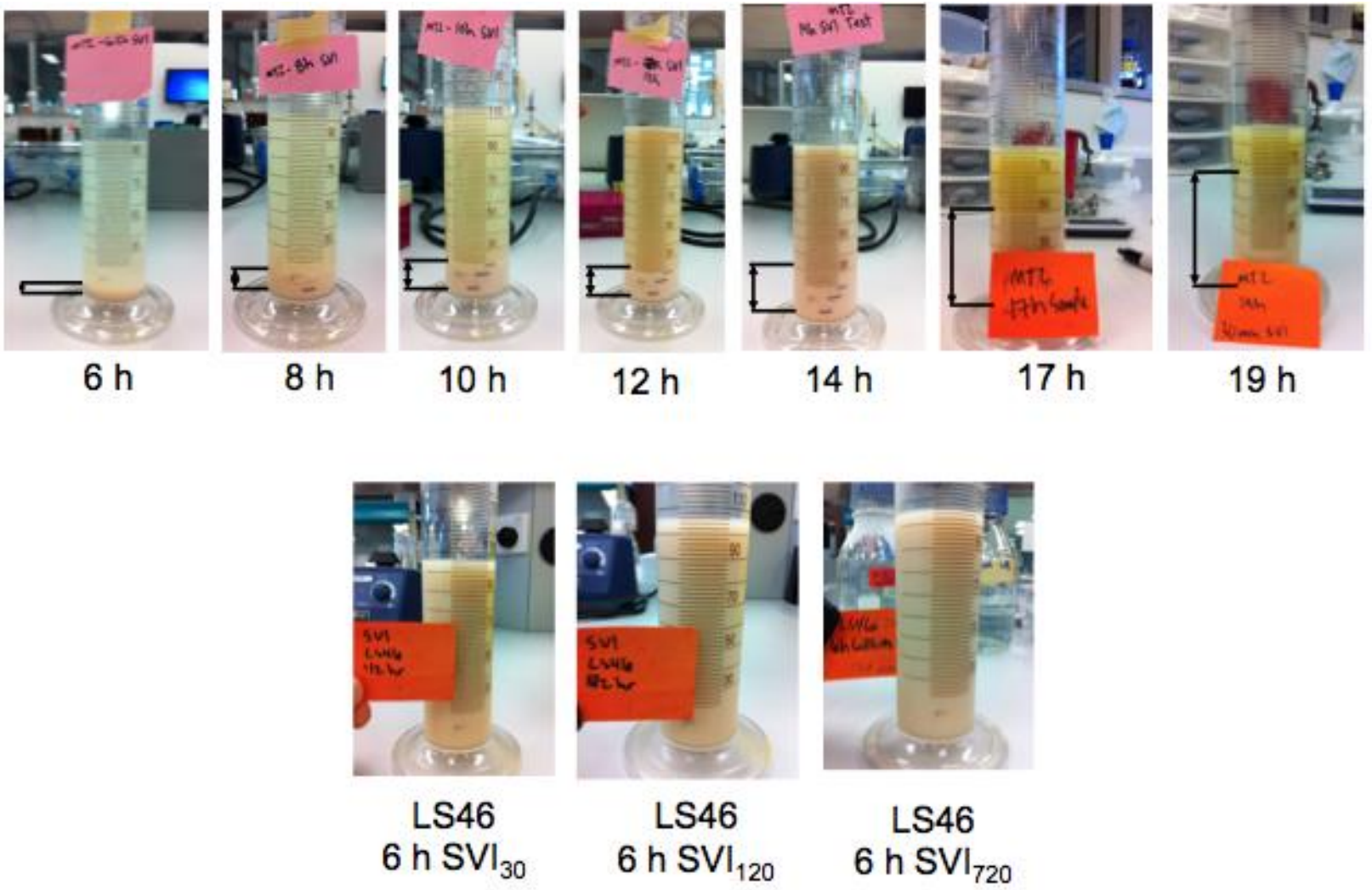

Figure A.2. Settling characteristics (after 30 minutes unless otherwise indicated) of *P. putida* mt-2 (top) and *P. putida* LS46 (bottom).

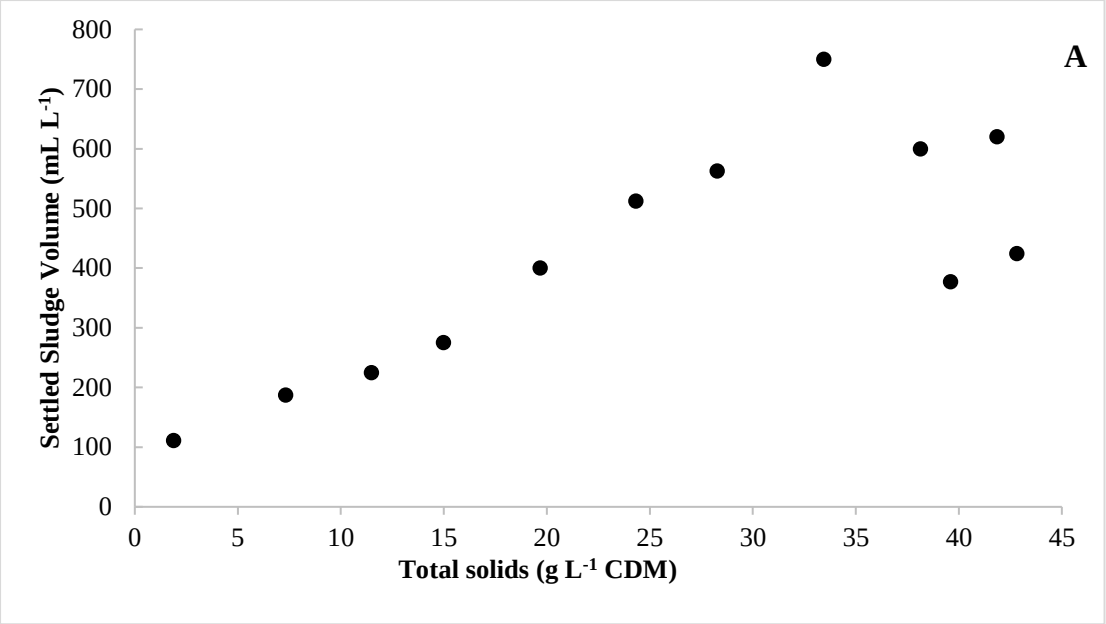

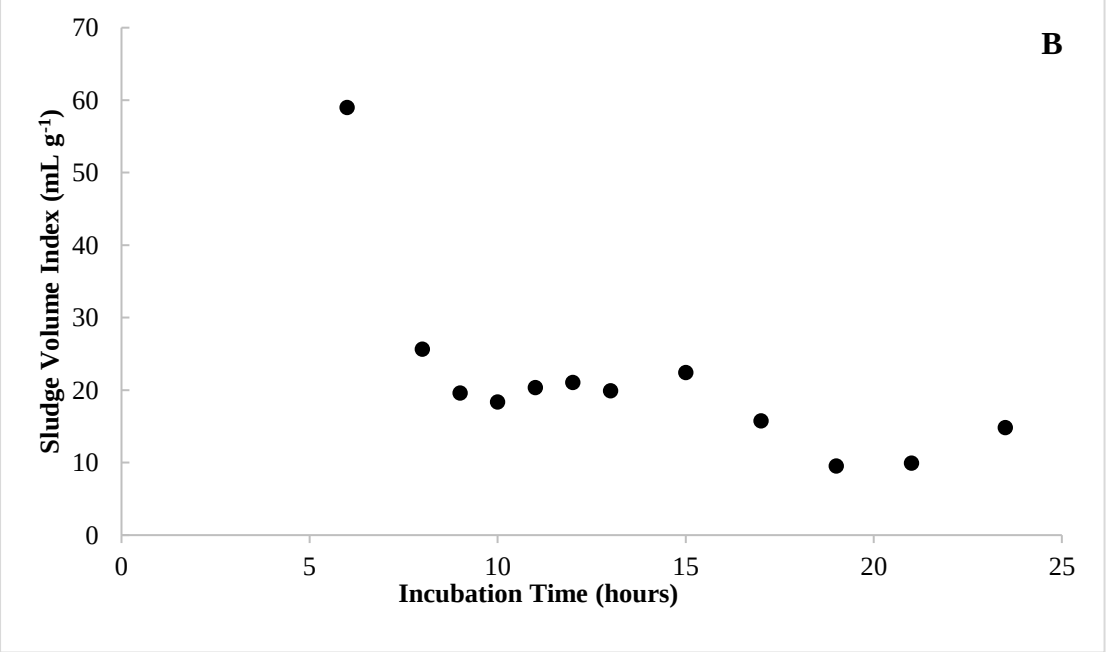

Figure A.3. A. Settled sludge volume after 30 minutes as a function of total biomass concentration **B)** SVI of *P. putida* mt-2 cultures over time.

A.4. Conclusions

Increasing the driving force by bioreactor pressurization appeared to be a viable strategy for increasing total biomass more rapidly in LS46, but it didn't appear to work well during the PHA accumulation phase, regardless of scale or whether feeding was done on the basis of pH or DO signals. This behavior was unexpected and the reasons for it remain unclear, although since slightly better overall results were achieved at the 152 L scale, it appears to be a fundamental issue and not a scale-up issue.

Curiously, *P. putida* mt-2 performed well during the PHA accumulation phase and reached total biomass of up to 45 g L^{-1} with PHA contents of over 70% CDM in both the 14 L scale and 152 L scale, and Q_v was around 1 g L^{-1} h^{-1}. However, the time required to reach these results was approximately 33% longer in the 152 L scale. This shows that: 1) good results can be achieved when the cultivation scale is increased by an order of magnitude, although more time is required to achieve the same result; and 2) and O_2-limited PHA accumulation strategy also works in other *Pseudomonas* sp., and not just LS46. In fact, the O_2-limited storage phase in this work actually appeared to work better with mt-2 than LS46 using the bioreactor setup described in this chapter.

Finally, some significant differences were observed (mostly qualitatively) on culture characteristics of mt-2 compared to LS46. Most notably was the observation that mt-2 settled out of suspension rapidly compared to LS46. This behavior could open up new process engineering opportunities, like application of SBRs with a biomass settling phase, which would have likely decreased the time of the react phase (and built higher biomass inventories with less wasted carbon) in Chapter 9.

Appendix B: Zoomed-in profile of DO and off-gas CO_2 signals for control of pulse-feed experiments (Chapter 7)

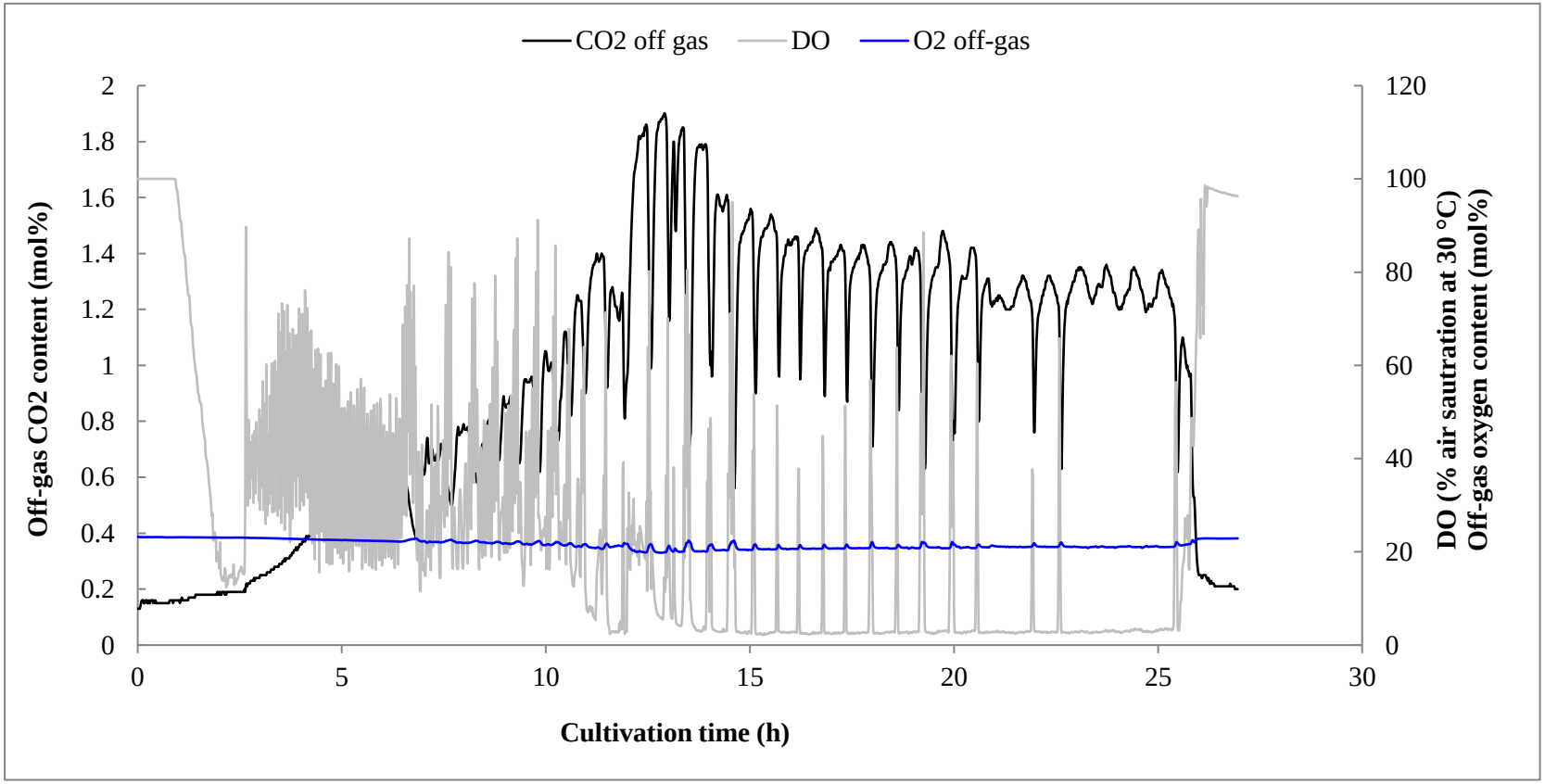

Figure B.1. Zoomed in plot of Figure 7.1(b) to better show how the DO and/or off-gas CO_2 signals reacted to carbon limitation, indicating need for addition of the next pulse of octanoic acid (and ammonium sulfate until 20h).

Appendix C: Effects of culture rheology on downstream processing operations

C.1. Introduction

This section gives some details on the effects that the rheological observations (discussed in Chapter 8) have on downstream unit processing operations, specifically filtering and centrifugation operations. This was motivated by our own observations of difficulties involved in centrifuging samples obtained from HCD cultivations, as well as the difficulties in forcing the supernatant through filters for sample processing. Given that one of the intial discussions in determining a research direction for this thesis involved application of membrane bioreactors to mcl-PHA production, this seemed worth exploring.

C.1. Methods: measurement of clarification efficiency of HCD cultures

To understand how rheological changes to the medium may affect downstream unit operations, two tests were conducted to model solids separation by both filtration and centrifugation. The filterability test is a dimensionless measure of the resistance to filtration, obtained by dividing the time required to filter a given volume of sample by the time required to filter an equivalent volume of water (Ives 1979). A modified approach of this concept was adapted for the purposes of these experiments. A Whatman 1 filter (11 μm pore size) was used as the filter and the sample volume ranged from 25 to 50 mL, depending on the difficulty of filtration. The efficiency of solids removal by centrifugation was assessed by the difference in CDM obtained from centrifuging samples at 4000×g compared to 12,500×g, both for 10 min.

C.3. Results

The observed increase in viscosity also affects downstream unit operations such as filtration (Okamoto 2001) and centrifugation (Tustian et al. 2007). The rates of both filtration and particle settling velocity (according to Stokes Law) during centrifugation are inversely proportional to the viscosity of the medium. As shown in Figure C.2, the filterability of the medium increased sharply from 21-27 h, during the time of maximum Qv, $[X_{PHA}]$ and $\%_{PHA}$. It should be noted that for the purpose of this test, the samples generally passed somewhat easily (within minutes) through the filter (pore size: 11 μm). However, the samples from the later stages of cultivation would completely block 0.2 μm filters, which might suggest that bioreactor configurations that employ microfiltration or ultrafiltration membrane cassettes may not be ideal in this application. In addition, the percentage of solids remaining after centrifugation at 4000 × g increased throughout the cultivation to more than 17% of the CDM by the final sample, which implies product loss could become problematic.

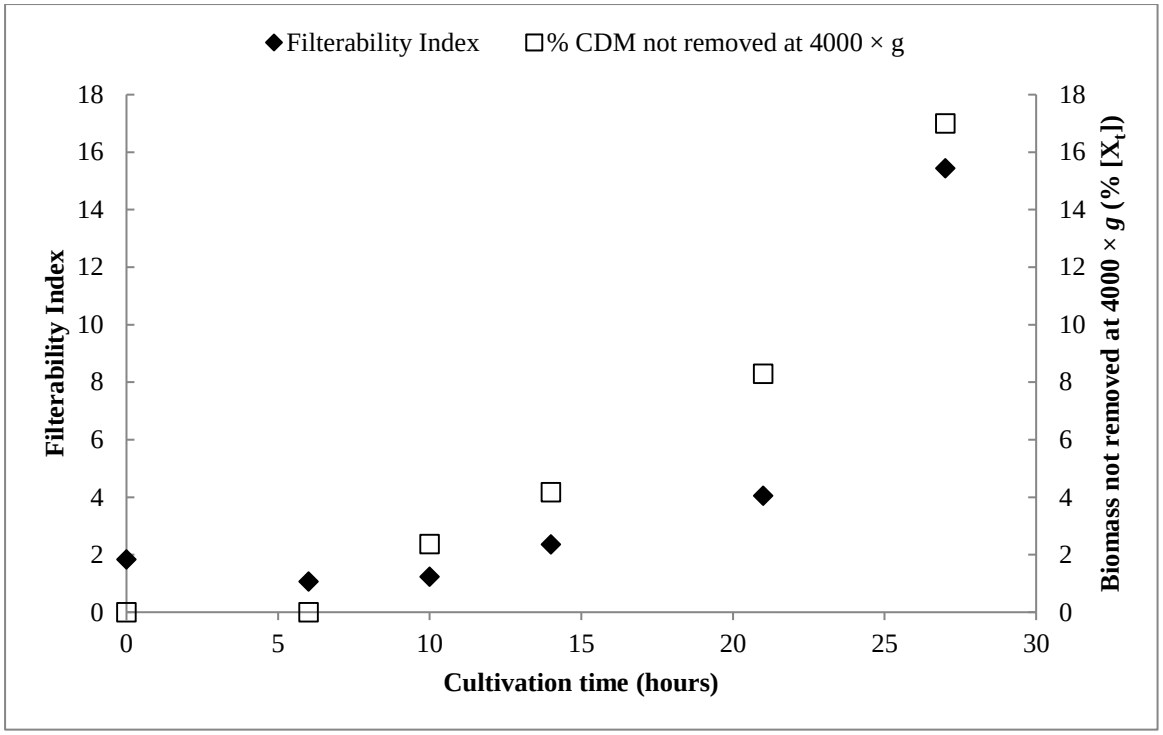

Figure C.2. Clarification or separation efficiency of the culture over time.

C.4. Works cited

Ives KJ (1979) A NEW CONCEPT OF FILTERABILITY. In: Ninth International Conference on Water Pollution Research. Elsevier, pp 123–137

Okamoto Y (2001) Harvest time effects on membrane cake resistance of *Escherichia coli* broth. J Membr Sci 190:93–106. doi: 10.1016/S0376-7388(01)00431-8

Tustian AD, Salte H, Willoughby NA, Hassan I, Rose MH, Baganz F, Hoare M, Titchener-Hooker NJ (2007) Adapted ultra scale-down approach for predicting the centrifugal separation behavior of high cell density cultures. Biotechnol Prog 23:1404–1410. doi: 10.1021/bp070175d

Appendix D: Application of a high cell-density fed batch process for non-sterile mcl-PHA production

D.1. Introduction

This work is an addendum to Chapter 9, in which the automated drip feed process developed in Chapter 7 for HCD fed batch cultivations was run under non-sterile conditions. The hypothesis that maintaining a sufficient concentration of octanoic acid maintained a selection pressure for *P. putida* LS46, but the data obtained in Chapter 9 certainly appeared to indicate that this wasn't really the case, and in fact any concentration of octanoic acid appeared to maintain the selection pressure. As such, the drip-feed process was used in this Appendix section.

D.2. Methods

Oxygen-limited fed batch experiments were conducted using the same fed-batch bioreactor setup described in Section 7.4.2 and automated drip-feed method described in Section 7.5.5. For test experiments, neither the bioreactor nor the medium was autoclaved; the bioreactor was prepared (with octanoic acid added to the medium), left overnight and axenic *P. putida* LS46 inoculum was added the following morning. For control experiments, the bioreactor was autoclaved at 121 °C for an exposure time of 40 min. The initial concentration of octanoic acid in all fed-batch bioreactor experiments was 2.88 g L^{-1} (20 mM), and a glycol-based antifoaming agent (Sigma 204) was also added to the medium (100 μL L^{-1}) prior to autoclaving.

D.3. Results

In the results presented above, we have taken preliminary results from shake flasks and scaled it to a semi-continuously running bench-scale SBR. Although productivity was by no means optimized in this SBR system, it was useful to show how mcl-PHA-producing

organism(s) perform in this environment over time. In industrial biotechnology however, HCD fed-batch cultivation is still (by far) the most commonly applied method for production and scale-up of PHAs. Since the requirement for medium sterility becomes increasingly impractical in larger-scale bioreactors, a (comparatively) high-productivity fed-batch process for mcl-PHA production was studied under non-sterile conditions as an addendum to this work. The approach followed the oxygen-limited drip feed process developed in Chapter 7.

Overall, the fed-batch process behaved nearly identically using non-sterile bioreactor equipment and medium as the sterile process described in Section 7.5.5, and further details are available there. Several key process performance metrics from the non-sterile fed-batch studies are summarized in Table D.1. The $Y_{PHA/S}$, Q_v, and Q_s values show that the carbon source was assimilated to mcl-PHA with the same rate and efficiency regardless of the process being performed in a sterile or non-sterile environment. Statistical analysis showed no significant difference in either $\%_{PHA}$ or Q_v under non-sterile conditions.

Table D.1. Performance of a non-sterile fed-batch process for mcl-PHA production using *P. putida* LS46 with respect to sterile control.

Condition	**Replicates**	**[X_t]**	**$\%_{PHA}$**	**$Y_{PHA/S}$[a]**	**Max. Q_v**	**Max. Q_s[b]**
	n=	g L^{-1}	% CDM	g g^{-1}	g L^{-1} h^{-1}	g g X_r^{-1} h^{-1}
Non-sterile	4	32.7 ± 0.4	50.9 ± 0.7	0.43 ± 0.00	0.61 ± 0.00	0.12 ± 0.02
Sterile	2	30.7 ± 1.3	51.9 ± 3.0	0.39 ± 0.00	0.60 ± 0.04	0.10 ± 0.00
Significance		p = 0.40	p = 0.52	p = 0.59	p = 0.80	p = 0.72

[a]$Y_{PHA/S}$ taken as the average value during the PHA accumulation phase (14-27 h); [b]measurement taken as the maximum observed value during the PHA accumulation phase (14-27 h). Statistical significance determined as a two-tailed comparison of means using confidence intervals of 95%.

Appendix E: The potential of non-sterile mcl-PHA production from biodiesel waste free fatty acids and mixed culture mcl-PHA production

E.1. Introduction

This section provides some supplemental data for Chapter 9, which may have important implications for future research directions from that work. Results for two aspects are shown: 1) mcl-PHA production from LCFAs derived from biodiesel waste, which was referred to in Chapter 9; and 2) mcl-PHA production from an enriched mixed culture obtained from a sample of secondary sludge.

E.2. Methods

E.2.1. Medium, substrates, and microorganism(s)

Ramsay's medium was used in all studies as described in Section 3.2. The pH of the medium was adjusted to 6.5 after addition of the carbon substrate.

For the experiments investigating non-sterile mcl-PHA production from waste LCFAs, the substrate was free fatty acids (FFAs) separated from biodiesel glycerin bottoms obtained from the Renewable Energy Group (Danville, IL). These were added to an initial concentration of 1% (vol/vol). These experiments employed *P. putida* LS46, for which strain maintenance and culturing practices were identical to those described in Section 3.2.

For the tests evaluating mcl-PHA production from an enriched mixed culture, the carbon substrate was octanoic acid. This was typically added to a final concentration of 5 to 40 mM (as described in Chapter 9). The inoculum was a sample of secondary sludge obtained from

Winnipeg's west side treatment plant (December 12, 2017). This was first enriched by adding 20 µL of the sample (thoroughly vortexed) to a flask containing 20 mM octanoic acid in Ramsay's medium, and incubated for 48 h, until significant growth was observed.

E.2.2. Experimental setup

All tests were conducted in 500 mL baffled flasks with a 100 mL working volume. These were incubated at 30 °C with 150 rpm orbital shaking. Samples (40 mL) were then taken and prepared for gravimetric analysis of CDM, and GC-FID determination of PHA content and composition as described in Chapter 3.

The experiments using biodiesel FFAs were initiated with the addition of a 1% (vol/vol) inoculum from an overnight (axenic) culture grown under identical conditions as the test. These were harvested at 48 h post inoculation. Samples (40 mL) were then taken and prepared for gravimetric analysis of CDM, and GC-FID determination of PHA content and composition as described in Chapter 3. However, in these experiments the pellet was washed once in hexane to remove residual LCFAs. These experiments were performed twice, with each experiment consisting of triplicate flasks for each condition.

The mixed-culture experiments were inoculated as 1% (vol/vol) from an overnight culture grown under identical conditions. The culture was also mixed with *P. putida* LS46 (on an equivalent OD_{600} basis with final inoculum volume of 1%) and compared with performance of pure *P. putida* LS46 cultures at several concentrations or octanoic acid. These experiments were only performed once and need to be replicated. Cultures were harvested at 24 h and the total biomass and PHA contents were determined as described above. In a second part of the experiment, the stability of enriched mixed culture was evaluated over a period of 5 days with

samples every 24 h. Briefly, in these experiments, a 1% vol/vol inoculum was transferred to a new flask under the same conditions at the time of harvest.

E.3. Results

E.3.1. Non-sterile mcl-PHA production from biodiesel waste LCFAs

The results for these tests are shown in Table E.1. As shown, there was no significant difference in either the total biomass produced, the PHA content of that biomass, or the overall volumetric productivity. The obtained monomer compositions in each cases were similar to that reported for LCFAs in Table 5.3. These results imply that longer chain fatty acids exert similar selectivity toward mcl-PHA producers as octanoic acid, but may be a less expensive alternative. Further investigation is required, and may be a possible avenue for follow-up work arising from this thesis.

Table E.1. Results for non-sterile mcl-PHA production from biodiesel waste free fatty acids compared to sterile conditions using *P. putida* LS46.

	Mean ± St.Dev (sterile)	Mean ± St.Dev (non-sterile)	*p*-value	Significant?
$[X_t]$ (g L^{-1} CDM)	5.7 ± 0.7	5.9 ± 0.3	0.72	No
$\%_{PHA}$ (% CDM)	37.4 ± 0.5	36.6 ± 0.9	0.38	No
Q_v (mg L^{-1} h^{-1})	44.3 ± 6.2	45.0 ± 3.2	0.90	No

E.3.2. Non-sterile mcl-PHA production using an enriched mixed culture

The mcl-PHA production capacity of the enriched mixed culture (WW) is shown in Figure E.1 along with an axenic *P. putida* LS46 culture and a culture of *P. putida* LS46 mixed with the enriched culture (LS46 = WW) for comparison. Remarkably, after an acclimation period of only 48 h, the mixed culture produced 22.6 % mcl-PHA (Table E.2) and the monomer composition was similar to that of pure *P. putida* LS46 at 89% C8, 6% C6, and 3% C10 with traces of C12 and C14. PHB was not detected in any of the samples. On the subsequent

subculture, the enriched mixed culture produced 43.8% mcl-PHA after 24 h from 40 mM octanoic acid, whereas pure *P. putida* LS46 produced 54.9% mcl-PHA. When the enriched mixed culture was spiked with *P. putida* LS46 (inoculated on an equivalent OD_{600} basis to a total inoculum size of 1% vol/vol), little difference was observed when compared to the mixed culture alone.

Figure E.1. PHA contents obtained from the enriched mixed cultures with respect to a pure culture of *P. putida* LS46 (in a sterile environment). LS46 – pure *P. putida* LS46 cultured under sterile conditions; LS46 + WW – an inoculum containing half of the enriched mixed culture and half of the axenic *P. putida* LS46 culture; WW – enriched culture from activated sludge.

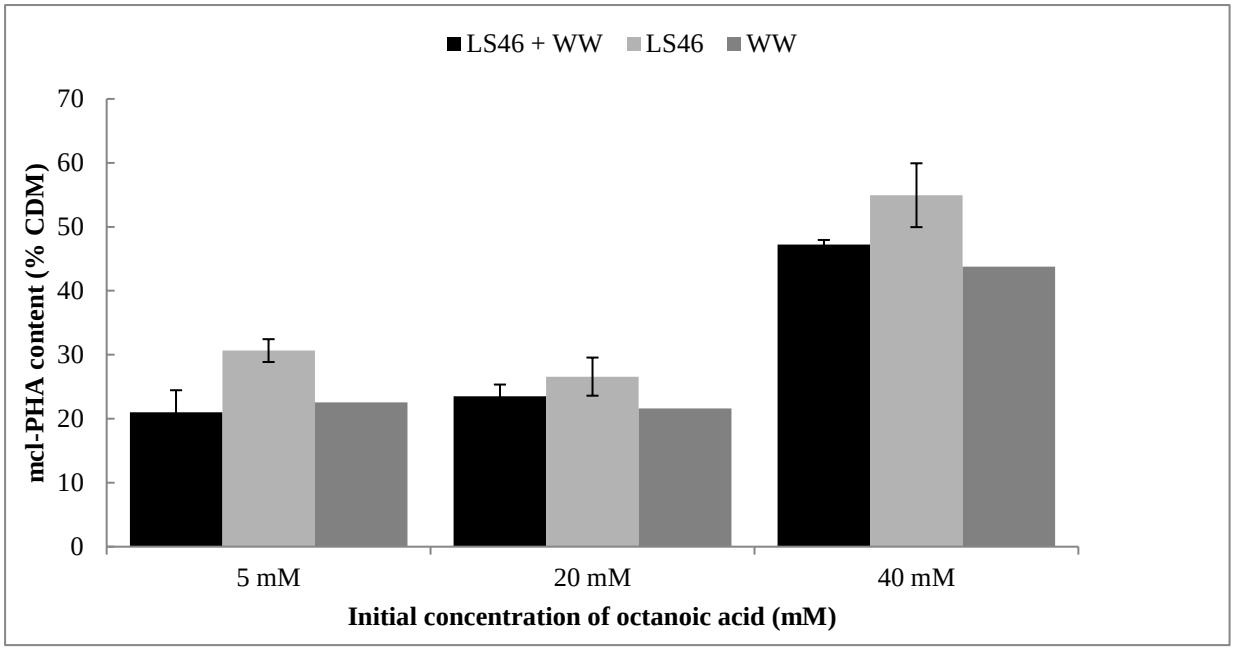

Table E.2. Total biomass, mcl-PHA content, and volumetric productivity obtained from the mixed cultures with respect to an axenic culture of *P. putida* LS46.

Conc.	Culture	$[X_t]$ (g L^{-1} CDM)	$\%_{PHA}$ (% CDM)	Q_v (mg L^{-1} h^{-1})
5 mM	LS46	0.48 ± 0.01	30.7 ± 1.8	6.2 ± 0.5
	LS46 + WW	0.42 ± 0.01	21.0 ± 3.4	3.6 ± 0.5
	WW	0.42	22.6	3.9
20 mM	LS46	2.18 ± 0.01	26.6 ± 3.0	25.8 ± 0.3
	LS46 + WW	2.00 ± 0.06	23.5 ± 1.8	19.6 ± 1.4
	WW	1.91	21.6	18.1
40 mM	LS46	3.79 ± 0.15	54.4 ± 5.0	87.0 ± 11.3
	LS46 + WW	3.36 ± 0.12	47.2 ± 0.7	66.0 ± 2.0
	WW	2.77	43.8	50.6
20 mM	LS46 inoculum	-	45.6	-
20 mM	WW inoculum (after 48 h)	-	22.6	-

Table E.3. Monomer compositions obtained from the mixed cultures with respect to an axenic culture of *P. putida* LS46.

Conc.	Culture	%C6	%C8	%C10	%C12
5 mM	LS46	7.9 ± 0.0	87.2 ± 0.9	3.7 ± 0.9	0.2 ± 0.0
	LS46 + WW	8.0 ± 1.0	86.9 ± 0.9	3.1 ± 0.8	0.6 ± 0.3
	WW	6.8	87.6	3.5	0.4
20 mM	LS46	6.8 ± 0.1	88.9 ± 3.0	2.7 ± 0.3	0.3 ± 0.0
	LS46 + WW	7.0 ± 0.0	87.5 ± 1.8	3.5 ± 0.1	0.4 ± 0.0
	WW	6.9	87.8	3.1	0.5
40 mM	LS46	6.2 ± 0.1	90.2 ± 0.2	3.0 ± 0.1	0.2± 0.0
	LS46 + WW	6.5 ± 0.1	88.8 ± 0.2	3.9 ± 0.1	0.2 ± 0.1
	WW	6.1	43.8	50.6	
20 mM	LS46 inoculum	5.0	90.1	3.0	0.1
20 mM	WW inoculum	6.2	89.0	3.6	0.3

Since the enriched mixed culture showed good mcl-PHA content and productivity, on only the second subculture from the original activated sludge the next question asked was is this behavior stable over time. A sample was taken from the activated sludge (20 uL) and subcultured on 20 mM octanoic acid fro the first 24 h and then 40 mM octanoic acid for four additional subcultures afterward. As shown in Figure E.4, the culture appeared to stabilize after 72 h at 3.3 g L^{-1} X_t with 40% PHA, resulting in an overall volumetric productivity of about 50 mg mcl-PHA L $culture^{-1}$ h^{-1}.

Figure E.4. Results for continual subculturing of the mcl-PHA producing culture enriched from activated secondary sludge using octanoic acid.

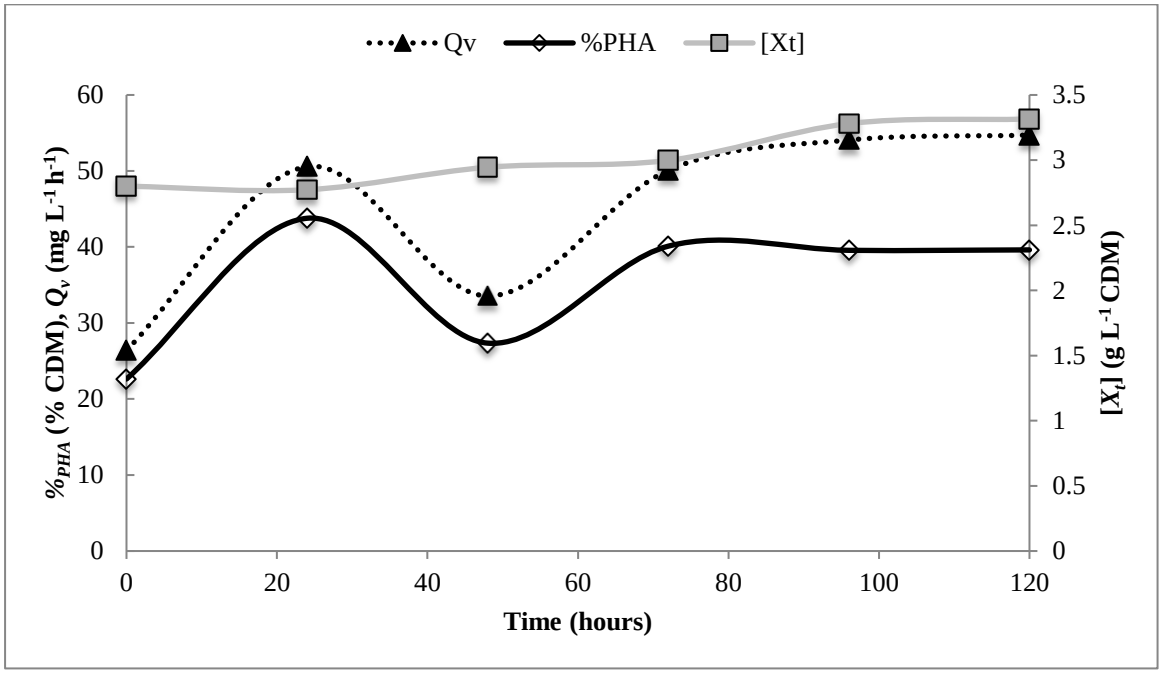

E.4. Conclusions

As supporting evidence for Chapter 9, this section has shown that non-sterile production of mcl-PHA from a more crude carbon source like biodiesel waste FFAs is possible in short-term (48 h) batch cultures when using an axenic *P. putida* LS46 inoculum. However, of perhaps

greater interest and relevance is the observation that mcl-PHA can be produced from fatty acids under non-sterile conditions using an enriched mixed culture. This suggests that the addition of octanoic acid to the culture medium applies a strong selective pressure for mcl-PHA producing organisms. Further work is needed in this area, but a possible future research direction to follow up on from this thesis would involve: 1) confirmation of these results; 2) elucidation of the population dynamics using next-generation sequencing technology such as Illumina sequencing; and 3) some kind of process optimization as either non-sterile semi-continuous sequencing batch reactors or a fully continuous system.